

Study Effect of Catalyst Shape on The Ethylbenzene Dehydrogenation in Fixed Bed
Reactor by Using Various Mathematical Models



A Thesis Submitted in Partial Fulfillment of the Requirements
for the Degree of Master of Engineering in Chemical Engineering

Department of Chemical Engineering

FACULTY OF ENGINEERING

Chulalongkorn University

Academic Year 2019

Copyright of Chulalongkorn University

การศึกษาผลของรูปร่างตัวเร่งปฏิกิริยาต่อการเกิดปฏิกิริยาเอทิลเบนซีนดีไฮโดรจีเนชันในเครื่อง
ปฏิกรณ์แบบเบดนิ่งโดยอาศัยแบบจำลองทางคณิตศาสตร์หลายรูปแบบ



วิทยานิพนธ์นี้เป็นส่วนหนึ่งของการศึกษาตามหลักสูตรปริญญาวิศวกรรมศาสตรมหาบัณฑิต
สาขาวิชาวิศวกรรมเคมี ภาควิชาวิศวกรรมเคมี
คณะวิศวกรรมศาสตร์ จุฬาลงกรณ์มหาวิทยาลัย
ปีการศึกษา 2562
ลิขสิทธิ์ของจุฬาลงกรณ์มหาวิทยาลัย

Thesis Title	Study Effect of Catalyst Shape on The Ethylbenzene Dehydrogenation in Fixed Bed Reactor by Using Various Mathematical Models
By	Miss Pawinee Maithong
Field of Study	Chemical Engineering
Thesis Advisor	Assistant Professor APINAN SOOTTITANTAWAT, D.Eng.
Thesis Co Advisor	Professor Emeritus Wiwut Tanthapanichakoon, Ph.D

Accepted by the FACULTY OF ENGINEERING, Chulalongkorn University in Partial Fulfillment of the Requirement for the Master of Engineering

..... Dean of the FACULTY OF
ENGINEERING
(Professor SUPOT TEACHAVORASINSKUN, Ph.D.)

THESIS COMMITTEE

..... Chairman
(Assistant Professor AMORNCHAI ARPORNWICHANOP,
D.Eng.)

..... Thesis Advisor
(Assistant Professor APINAN SOOTTITANTAWAT, D.Eng.)

..... Thesis Co-Advisor
(Professor Emeritus Wiwut Tanthapanichakoon, Ph.D)

..... Examiner
(Rungthiwa Methaapanon, Ph.D.)

..... External Examiner
(Khavinet Lourvanij, Ph.D)

ภาวิณี ไหมทอง : การศึกษาผลของรูปร่างตัวเร่งปฏิกิริยาต่อการเกิดปฏิกิริยาเอทิลเบนซีนดีไฮโดรจีเนชันในเครื่องปฏิกรณ์แบบเบดนิ่งโดยอาศัยแบบจำลองทางคณิตศาสตร์หลายรูปแบบ. (Study Effect of Catalyst Shape on The Ethylbenzene Dehydrogenation in Fixed Bed Reactor by Using Various Mathematical Models) อ.ที่ปรึกษาหลัก : ผศ. ดร.อภิรักษ์ สุทธิธรรวัช, อ.ที่ปรึกษาร่วม : ศ.กิตติคุณ ดร.วิวัฒน์ ตัณฑะพานิชกุลPh.D

ในปัจจุบันสารเคมีโดยส่วนใหญ่ผลิตได้โดยกระบวนการใช้ตัวเร่งปฏิกิริยาในเครื่องปฏิกรณ์แบบเบดนิ่ง รูปร่างของตัวเร่งปฏิกิริยามีผลต่อประสิทธิภาพของเครื่องปฏิกรณ์ ผลของตัวเร่งสามารถศึกษาได้โดยแบบจำลองทางคณิตศาสตร์ที่มีหลากหลายรูปแบบเพื่อให้เสมือนจริง ดังนั้นวัตถุประสงค์ของงานวิจัยนี้คือการศึกษาผลของรูปร่างตัวเร่งปฏิกิริยาต่อเครื่องปฏิกรณ์ของกระบวนการดีไฮโดรจีเนชันของเอทิลเบนซีนเป็นสไตรีนซึ่งเป็นปฏิกิริยาวิฤภาคแก๊สด้วยแบบจำลองที่พัฒนาขึ้นหลากหลายรูปแบบ แบบจำลองแบบเอกพันธ์ (แบบจำลอง1) เป็นแบบจำลองที่ง่ายที่สุด ทำนายค่าร้อยละการเปลี่ยนแปลงของสารตั้งต้นได้ 36.52% ส่วนแบบจำลองที่ซับซ้อนขึ้นคือแบบจำลองวิวิธพันธ์ที่พิจารณาการถ่ายเทสารภายในเม็ดตัวเร่งปฏิกิริยา (แบบจำลอง2) ทำนายได้ 34.49% โดยเท่ากับการทำนายของแบบจำลองที่พิจารณาทั้งการถ่ายเทของสารและความร้อนภายในเม็ดตัวเร่ง (แบบจำลอง3) จากผลการทำนายแสดงว่าการถ่ายเทสารภายในเม็ดตัวเร่งปฏิกิริยามีผลต่อการเกิดปฏิกิริยา ในขณะที่แบบจำลองวิวิธพันธ์ที่พิจารณาการถ่ายเททั้งภายในและภายนอกเม็ดตัวเร่งปฏิกิริยา (แบบจำลอง4) ทำนายได้ 34.46% และเมื่อเพิ่มผลของการแพร่สารในทิศทางทวนไหลในแบบจำลอง3 และ 4 พบว่าทั้งสองแบบจำลองทำนายได้ 34.46% ดังนั้นการถ่ายเทภายนอกและการแพร่ของสารในทิศทางทวนไหลไม่มีผลต่อค่าร้อยละการเปลี่ยนแปลง สำหรับผลของรูปร่างตัวเร่งปฏิกิริยาจะศึกษาโดยแบบจำลองวิวิธพันธ์ที่พัฒนาขึ้นมาในหลายรูปแบบ พบว่าผลการทำนายของแต่ละแบบจำลองมีค่าแตกต่างกันอย่างไม่มีนัยสำคัญ รูปร่างของตัวเร่งปฏิกิริยาที่มีเส้นผ่านศูนย์กลางสมมูลเท่ากันนั้นพบว่าปริมาณน้ำหนักตัวเร่งปฏิกิริยาที่ทำให้ได้ค่าเปอร์เซ็นต์การเปลี่ยนแปลงของสารตั้งต้นที่เท่ากันเรียงลำดับรูปร่างของตัวเร่งจากน้อยไปมากได้ ทรงสามกليب, ทรงกลม, และ ทรงกระบอก ตามลำดับ เนื่องจากรูปร่างของตัวเร่งปฏิกิริยามีผลต่อประสิทธิภาพการแพร่ภายในเม็ดตัวเร่งและความดันตกของระบบ

สาขาวิชา วิศวกรรมเคมี

ลายมือชื่อนิสิต

ปีการศึกษา 2562

ลายมือชื่อ อ.ที่ปรึกษาหลัก

ลายมือชื่อ อ.ที่ปรึกษาร่วม

6170392221 : MAJOR CHEMICAL ENGINEERING

KEYWORD: Heterogeneous reactor model, Catalyst shape

Pawinee Maithong : Study Effect of Catalyst Shape on The Ethylbenzene Dehydrogenation in Fixed Bed Reactor by Using Various Mathematical Models. Advisor: Asst. Prof. APINAN SOOTTITANTAWAT, D.Eng. Co-advisor: Prof. Emer. Wiwut Tanthapanichakoon, Ph.D

Nowadays, the chemicals are mostly manufactured by catalytic reactions in fixed bed reactor. Catalyst shape affects to reactor performance and the effect is studied by mathematic models which are varied forms to more realistic. Therefore, the objective of research is to study the effect of catalyst shape on the behavior of reactor for ethylbenzene dehydrogenation to styrene in gas phase by varied form. The simplest model, pseudohomogeneous model (model1), predicts 36.52% ethylbenzene conversion. The more complex model, heterogeneous model accounting for internal mass transfer (model2), predicts 34.49% conversion that equals to the model accounting for internal mass and heat transfer(model3). This result shows that internal mass transfer affects to overall the reaction. The more complex, heterogeneous model accounting for internal and external transfer(model4), predict 34.46% conversion. Addition of axial mixing to model3 and model4, both results are 34.46% conversion. Thus, external transfer and mass axial dispersion are little effect. Effect of catalyst shape on reactor performance is studied by varied form of heterogeneous model. The results of each models are little different. For the catalyst shape of same equivalent diameter, the required catalyst weight to achieve specific conversion increases in order trilobe < sphere < cylinder since the catalyst shape affects on effectiveness factor and pressure drop.

Field of Study: Chemical Engineering

Student's Signature

Academic Year: 2019

Advisor's Signature

Co-advisor's Signature

ACKNOWLEDGEMENTS

Firstly, I would like to thank the department of chemical engineering, Chulalongkorn University for offering me the scholarship to achieve my master's degree.

I am sincerely grateful to my advisor, Asst. Prof. Apinan Soottitantawat, who show a great confident in me to give me responsibility in this study and provided me with a great deal of support and shared his knowledge and expertise with me. I would also like to thank my thesis co-advisor, Prof. Emer. Wiwut Tanthapanichakoon, who always open whenever I ran into a trouble spot or had a question about my research. Without their assistance and dedicated involvement in every step throughout the process, this thesis would have never been accomplished. I would like to thank you very much for your support and understanding

I also would like to thank the member of my defense thesis committee for their effort, time and commend that improved the quality of the thesis. They were Asst. Prof. Amornchai Arpornwichanop, Dr. Rungthiwa Methaapanon, and Dr. Khavinet Lourvanij.

I would like to thank Process Scale-up Technology Group of SCG Chemicals company for financial support, knowledge, and suggestion.

Finally, I must express my present gratitude to my parents and my colleague for providing me with unfailing support and continuous encouragement throughout my years of study and through the process of researching and writing this thesis. This accomplishment would not have been possible without them. Thank you.

Pawinee Maithong

TABLE OF CONTENTS

	Page
ABSTRACT (THAI).....	iii
ABSTRACT (ENGLISH).....	iv
ACKNOWLEDGEMENTS.....	v
TABLE OF CONTENTS.....	vi
Chapter 1 Introduction.....	11
1.1 Motivation of Research.....	11
1.2 Objective of Research.....	12
1.3 Scopes of Research.....	12
1.4 Expected Benefits of Research.....	13
Chapter 2 Fundamentals and Literature Reviews.....	14
2.1 Fixed bed reactor.....	14
2.1.1 External transfer.....	15
2.1.2 Internal transfer.....	16
2.1.3 Reaction.....	18
2.1.4 Axial dispersion.....	18
2.2 Modeling of fixed bed reactor.....	19
2.2.1 Pseudohomogeneous model.....	20
2.2.2 Heterogeneous model accounting only for internal mass diffusion.....	20
2.2.3 Heterogeneous model accounting for both internal diffusion inside and external diffusion around a pellet.....	22
2.2.4 Heterogeneous model accounting for both internal diffusion inside and external diffusion around a pellet and mass axial dispersion.....	23

2.2.5 Auxiliary Equations and Correlations	23
2.3 Effect of catalyst shape	26
2.4 Ethylbenzene dehydrogenation to styrene process.....	30
Chapter 3 Methodology	37
3.1 Validation	37
3.2 Developed model.....	37
3.2.1 Pseudohomogeneous model (Model1)	37
3.2.2 Heterogeneous model accounting for internal diffusion (Model2).....	38
3.2.3 Heterogeneous model accounting for internal mass and heat transfer (Model3)	39
3.2.4 Heterogeneous model accounting for internal mass and heat transfer and external mass and heat transfer (Model4).....	40
3.2.5 Heterogeneous model accounting for internal mass and heat transfer and mass axial dispersion. (Model5).....	41
3.2.6 Heterogeneous model accounting for internal mass and heat transfer, external mass and heat transfer and mass axial dispersion. (Model6)	43
3.3 Determine the effect of catalyst.....	44
Chapter 4 Result and discussion	46
4.1 Developed model of fixed bed reactor for dehydrogenation ethylbenzene to styrene	46
4.1.1 Validate simulation result of model with publication	46
4.1.2 Developed models of fixed bed reactor for dehydrogenation ethylbenzene to styrene	48
4.1.2.1 Heterogeneous model accounting for internal mass transfer	49
4.1.2.2 Heterogeneous model accounting for internal mass and heat transfer	51

4.1.2.3 Heterogenous model accounting for internal and external transportation	53
4.1.2.4 Heterogeneous model with axial mixing	56
4.1.3 Estimate the important of transfer effect on reaction by criteria	60
4.1.3.1 Estimate the importance of internal transfer on reaction for commercial process	60
4.1.3.2 Estimate the importance of the external transfer on reaction by criteria	62
4.1.3.2.1 Estimate the importance of the external transfer on reaction for commercial process.....	62
4.1.3.2.2 Estimate the importance of the external transfer on reaction for process that affected by external transfer .	64
4.1.3.3 Estimate the importance of mass axial dispersion on reaction by criteria	67
4.1.3.3.1 Estimate the importance of mass axial dispersion on reaction for commercial process.....	67
4.1.3.3.2 Estimate the importance of mass axial dispersion on reaction for process that affected by mass axial dispersion	68
4.1.4 Comparison of simulation result	70
4.1.4.1 Comparison of simulation result with simulation result of reference paper	70
4.1.4.2 Comparison of simulation result with industrial result	71
4.2 Study the effect of catalyst shape on reactor performance by same effective diameter catalyst	73
4.2.1 Effect of catalyst shape on required catalyst mass and reactor length ...	76

4.2.2 Effect of catalyst shape on effectiveness factor	78
4.2.3 Effect of catalyst shape on pressure drop	79
4.2.4 Effect of catalyst shape on observe reaction rate.....	80
4.2.5 Effect of catalyst shape on intermediate parameters relate to required catalyst weight and bed length.....	83
4.3 Study the effect of catalyst shape on reactor performance by catalyst shape in commercial size	84
Chapter 5 Conclusion	87
REFERENCES	89
NOMENCLATURE	90
REFERENCES	94
Appendix A Kinetic parameter estimation.....	98
Appendix B Data for Modeling.....	107
Appendix C Result of studied effect of catalyst that same equivalent diameter	113
Appendix D Result of studied effect of commercial catalyst	122
Appendix E Fixed bed reactor model code.....	123
1. Model1 : Pseudohomogeneous model.....	123
2. Model2 : Heterogeneous model account for internal mass transfer	128
3. Model3 : Heterogeneous model account for internal mass and heat transfer .	135
4. Model4 : Heterogeneous model account for internal and external transfer	145
5. Model5 : Heterogeneous model account for internal transfer and mass axial dispersion	158
6. Model6 : Heterogeneous model account for internal transfer, external transfer and mass axial dispersion	165
VITA.....	172

Chapter 1 Introduction

1.1 Motivation of Research

Nowadays, the greatest tonnages of synthesis chemicals are mostly manufactured by catalytic reactions. They are generally occurred in fixed bed reactor, because of simplicity of technology and operation [1]. Catalyst is the important part of fixed bed reactor since the reaction process occurs on them. For gas-solid reactor, the reactant transfers from gas phase to active site and reacts to product on active site. The catalyst should have large specific external catalyst surface for more external mass transfer, therefore, there are many shapes of catalyst to response the requirement. However, the catalyst shape also affects to process in reactor example of pressure drop, void of bed or flow pattern in reactor [2]. In consequence, the effect of catalyst shape should be considered for selection a suitable catalyst shape that can be complete specified only for a specific process.

The effect of catalyst shape is studied by mathematic model which can predict the performance of the reactor. There are several publications which use mathematic model to study the effect of catalyst shape. Example of Fischer-Tropsch synthesis reactor[3], the heterogeneous model is used to understand the effect of catalyst shape on effectiveness factor, bed void fraction, and overall heat transfer coefficient. For hydrodesulfurization reactor[2], the heterogeneous model accounting for internal and external mass transfer is used to examine the effect on phenomena inside reactor, such as liquid hold up, internal, and external concentration gradient, and pressure drop.

Mathematic models are varied forms which range from simple form to complex form aiming at more realistic description of phenomena in reactor. The model is classified two categories, pseudohomogeneous and heterogeneous model. Pseudohomogeneous models do not explicitly account for the presence of catalyst, while the heterogeneous models consist of separate conservation equations for fluid and catalyst [4]. The heterogeneous models account for the role of internal and external transfer which affect to reaction rate. These models

are required for process with significant temperature and concentration differences between the phases, such as steam methane reforming [1], partial oxidation of methanol to formaldehyde [5], or methanation of carbon dioxide process [6]. Moreover, to simulate real reactor, axial dispersion model is used to determine residence time distribution instead of plug flow model [7], such as water-gas shift process [8]. Most of the Chemical Industries, reactors are non-ideal, therefore, it is important to know the modeling and simulation of real reactor in practice.

From previous publication, the effect of catalyst is studied by model which accounts for only internal or external mass transfer [2, 3, 9]. Therefore, this research focuses to study the effect of catalyst shape on reactor behaviors by developed model which accounts for internal heat and mass transfer, external heat and mass transfer and axial dispersion for industrial ethylbenzene dehydrogenation reactor.

1.2 Objective of Research

To study the effect of catalyst shape on the behavior of fixed bed reactor by developed models which account for internal heat and mass transfer, external heat and mass transfer and axial dispersion.

1.3 Scopes of Research

- 1.3.1 This research studies ethylbenzene dehydrogenation to styrene on iron oxide catalysts promoted by potassium process.
- 1.3.2 The information of process including reaction rate, operating condition, and reactor properties obtain from literature review [10].
- 1.3.3 The effect of different catalyst is studied by heterogeneous model which accounts for internal heat and mass transfer, external heat and mass transfer and axial dispersion.
- 1.3.4 This research studies the effect of different catalyst particle shapes (sphere, cylinder, and 3-lobe) on the characteristics and behavior of

catalyst and reactor, such as catalyst effectiveness, amount of catalyst, pressure drop per unit length.

- 1.3.5 The spherical catalyst shape sizes 5.5 mm of diameter. The cylinder catalyst shape sizes 5 mm of length and 3.5 diameter. The 3-lobe catalyst sizes 5 mm of circumference and 5 mm of length.

1.4 Expected Benefits of Research

The mathematic model is properly selected for prediction the reactor. The model is used for analysis the effect of catalyst shape to the performance of reactor. The result from the analysis are information to select the appropriate catalyst shape for fixed bed reactor.

Chapter 2 Fundamentals and Literature Reviews

This chapter describes literature reviews including phenomena in fixed bed reactor, modeling of fixed bed reactor, effect of catalyst shape, and ethylbenzene dehydrogenation to styrene process.

2.1 Fixed bed reactor

Catalytic reactions are generally carried out in fixed bed reactors, because of simplicity of technology and operation. The steps of catalytic reaction process are shown in Figure 1.

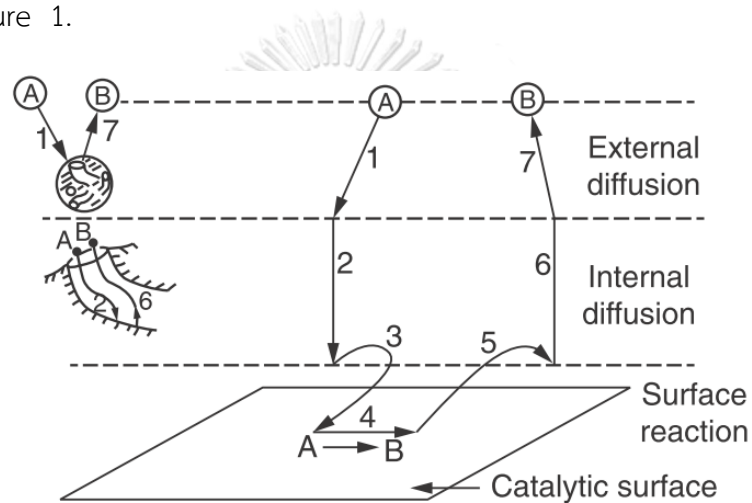


Figure 1 Step in catalytic reaction

Step in catalytic reaction [11]

1. Mass transfer of the reactant from bulk fluid to the external surface of catalyst
2. Diffusion of reactant from the pore mouth through the catalyst pores to internal catalytic surface
3. Adsorption of reactant onto active sites
4. Reaction on the surface of the active sites
5. Desorption of products
6. Diffusion of the products from interior of catalyst to pore mouth at the external catalyst
7. Mass transfer of products from external catalyst surface to the bulk fluid

The overall rate of reaction is equal to the rate of the slowest step in mechanism. When the diffusion steps (step 1, 2, 6, and 7) are very fast compared with the reaction step (step 3, 4, and 5), the concentrations are not significantly different between the bulk of fluid and external surface or between external surface and active site. Therefore, the diffusion does not affect the overall rate of reaction. If the reaction steps are very fast compared with the diffusion, mass transport affects the reaction rate.

2.1.1 External transfer

External diffusion of mass is transfer from bulk fluid to external surface of catalyst. The resistance to transfer is boundary layer surrounding the pellet. The reactant at a bulk concentration (C_b) must transfer through the boundary layer to external surface of pellet where the concentration is C_s . The rate of transfer [11] is

$$\text{Rate of mass transfer} = k_c(C_b - C_s)$$

where the mass transfer coefficient, k_c , is a function of the hydrodynamic conditions, namely fluid velocity, and particle diameter. The coefficient correlated in terms of three dimensionless group: the Sherwood number, Sh ; the Reynolds number, Re ; and the Schmidt numbers.

The mass transfer coefficient is inversely proportional to boundary layer thickness and directly proportional to diffusion coefficient. At low velocities of fluid, the boundary layer is thick, and take long time to transfer to external surface, resulting in small mass transfer coefficient. As a result, mass transfer through the boundary is slow and limits the rate of overall reaction. As the velocities increase, the boundary layer become smaller and mass transfer rate is increase. As a result, external mass transfer does not limit the rate of overall reaction.

The energy is transferred between fluid bulk and catalyst surface, since the reaction which occurs at catalyst releases or consumes the energy. The rate of transfer is

$$\text{Rate of heat transfer} = h(T - T_s)$$

Mears' criterion is used to identify the importance of external diffusion limitation. Mass transport from the bulk gas phase to the surface of catalyst is very fast and concentration gradient can be neglected [11] when

$$\frac{r_c \rho_B R n}{k_c C_i} < 0.15$$

Similarly, energy transport from the bulk gas phase to surface of catalyst is very fast and temperature gradient can be neglected [11] when

$$\left| \frac{-\Delta H_r(r_c) \rho_B R E}{h T^2 R_g} \right| < 0.15$$

2.1.2 Internal transfer

Internal diffusion of mass is the diffusion from the external surface into the interior of catalyst. The pores in the pellet are not straight and cylindrical; consequently, we shall define an effective diffusion coefficient to describe the average diffusion. The effective diffusivity, D_e , accounts for tortuous path inside catalyst and varying cross-sectional areas of pores. An equation that relates D_e to either bulk or the Knudsen diffusivity [11] is

$$D_e = \frac{D_{AB} \phi_p \sigma_c}{\tau}$$

Where $\tau = \text{tortuosity} = \frac{\text{Actual distance a molecule travels between two points}}{\text{Shortest distance between those two points}}$

$\phi_p = \text{pellet porosity}$

$\sigma_c = \text{Constriction factor}$

The molar flux of internal diffusion is

$$W_r = -D_e \frac{dC}{dr}$$

For the large pellets, it takes a long time for diffusion into the interior of catalyst. While the very small pellets, it takes very little time to diffuse, as a result, internal diffusion does not limit the rate of overall reaction.

Weisz-Ptrater criterion can estimate effect of internal diffusion on overall reaction rate by value of C_{WP} .

$$C_{WP} = \frac{\text{actual reaction rate}}{\text{diffusion rate}}$$

$$C_{WP} = \frac{r_c \rho_c R^2}{D_e C_s}$$

If the above parameter $C_{WP} \ll 1$, there is no mass diffusion limitation and consequently concentration gradient inside the pellet is negligible. If $C_{WP} \gg 1$, internal diffusion limits the observed overall reaction rate [11].

When catalytic reaction rate occurs inside catalyst, the energy is transferred to release or consume by reaction. Temperature gradients may exist within the catalyst. The effective thermal conductivity determines whether or not appreciable temperature gradients. An approximation for predicting effective thermal conductivities is

$$k_e = k_s^{1-\varepsilon_p} k_f^{\varepsilon_p}$$

Where k_f and k_s are the thermal conductivities of fluid and solid, respectively, and ε_p is the porosity of catalyst.

The heat flux is

$$q_r = k_e \frac{dT}{dr}$$

The rate of endothermic heat consumption is equal to the rate of heat conduction into the pellet, as show in following equation.

$$k_e(T_0 - T) = \Delta H \cdot \text{Reaction rate}$$

Because reaction rate inside catalyst must be equal to the rate transfer inside, the equation may be written

$$k_e(T_0 - T) = \Delta H \cdot D_e(C_0 - C)$$

Where T_0 and C_0 are the temperature and concentration at catalyst surface, respectively. From the equation, temperature gradient inside catalyst depends on effective thermal conductivity. When k_e is high, the temperature gradient is low. Moreover, energy conversion parameter (β) [12], which represent the ratio of maximum temperature difference to external surface temperature, may be regard as zero for isothermal catalyst.

$$\beta = \frac{(-\Delta H)D_e C_0}{k_e T_0}$$

2.1.3 Reaction

The heterogeneous reaction composes of three reaction steps in series (adsorption, surface reaction, and desorption)[11]. One step in the series is rate limiting which is limiting the overall rate of reaction.

The approach for determining catalytic mechanisms is usually term Langmuir-Hinshelwood approach. It is derived from ideas proposed by Hinshelwood based on Langmuir's principle. The Langmuir-Hinshelwood approach was popularized by Hougen and Watson and occasionally include their name. First, the rate limit is assumed and then formulate the reaction rate law in term of the species present.

2.1.4 Axial dispersion

In real vessel, flow is small deviate from plug flow (ideal flow). The substances spread as it passes through the vessel. The spreading is molecular diffusion in axial direction which is described by Fick's law equation [13].

$$\text{Flux of axial dispersion} = D_{ea} \frac{dc}{dx}$$

The deviation from plug flow can be estimated by vessel dispersion number (D_{ea}/uL), is the parameter that measures the extent of axial dispersion. When D_{ea}/uL is lower than 0.01, it means small deviation from plug flow. While D_{ea}/uL is higher than 0.01, the deviation from plug flow is large, the dispersion flow must be considered. [13]

2.2 Modeling of fixed bed reactor

The modeling of reactor is the mathematic equation describing the phenomena occurring in a reactor including reaction rate equation and the continuity, energy, and momentum equations.

The model extensively explores reactor design and performance as the development of chemical reaction engineer and increasing possibilities of computer. Model form now range from the very simple form to very sophisticated ones aiming at a more representative description of geometry and phenomena. The degree of sophistication depends on reaction scheme and on operating conditions [4].

The fixed bed reactor can be modeled in various ways. The models are classified in two categories: pseudohomogeneous and heterogeneous. Pseudohomogeneous models do not account for the existing of catalyst, in contrast with heterogeneous models which separate conservation equations for fluid and catalyst. The transport occurring in reactor consists of transport in axial direction and transport in reaction process. The transport in axial direction has 2 type: plug flow and axial dispersion. The transport in the reaction is divided into two parts: heat and mas transfer between the bulk of fluid and surface of catalyst (interparticle transport), and inside catalyst (intraparticle transport). The classification of fixed bed reactor models is present in following table

Table 1 Classification of fixed bed reactor model

Pseudohomogeneous models	Heterogeneous models
Plug flow	Plug flow + Intraparticle transport
	Plug flow + Intraparticle transport + Interparticle transport
Mass axial dispersion	Axial dispersion + Intraparticle transport
	Mass axial dispersion + Intraparticle transport + Interparticle transport

The basic structure of each model is composed of heat and mass conservation equations coupled through thermodynamic and kinetic relations as well as equation for estimating pressure drop through the packed bed. Published auxiliary correlations are used to estimate the necessary physical properties, coefficients of heat and mass transfer and friction factor in packed beds.

2.2.1 Pseudohomogeneous model

Pseudohomogeneous model does not explicitly account for the presence of catalyst pellets and assume that gradients of temperature and concentrations between the fluid and solid phases can be ignored. As a result, the equations for the two phases can be combined. The resulting fluid-phase balances are as follows[4]:

Mass balance:

$$\frac{du_s C_i}{dz} = \sum \rho_B v_{ij} r_{cj} + \sum \varepsilon_B v_{ij} r_{tj} \quad (1)$$

Energy balance:

$$\sum_{i=1}^6 \frac{\dot{m}_i C_{pi}}{A_c} \frac{dT}{dz} = \sum_{i=1}^4 (-\Delta H_{rj})(r_{cj} \rho_B + r_{tj} \varepsilon_B) \quad (2)$$

The boundary conditions at reactor inlet:

$$z = 0 ; C_i = C_{i0}, T = T_0$$

2.2.2 Heterogeneous model accounting only for internal mass diffusion

Heterogeneous model accounting only for internal mass diffusion leads to separate heat and mass balance equations for the fluid and solid (catalyst pellet) phases. The latter accounts for the resistance to mass and heat transport inside the catalyst pellet. By assuming sufficiently rapid heat and mass transport between the bulk fluid stream and the pellet surface, this model essentially neglects the concentration gradients between them. It is also assumed that negligible temperature gradient exists inside the pellet and intra-pellet heat transport can be ignored.

Solid phase (spherical catalyst pellet) mass balance[11]:

$$0 = \frac{D_{ei}}{r^2} \frac{d}{dr} \left(r^2 \frac{dC_i^s}{dr} \right) + \rho_s \sum_{j=1}^n v_{ij} r_{cj} + \varepsilon_s \sum_{j=1}^n v_{ij} r_{tj} \quad (3)$$

The boundary conditions for the pellets (BC)

$$r = 0 ; \frac{dC_i^s}{dr} = 0$$

$$r = R ; C_i^s = C_i$$

The above differential equation along with the pellet's BC for each species i can be simultaneously integrated numerically to yield the concentration profile of each species as function of radial position inside a pellet. This in turn can be used to estimate the following catalyst effectiveness factor η_j of each reaction j , which also depends on the axial position of the pellet in the reactor.

$$\eta_j = \frac{\text{Actual rate of reaction } j}{\text{Rate of reaction } j \text{ at external surface condition}}$$

$$\eta_j = \frac{\int_0^V [r_{cj}(P_{s,i})\rho_s + r_{tj}(P_{s,i})\varepsilon_s] dV}{[r_{cj}(P_i)\rho_s + r_{tj}(P_i)\varepsilon_s]V} \quad (4)$$

Gas phase mass balance:

$$\frac{du_s C_i}{dz} = \sum \rho_B \eta_j v_{ij} r_{cj} + \sum \varepsilon_B v_{ij} r_{tj} \quad (5)$$

Gas phase energy balance:

$$\sum_{i=1}^6 \frac{\dot{m}_i C_{pi}}{A_c} \frac{dT}{dz} = \sum_{i=1}^4 (-\Delta H_{rj}) (\eta_j r_{cj} \rho_B + r_{tj} \varepsilon_B) \quad (6)$$

The boundary conditions at the reactor inlet:

$$z = 0 ; C_i = C_{i0}, T = T_0$$

The above set of differential equations can be integrated numerically together with the estimated values of the effectiveness factors at each axial position to obtain the concentration profile of each species and the temperature profile along the axial position or length of the reactor.

2.2.3 Heterogeneous model accounting for both internal diffusion inside and external diffusion around a pellet

Solid phase (catalyst pellet) mass balance[4]:

$$0 = \frac{D_{ei}}{r^2} \frac{d}{dr} \left(r^2 \frac{dC_i^s}{dr} \right) + \rho_s \sum_{j=1}^n v_{ij} r_{cj} + \varepsilon_s \sum_{j=1}^n v_{ij} r_{tj} \quad (7)$$

Solid phase (catalyst pellet) energy balance:

$$0 = \frac{k_e}{r^2} \frac{d}{dr} \left(r^2 \frac{dT^s}{dr} \right) + \sum_{j=1}^n (-\Delta H_{rj}) (\rho_s r_{cj} + \varepsilon_s r_{tj}) \quad (8)$$

The boundary conditions for the pellet:

$$r = 0; \frac{dC_i}{dr} = 0, \frac{dT}{dr} = 0$$

$$r = R; C_i^s = C_{si}, T^s = T_s$$

The above differential equations along with the pellet's BC can be used to calculate the radial concentration and temperature profiles inside the pellet, which also depends on the axial position of the pellet in the reactor.

Gas phase mass balance:

$$\frac{\partial u_s C_i}{\partial z} = k_c a_p (C_i - C_{si}) + \sum \varepsilon_B v_{ij} r_{ti} \quad (9)$$

Gas phase energy balance:

$$u_s \rho_g C_p \frac{\partial T}{\partial z} = h a_p (T - T_s) \quad (10)$$

The boundary conditions at the reactor inlet:

$$z = 0 ; C_i = C_{i0}, T = T_0$$

The above set of differential equations along with the BC can be used to obtain the concentration profile of each species and temperature profile along the axial position or length of the reactor.

2.2.4 Heterogeneous model accounting for both internal diffusion inside and external diffusion around a pellet and mass axial dispersion

Accounting for axial mixing, the steady-state mass balance of gas phase may be written[14]

$$\frac{\partial u_s C_i}{\partial z} = k_c a_p (C_i - C_{si}) + \sum \varepsilon_B v_{ij} r_{ti} + \frac{\partial}{\partial z} (\varepsilon_B D_{ea} \frac{\partial C_i}{\partial z}) \quad (11)$$

The boundary conditions for gas phase:

$$z = 0 ; u_s (C_{i0} - C_i) = -\varepsilon_B D_{ea} \frac{\partial C_i}{\partial z}$$

$$z = L_b ; \frac{\partial C_i}{\partial z} = 0$$

2.2.5 Auxiliary Equations and Correlations

The pressure drop along the axial direction of the catalytic bed is calculated based on the following differential form of the Ergun equation

$$-\frac{dP_t}{dz} = f \frac{u_s G}{d_p} \times \frac{10^{-5}}{3600^2} \quad (12)$$

$$f = \frac{1 - \varepsilon_B}{\varepsilon_B^3} \left[a + \frac{b(1 - \varepsilon_B)}{Re} \right] \quad (13)$$

Here a = 1.75 and b = 150.

The BC at the reactor inlet:

$$P = P_0$$

In addition, some parameters are needed in the heterogeneous models such as film heat and mass transfer coefficients between the gas and solid phases. Similarly, suitable temperature-, pressure- and/or component-dependent correlations are needed to estimate the physical properties of components and mixture such as viscosity, specific heat capacity, thermal conductivity, and diffusion coefficients along the reactor. The relevant correlations are summarized in Table 2.

Table 2 Correlations for model simulation

Correlation	Formula
Viscosity [15] (for H ₂ , H ₂ O)	$\mu = 26.69 \frac{\sqrt{MwT}}{\sigma^2 \Omega_v} \times 10^{-7}$ $H_2: \Omega_v = \Omega_v(\text{Lennard} - \text{Jones})$ $H_2O: \Omega_v = \Omega_v(\text{Lennard} - \text{Jones}) + \frac{0.2\delta^2}{T^*}$ $\Omega_v(\text{Lennard} - \text{Jones}) = \frac{A}{T^*B} + Ce^{-DT^*} + Ee^{-FT^*}$ $T^* = (k/\epsilon) T, A = 1.16145, B = 0.14874, C = 0.52487, D = 0.77320,$ $E = 2.16178, F = 2.43787$
Viscosity [16] (for C ₈ H ₁₀ , C ₈ H ₈ , C ₇ H ₈ , C ₆ H ₆)	$\mu\xi = (4.610T_r^{0.618} - 2.04e^{-0.449T_r} + 1.94e^{-4.058T_r} + 0.1) \times 10^{-7}$ $\xi = T_c^{1/6} Mw^{-1/2} P_c^{-2/3}$
Mixture viscosity [15]	$\mu = \sum_i^n \frac{y_i \mu_i}{\sum_j^n y_j \phi_{ij}}$ $\phi_{ij} = \frac{\left[1 + \left(\frac{\mu_i}{\mu_j} \right)^{\frac{1}{2}} \left(\frac{Mw_j}{Mw_i} \right)^{\frac{1}{4}} \right]^2}{\left[8 \left(1 + \frac{Mw_i}{Mw_j} \right)^{\frac{1}{2}} \right]}$
Binary mass diffusion coefficient i in j [15]	$D_{ij} = \frac{0.00143T^{1.75}}{PM_{ij}^{\frac{1}{2}} \left[(\sum v)_i^{\frac{1}{3}} + (\sum v)_j^{\frac{1}{3}} \right]}$ $M_{ij} = 2 \left[\frac{1}{Mw_i} + \frac{1}{Mw_j} \right]^{-1}$
Mass diffusion coefficient in mixture [17]	$D_{mi} = \frac{1 - y_i}{\sum \frac{y_i}{D_{ij}}}$

Mass transfer coefficient [18]	$k_c = 1.17Re^{-0.42}Sc^{-0.67}u_s$
Thermal conductivity of gas mixture [15]	$k_e = \frac{\sum y_i k_i}{\sum y_i A_{ij}}$ $A_{ij} = \frac{\varepsilon \left[1 + (\lambda_{tri}/\lambda_{trj})^{1/2} / (M_i/M_j)^{1/4} \right]^2}{[8(1 + M_i/M_j)]^{1/2}}$ $\frac{\lambda_{tri}}{\lambda_{trj}} = \frac{\Gamma_j [\exp(0.0464T_{ri}) - \exp(0.2412T_{ri})]}{\Gamma_i [\exp(0.0464T_{rj}) - \exp(0.2412T_{rj})]}$ $\Gamma = 210 \left(\frac{T_c M^3}{P_c^4} \right)^{1/6}$
Heat transfer coefficient [19]	$h = \frac{0.458}{\varepsilon_B} Re^{-0.407} Pr^{-0.67} C_p \rho_g u_s$

The conservation equations of mass, heat and momentum are derived to simulate the concentration, temperature, and pressure profiles along the reactor length and inside catalyst pellets. The models of reactor are convenient to study the effect on products of changes in feed and catalyst, scale up from laboratory to industry scales, optimization of the reactor performance and Interpretations of laboratory measurements.

2.3 Effect of catalyst shape

Catalyst shape should be parametric studies on fixed bed catalytic reactors. Characteristic of catalyst affects on performance of reactor such as diffusion characteristics, pressure drop limitations, catalyst pore size, catalyst loading techniques, and catalytic activity requirements. An appropriate selection of catalyst shape depends on the type of feed and operating conditions in order to optimize catalyst behavior [2]. The effect of catalyst shape is studied by mathematical model.

The iron catalyst is determined the effect of catalyst shape on the reactor for Fischer-Tropsch Synthesis by Kyle M. Brunner et al [3]. There are 4 studied catalyst shape i.e. sphere, cylinder, trilobes, and hollow cylinder. The heterogeneous model accounting for internal mass diffusion is used for simulation reactor and determined the effect of catalyst in term of bed void fraction and effectiveness factor. The correlation developed by Benyahia and O'Neill calculate bed void fraction. The correlation depends on sphericity, ϕ_p .

$$\varepsilon_b = 0.1504 + \frac{0.2024}{\phi_p} + \frac{1.0814}{\left(\frac{d_t}{d_{pe}} + 0.1226\right)^2} \quad (14)$$

Where sphericity is ratio of surface area of sphere of equivalent volume to surface area of catalyst. d_t is diameter of reactor and d_{pe} is equivalent diameter of catalyst.

The effectiveness factor accounts for diffusion within catalyst. It depends on effective diffusion length, L_{pe} , ratio of catalyst volume to surface area.

$$\text{Effectiveness factor} = \eta = \frac{\tanh(\phi)}{\phi} \quad (15)$$

$$\text{Thiele modulus} = \phi = L_{pe} \sqrt{\frac{k_e C_A^n (n+1)}{2D_e C_A}} \quad (16)$$

The performances of reactor which is affected by catalyst shape are required catalyst mass, pressure drop, pore diffusion and heat transfer. Effect on required catalyst mass and reactor length, they decrease with catalyst shape in order sphere > cylinder > hollow cylinder > trilobe. Effect on effectiveness factor, the order of increasing effectiveness factor with shape is sphere < cylinder < hollow cylinder < trilobe. Effect on pressure drop, the pressure drop per length of reactor with respect to shape decreases in order sphere > cylinder > trilobe > hollow cylinder. These results show in Figure 2. These results are agreement with the report about steam reforming catalyst.

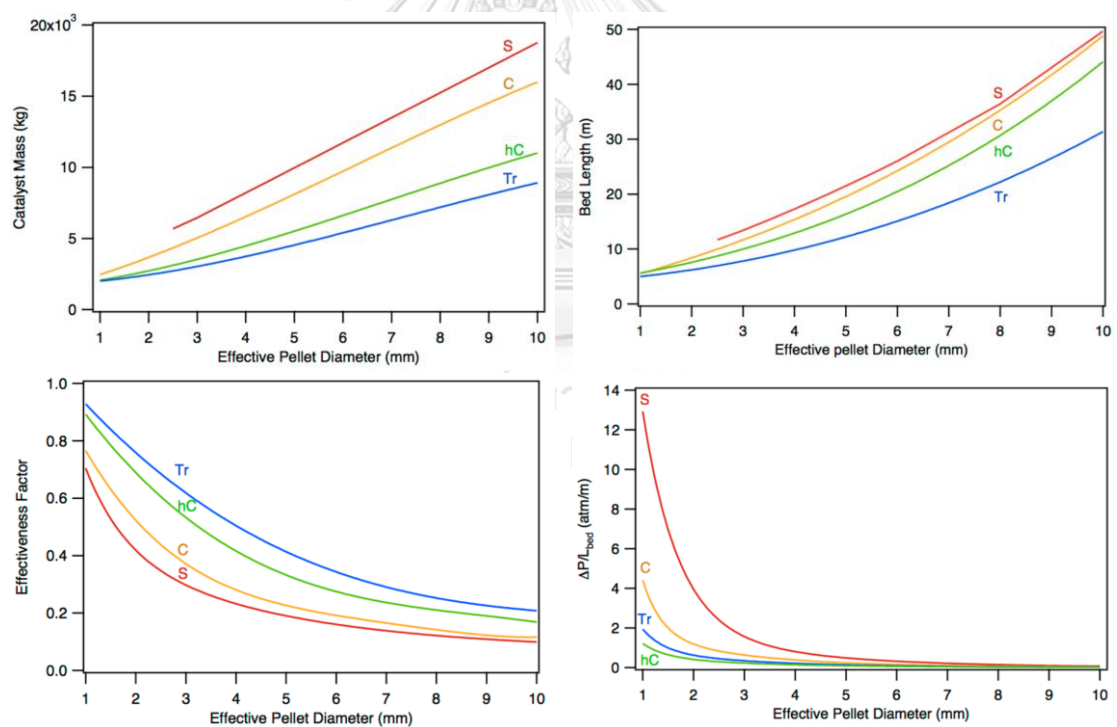


Figure 2 Effect of d_{pe} and shape on required catalyst mass, reactor length, effectiveness factor and pressure drop per bed length [3]

For hydrodesulfurization of gas oil [2], the heterogenous model accounting for internal and external mass transfer is used to study the effect of different particle shapes on catalyst behavior. The effect of shape catalyst is determined in term of bed void fraction, effectiveness factor and thiele modulus. Effect on effectiveness factor increases with catalyst shape in order sphere < pellet < cylinder < 2-lobe < 3-lobe < 4-lobe, show in Figure 3.

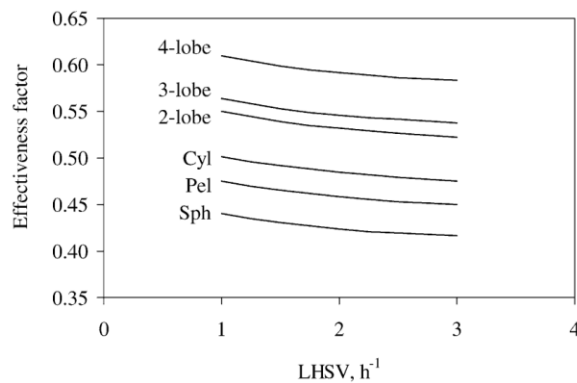


Figure 3 Catalyst effectiveness for different particle shapes [2]

For oxidation of phenol [9]. The model determines the effect of difference catalyst geometry in term of effectiveness factor and thiele modulus. The model results of conversion are compared with experimental data show in Figure 4.

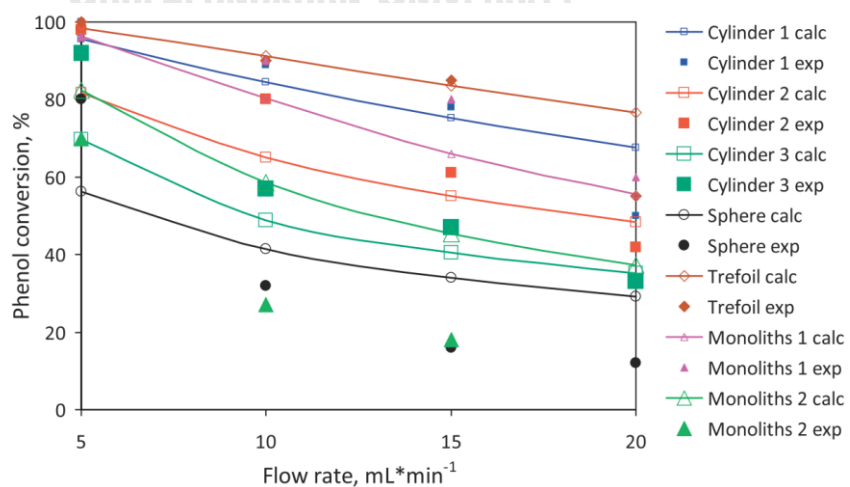


Figure 4 Experimental (points) and calculated (lines) conversions of phenol [9]

From the previous publication [2, 3, 9], the effect of catalyst shape is determined by thiele modulus and effectiveness factor in eq 15-16. The equation is derived from slab balance inside catalyst, the equation of mass balance can be written [4]

$$0 = \frac{d}{dy} \left(D_{ei} \frac{dC_i}{dy} \right) + \rho_s \sum_{j=1}^n v_{ij} r_{cj} + \varepsilon_s \sum_{j=1}^n v_{ij} r_{tj} \quad (17)$$

The boundary conditions for the pellet:

$$y = 0; \frac{dC_i}{dy} = 0$$

$$y = L; C_i^s = C_{si}$$

For generalized modulus, L is the ratio of catalyst volume to surface area, called effective diffusion length.

2.4 Ethylbenzene dehydrogenation to styrene process

There are many researches about modeling of dehydrogenation ethylbenzene to styrene. Sheel and Crowe (1969) [20] are first who reported modeling of an industrial styrene reactor. They employed six reactions with a pseudo homogeneous model for modeling adiabatic reactor. Clough et al (1976) [21] developed model for a styrene pilot plant reactor by the kinetic reaction of Sheel and Crowe and optimized the location of steam injection. Sheppard et al. (1986) [22] developed the model using various kinetic and fitted the result with plant data. The fitted kinetic is used to simulate industrial reactor and economic analysis. Elnashaie et al. (1993) [23] developed a heterogeneous model for internal diffusion and reaction in the catalyst pellet. This model was used to extract intrinsic kinetic parameter from industrial reactor. Elnashaie and Elshishini (1994) [24] developed both pseudohomogeneous and heterogeneous models for simulating an industrial styrene reactor. Both works used the kinetic reaction by Sheel and Crowe. Elnashaie et al. (2001) [25] used the intrinsic kinetic to simulate reactor for different configuration namely fixed bed with/without membrane and fluidized bed with/without membrane. The kinetic reaction by Sheel and Crowe is used for modeling reactor to optimize in various publication i.e. the publication by Yue Li et al (2003) [26], B.V. Babu et al (2005) [27], Ashish M. Gujarathi and B.V. Babu (2010) [28], and Salim et al. (2012) [29].

Lee (2008) [10] makes a detail study for reaction kinetic, design and simulation of industrial ethylbenzene dehydrogenation reactor. Kinetic experiments are carried out using a commercial potassium-promoted iron catalyst and fitted the experimental data for kinetic parameter. He used intrinsic kinetic parameters with the heterogeneous fixed bed reactor model which accounts for the diffusional limitations inside the porous catalyst.

The catalyst for ethylbenzene dehydrogenation to styrene in commercial is extrude catalyst. [30] The shapes of the catalyst are various form example of cylindrical and trilobe. [31]

The dehydrogenation of ethylbenzene to styrene occurs simultaneously via thermal and catalytic reactions. Relying on free radical mechanisms, thermal reactions are important only in the zone without catalyst and in the void of the catalyst bed. They, however, give low thermal conversions. Catalytic reaction is more active and can be represented by Hougen-Watson type kinetic model, which accounts for the adsorption of reactants on the active sites, surface reaction and desorption of resulting products. The published reaction scheme and reaction rate expressions are summarized in Table 3. Subscripts 1 to 4 stand for the respective listed reactions.

Table 3 Reaction scheme and expressions of thermal, catalytic reaction rates [10]

Reaction	Thermal reaction rate	Catalytic reaction rate
$C_8H_{10} \leftrightarrow C_8H_8 + H_2$	$r_{t1} = k_{t1} \left(P_{EB} - \frac{P_{ST} P_{H_2}}{K_{eq}} \right)$	$r_{c1} = \frac{k_1 K_{EB} (P_{EB} - P_{ST} P_{H_2} / K_{eq})}{(1 + K_{EB} P_{EB} + K_{H_2} P_{H_2} + K_{ST} P_{ST})^2}$
$C_8H_{10} \rightarrow C_6H_6 + C_2H_4$	$r_{t2} = k_{t2} P_{EB}$	$r_{c2} = \frac{k_2 K_{EB} P_{EB}}{(1 + K_{EB} P_{EB} + K_{H_2} P_{H_2} + K_{ST} P_{ST})^2}$
$C_8H_{10} + H_2 \rightarrow C_7H_8 + CH_4$	$r_{t3} = k_{t3} P_{EB}$	$r_{c3} = \frac{k_3 K_{EB} P_{EB} K_{H_2} P_{H_2}}{(1 + K_{EB} P_{EB} + K_{H_2} P_{H_2} + K_{ST} P_{ST})^2}$
$C_8H_8 + H_2 \rightarrow C_7H_8 + CH_4$	-	$r_{c4} = \frac{k_4 K_{ST} P_{ST} K_{H_2} P_{H_2}}{(1 + K_{EB} P_{EB} + K_{H_2} P_{H_2} + K_{ST} P_{ST})^2}$

The kinetic parameters for thermal and catalytic reactions are shown in Table 4 and the adsorption equilibrium constants in Table 5.

Table 4 Reaction rate constants [10]

$k_j = A_j \exp\left(-\frac{E_j \times 10^3}{R_g T}\right)$	A_j	E_j
k_{t1}	2.2215×10^{16}	272.23
k_{t2}	2.4217×10^{20}	352.79
k_{t3}	3.8224×10^{17}	313.06
k_1	4.594×10^9	175.38
k_2	1.060×10^{15}	296.29
k_3	1.246×10^{26}	474.76
k_4	8.024×10^{10}	213.78

Table 5 Adsorption equilibrium constants [10]

$K_i = A_i \exp\left(-\frac{\Delta H_i \times 10^3}{R_g T}\right)$	A_i	ΔH_i
K_{EB}	1.014×10^{-5}	-102.22
K_{ST}	2.678×10^{-5}	-104.56
K_{H2}	4.519×10^{-7}	-117.95

The catalyst properties, operating conditions and reactor dimensions used in the simulation are summarized in Table 6.

Table 6 Catalyst properties, operating conditions and reactor dimensions [10]

Parameter	Value
Catalyst properties	
Catalyst bulk density [kgcat/m ³]	1422
Catalyst pellet density [kgcat/m ³]	2500
Void fraction of the bed	0.4312
Catalyst Internal void fraction	0.4
Tortuosity of the catalyst	3
Catalyst equivalent pellet diameter [m]	0.0055
Feed conditions (after mixing fresh and recycled streams)	
Feed molar flow rate [kmol/h]	
Ethylbenzene	707
Styrene	7.104
Benzene	0.293
Toluene	4.968
Steam	7777
Total feed molar flow rate [kmol/h]	8496.37
Temperature [K]	886
Pressure [bar]	1.25
Reactor dimensions	
Inner radius of reactor [m]	3.5
Length of bed [m]	1.33

The industrial styrene reactor simulation result using the pseudohomogeneous model together with the intrinsic kinetic parameters is shown in Table 7.

Table 7 Simulation result of a 3-bed adiabatic reactor by pseudohomogeneous model [10]

	BED1	BED2	BED3
Weight of catalyst, kg *	72 950	82 020	78 330
Space time §	103.18	219.19	329.98
X_{EB} , % ¶	39.25	68.64	86.82
S_{ST} , % ¶	98.84	96.09	91.43
S_{BZ} , %	0.94	1.34	1.67
S_{TO} , %	0.23	2.58	6.90
P_{in} , bar ³	1.25	1.066	0.787
T_{in} , K ³	886	898.2	897.6
T_{out} , K	806.2	843.6	873.7



The industrial styrene reactor simulation result using the heterogeneous model accounting for internal diffusion is shown in Table 8.

Table 8 Simulation result of a 3-bed adiabatic reactor by heterogeneous model [10]

	BED1	BED2	BED3
Weight of catalyst, kg *	72 950	82 020	78 330
Space time §	103.18	219.19	329.98
X_{EB} , % ¶	36.89	65.78	83.76
S_{ST} , % ¶	98.49	95.10	90.43
S_{BZ} , %	1.000	1.423	1.754
S_{TO} , %	0.507	3.480	7.809
P_{in} , bar *	1.25	1.06	0.783
T_{in} , K *	886	898.2	897.6
T_{out} , K	811.36	845.71	873.6

Compare the simulation result using heterogeneous model to using pseudohomogeneous model, the conversion of ethylbenzene and selectivity of styrene is decrease show in Figure 5.

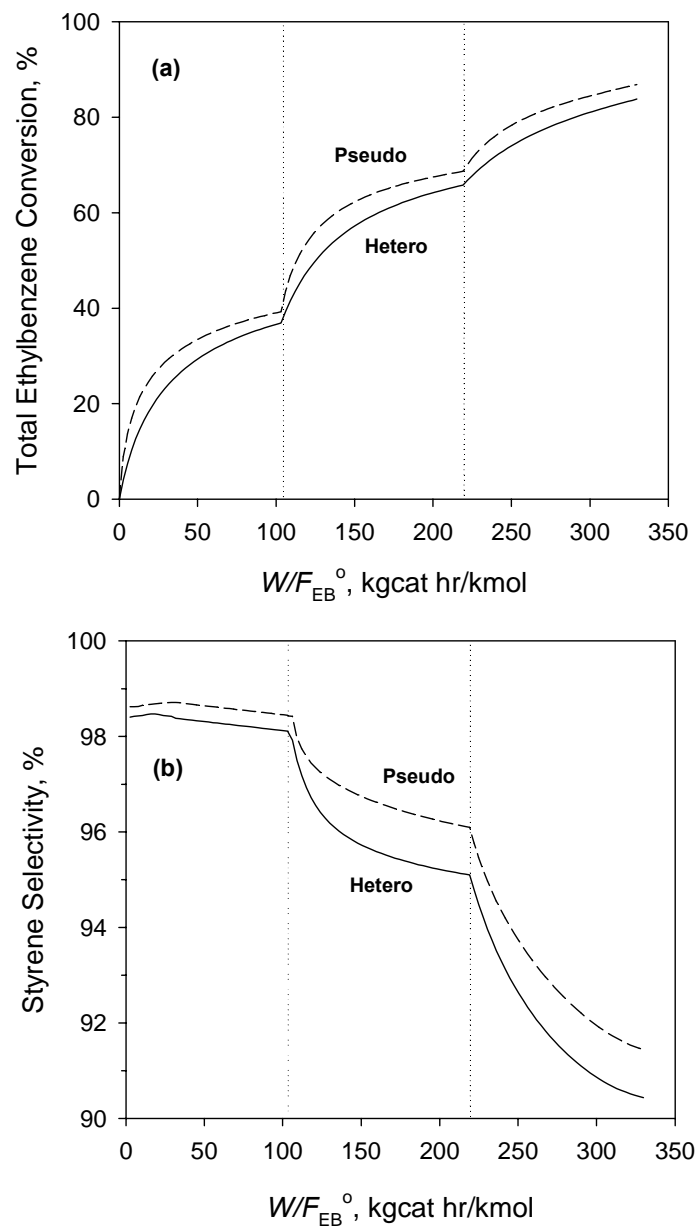


Figure 5 Comparison of simulated total ethylbenzene conversion profiles (a) and styrene selectivity profiles (b) in a 3-bed adiabatic reactor between the heterogeneous model and the pseudohomogeneous model [10]

Chapter 3 Methodology

This research applies the EQUATRAN program to solving the set of differential equation in mathematical model. This methodology in this research is divided to 3 section, there are

3.1 Validation

First, the kinetic parameters of catalytic reaction are estimated by the mathematic model from the experimental data of the literature [32]. The kinetic parameters were obtained by minimize the sum squares of difference between predicted and experimental conversions. The estimates kinetic parameters are used to predict conversions and the results are compared with experimental data.

3.2 Developed model

The mathematic model will be developed models which account for internal mass and heat transfer, external mass and heat transfer and axial dispersion by using the industrial reactor data which is reported by literature review including catalyst properties, operating conditions and reactor dimensions, as shown in Table 6

3.2.1 Pseudohomogeneous model (Model1)

The pseudohomogeneous model is a simple model. The concentration and temperature gradients only occur in axial direction for gas phase which is plug flow. The steady state equations of mass and energy balance are

Mass balance:

$$\frac{du_s C_i}{dz} = \sum \rho_B v_{ij} r_{c_j} + \sum \varepsilon_B v_{ij} r_{t_j}$$

Boundary condition $z = 0 ; C_i = C_{i0}$

Energy balance:

$$\sum_{i=1}^6 \frac{\dot{m}_i C_{pi}}{A_c} \frac{dT}{dz} = \sum_{i=1}^4 (-\Delta H_{rj})(r_{cj} \rho_B + r_{tj} \varepsilon_B)$$

$$\text{Boundary condition } z = 0 ; T = T_0$$

3.2.2 Heterogeneous model accounting for internal diffusion (Model2)

Heterogeneous model accounting for internal diffusion considers the concentration gradient inside catalyst due to internal mass transfer. While concentration gradient between fluid and catalyst surface is neglected. Temperature gradient inside catalyst is also neglected. The flow is plug flow. The balance equations are separate for solid phase and gas phase. The steady state equations of mass balance inside spherical catalyst which account for reaction and internal transfer are

$$0 = \frac{D_{ei}}{r^2} \frac{d}{dr} \left(r^2 \frac{dC_i^s}{dr} \right) + \rho_s \sum_{j=1}^n v_{ij} r_{cj} + \varepsilon_s \sum_{j=1}^n v_{ij} r_{tj}$$

$$\text{Boundary conditions } r = 0 ; \frac{dC_i^s}{dr} = 0$$

$$r = R ; C_i^s = C_i$$

Intrinsic reaction and internal transport throughout catalyst are integrated and led to calculate effectiveness factor. Since the effectiveness factor varies along the reactor length, it is calculated at each integration step.

$$\eta_j = \frac{\int_0^V [r_{cj}(P_{s,i}) \rho_s + r_{tj}(P_{s,i}) \varepsilon_s] dV}{[r_{cj}(P_i) \rho_s + r_{tj}(P_i) \varepsilon_s] V}$$

The steady state mass and energy balance equations along the reactor are

$$\frac{du_s C_i}{dz} = \sum \rho_B \eta_j v_{ij} r_{cj} + \sum \varepsilon_B v_{ij} r_{tj}$$

Boundary condition $z = 0 ; C_i = C_{i0}$

$$\sum_{i=1}^6 \frac{\dot{m}_i C_{pi}}{A_c} \frac{dT}{dz} = \sum_{i=1}^4 (-\Delta H_{rj}) (\eta_j r_{cj} \rho_B + r_{tj} \varepsilon_B)$$

Boundary condition $z = 0 ; T = T_0$

3.2.3 Heterogeneous model accounting for internal mass and heat transfer

(Model3)

Heterogeneous model accounting for internal mass and heat transfer considers the gradients of both concentration and temperature inside catalyst. The flow is plug flow. The external transfer is neglected. The steady state mass and energy balance equations are

Mass balance:

Solid phase (spherical catalyst)

$$0 = \frac{D_{ei}}{r^2} \frac{d}{dr} \left(r^2 \frac{dC_i^s}{dr} \right) + \rho_s \sum_{j=1}^n v_{ij} r_{cj} + \varepsilon_s \sum_{j=1}^n v_{ij} r_{tj}$$

Boundary conditions $r = 0 ; \frac{dC_i^s}{dr} = 0$

$$r = R ; C_i^s = C_i$$

$$\eta_j = \frac{\int_0^V [r_{cj}(P_{s,i}) \rho_s + r_{tj}(P_{s,i}) \varepsilon_s] dV}{[r_{cj}(P_i) \rho_s + r_{tj}(P_i) \varepsilon_s] V}$$

Gas phase

$$\frac{du_s C_i}{dz} = \sum \rho_B \eta_j v_{ij} r_{cj} + \sum \varepsilon_B v_{ij} r_{tj}$$

Boundary condition $z = 0 ; C_i = C_{i0}$

Energy balance

Solid phase (spherical catalyst)

$$0 = \frac{k_e}{r^2} \frac{d}{dr} \left(r^2 \frac{dT^s}{dr} \right) + \sum_{j=1}^n (-\Delta H_{rj}) (\rho_s r_{cj} + \varepsilon_s r_{tj})$$

$$\text{Boundary conditions } r = 0; \frac{dT}{dr} = 0$$

$$r = R; T^s = T_s$$

Gas phase

$$\sum_{i=1}^6 \frac{\dot{m}_i C_{pi}}{A_c} \frac{dT}{dz} = \sum_{i=1}^4 (-\Delta H_{rj}) (\eta_j r_{cj} \rho_B + r_{tj} \varepsilon_B)$$

$$\text{Boundary condition } z = 0; T = T_0$$

3.2.4 Heterogeneous model accounting for internal mass and heat transfer and external mass and heat transfer (Model4)

Heterogeneous model accounting for internal mass and heat transfer and external mass and heat transfer considers the gradients both inside catalyst and between bulk gas and catalyst surface. The flow is plug flow. The steady state mass and energy balance equations are

Mass balance:

Solid phase (spherical catalyst)

$$0 = \frac{D_{ei}}{r^2} \frac{d}{dr} \left(r^2 \frac{dC_i^s}{dr} \right) + \rho_s \sum_{j=1}^n v_{ij} r_{cj} + \varepsilon_s \sum_{j=1}^n v_{ij} r_{tj}$$

$$\text{Boundary conditions } r = 0; \frac{dC_i}{dr} = 0$$

$$r = R; C_i^s = C_{si}$$

Gas phase

$$\frac{\partial u_s C_i}{\partial z} = k_c a_p (C_i - C_{si}) + \sum \varepsilon_B v_{ij} r_{ti}$$

Boundary condition $z = 0 ; C_i = C_{i0}$

Energy balance

Solid phase (spherical catalyst)

$$0 = \frac{k_e}{r^2} \frac{d}{dr} \left(r^2 \frac{dT^s}{dr} \right) + \sum_{j=1}^n (-\Delta H_{rj}) (\rho_s r_{cj} + \varepsilon_s r_{tj})$$

Boundary conditions $r = 0 ; \frac{dT}{dr} = 0$
 $r = R ; T^s = T_s$

Gas phase

$$u_s \rho_g C_p \frac{\partial T}{\partial z} = h a_p (T - T_s)$$

Boundary condition $z = 0 ; T = T_0$

3.2.5 Heterogeneous model accounting for internal mass and heat transfer and mass axial dispersion. (Model5)

Accounting for axial mixing, the steady state equations are written

Mass balance:

Solid phase (spherical catalyst)

$$0 = \frac{D_{ei}}{r^2} \frac{d}{dr} \left(r^2 \frac{dC_i^s}{dr} \right) + \rho_s \sum_{j=1}^n v_{ij} r_{cj} + \varepsilon_s \sum_{j=1}^n v_{ij} r_{tj}$$

Boundary conditions $r = 0 ; \frac{dC_i^s}{dr} = 0$
 $r = R ; C_i^s = C_i$

$$\eta_j = \frac{\int_0^V [r_{cj}(P_{s,i})\rho_s + r_{tj}(P_{s,i})\varepsilon_s] dV}{[r_{cj}(P_i)\rho_s + r_{tj}(P_i)\varepsilon_s]V}$$

Gas phase

$$\frac{du_s C_i}{dz} = \sum \rho_B \eta_j v_{ij} r_{cj} + \sum \varepsilon_B v_{ij} r_{tj} + \frac{\partial}{\partial z} (\varepsilon_B D_{ea} \frac{\partial C_i}{\partial z})$$

Boundary conditions $z = 0$; $u_s(C_{i0} - C_i) = -\varepsilon_B D_{ea} \frac{\partial C_i}{\partial z}$

$$z = L_b ; \frac{\partial C_i}{\partial z} = 0$$

Energy balance

Solid phase (spherical catalyst)

$$0 = \frac{k_e}{r^2} \frac{d}{dr} \left(r^2 \frac{dT^s}{dr} \right) + \sum_{j=1}^n (-\Delta H_{rj}) (\rho_s r_{cj} + \varepsilon_s r_{tj})$$

Boundary conditions $r = 0$; $\frac{dT}{dr} = 0$

$$r = R ; T^s = T_s$$

Gas phase

$$\sum_{i=1}^6 \frac{\dot{m}_i C_{pi}}{A_c} \frac{dT}{dz} = \sum_{i=1}^4 (-\Delta H_{rj}) (\eta_j r_{cj} \rho_B + r_{tj} \varepsilon_B)$$

Boundary condition $z = 0$; $T = T_0$

3.2.6 Heterogeneous model accounting for internal mass and heat transfer, external mass and heat transfer and mass axial dispersion. (Model6)

Mass balance

Solid phase (spherical catalyst)

$$0 = \frac{D_{ei}}{r^2} \frac{d}{dr} \left(r^2 \frac{dC_i^s}{dr} \right) + \rho_s \sum_{j=1}^n v_{ij} r_{cj} + \varepsilon_s \sum_{j=1}^n v_{ij} r_{tj}$$

$$\text{Boundary conditions } r = 0; \frac{dC_i}{dr} = 0,$$

$$r = R; C_i^s = C_{si},$$

Gas phase

$$\frac{\partial u_s C_i}{\partial z} = k_c a_p (C_i - C_{si}) + \sum \varepsilon_B v_{ij} r_{ti} + \frac{\partial}{\partial z} (\varepsilon_B D_{ea} \frac{\partial C_i}{\partial z})$$

$$\text{Boundary conditions } z = 0; u_s (C_{i0} - C_i) = -\varepsilon_B D_{ea} \frac{\partial C_i}{\partial z}$$

$$z = L_b; \frac{\partial C_i}{\partial z} = 0$$

Energy balance

Solid phase (spherical catalyst)

$$0 = \frac{k_e}{r^2} \frac{d}{dr} \left(r^2 \frac{dT^s}{dr} \right) + \sum_{j=1}^n (-\Delta H_{rj}) (\rho_s r_{cj} + \varepsilon_s r_{tj})$$

$$\text{Boundary conditions } r = 0; \frac{dT}{dr} = 0$$

$$r = R; T^s = T_s$$

Gas phase

$$u_s \rho_g C_p \frac{\partial T}{\partial z} = h a_p (T - T_s)$$

$$\text{Boundary condition } z = 0; T = T_0$$

3.3 Determine the effect of catalyst

After the models are developed, the developed models are used to determine the effect of shape catalyst on performance reactor which are amount of required catalyst mass and reactor length. Finally, the results from each developed model are compared.

The effect of catalyst is determined in term of volume of catalyst, surface of catalyst, and bed porosity. From the previous publications which studied effect of catalyst shape, the effect of catalyst shape is determined in term effectiveness factor and thiele modulus that are derived from slab balance. Therefore, the developed model determined inside catalyst by slab balance. The steady state equations can be written

Mass balance:

$$0 = \frac{d}{dy} \left[D_{ei} \frac{dC_i}{dy} \right] + \rho_s \sum_{j=1}^n v_{ij} r_{cj} + \varepsilon_s \sum_{j=1}^n v_{ij} r_{tj}$$

$$\text{Boundary conditions } y = 0; \frac{dC_i}{dy} = 0$$

$$y = L; C_i^s = C_{si}$$

Energy balance:

$$0 = \frac{d}{dy} \left(k_e \frac{dT^s}{dy} \right) + \sum_{j=1}^n (-\Delta H_{rj}) (\rho_s r_{cj} + \varepsilon_s r_{tj})$$

$$\text{Boundary conditions } y = 0; \frac{dT}{dy} = 0$$

$$y = L; T^s = T_s$$

The catalyst shapes are determined including sphere, cylinder and trilobe, as shown in Figure 6. First study the effect, the catalyst size of all shape is same as

0.0055 mm effective diameter which is the diameter of a sphere having same catalyst volume as the actual catalyst.

Next the real catalyst size of each shape is determined the effect on performance reactor, as shown in Table 9.

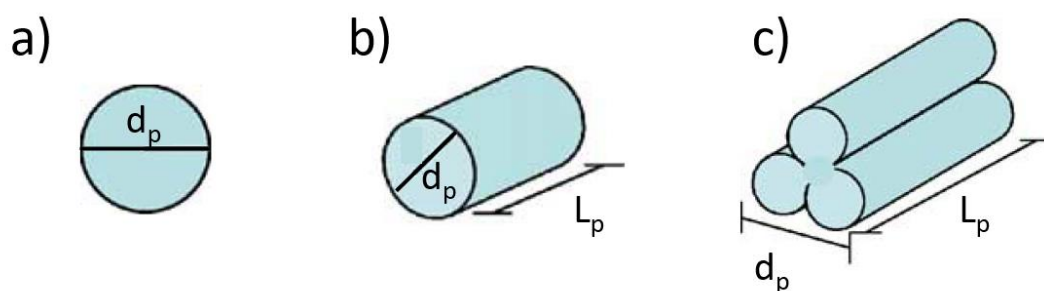


Figure 6 Catalyst shape used in the model: a) spheres, b) cylinders, and c) trilobes

Table 9 Geometry and properties of commercial catalyst in each shape

Properties	Sphere	Cylinder	Trilobe
Diameter of catalyst (D_p) [m]	5.50E-03	3.50E-03	5.00E-03
Length of catalyst (L_p) [m]	-	5.00E-03	5.00E-03

Chapter 4 Result and discussion

4.1 Developed model of fixed bed reactor for dehydrogenation ethylbenzene to styrene

4.1.1 Validate simulation result of model with publication

From the experimental data [32], the kinetic rate parameters were obtained by using the Marquardt method to minimize the sum of squares of difference between predicted and actual conversions provided in EQUATRAN software. Table 10 shows the estimates kinetic parameters for catalytic reaction rate. Figure 7 shows comparison of conversion of experimental data and calculated using estimated kinetic parameters and they are good the fit of experimental data.

Table 10 Value of estimated kinetic parameters of catalytic reaction rate

Parameter	unit	Value
A_1	kmol/(kgcat·hr)	2.33E+11
A_2	kmol/(kgcat·hr)	2.65E+16
A_3	kmol/(kgcat·hr)	9.01E+15
A_4	kmol/(kgcat·hr)	8.54E+17
A_{eb}	1/bar	2.55E-10
A_{st}	1/bar	2.26E-06
A_{h2}	1/bar	3.93E-09
E_1	kJ/mol	204.66
E_2	kJ/mol	320.35
E_3	kJ/mol	320.97
E_4	kJ/mol	333.48
H_{eb}	kJ/mol	-180.51
H_{st}	kJ/mol	-122.26
H_{h2}	kJ/mol	-152.11

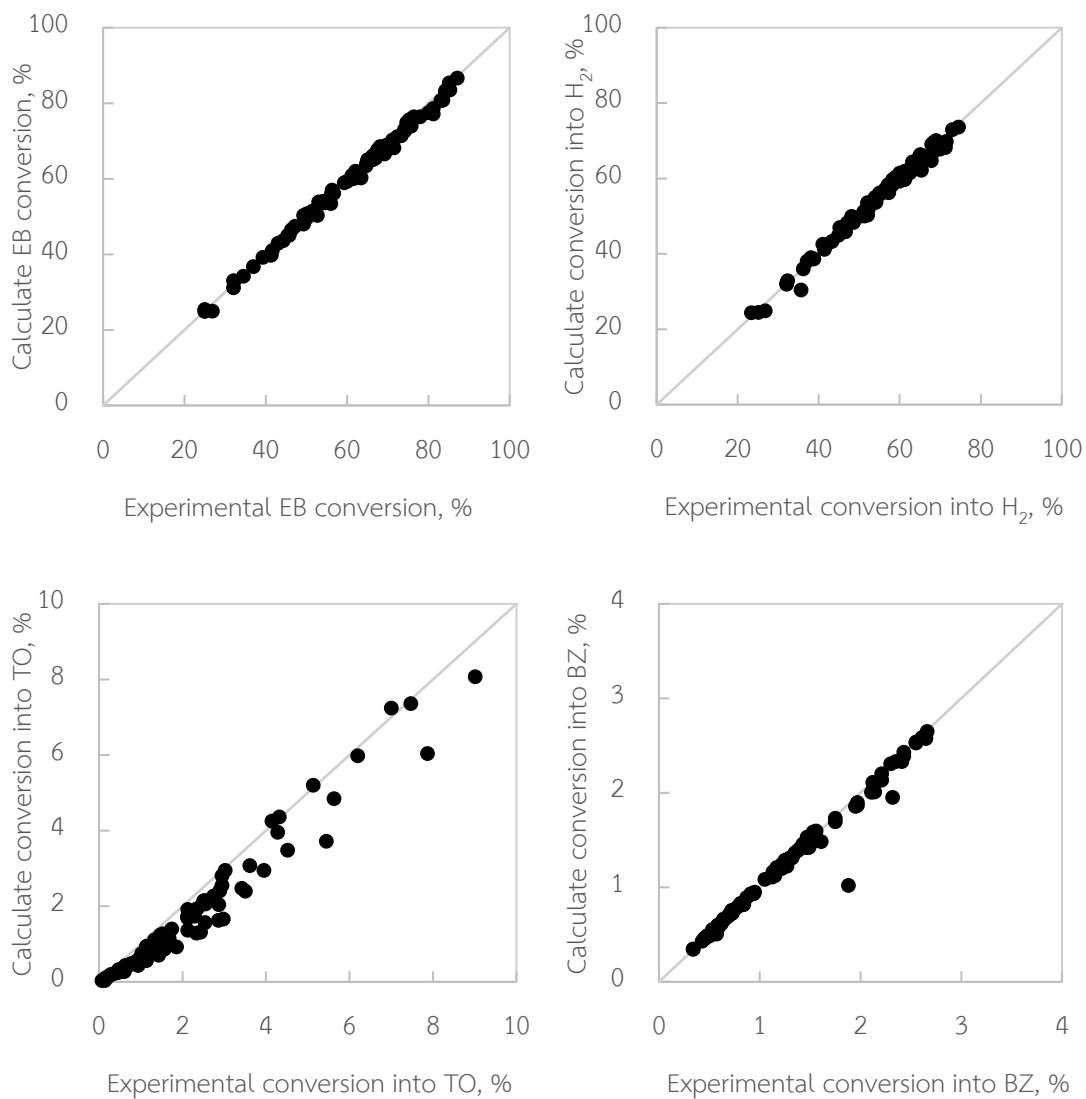


Figure 7 Comparison of experimental and calculated conversions for ethylbenzene (EB), hydrogen (H_2), toluene (TO), and benzene (BZ) at all reaction conditions.

4.1.2 Developed models of fixed bed reactor for dehydrogenation ethylbenzene to styrene

The mathematic models are developed into varied forms. Firstly, the reactor performance is predicted by pseudohomogeneous model (Model1) and heterogeneous model with internal mass transfer (Model2). More realistic heterogeneous model (Model3) accounts for internal both mass and heat transfer. And more complex heterogeneous model (Model4) accounts for both internal and external transfer of mass and heat. Heterogeneous model (Model5) accounts for internal mass and heat transfer and mass axial dispersion. The latest heterogeneous model (Model6) accounts for internal mass and heat transfer, external mass and heat transfer and mass axial dispersion. The whole set of mass, energy and momentum balance equations are numerically integrated for the commercial adiabatic reactor using the 4-th Runge-Katta method with variable step size provided in EQUATRAN software for plug flow model (Model1, Model2, Model3, and Model4) while using the trapezoid method for dispersion model (Model5 and Model6). The operating condition and reactor geometry are shown in Table 6, which are identical to every model. The simulations results are shown in Table 11.

Table 11 Simulation result of reactor by difference model forms

Output	Model1	Model2	Model3	Model4	Model5	Model6
X_{EB} [%]	36.52	34.49	34.49	34.46	34.46	34.46
S_{ST} [%]	98.34	97.90	97.90	97.88	97.78	97.99
S_{BZ} [%]	1.06	1.13	1.13	1.13	1.17	1.17
S_{TO} [%]	0.61	0.97	0.97	0.99	0.95	0.98
P_{out} [bar]	1.05	1.04	1.04	1.04	1.04	1.04
T_{out} [K]	822.57	826.44	826.45	826.63	826.08	826.43

The pseudohomogeneous model (Model1) does not account for the role of internal and external transfer. The simulation results using Model1, the ethylbenzene conversion and styrene selectivity at the outlet of the reactor are 36.52% and 98.34%. More complex models are developed to account for the effect of more phenomena occurred in the reactor including internal transfer, external transfer, and mass axial dispersion.

4.1.2.1 Heterogeneous model accounting for internal mass transfer

The heterogeneous model accounts for internal mass transfer (Model2), the simulation results are 34.49% of ethylbenzene conversion and 97.90% of styrene selectivity. Compared to the simulation results using the model1, the ethylbenzene conversion and styrene selectivity decrease. This shows that the internal mass transfer affects on reactor performance. The decrease of ethylbenzene conversion can be explained by the effectiveness factor. The effectiveness factor of reaction 1 dehydrogenation ethylbenzene to styrene, the main reaction, shows in Figure 8, the effectiveness factors are smaller than unity, which means that the internal mass diffusion limits the overall reaction rate[11]. The effectiveness factor gradually increases along the reactor length as the reaction rate decreases. At the inlet of reactor, the temperature is high, so the reaction rate is high. While at the outlet of reactor, the temperature decreases, the reaction rate is slower, therefore, the difference of mass diffusion and reaction rate is lower, as show in Figure 9. The effect of mass diffusion decreases result in increase the effectiveness factor.

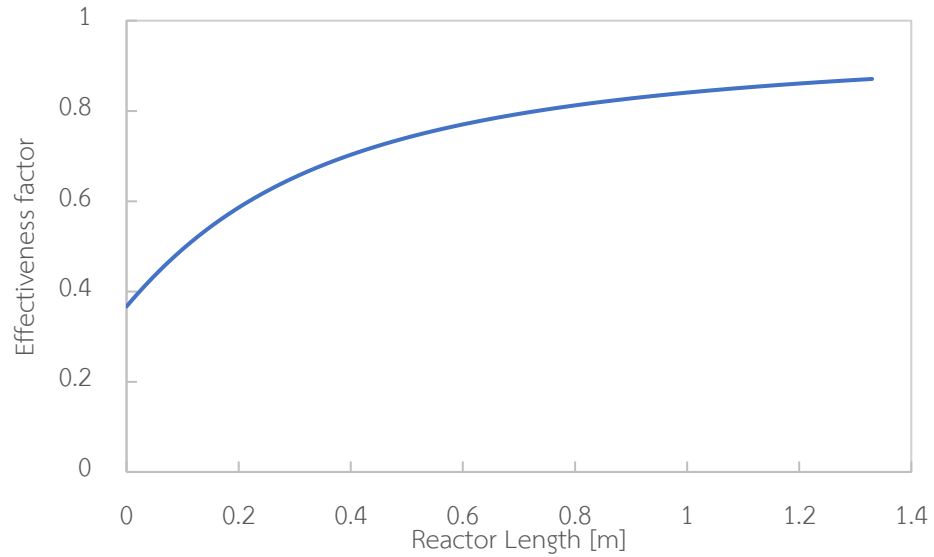


Figure 8 Effectiveness factor of main reaction along the reactor

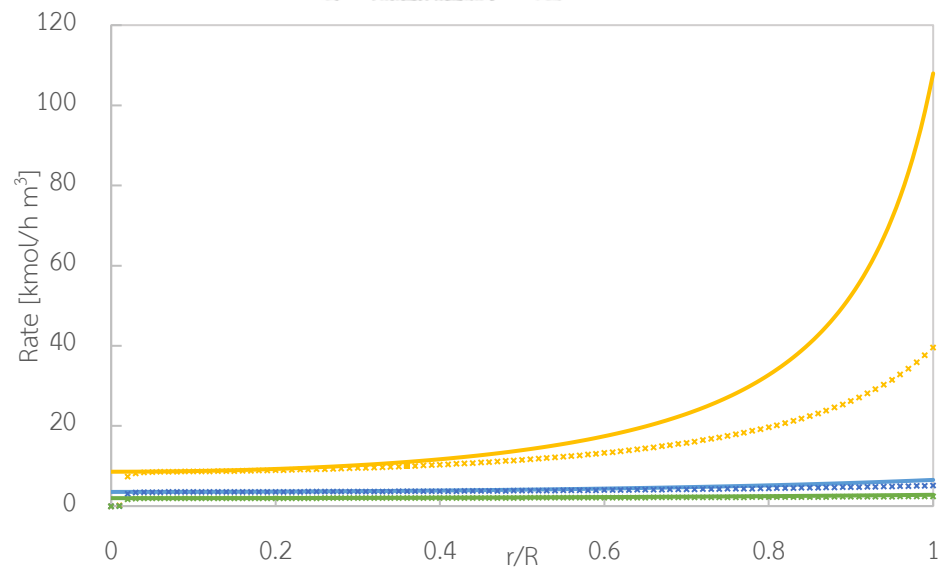


Figure 9 Mass transfer rate (dash line) and reaction rate (symbol line) inside catalyst at different points of the reactor; inlet of reactor (yellow), center of reactor (blue), outlet of reactor (green).

4.1.2.2 Heterogeneous model accounting for internal mass and heat transfer

The heterogeneous model accounts for internal mass and heat transfer (Model3), the simulation results are same the simulation results using the model2. This means that the internal heat transfer dose not affect on the reaction. Figure 10 shows the calculated intrapellet temperature profile. The intrapellet radial temperature profile at the entrance, center, and exit of reactor remains essentially the same because the rate of endothermic heat consumption is equal to the rate of heat conduction into the pellet, as show in following equation.

$$k_e(T_0 - T) = \Delta H \cdot \text{Reaction rate}$$

Because reaction rate inside catalyst must be equal to the rate transfer inside, the equation may be written

$$k_e(T_0 - T) = \Delta H \cdot D_e(C_0 - C)$$

Where T_0 and C_0 are the temperature and concentration at catalyst surface, respectively. From the equation, temperature gradient inside catalyst depends on effective thermal conductivity (k_e). When k_e is high, the temperature gradient is low. Moreover, energy conversion parameter (β) [12], which represents the ratio of maximum temperature difference to external surface temperature, may be written

$$\beta = \frac{(-\Delta H)D_eC_0}{k_eT_0}$$

The value of β may be regard as zero for isothermal catalyst. The value of β for this process is much lower close to zero, so the catalyst is isothermal, as shown in Table 12.

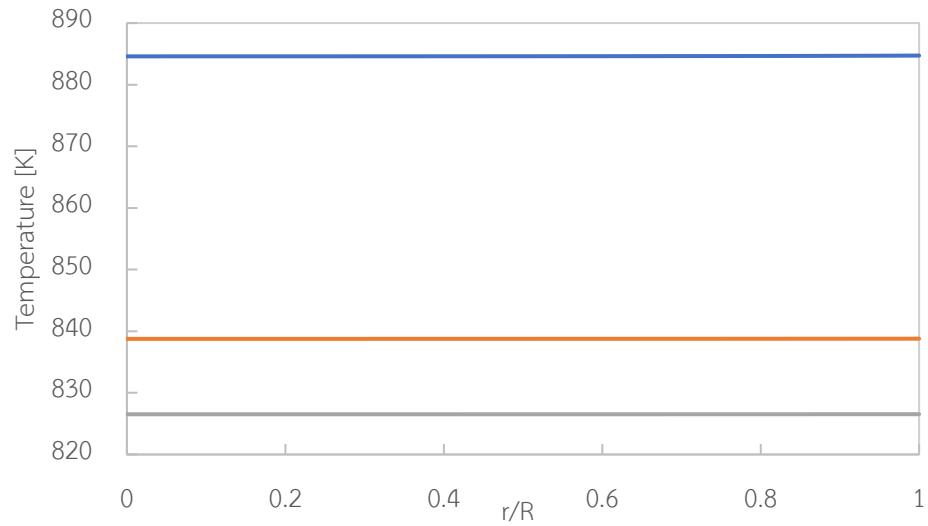


Figure 10 Intrapellet radial temperature profile at different points of the reactor; inlet of reactor(blue), center of reactor (orange), outlet of reactor(grey).

Table 12 The energy conversion parameter (β) of catalytic reaction 1-4 at different points of the reactor

Position	Reaction 1	Reaction 2	Reaction 3	Reaction 4
Inlet of reactor	-1.97E-04	-1.61E-04	1.03E-04	3.32E-06
Center of reactor	-1.56E-04	-1.27E-04	8.04E-05	9.03E-05
Outlet of reactor	-1.42E-04	-1.17E-04	7.33E-05	1.13E-04

4.1.2.3 Heterogenous model accounting for internal and external transportation

The heterogeneous model accounts for both internal and external transfer (Model4), the simulation results are 34.46% of ethylbenzene conversion and 97.88% of styrene selectivity. Compared to the simulation results using the model3, the ethylbenzene conversion and styrene selectivity slightly decrease. The concentration and temperature between bulk of fluid and catalyst surface are slightly different, as shown in Figure 11 and Figure 12. The results show that the external transfer little affect on performance reactor and more effect occur at entrance region. Since the moles of product are more than the moles of reactant in the reaction, the volume of gas increases result in increasing of fluid velocity, as shown in Figure 13. The increasing of fluid velocity increases mass transfer coefficient, as shown in Figure 14, because film around catalyst decreases. Therefore, external transfer decreases the effect on overall reaction.

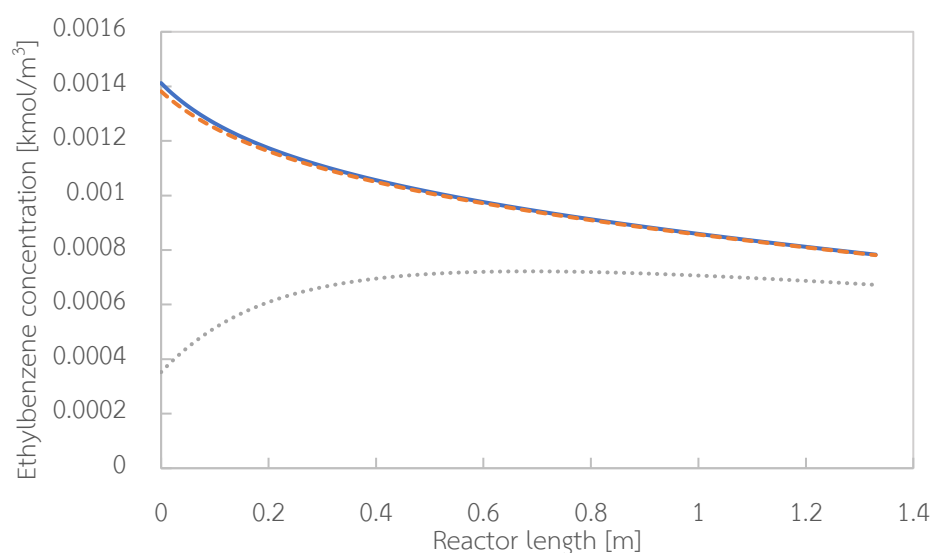


Figure 11 Concentration profile along the reactor at bulk of fluid (blue), surface of catalyst (orange), and center of catalyst (grey)

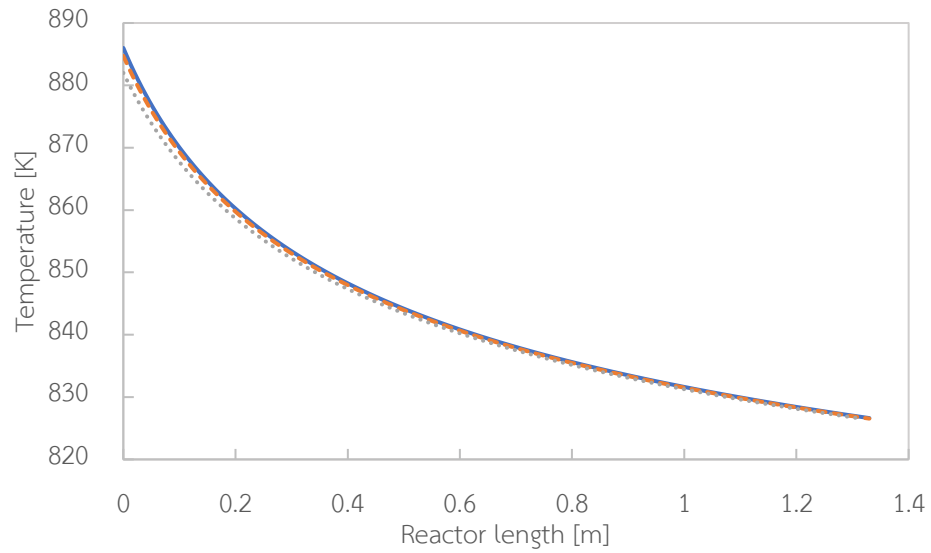


Figure 12 Temperature profile along the reactor at bulk of (blue), surface of catalyst (orange), and center of catalyst (grey)

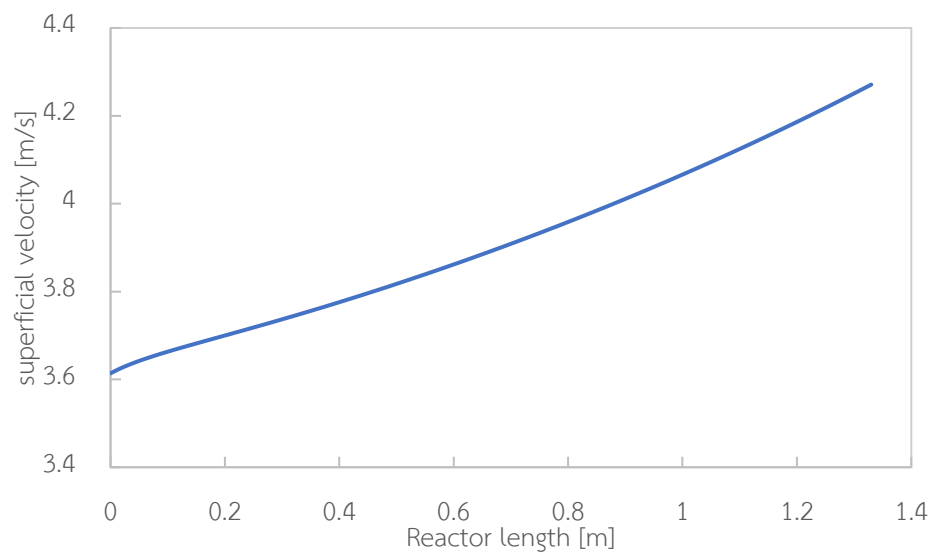


Figure 13 Superficial velocity of fluid along the reactor

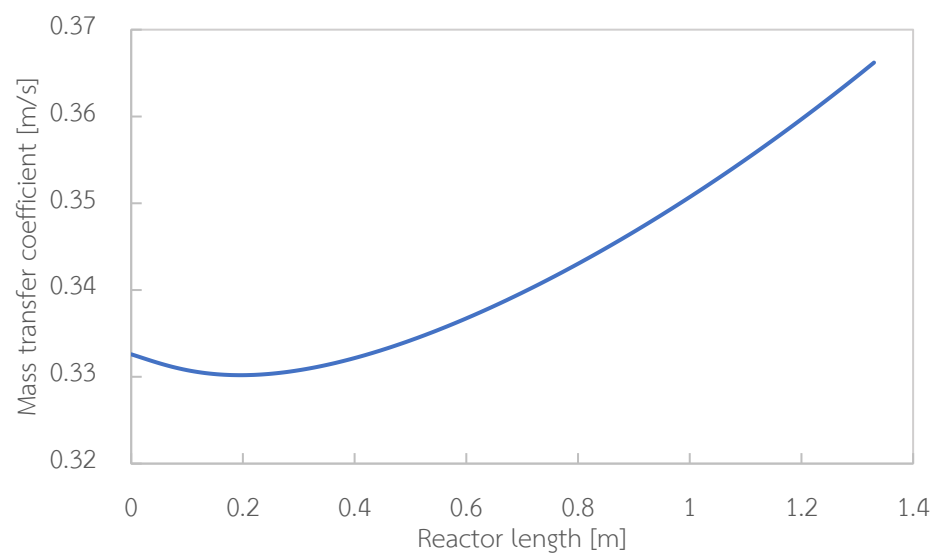


Figure 14 Mass transfer coefficient of ethylbenzene along the reactor



4.1.2.4 Heterogeneous model with axial mixing

The heterogeneous models accounting for internal transfer are compared between plug flow (Model3) and mass dispersion (Model5), the simulation results are little different. The heterogeneous models accounting for internal and external transfer, the comparison between plug flow (Model4) and mass dispersion (Model6) are little different too. The ethylbenzene concentration along the reactor show in Figure 15 and Figure 16 , the concentration of mass dispersion model is little lower than plug flow model. The result shows that mass dispersion little affects on overall reaction rate, therefore, it can be neglect. The little effect of axial dispersion may be occurred due to the reactor length. The effect is determined by value of D_{ea}/uL . When D_{ea}/uL is lower than 0.01, the effect of axial dispersion can be neglected [13]. Figure 17 shows that the effect of axial dispersion decreases when reactor length increases. The deviation from plug flow is occurred by different routes of fluid taking through the reactor that may take different lengths of time to pass through the vessel. The distribution of these times for the stream of fluid leaving the vessel is called the exit age distribution, E [13]. Figure 18 shows that the residence time distribution of process flow is small deviate from plug flow. For plug flow, the material of cross-section area of reactor together flows and does not mix in flow direction result in equal residence time, while material of dispersed flow spread result in difference residence time.

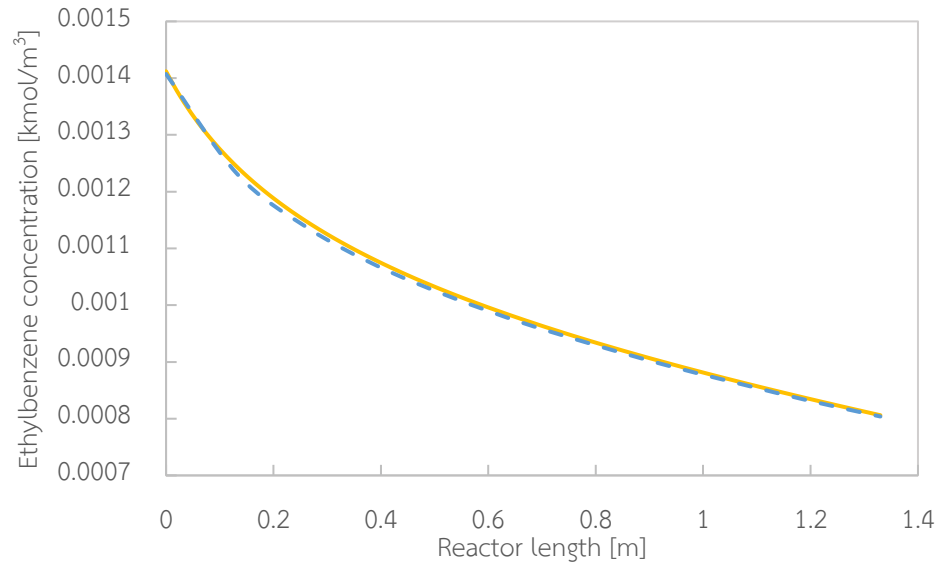


Figure 15 Concentration profile along the reactor by heterogeneous accounting for internal transfer model3 (yellow line) with plug flow and model5 (blue line) with dispersion flow.

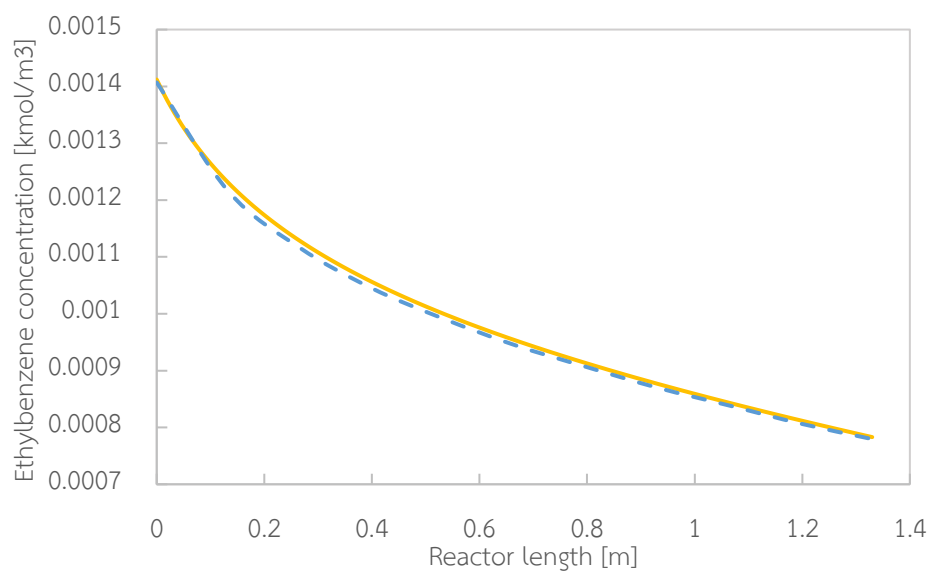


Figure 16 Concentration profile along the reactor by heterogeneous accounting for internal and external transfer model4 (yellow line) with plug flow and model6 (blue line) with dispersion flow.

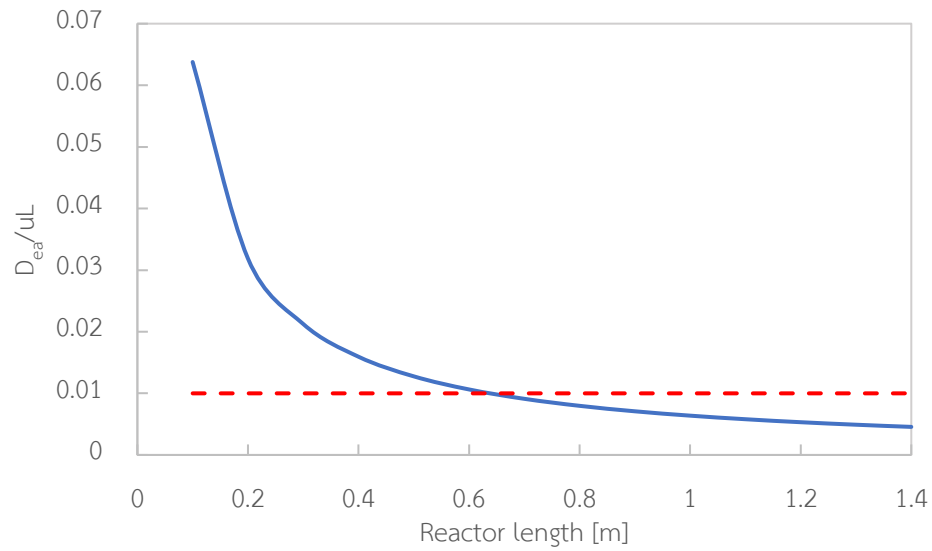


Figure 17 The value of D_{ea}/uL for different length of reactor

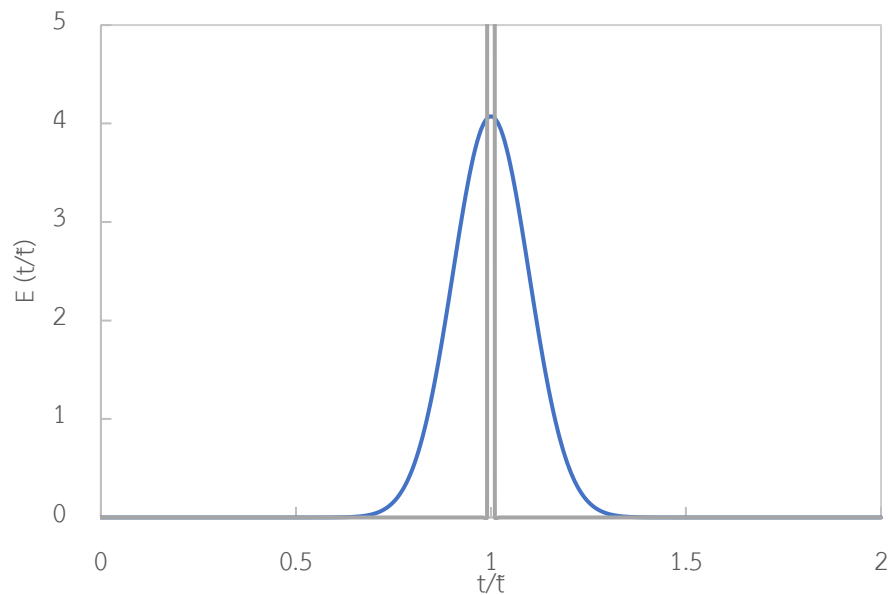


Figure 18 The residence time distribution curve of this process (blue) and plug flow (grey), E is exit age distribution, t is actual residence time and \bar{t} is average residence time.

In response to the differences in ethylbenzene conversion level among the models, the temperature profile of model1 is smallest at the reactor outlet because the main dehydrogenation reaction is endothermic and the conversion of ethylbenzene of model1 is highest. The axial pressure profiles of the models are essentially the same because the feed stream contains more than 90% steam (to provide endothermic heat of reaction) and less than 10% ethylbenzene.

The comparison of simulation result by different forms of model shows that internal mass transfer is stronger effect on output result, while external transfer and mass axial dispersion affect in entrance region and little affect on overall result at outlet of reactor. The prediction results of heterogeneous model are slightly different, and the more complex model is used to significantly improve the accuracy of the reactor performance prediction according to previous publication[8, 33, 34]. For methanol production[33], the prediction results by heterogeneous model accounting for both internal and external transfer are lower percent error from plant data than results by heterogeneous model accounting for only internal transfer. For water-gas shift reaction[8], the results from model accounting for external transfer and mass axial dispersion are closer the experiment data than model without accounting for them. For hydrogenation of acetylene[34], the results of model with dispersed flow are close to plant data than model of plug flow.

4.1.3 Estimate the important of transfer effect on reaction by criteria

4.1.3.1 Estimate the importance of internal transfer on reaction for commercial process

The effect of internal mass diffusion is determined by Weisz-Ptrater criteria. Weisz-Ptrater parameter (C_{wp}) which is the ratio of actual reaction rate to internal diffusion rate is calculated by following equation.

$$C_{WP} = \frac{r_c \rho_c R^2}{D_e C_s}$$

If C_{wp} is lower than unity, internal diffusion rate does not limit the reaction. In the contrast if C_{wp} is higher than unity, internal diffusion rate limits the reaction. The value of C_{wp} along the reactor is shown in Figure 19. The value is much higher than unity at the inlet, then the internal mass diffusion would limit the overall rate [11]. The result that is determined by Weisz-Ptrater criteria appear like the simulation result. The criteria is also used to estimate internal mass transfer and confirmed with the experiment. Teppei Nunoura and et al [35] experiment water oxidation of phenol in fixed bed reactor. They found that the phenol conversion increases with decrease of catalyst diameter, the internal transfer limits the reaction. The result was confirmed with Weisz-Prater criterion which C_{wp} was calculated to be 1.73.

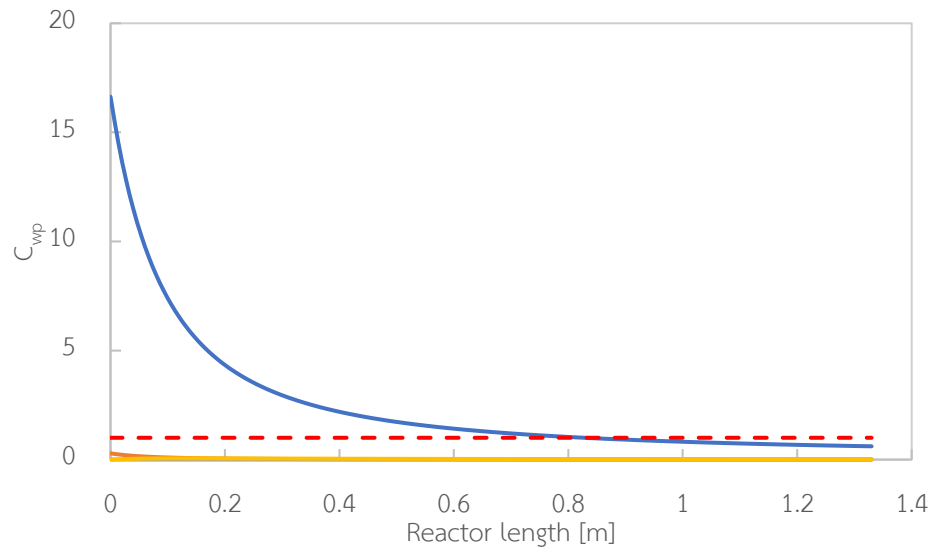
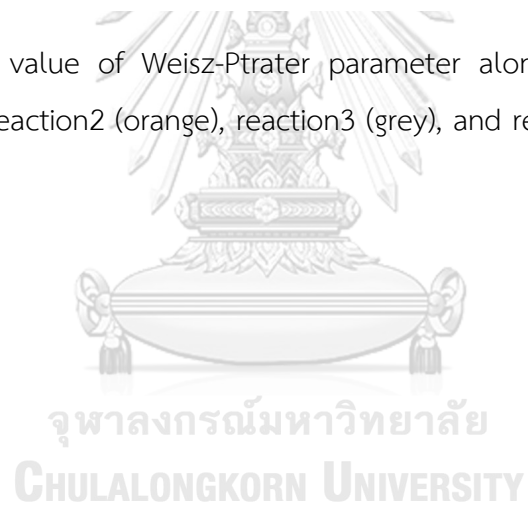


Figure 19 The value of Weisz-Prater parameter along the reactor length for reaction1 (blue), reaction2 (orange), reaction3 (grey), and reaction4 (yellow). Red line is criteria.



4.1.3.2 Estimate the importance of the external transfer on reaction by criteria

4.1.3.2.1 Estimate the importance of the external transfer on reaction for commercial process

The effect of external transfer is determined by Mear's criteria[11]. Mass transfer from bulk gas to catalyst surface can be neglect when

$$\frac{r_c \rho_B R n}{k_c C_i} < 0.15$$

Heat transfer from bulk gas to catalyst surface can also be neglect when

$$\left| \frac{-\Delta H_r (r_c) \rho_B R E}{h T^2 R_g} \right| < 0.15$$

The absolute values of Mears' mass-transport and heat-transport parameters are smaller than 0.15 shown in Figure 20 and Figure 21 respectively, then the corresponding external transport effect may be neglected. The criteria is also used with the experiment of oxidation of phenol [35], the Mears' mass transfer parameter is lower than 0.15, which means external transfer can be neglect. The result was confirmed with the experiment since the phenol conversion was not affected by increase of the flow rate.

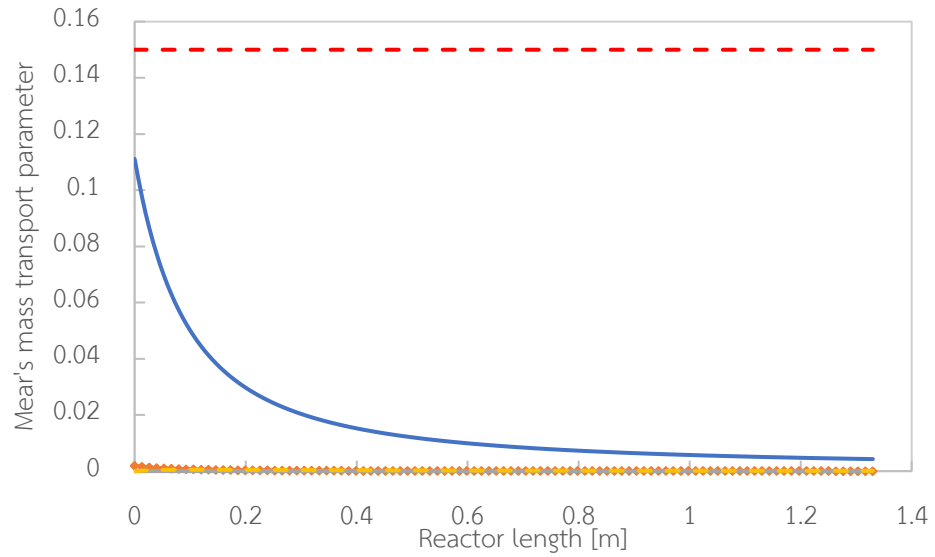


Figure 20 The absolute values of Mear's mass-transport parameter along the reactor for reaction1 (blue), reaction2 (orange), reaction3 (grey), and reaction4 (yellow). Red line is criteria.

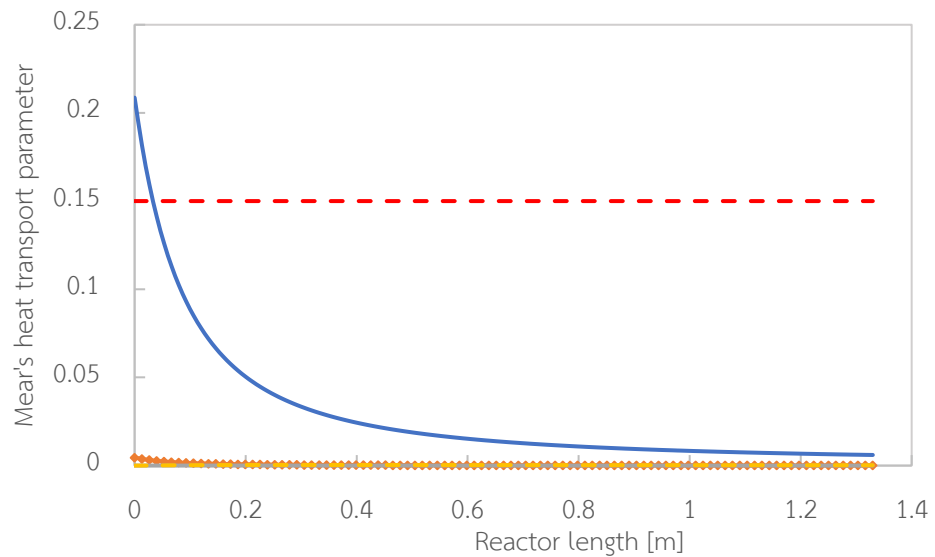


Figure 21 The absolute values of Mear's heat-transport parameter along the reactor for reaction1 (blue), reaction2 (orange), reaction3 (grey), and reaction4 (yellow). Red line is criteria.

4.1.3.2.2 Estimate the importance of the external transfer on reaction for process that affected by external transfer

Commercial operating condition, the flow rate is high lead to high external transfer, thus gradient concentration between bulk and surface can be neglect. Therefore, case study 1 which is low flow rate by constant space velocity (equal to commercial process) is studied and the condition is shown in Table 13. The result shows that the effect of external transfer on reaction increases when the flow rate decreases, as shown output parameter in Table 14. From Figure 22 and Figure 23, Mears' mass and heat parameters are much higher than 1.5, which means external transfer affects on overall reaction rate [11].

From case study 1, the results show that if external transfer affects on reaction rate by estimation of Mears' criterion, the complex model accounting for external transfer should be used to predict reactor performance.

Table 13 Operating Condition of process

Initial condition	Commercial	Case study 1
Feed molar flow rate [kmol/h]		
Ethylbenzene	707	14.14
Styrene	7.104	0.142
Benzene	0.293	0.006
Toluene	4.968	0.099
Hydrogen	0	0
Steam	7777	155.54
Pressure [bar]	1.25	1.25
Bed length [m]	1.33	0.03325
velocity [m/h]	13010.11	325.25

Table 14 The simulation result of heterogeneous model in case study 1

Output Result	Heterogeneous model accounting for internal transfer	Heterogeneous model accounting for internal and external transfer
X_{EB} [%]	35.87	34.66
S_{ST} [%]	97.80	97.71
S_{BZ} [%]	1.12	1.09
S_{TO} [%]	1.08	1.20
P_{out} [bar]	1.25	1.25
T_{out} [K]	824.16	826.60

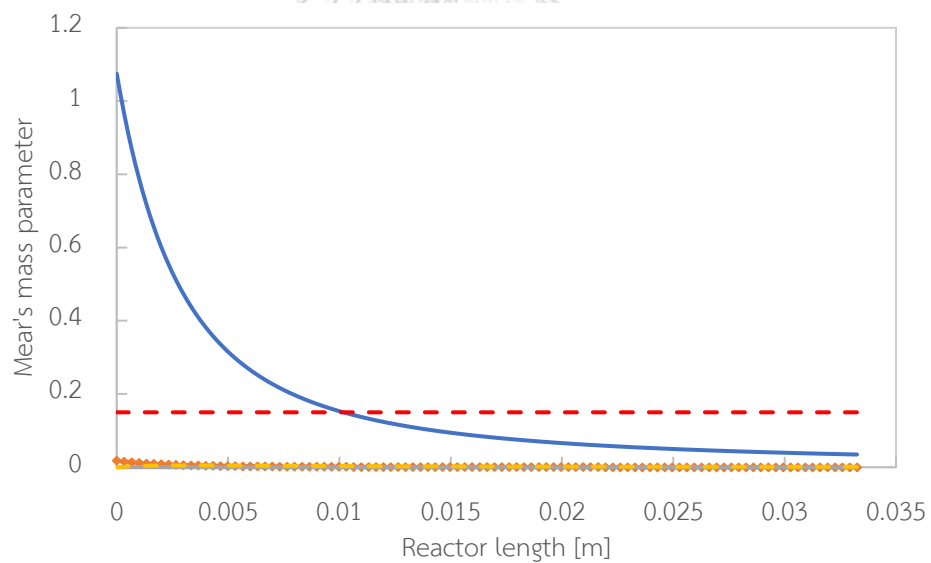


Figure 22 The absolute values of Mears' mass-transport parameter along the reactor for reaction1 (blue), reaction2 (orange), reaction3 (grey), and reaction4(yellow). Red line is criteria.

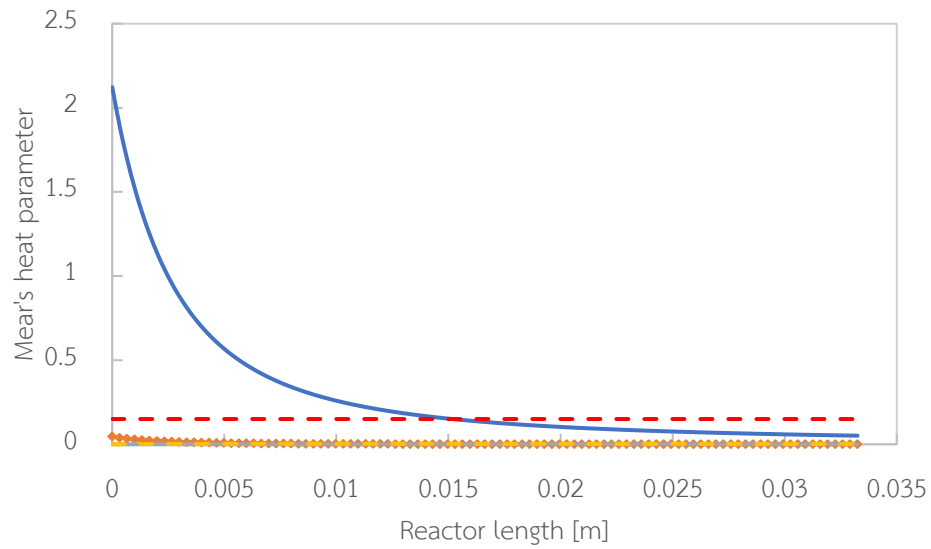
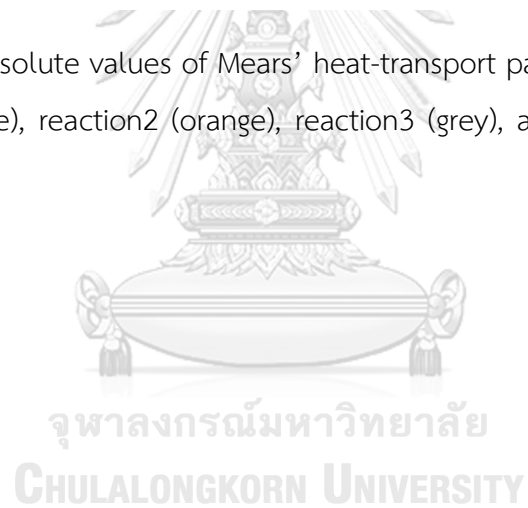


Figure 23 The absolute values of Mear's heat-transport parameter along the reactor for reaction1 (blue), reaction2 (orange), reaction3 (grey), and reaction4(yellow). Red line is criteria.



4.1.3.3 Estimate the importance of mass axial dispersion on reaction by criteria

4.1.3.3.1 Estimate the importance of mass axial dispersion on reaction for commercial process

The effect of mass axial dispersion is determined by vessel dispersion number (D/uL). The value of this process is 0.0048, it is lower than 0.01, which means the flow is deviate from plug flow [13]. The residence time distribution curve shows in Figure 24 which the process flow is small deviate from plug flow.

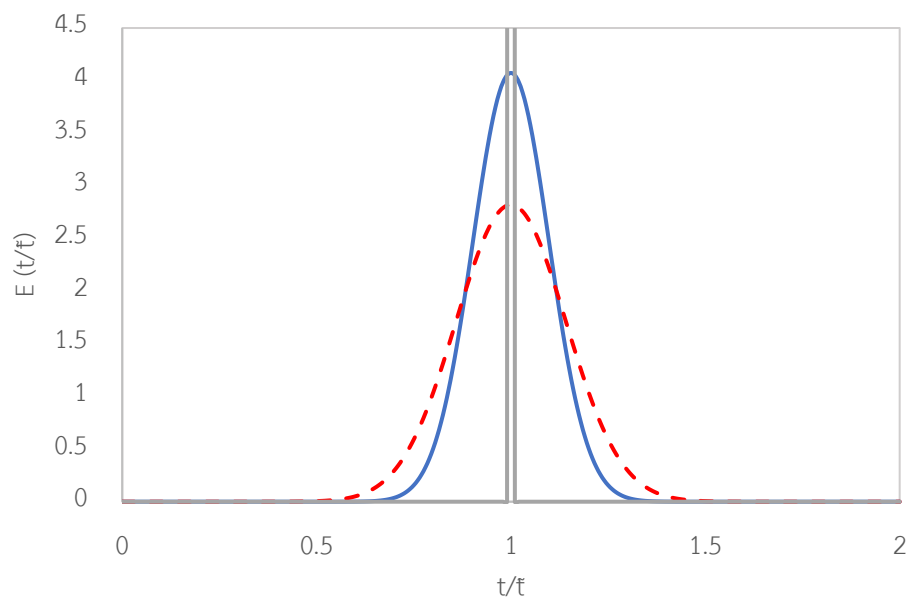


Figure 24 The residence time distribution curve of process (blue), plug flow (grey), and criteria (red), E is exit age distribution, t is actual residence time and \bar{t} is average residence time.

4.1.3.3.2 Estimate the importance of mass axial dispersion on reaction for process that affected by mass axial dispersion

Commercial operating condition, the value of D_{ea}/uL is lower than 0.01, axial dispersion effect can be neglect[13]. Moreover, mass axial dispersion can be diminished by increasing flow rate and reactor length. Therefore, case study 2 is studied in condition of decreasing bed length and flow rate, as shown in Table 15. The result shows that the effect of axial dispersion on reaction increases as the flow rate and bed length decrease, as shown in Table 16. The value of D_{ea}/uL is 0.0127 which is higher than 0.01. The residence time distribution curve shows large deviation from plug flow, as shown in Figure 25.

Table 15 Operating Condition of process

Initial condition	Commercial	Case study 2
Feed molar flow rate [kmol/h]		
Ethylbenzene	707	141.4
Styrene	7.104	1.42
Benzene	0.293	0.06
Toluene	4.968	0.99
Hydrogen	0	0
Steam	7777	1555.4
Pressure [bar]	1.25	1.25
Bed length [m]	1.33	0.5
velocity [m/h]	13010.11	2602.02

Table 16 The simulation result of heterogeneous model in case study 2

Output Result	Heterogeneous model accounting for internal transfer	Heterogeneous model accounting for internal transfer and mass axial dispersion
X_{EB} [%]	39.25	34.87
S_{ST} [%]	97.68	95.44
S_{BZ} [%]	1.09	1.20
S_{TO} [%]	1.23	1.14
P_{out} [bar]	1.25	1.25
T_{out} [K]	818.46	817.02

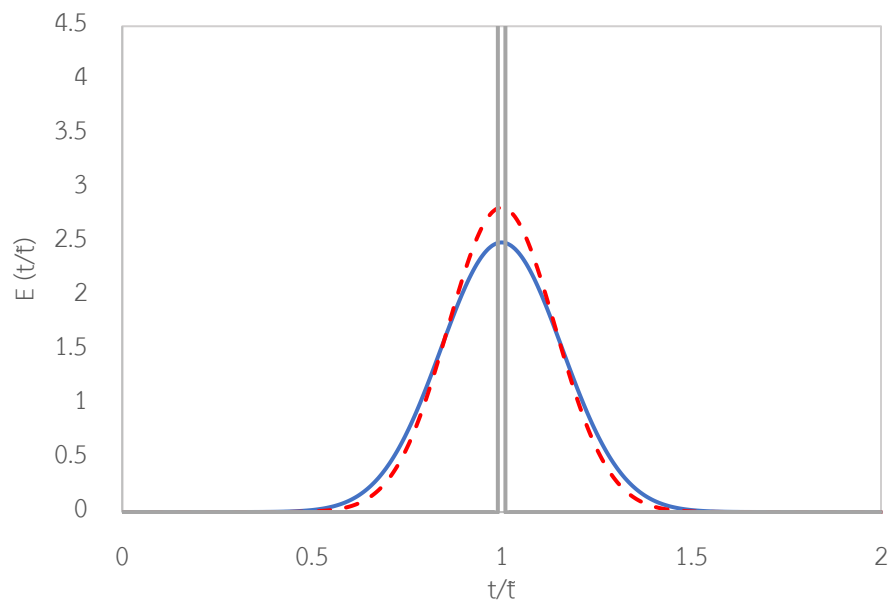


Figure 25 The residence time distribution curve of this process (blue), plug flow (grey), and criteria (red), E is exit age distribution, t is actual residence time and \bar{t} is average residence time.

From case study 2 shows that the process which affects by mass axial dispersion should use dispersed flow model to predict reactor performance and the effect is estimated by the value of vessel dispersion number (D/uL).

Obviously, the three criteria confirm that internal mass transfer affects the overall reaction rate. While external transfer and mass axial dispersion effect occur at only entrance region of reactor and they can be neglected.

4.1.4 Comparison of simulation result

4.1.4.1 Comparison of simulation result with simulation result of reference paper

The reactors are predicted by mathematical model for 3 reactors according to the industrial process. To double-check the reliability of the present simulation results, the ethylbenzene conversion, selectivity, reaction temperature and pressure at the reactor outlet are compared with those given under the same conditions in the referenced publication [10], as shown in

Table 17. The results are some difference, but the result of toluene selectivity is large difference. The different may be occurred by the used kinetic parameters and property data i.e. mass transfer coefficient, since the reference data does not show the used value.

Table 17 The comparison of reactor outlet results between the publication and this research

Output	This research			Publication [10]			%Difference		
	R1	R2	R3	R1	R2	R3	R1	R2	R3
X _{EB} [%]	34.49	65.35	84.80	36.89	65.78	83.76	-6.50	-0.65	1.24
S _{ST} [%]	97.90	94.06	89.54	98.49	95.1	90.43	-0.60	-1.09	-0.99
S _{BZ} [%]	1.13	1.52	1.85	1	1.423	1.754	12.90	6.77	5.43
S _{TO} [%]	0.97	4.42	8.61	0.507	3.48	7.809	91.78	27.02	10.31
P _{out} [bar]	1.04	0.75	0.24	1.06	0.783	0.3	-1.43	-4.16	-19.73
T _{out} [K]	826.44	852.04	876.18	811.36	845.71	873.6	1.86	0.75	0.30

*R = reactor

4.1.4.2 Comparison of simulation result with industrial result

The total ethylbenzene conversion and styrene selectivity in industrial have been reported in the range of 60-70% and 97%, respectively [36]. The simulation result of reactor output from each model are shown in

Table 18 and compared with industrial output. The heterogeneous models which account for internal mass transfer, the dominant effect, (model2-4) predict the same reactor output results for all reactor and less percent error from industrial output than pseudohomogeneous model. The models which increase accounting for mass axial dispersion (model5-6) predict the slightly less ethylbenzene conversion and styrene selectivity than plug flow model (model3-4) for reactor1 and reactor2, while the reactor3 predict more different so the percent error from industrial output. There is some error of simulation reactor3 from model6 since the styrene selectivity excess 100.



Table 18 The comparison of reactor outlet results from each model

Model	Reactor1		Reactor2		Reactor3		%Error*	
	X _{EB} [%]	S _{ST} [%]	X _{EB} [%]	S _{ST} [%]	X _{EB} [%]	S _{ST} [%]	X _{EB} [%]	S _{ST} [%]
Model1	36.5	98.3	68.2	95.1	88.0	90.6	29.5	-6.59
Model2	34.5	97.9	65.4	94.1	84.8	89.5	24.7	-7.69
Model3	34.5	97.9	65.3	94.1	84.8	89.5	24.7	-7.69
Model4	34.5	97.9	65.4	94.0	84.8	89.5	24.7	-7.69
Model5	34.5	97.8	64.8	93.8	81.0	98.1	19.2	1.09
Model6	34.5	98.0	64.9	93.7	79.7	103.8	17.1	7.06

* Percent error from 68% conversion of ethylbenzene and 97% selectivity of styrene



4.2 Study the effect of catalyst shape on reactor performance by same effective diameter catalyst

The model can be used to predict reactor performance response to change in shape catalyst. Previous section, the inside catalyst is determined by spherical balance equation which can be written

$$0 = \frac{D_{ei}}{r^2} \frac{d}{dr} \left(r^2 \frac{dC_i^s}{dr} \right) + \rho_s \sum_{j=1}^n v_{ij} r_{cj} + \varepsilon_s \sum_{j=1}^n v_{ij} r_{tj}$$

The boundary conditions

$$r = 0 ; \frac{dC_i^s}{dr} = 0$$

$$r = R ; C_i^s = C_i$$

The above differential equation with boundary conditions of spherical balance is integrated as function of radial position inside catalyst from center of catalyst ($r = 0$) to catalyst surface ($r =$ catalyst radius, R).

Previous publications of studied effect of catalyst shape, the effect is determined in term of thiele modulus and effectiveness factor which are derived by slab balance of mass inside catalyst. The slab balance equation can be written

$$0 = \frac{d}{dy} \left(D_{ei} \frac{dC_i}{dy} \right) + \rho_s \sum_{j=1}^n v_{ij} r_{cj} + \varepsilon_s \sum_{j=1}^n v_{ij} r_{tj}$$

The boundary conditions

$$y = 0 ; \frac{dC_i}{dy} = 0$$

$$y = L ; C_i^s = C_{si}$$

For generalized modulus, L is the ratio of catalyst volume to surface area, called effective diffusion length. For slab balance, the differential equation with boundary

conditions is integrated as function of y -coordinate from center of catalyst ($y = 0$) to catalyst surface ($y = L$).

Therefore, the heterogeneous models for studied the effect determine inside catalyst by slab balance and the simulation result shows in Table 19.

Table 19 Simulation result of reactor by difference model forms with slab balance inside catalyst

Output	Model2	Model3	Model4	Model5	Model6
X_{EB} [%]	35.16	35.16	35.06	35.11	35.05
S_{ST} [%]	98.04	98.04	98.03	98.00	98.32
S_{BZ} [%]	1.11	1.11	1.11	1.16	1.16
S_{TO} [%]	0.85	0.85	0.87	0.83	0.86
P_{out} [bar]	1.05	1.05	1.04	1.05	1.04
T_{out} [K]	825.17	825.17	825.30	824.73	825.09

The simulation results of slab balance inside catalyst models compared to spherical balance inside catalyst models, the results are slightly different. The diffusion length is integration length for differential equation of inside catalyst. For catalyst size 0.0055 m of diameter, the predicted ethylbenzene conversion by slab balance increases. Because slab balance model is integrated with the diffusion length which is the ratio of volume to surface catalyst (0.000917 m), while spherical balance model is integrated with the diffusion length which is radius of catalyst (0.00275 m). The lower of diffusion length affects on higher effectiveness factor, as shown in Figure 26.

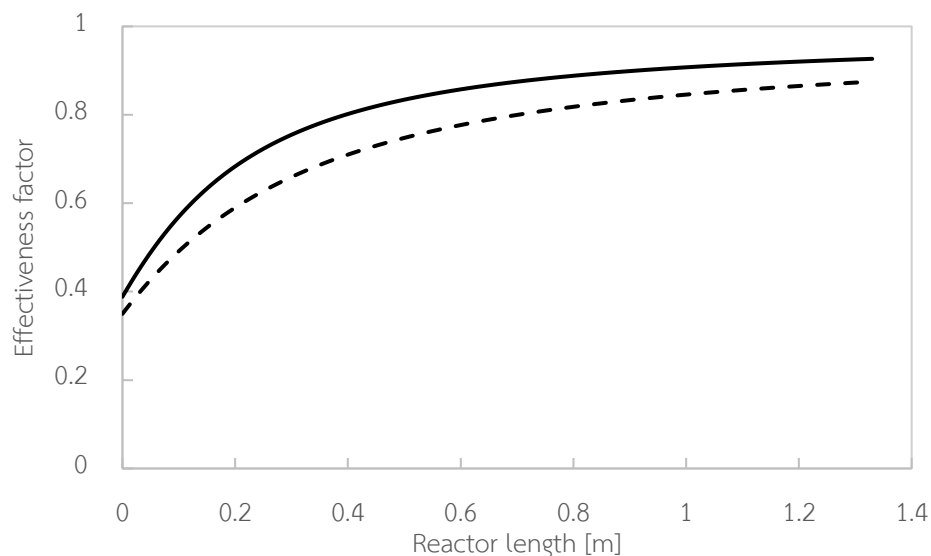


Figure 26 The effectiveness factor of main reaction along the reactor by spherical balance (dash line) and slab balance (solid line) inside catalyst.

The developed models were employed to describe the effect of catalyst shape on performance of adiabatic fixed bed reactor. The studied performance is catalyst weight and bed length to achieve 36% conversion of ethylbenzene. To fair the comparison of catalyst shape, size of catalyst is fixed at 5.5 mm effective diameter which is the diameter of a sphere having same catalyst volume as the actual catalyst. The physical properties, including surface area, sphericity, bed void fraction and diffusion length, of three catalyst shape of this study (Sphere, Cylinder, and Trilobe) with 5.5 mm equivalent diameter are summarized in Table 20.

Table 20 Properties for 5.5 mm effective diameter of three catalyst shape

Physical Properties	Sphere	Cylinder	Trilobe
Surface area [m ²]	9.50E-05	1.26E-04	1.53E-04
Sphericity	1.000	0.755	0.622
Bed void fraction	0.353	0.418	0.476
Diffusion length [m]	9.17E-04	7.91E-04	4.44E-04

The developed models are used to describe the effect of catalyst shape on catalyst weight, reactor bed length, effectiveness factor and pressure drop. The results are shown in Figure 27 - Figure 30. The results from different form of model are little different since every model account for internal mass transfer which is strong effect to overall reaction. Moreover, the three criteria also confirm that internal mass transfer affects the overall reaction rate, and external transfer and mass axial dispersion effect can be neglect show in appendix C.

4.2.1 Effect of catalyst shape on required catalyst mass and reactor length

Catalyst weight decreases with catalyst shape in order cylinders > spheres > trilobes, as shown in Figure 27.

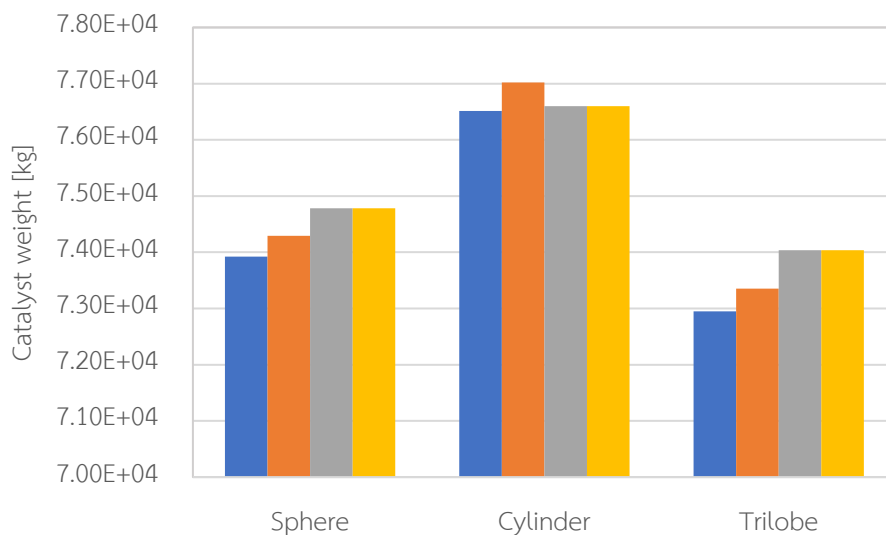


Figure 27 Effect of catalyst shape on catalyst weight required to achieve ethylbenzene conversion 36% calculated by model3 (blue), model4 (orange), model5 (grey), and model6 (yellow).

Model simulations determine the affect on reactor bed length, using catalyst density of 2500 kg/m^3 . Bed length depends on the bed density, which is related to bed void fraction. Figure 28 shows the increase of bed length with catalyst shape in order trilobes > cylinders > spheres.

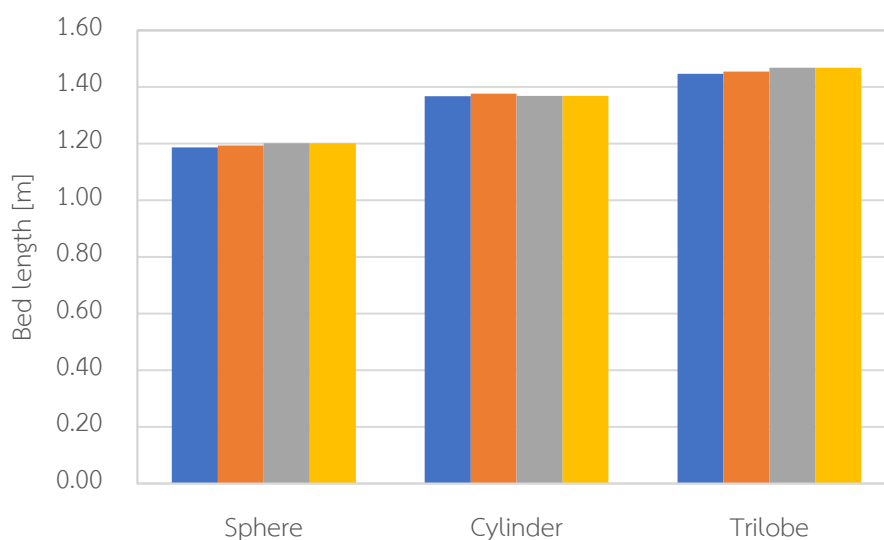


Figure 28 Effect of catalyst shape on bed length required to achieve ethylbenzene conversion 36% calculated by model3 (blue), model4 (orange), model5 (grey), and model6 (yellow).

Even though Figure 27 and Figure 28 show the overall effect of catalyst shape on reactor performance or design. The results arise from combination of effects of several other variables that are affected by catalyst shape. The following discussion considers the individual contributions of catalyst effectiveness factor and pressure drop to the overall effect of catalyst shape on catalyst weight and reactor bed length.

4.2.2 Effect of catalyst shape on effectiveness factor

The catalyst shape affects on overall reaction rate via the internal balance, which depends on diffusion length. Figure 29 shows the effect of catalyst shape on effectiveness factor of main reaction. The order of increasing the effectiveness factor is spheres < cylinders < trilobes. The increase of effectiveness factor can be explained by diffusion length. The diffusion length is the ratio of volume to surface area and is the indication of resistance to diffusion. As diffusion length decreases (increasing surface area), diffusion resistance decreases, and effectiveness factor increases. The simulation results of catalyst shape affect on effectiveness factor are in agreement with simulation results by Kyle M. Brunner and et al. for Fischer-Tropsch synthesis [3] and M.J. Macias and J. Ancheyta for hydrodesulfurization [2].

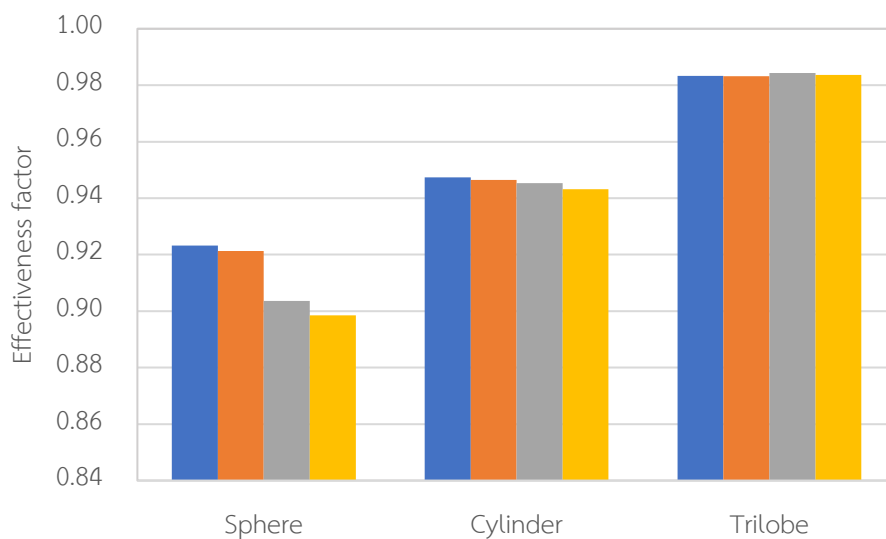


Figure 29 Effect of catalyst shape on effectiveness factor of main reaction at outlet calculated by model3 (blue), model4 (orange), model5 (grey), and model6 (yellow).

4.2.3 Effect of catalyst shape on pressure drop

The effect of catalyst shape on pressure drop per unit bed length ($\Delta P/L_{bed}$) affects the catalyst weight required to achieve a specified ethylbenzene conversion. The pressure drop per unit bed length depends on bed void fraction. The effect of catalyst shape on bed void fraction shows in Table 20. Void bed fraction increases with catalyst shape in order of sphere < cylinder < trilobe, result in $\Delta P/L_{bed}$ decreases in the order sphere > cylinder > trilobe, as shown Figure 30. The simulation results of catalyst shape affect on pressure drop also agree with simulation results by Kyle M. Brunner and et al. for Fischer-Tropsch synthesis [3] and M.J. Macias and J. Ancheyta for hydrodesulfurization [2].

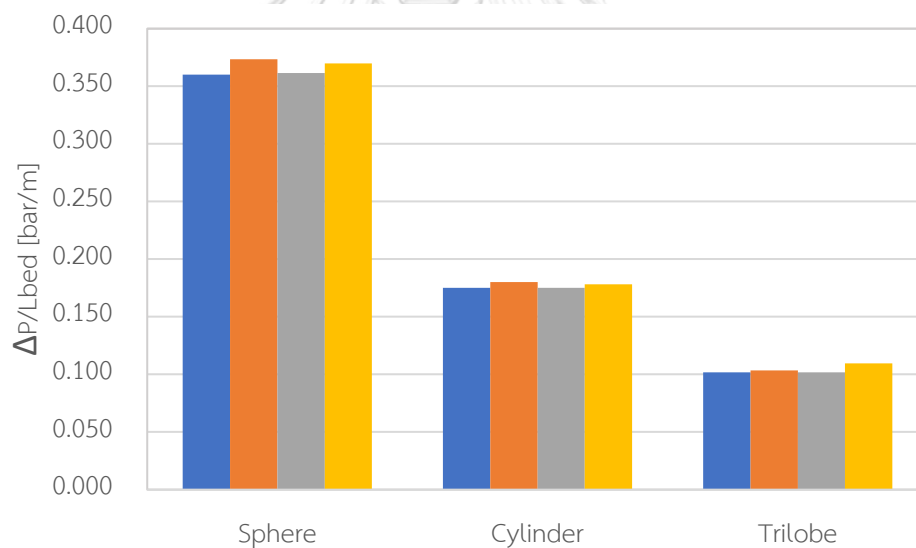


Figure 30 Effect of catalyst shape on $\Delta P/L_{bed}$ calculated by model3 (blue), model4 (orange), model5 (grey), and model6 (yellow).

4.2.4 Effect of catalyst shape on observe reaction rate

Figure 33 shows the observe reaction rate, which depends on effectiveness factor (Figure 32) and reaction rate at catalyst surface condition (Figure 31). The reaction rate at catalyst surface condition decreases with catalyst shape order spheres > cylinders > trilobes. The result shows that decreasing $\Delta P/L_{bed}$ affects to increase partial pressure, then reaction rate decreases. This result agrees with simulation result presented by Won Jae Lee and Gilbert F. Froment [10] for identical process of ethylbenzene dehydrogenation to benzene, when the total pressure decreases from 1.25 bar to 0.70 bar, the ethylbenzene conversion increase from 81.09% to 82.12%. The result also agrees with conversion to styrene of bench-scale lab [37], when the pressure decreases from 1.27 to 0.68 atm, the conversion to styrene increases from 33.9% to 37.6% at 566°C, 51.9% to 56.1% at 593°C, 64.7% to 68.3% at 621°C.

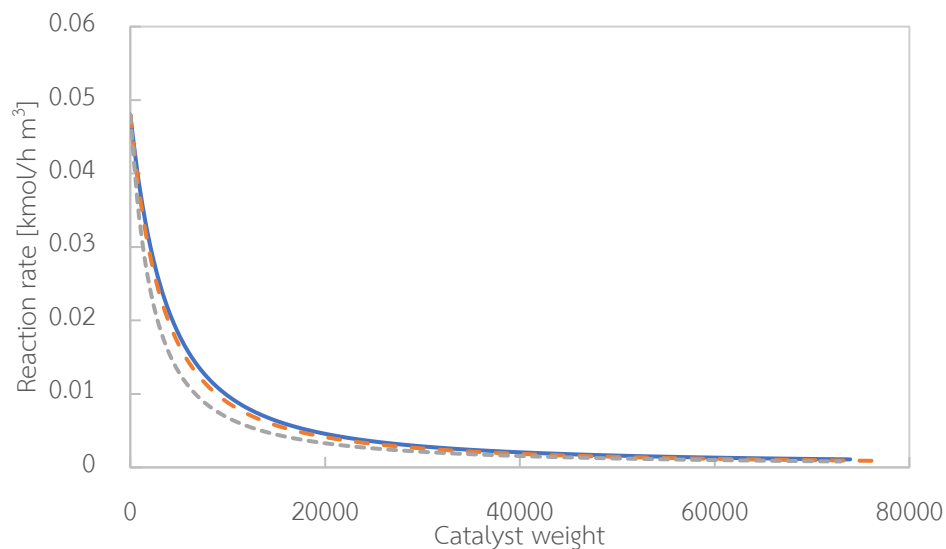


Figure 31 Reaction rate of main reaction of different catalyst shape i.e. sphere (blue), cylinder (orange), and trilobe (grey) by model3.

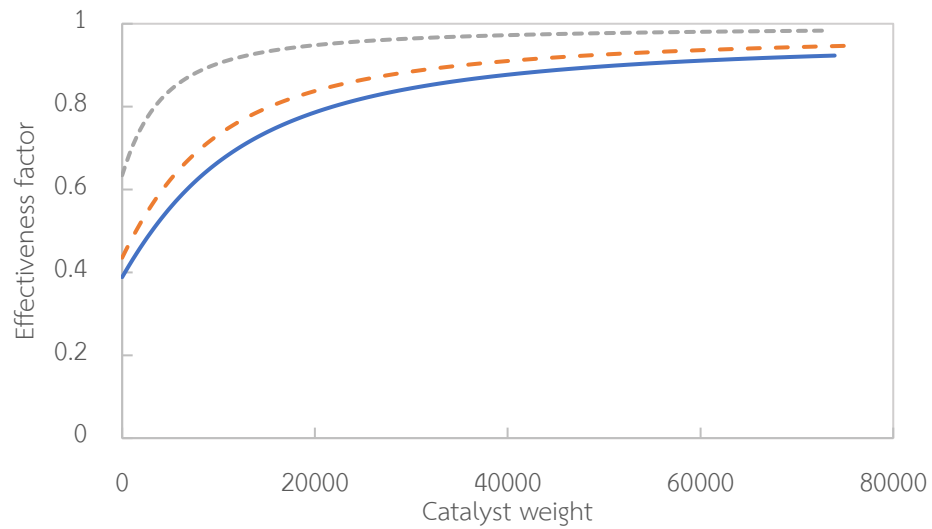


Figure 32 Effectiveness factor of main reaction of different catalyst shape i.e. sphere (blue), cylinder (orange), and trilobe (grey) by model3.

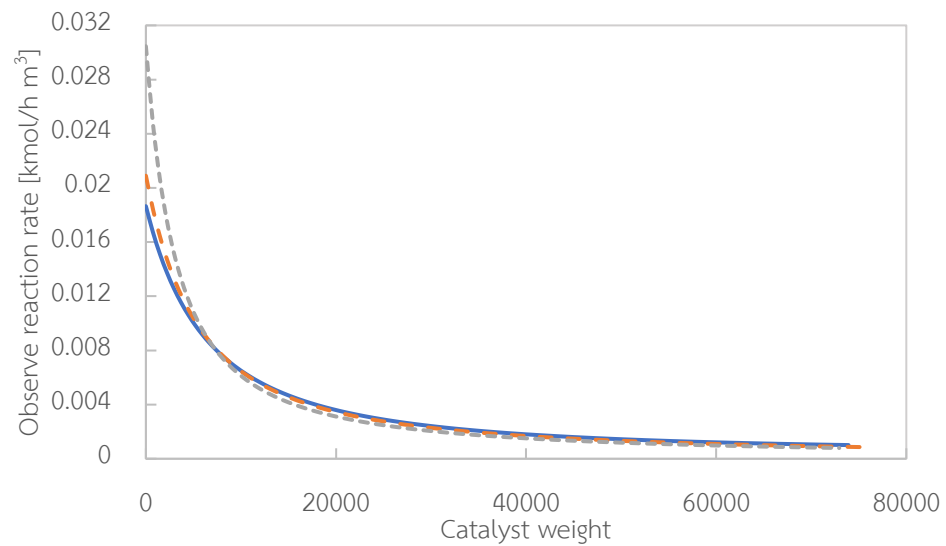


Figure 33 Observe reaction rate of main reaction of different catalyst shape i.e. sphere (blue), cylinder (orange), and trilobe (grey) by model3.

From Figure 33, the observed reaction rate result of trilobe is much higher than sphere and cylinder, because of the effectiveness factor. Therefore, the catalyst weight required of trilobe is lowest, as shown in Figure 27. Although the effectiveness factor of cylinder is higher than sphere, the reaction rate is lower than sphere result in highest catalyst, as shown in Figure 27. For ethylbenzene dehydrogenation to styrene process, the catalyst weight required decreases in catalyst shape order cylinders > spheres > trilobes. Compare the results of catalyst shape effect with Fischer-Tropsch synthesis[3], the required catalyst weight decreases with catalyst shape in order spheres > cylinders > trilobes, it is different from the result of ethylbenzene dehydrogenation to styrene process. Since the required catalyst weight depends on observed reaction rate, which related to effectiveness factor and reaction rate at catalyst surface condition. For Fischer-Tropsch synthesis, the decreasing pressure drop affects to increase partial pressure and increase reaction rate at catalyst surface condition, since the reaction is one reaction and irreversible reaction. So, the reaction rate at catalyst surface condition increases with catalyst shape order spheres < cylinders < trilobes. The effect combines with the effect of effectiveness factor which increases with order spheres < cylinders < trilobes. The overall effect leads to increase the observed reaction rate with order spheres < cylinders < trilobes, in consequence, the required catalyst weight decreases in catalyst shape order spheres > cylinders > trilobes. While ethylbenzene dehydrogenation to styrene process, the reaction is multiple reaction and reversible. When decreasing pressure drop, partial pressure increases result in decreasing reaction rate at catalyst surface condition. It is attributed to Le Chatelier's principle for the reversible reaction in which the total number of moles of gaseous products is two times that of the reactant. In this case the reaction equilibrium (reactant conversion) is favored by a lower total pressure. So, the reaction rate at catalyst surface condition decreases with catalyst shape order spheres > cylinders > trilobes,

while the effect of effectiveness factor which increases with order spheres < cylinders < trilobes. The effect on observe reaction rate depends on the trade-off between the effect of effectiveness factor and reaction rate at catalyst surface condition. And the observe reaction rate affects to required catalyst. The effect of bed length also tradeoffs between the catalyst weight required and bed void fraction.

For reversible reaction, effect of catalyst shape which increases surface increases effectiveness factor but decreases reaction rate at surface condition. Therefore, the effect of catalyst shape on actual reaction rate is traded off between the effect on effectiveness factor and reaction rate at surface condition. If the effect on effectiveness factor dominate, the actual reaction rate increases result in lower catalyst weight. In contrast if the effect on reaction rate at surface condition dominate, the higher catalyst weight is required.

From simulation result for equal effective diameter at 5.5 mm of catalyst, catalyst shape which require lowest catalyst weight to achieve specific conversion is trilobe.

จุฬาลงกรณ์มหาวิทยาลัย
CHULALONGKORN UNIVERSITY

4.2.5 Effect of catalyst shape on intermediate parameters relate to required catalyst weight and bed length

For given equivalent diameter, the effect of catalyst shape on intermediate parameters, which affects on catalyst weight and reactor bed length, is presented on the schematic in Figure 34. This schematic shows the interaction between parameters that are affected by change catalyst shape and contribute to catalyst weight required and bed length. The green arrows indicate that a parameter increases because of change in the previous parameter. Red arrows indicate that a parameter decreases.

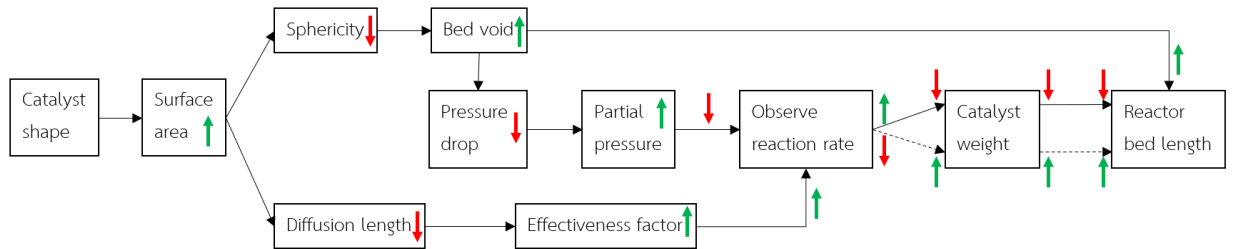


Figure 34 Schematic representation of the effect of catalyst shape on parameters that contribute to catalyst weight and bed length required to achieve specific conversion

4.3 Study the effect of catalyst shape on reactor performance by catalyst shape in commercial size

Commercial catalyst size of each shape is summarized in Figure 6 and Table 21, with the physical properties.

Table 21 Geometry and properties of commercial catalyst in each shape

Properties	Sphere	Cylinder	Trilobe
Diameter of catalyst (D_p) [m]	5.50E-03	3.50E-03	5.00E-03
Length of catalyst (L_p) [m]	-	5.00E-03	5.00E-03
Surface area [m^2]	9.50E-05	7.42E-05	1.06E-04
Effective diameter [m]	5.50E-03	4.51E-03	5.10E-03
Diffusion length [m]	9.17E-04	8.75E-04	6.25E-04
Sphericity	1.000	0.862	0.768
Bed void fraction	0.353	0.385	0.414

The simulation result of reaction performance affect by each catalyst shape show in Table 22.

Table 22 Effect of catalyst shape with commercial size by Model3

Result	Sphere	Cylinder	Trilobe
Catalyst weight [kg]	7.39E+04	7.37E+04	7.28E+04
Reactor bed length [m]	1.19	1.25	1.29
Effectiveness factor	0.923	0.930	0.966
Pressure drop per length of reactor [bar/m]	0.360	0.324	0.201

Effectiveness factor increases in shape order trilobe > cylinder > sphere because of the diffusion length. Since there is the effect of size catalyst on pressure drop, the pressure drop is not much different of each catalyst shape. The decreasing catalyst size increases the pressure drop. The observe reaction rate increases with catalyst shape order trilobe > cylinder > sphere because larger effect of effectiveness factor than effect of pressure drop on reaction rate, as shown in Figure 35. Therefore, catalyst weight required decreases with catalyst shape order sphere > cylinder > trilobe. And reactor bed length is dominant effected by void bed fraction, bed length increase with catalyst shape order sphere < cylinder < trilobe. This effect shows that besides the catalyst shape affects to reactor performance, catalyst size also affects too. Therefore, catalyst selection should determine both shape and size of catalyst.

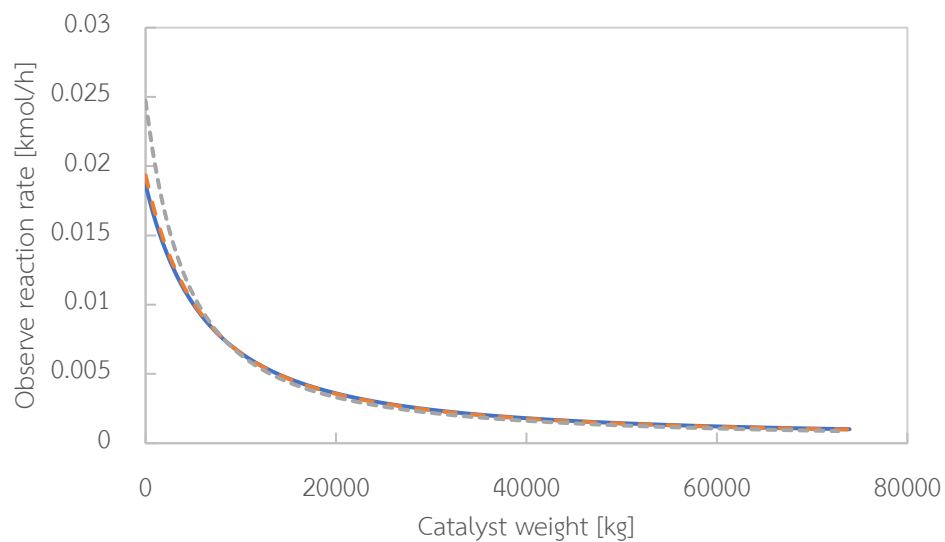


Figure 35 Observe reaction rate of main reaction of different catalyst shape i.e. sphere (blue), cylinder (orange), and trilobe (grey) by model3.



Chapter 5 Conclusion

The simulation study investigates the effect of internal mass transfer, external mass transfer and mass axial dispersion on the conversion of ethylbenzene and product selectivity, when the adiabatic dehydrogenation system is carried out under typical commercial operating conditions. The simulation results reveal that pseudohomogeneous model1 predicts the highest ethylbenzene conversion (36.52%) and highest ST selectivity (98.34%) at the reactor outlet. Effect of internal mass transfer is described by heterogeneous model2 and model3, the models predict lower ethylbenzene conversion (34.49%) and lower styrene selectivity (97.90%) than pseudohomogeneous model1. Effect of external mass transfer is described by heterogeneous model4, the results are 34.46% ethylbenzene conversion and 97.88% styrene selectivity. Effect of mass axial dispersion is described by model5 and model6, the models predict slightly different result from plug flow. This clearly shows that both internal diffusion inside and external diffusion around catalyst pellets contribute to significant deviations in the reactor performance. The effect of intrapellet diffusion is stronger than that of external diffusion between the bulk fluid and catalyst surface and axial dispersion. The results also confirm that the well-known Weisz-Ptater, Mears' criteria and vessel dispersion number can reliably determine whether the roles of intrapellet diffusion, external diffusion between the bulk fluid stream and catalyst surface and axial dispersion are significant for the reaction system of interest or not.

The heterogeneous models were used to understand the effect of catalyst shape on reactor design and performance. The used models compose of model accounting for internal mass transfer (model3), model accounting for internal and external transfer (model4), model accounting for internal transfer and mass axial dispersion (model5), and model accounting for internal and external transfer and mass axial dispersion(model6). The result of all models is slightly different since the

effect of external transfer and mass axial dispersion is little effect on reactor performance which mean it can be neglect. The effect of catalyst shape on required catalyst weight to achieve same conversion increases in order trilobe < sphere < cylinder since the effect of catalyst on effectiveness factor and pressure drop. The effectiveness factor is highest by trilobe shape (0.983) and decreases in order cylinder shape (0.947) and spherical shape (0.923). As the pressure drop increases, total pressure decreases, and reaction rate at surface condition increases. The reaction rate at surface condition is highest by spherical shape and decreases in order cylinder > trilobe. The effect of catalyst shape on catalyst weight depends on overall reaction which relates to the dominant effect between effectiveness factor and reaction rate at catalyst surface. And the effect of catalyst shape on bed length depends on dominant effect between required catalyst weight and bed void fraction. From simulation result, catalyst shape which require lowest catalyst weight to achieve specific conversion is trilobe.



REFERENCES



จุฬาลงกรณ์มหาวิทยาลัย
CHULALONGKORN UNIVERSITY

NOMENCLATURE

A_c = cross-section area of reactor, m^2

A_j = pre-exponential factor of catalytic reaction j , $kmol/(kgcat\ h)$

A_i = pre-exponential factor for adsorption of species i , $1/bar$

a_p = external surface area, $1/m$

C_{0i} = concentration of component i in bulk fluid at initial, $kmol/m^3$

C_i = concentration of component i in bulk fluid, $kmol/m^3$

C_i^s = concentration of component i inside the catalyst, $kmol/m^3$

C_{pi} = Specific heat of component i , $kJ/(kg\ K)$

C_{si} = concentration of component i at surface of catalyst, $kmol/m^3$

C_{WP} = Weisz-Prater parameter

D_{ea} = effective axial dispersion coefficient, m^2/h

D_{ei} = effective diffusivity of component i , m^2/h

D_{ij} = binary mass diffusion coefficient i in j , m^2/s

D_{mi} = mass diffusion coefficient in mixture, m^2/s

d_p = catalyst equivalent pellet diameter, m

d_t = diameter of bed, m

E = active energy of reaction, kJ/mol

f = friction factor

G = superficial mass flow velocity, $kg/(m^2\ h)$

h = heat transfer coefficient, $kJ/(m^2\ h\ K)$

ΔH_i = adsorption enthalpy of adsorbed component i, kJ/kmol

ΔH_{rj} = heat of reaction j, kJ/kmol

k = Boltzmann's constant, 1.3805×10^{-23} J/K

k_c = mass transfer coefficient, m/h

k_e = effective thermal conductivity, kJ/ (m h K)

k_j = rate coefficient of catalytic reaction j, kmol/ (kgcat h)

k_{tj} = rate coefficient of thermal reaction j, kmol/ (m³ bar h)

K_i = adsorption equilibrium constant of component i, 1/bar

K_{eq} = reaction equilibrium constant, bar

\dot{m}_i = mass flow rate of component i, kg/h

Mw = molecular weight, kg/kmol

n = reaction order

P_c = critical pressure, bar

P_i = partial pressure of component i in bulk fluid, bar

Pr = Prandtl number

$P_{s,i}$ = partial pressure of component i inside the catalyst, bar

P_t = total pressure, bar

R_g = gas constant, J/ (mol K)

R = radius of catalyst, m

r = radial coordinate of catalyst, m

Re = Reynolds number

r_{tj} = rate of thermal reaction j , kmol/ (m³ h)

r_{cj} = rate of catalytic reaction j , kmol/ (kgcat h)

S_i = selectivity of component i , %

Sc = Schmidt number

T_0 = temperature in bulk fluid at initial, K

T = temperature in bulk fluid, K

T_c = critical temperature, K

T_r = reduce temperature

T^s = temperature inside the catalyst, K

T_s = temperature at surface of catalyst, K

u_s = superficial velocity, m/h

X_{EB} = conversion of ethylbenzene, %

y_i = mole fraction

z = axial coordinate of reactor, m



Greek

δ = polar parameter

ϵ = minimum of the pair-potential energy, J

ϵ_B = void fraction of bed

ϵ_s = internal void fraction of catalyst

η_j = effectiveness factor of reaction j

μ = viscosity of mixture, kg/ (m h)

μ_i = viscosity of species i, kg/ (m h)

v = atomic diffusion volume

ρ_B = bulk density of bed, kgcat/m³

ρ_s = catalyst density, kgcat/m³cat

ρ_g = gas density, kgcat/m³cat

σ = hard-sphere diameter, Å

ν_{ij} = stoichiometric coefficient of component i in reaction j

Ω_v = viscosity collision integral



REFERENCES

Uncategorized References

1. Jakobsen, H.A., *Chemical Reactor Modeling – Multiphase Reactive Flows*. 2008. 1-1244.
2. Macías, M.J. and J. Ancheyta, *Simulation of an isothermal hydrodesulfurization small reactor with different catalyst particle shapes*. *Catalysis Today*, 2004. **98**(1-2): p. 243-252.
3. Brunner, K.M., et al., *Effects of Particle Size and Shape on the Performance of a Trickle Fixed-Bed Recycle Reactor for Fischer–Tropsch Synthesis*. *Industrial & Engineering Chemistry Research*, 2015. **54**(11): p. 2902-2909.
4. Froment, G.F., K.B. Bischoff, and J. De Wilde, *Chemical Reactor Analysis and Design, 3rd Edition*. 2010: John Wiley & Sons, Incorporated.
5. Iordanidis, A.A., *Mathematical modeling of catalytic fixed bed reactors*. 2002: Twente University Press Enschede, The Netherlands.
6. Schlereth, D., *Kinetic and Reactor Modeling for the Methanation of Carbon Dioxide*. 2015, Technische Universität München.
7. Kalam, M., *Modeling and Simulation of Real Reactor*. 2016.
8. Manrique, Y., et al., *Modeling and Simulation of a Packed-bed Reactor for Carrying out the Water-Gas Shift Reaction*. *International Journal of Chemical Reactor Engineering*, 2012. **10**.
9. Taran, O.P., et al., *Wet peroxide oxidation of phenol over Cu-ZSM-5 catalyst in a flow reactor. Kinetics and diffusion study*. *Chemical Engineering Journal*, 2015. **282**: p. 108-115.
10. Jae Lee, W. and G.F. Froment, *Ethylbenzene Dehydrogenation into Styrene: Kinetic Modeling and Reactor Simulation*. *Industrial & Engineering Chemistry Research*, 2008. **47**(23): p. 9183-9194.
11. Fogler, H.S., *Elements of Chemical Reaction Engineering*. 2006: Prentice Hall PTR.
12. Hill, C.G. and T.W. Root, *Introduction to Chemical Engineering Kinetics and Reactor Design*. 2014: Wiley.

13. Levenspiel, O., *Chemical reaction engineering*. 1999: Wiley.
14. Ancheyta, J., *Modeling and Simulation of Catalytic Reactors for Petroleum Refining*. 2011: Wiley.
15. Poling, B., J. Prausnitz, and J.O. Connell, *The Properties of Gases and Liquids*. 2000: McGraw-hill.
16. Yoonm, P. and G. Thodos, *Viscosity of nonpolar gaseous mixtures at normal pressures*. *AIChE Journal*, 1970. **16**(2): p. 300-304.
17. Satterfield, C.N., *Mass Transfer in Heterogeneous Catalysis*. 1970: M.I.T. Press.
18. Cussler, E.L. and E.L. Cussler, *Diffusion: Mass Transfer in Fluid Systems*. 2009: Cambridge University Press.
19. Rokhgireh, A., M. Farsi, and M. Javidi, *Steady State Modeling and Optimization of Styrene Production in an Industrial Axial Flow Adiabatic Reactor*. *Theoretical Foundations of Chemical Engineering*, 2017. **51**(6): p. 1070-1079.
20. Sheel, J.G.P. and C.M. Crowe, *Simulation and optimization of an existing ethylbenzene dehydrogenation reactor*. *The Canadian Journal of Chemical Engineering*, 1969. **47**(2): p. 183-187.
21. Clough, D.E. and W.F. Ramirez, *Mathematical modeling and optimization of the dehydrogenation of ethylbenzene to form styrene*. *AIChE Journal*, 1976. **22**(6): p. 1097-1105.
22. Sheppard, C.M., E.E. Maier, and H.S. Caram, *Ethylbenzene dehydrogenation reactor model*. *Industrial & Engineering Chemistry Process Design and Development*, 1986. **25**(1): p. 207-210.
23. Elnashaie, S.S.E.H., B.K. Abdalla, and R. Hughes, *Simulation of the industrial fixed bed catalytic reactor for the dehydrogenation of ethylbenzene to styrene: heterogeneous dusty gas model*. *Industrial & Engineering Chemistry Research*, 1993. **32**(11): p. 2537-2541.
24. Abdalla, B.K., et al., *Intrinsic kinetics and industrial reactors modelling for the dehydrogenation of ethylbenzene to styrene on promoted iron oxide catalysts*. *Applied Catalysis A: General*, 1994. **113**(1): p. 89-102.

25. Elnashaie, S., et al., *On the link between intrinsic catalytic reactions kinetics and the development of catalytic processes: Catalytic dehydrogenation of ethylbenzene to styrene*. *Catalysis today*, 2001. **64**(3-4): p. 151-162.
26. Li, Y., G.P. Rangaiah, and A.K. Ray, *Optimization of styrene reactor design for two objectives using a genetic algorithm*. *International Journal of Chemical Reactor Engineering*, 2003. **1**(1).
27. Babu, B., P.G. Chakole, and J.S. Mubeen, *Multiobjective differential evolution (MODE) for optimization of adiabatic styrene reactor*. *Chemical Engineering Science*, 2005. **60**(17): p. 4822-4837.
28. Gujarathi, A.M. and B. Babu, *Multi-objective optimization of industrial styrene reactor: Adiabatic and pseudo-isothermal operation*. *Chemical Engineering Science*, 2010. **65**(6): p. 2009-2026.
29. Fettaka, S., Y.P. Gupta, and J. Thibault, *Multiobjective optimization of an industrial styrene reactor using the dual population evolutionary algorithm (DPEA)*. *International Journal of Chemical Reactor Engineering*, 2012. **10**(1).
30. Rase, H.F., *Handbook of Commercial Catalysts: Heterogeneous Catalysts*. 2016: CRC Press.
31. Rubin, C., L. Cavalli, and E. Conca, *Catalyst for the dehydrogenation of ethylbenzene to styrene*. 2000, Google Patents.
32. Lee, W.J., *Ethylbenzene dehydrogenation into styrene: kinetic modeling and reactor simulation*, in *Chemical Engineering 2005*, Texas A&M University. p. 249.
33. Rezaie, N., et al., *A comparison of homogeneous and heterogeneous dynamic models for industrial methanol reactors in the presence of catalyst deactivation*. *Chemical Engineering and Processing: Process Intensification*, 2005. **44**(8): p. 911-921.
34. Bahrami, S., et al., *Modeling of Fixed-Bed Reactor for Hydrogenation of Acetylene in the Olefin Unit's*. *International Proceedings of Chemical, Biological and Environmental Engineering*, 2015: p. 54-58.

35. Nunoura, T., et al., *Reaction engineering model for supercritical water oxidation of phenol catalyzed by activated carbon*. Industrial & engineering chemistry research, 2003. **42**(15): p. 3522-3531.
36. *Petrochemical Processes handbook* 2014.
37. Sheppard, C.M., *Kinetic and reactor models for the ethylbenzene dehydrogenation reaction*. 1982.



Appendix A Kinetic parameter estimation

Table A1 Data of experiment [32]

No.	W/F _{eb0}	T	y _{eb0}	y _{st0}	y _{h20}	X _{H2}	X _{BZ}	X _{TO}	X _{EB}
1	15	913.15	0.0489	0	0	0.514	0.0161	0.0094	0.551
2	24	913.15	0.0489	0	0	0.653	0.0195	0.0153	0.692
3	29	913.15	0.0489	0	0	0.672	0.0214	0.0229	0.733
4	31	913.15	0.0489	0	0	0.681	0.0213	0.0236	0.741
5	37	913.15	0.0489	0	0	0.715	0.0221	0.0295	0.812
6	50	913.15	0.0489	0	0	0.73	0.0243	0.0428	0.843
7	61	913.15	0.0489	0	0	0.745	0.0265	0.0513	0.871
8	22	913.15	0.0477	0.0143	0	0.513	0.0155	0.0114	0.56
9	34	913.15	0.0477	0.0143	0	0.612	0.0197	0.0213	0.6701
10	45	913.15	0.0477	0.0143	0	0.678	0.0212	0.0302	0.742
11	58	913.15	0.0477	0.0143	0	0.699	0.0241	0.0414	0.812
12	25	913.15	0.0481	0.0096	0	0.573	0.0175	0.0147	0.634
13	42	913.15	0.0481	0.0096	0	0.675	0.0221	0.0295	0.758
14	57	913.15	0.0481	0.0096	0	0.712	0.0243	0.0432	0.831
15	22	913.15	0.0458	0	0.0367	0.541	0.0175	0.0351	0.634
16	30	913.15	0.0458	0	0.0367	0.585	0.0211	0.0545	0.715
17	43	913.15	0.0458	0	0.0367	0.626	0.0235	0.0787	0.78
18	54	913.15	0.0458	0	0.0367	0.629	0.0255	0.0901	0.836
19	26	913.15	0.047	0	0.0221	0.6	0.0197	0.0342	0.672
20	42	913.15	0.047	0	0.0221	0.671	0.023	0.0563	0.8
21	58	913.15	0.047	0	0.0221	0.678	0.0261	0.0747	0.853
22	25	913.15	0.0733	0	0	0.621	0.0232	0.0251	0.712
23	51.6	913.15	0.0733	0	0	0.694	0.0255	0.062	0.842
24	60	913.15	0.0733	0	0	0.713	0.0266	0.07	0.851
25	18.08	893.15	0.0489	0	0	0.466	0.0094	0.0052	0.472
26	29.7	893.15	0.0489	0	0	0.571	0.0122	0.0117	0.616
27	30.96	893.15	0.0489	0	0	0.581	0.0127	0.0113	0.621

No.	W/F _{eb0}	T	y _{eb0}	y _{st0}	y _{h20}	X _{H2}	X _{BZ}	X _{TO}	X _{EB}
28	36.28	893.15	0.0489	0	0	0.625	0.013	0.0135	0.651
29	36.28	893.15	0.0489	0	0	0.613	0.0132	0.0141	0.663
30	41.89	893.15	0.0489	0	0	0.631	0.0138	0.0174	0.681
31	46.77	893.15	0.0489	0	0	0.651	0.0143	0.0298	0.724
32	55.56	893.15	0.0489	0	0	0.679	0.0152	0.0262	0.747
33	57.53	893.15	0.0489	0	0	0.683	0.0154	0.0275	0.753
34	59.8	893.15	0.0489	0	0	0.69	0.0156	0.0289	0.764
35	6.5	893.15	0.0489	0	0	0.251	0.005	0.00068	0.269
36	22.02	893.15	0.0485	0.0048	0	0.46	0.0095	0.0063	0.493
37	30.13	893.15	0.0485	0.0048	0	0.535	0.0115	0.0113	0.567
38	40.05	893.15	0.0485	0.0048	0	0.582	0.0125	0.0154	0.647
39	50.23	893.15	0.0485	0.0048	0	0.641	0.0147	0.0212	0.698
40	32.43	893.15	0.0481	0.0096	0	0.511	0.0105	0.0116	0.53
41	42.45	893.15	0.0481	0.0096	0	0.565	0.0122	0.0151	0.612
42	52.12	893.15	0.0481	0.0096	0	0.6	0.0135	0.0213	0.664
43	33.28	893.15	0.0477	0.0143	0	0.47	0.0188	0.0102	0.501
44	42.19	893.15	0.0477	0.0143	0	0.521	0.0113	0.0133	0.563
45	64.3	893.15	0.0477	0.0143	0	0.624	0.0149	0.0251	0.683
46	64.3	893.15	0.0477	0.0143	0	0.618	0.0143	0.0254	0.691
47	26.82	893.15	0.0467	0	0.0266	0.521	0.0112	0.0243	0.547
48	36.27	893.15	0.0467	0	0.0266	0.55	0.0127	0.0287	0.626
49	47.11	893.15	0.0467	0	0.0266	0.589	0.0143	0.0395	0.675
50	53.21	893.15	0.0467	0	0.0266	0.611	0.0147	0.0452	0.712
51	30.12	893.15	0.0733	0	0	0.552	0.0117	0.0168	0.601
52	44.05	893.15	0.0733	0	0	0.626	0.0141	0.0255	0.682
53	58.06	893.15	0.0733	0	0	0.649	0.0153	0.0361	0.749
54	11.3	873.15	0.0489	0	0	0.268	0.0034	0.0014	0.25
55	20	873.15	0.0489	0	0	0.362	0.0057	0.0021	0.37
56	27	873.15	0.0489	0	0	0.42	0.0059	0.0037	0.443

No.	W/F _{eb0}	T	y _{eb0}	y _{st0}	y _{h20}	X _{H2}	X _{BZ}	X _{TO}	X _{EB}
57	35	873.15	0.0489	0	0	0.486	0.0069	0.0061	0.498
58	37	873.15	0.0489	0	0	0.494	0.007	0.0066	0.511
59	41	873.15	0.0489	0	0	0.522	0.0074	0.0082	0.543
60	45.14	873.15	0.0489	0	0	0.533	0.0078	0.0092	0.562
61	64	873.15	0.0489	0	0	0.613	0.0091	0.0158	0.648
62	20	873.15	0.0477	0.0143	0	0.234	0.0034	0.0015	0.25
63	30	873.15	0.0477	0.0143	0	0.321	0.0045	0.0029	0.321
64	39.43	873.15	0.0477	0.0143	0	0.371	0.0053	0.0047	0.393
65	50.01	873.15	0.0477	0.0143	0	0.433	0.0063	0.0078	0.454
66	62	873.15	0.0477	0.0143	0	0.471	0.0073	0.0105	0.493
67	23	873.15	0.0481	0.0096	0	0.356	0.0043	0.0022	0.321
68	34	873.15	0.0481	0.0096	0	0.388	0.0055	0.0046	0.412
69	45	873.15	0.0481	0.0096	0	0.449	0.0065	0.0073	0.463
70	55	873.15	0.0481	0.0096	0	0.482	0.0072	0.0113	0.516
71	22	873.15	0.0458	0	0.0367	0.323	0.0048	0.0094	0.345
72	30	873.15	0.0458	0	0.0367	0.381	0.0058	0.0143	0.416
73	36	873.15	0.0458	0	0.0367	0.41	0.0064	0.0186	0.458
74	45.31	873.15	0.0458	0	0.0367	0.452	0.0072	0.0233	0.527
75	53.47	873.15	0.0458	0	0.0367	0.481	0.0081	0.0286	0.541
76	19	873.15	0.047	0	0.0221	0.321	0.0046	0.0061	0.322
77	30	873.15	0.047	0	0.0221	0.414	0.0062	0.0114	0.43
78	40	873.15	0.047	0	0.0221	0.465	0.0072	0.0157	0.501
79	60	873.15	0.047	0	0.0221	0.539	0.0087	0.0254	0.593
80	25	873.15	0.0733	0	0	0.38	0.0058	0.0046	0.414
81	51.6	873.15	0.0733	0	0	0.521	0.0084	0.0142	0.562
82	68.3	873.15	0.0733	0	0	0.571	0.0091	0.0213	0.621

* y_{i0} = feed mole fraction of component i, X_i = fractional conversion into component i, EB = ethylbenzene, ST = styrene, H₂ = hydrogen, BZ = benzene, TO = toluene

From the experimental data shows in A1 Table, the pseudohomogeneous model is used to find the kinetic parameter which calculated less conversion error from the experiment for each temperature. The results show in Table A2.

Table A2 Parameter estimates

Parameter	Unit	Temperature [K]		
		873.15	893.15	913.15
k1	kmol/(kgcat•h)	0.130517	0.260011	0.448363
k2	kmol/(kgcat•h)	0.001793	0.004991	0.012382
k3	kmol/(kgcat•h)	0.012612	2.66E-06	0.100848
k4	kmol/(kgcat•h)	0.008067	0.037868	0.059874
KEB	1/bar	17.038	8.176689	5.74832
KST	1/bar	48.15129	30.07574	23.0579
KH2	1/bar	5.013077	3.012531	2.003256

The estimates kinetic parameters for all temperature (873.15 K, 893.15 K, and 913.15 K) show in Table A3.

Table A3 Kinetic parameter

Parameter	unit	Value
A1	kmol/(kgcat·hr)	2.33E+11
A2	kmol/(kgcat·hr)	2.65E+16
A3	kmol/(kgcat·hr)	9.01E+15
A4	kmol/(kgcat·hr)	8.54E+17
Aeb	1/bar	2.55E-10
Ast	1/bar	2.26E-06
Ah2	1/bar	3.93E-09
E1	kJ/mol	2.05E+02
E2	kJ/mol	3.20E+02
E3	kJ/mol	3.21E+02
E4	kJ/mol	3.33E+02
Heb	kJ/mol	-1.81E+02
Hst	kJ/mol	-1.22E+02
Hh2	kJ/mol	-1.52E+02

From the kinetic parameter in Table A3, they are used with the model to predict the conversion and compare with the experimental data show in Figure A1 - A3.

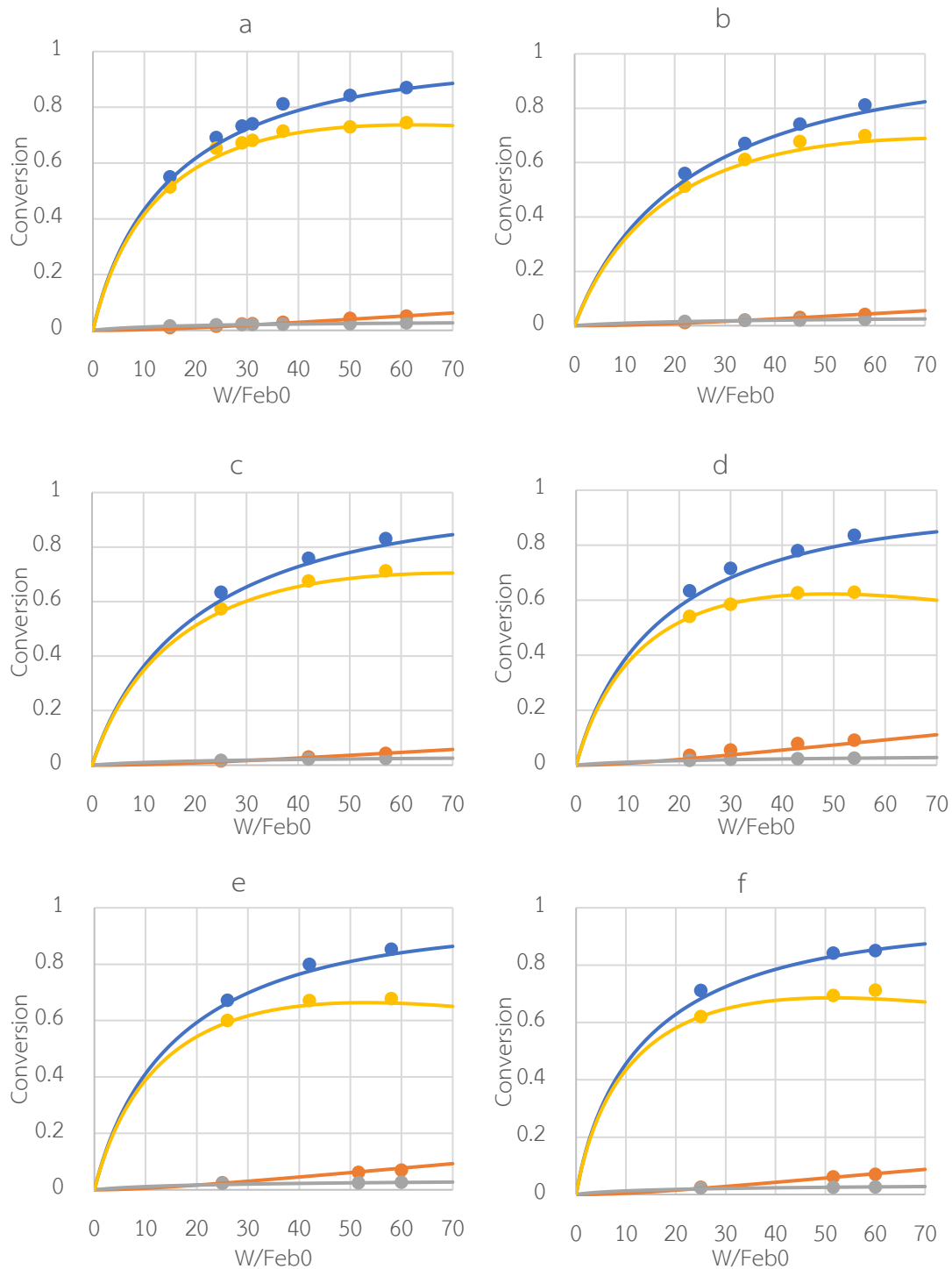


Figure A1 Comparison the simulation result (Line) and experiment data (Point) including conversion of ethylbenzene (blue), toluene (orange), benzene (grey), and hydrogen (yellow). a, b, c, d, e, and f show the comparison of experiment no.1 - 7, 8 - 11, 12 - 14, 15 - 18, 19 - 21, and 22 - 24, respectively.

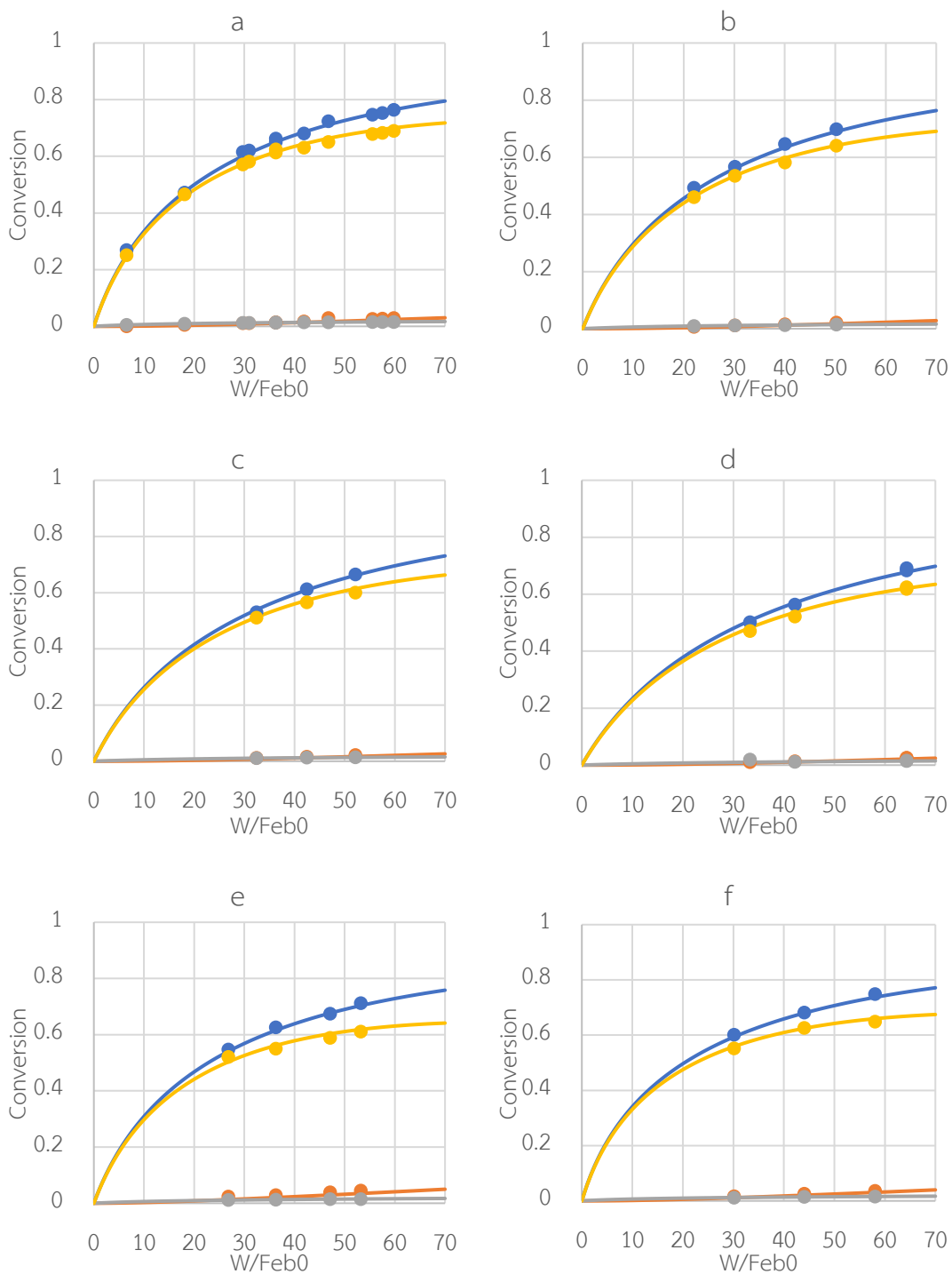


Figure A2 Comparison the simulation result (Line) and experiment data (Point) including conversion of ethylbenzene (blue), toluene (orange), benzene (grey), and hydrogen (yellow). a, b, c, d, e, and f show the comparison of experiment no.25 – 35, 36 – 39, 40 – 42, 43 – 46, 47 – 50, and 51 – 53, respectively.

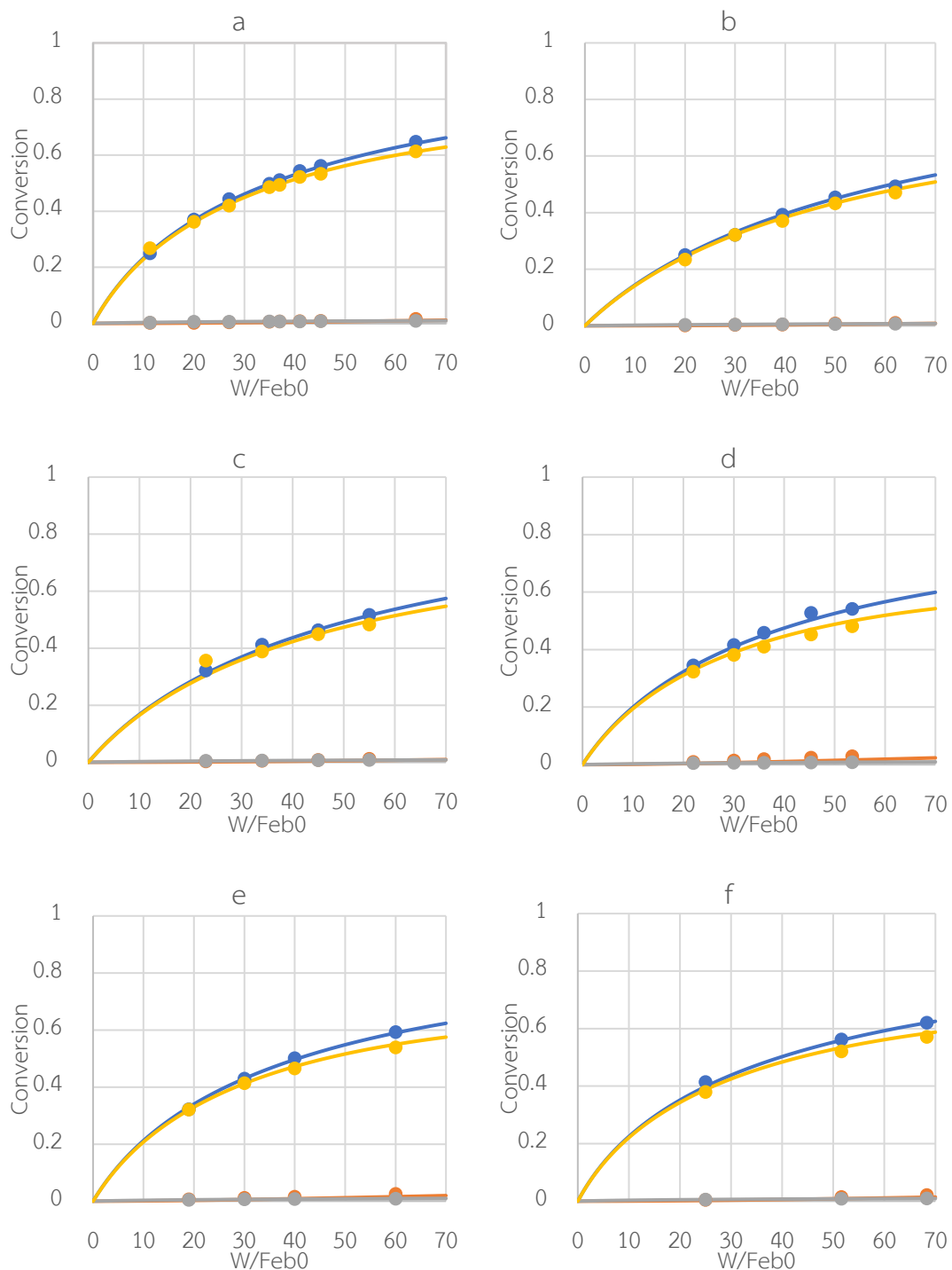


Figure A3 Comparison the simulation result (Line) and experiment data (Point) including conversion of ethylbenzene (blue), toluene (orange), benzene (grey), and hydrogen (yellow). a, b, c, d, e, and f show the comparison of experiment no.54 – 61, 62 – 66, 67 – 70, 71 – 75, 76 – 79, and 80 – 82, respectively.

From the experiment data, Lee [32] predicted the kinetic parameter, as shown in Table A4 and simulation result by use the kinetic parameter, as shown in Table A5.

Table A4 Kinetic parameter

Parameter	unit	Value
A_1	kmol/(kgcat·hr)	4.59E+09
A_2	kmol/(kgcat·hr)	1.06E+15
A_3	kmol/(kgcat·hr)	1.25E+26
A_4	kmol/(kgcat·hr)	8.02E+10
A_{eb}	1/bar	1.01E-05
A_{st}	1/bar	2.68E-05
A_{h2}	1/bar	4.52E-07
E_1	kJ/mol	175.38
E_2	kJ/mol	296.29
E_3	kJ/mol	474.76
E_4	kJ/mol	213.78
H_{eb}	kJ/mol	-102.22
H_{st}	kJ/mol	-104.56
H_{h2}	kJ/mol	-117.95

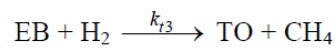
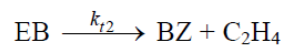
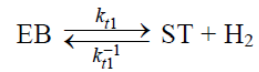
Table A5 Simulation result by the model

Output	Pseudohomogeneous model	Heterogeneous model with internal mass diffusion
X_{EB} [%]	39.25	36.89
S_{ST} [%]	98.84	98.49
S_{BZ} [%]	0.94	1
S_{TO} [%]	0.23	0.507
P_{out} [bar]	1.066	1.06
T_{out} [K]	806.2	811.36

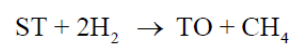
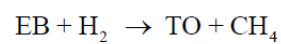
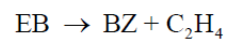
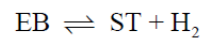
Appendix B Data for Modeling

Reaction [10]

- Thermal reaction



- Catalytic reaction



Reaction rate [10]

- Thermal reaction rate

$$r_{t1} = k_{t1} \left(P_{\text{EB}} - \frac{P_{\text{ST}} P_{\text{H}_2}}{K_{\text{eq}}} \right)$$

$$r_{t2} = k_{t2} P_{\text{EB}}$$

$$r_{t3} = k_{t3} P_{\text{EB}}$$

- Catalytic reaction rate

$$r_{c1} = \frac{k_1 K_{\text{EB}} \left(P_{\text{EB}} - \frac{P_{\text{ST}} P_{\text{H}_2}}{K_{\text{eq}}} \right)}{\left(1 + K_{\text{EB}} P_{\text{EB}} + K_{\text{H}_2} P_{\text{H}_2} + K_{\text{ST}} P_{\text{ST}} \right)^2}$$

$$r_{c2} = \frac{k_2 K_{\text{EB}} P_{\text{EB}}}{\left(1 + K_{\text{EB}} P_{\text{EB}} + K_{\text{H}_2} P_{\text{H}_2} + K_{\text{ST}} P_{\text{ST}} \right)^2}$$

$$r_{c3} = \frac{k_3 K_{\text{EB}} P_{\text{EB}} K_{\text{H}_2} P_{\text{H}_2}}{\left(1 + K_{\text{EB}} P_{\text{EB}} + K_{\text{H}_2} P_{\text{H}_2} + K_{\text{ST}} P_{\text{ST}} \right)^2}$$

$$r_{c4} = \frac{k_4 K_{\text{ST}} P_{\text{ST}} K_{\text{H}_2} P_{\text{H}_2}}{\left(1 + K_{\text{EB}} P_{\text{EB}} + K_{\text{H}_2} P_{\text{H}_2} + K_{\text{ST}} P_{\text{ST}} \right)^2}$$

Kinetic parameters

$$k_{ti} = A_{ti} e^{-\frac{E_{ati}}{RT}}$$

Table B1 Preexponential factors and activation energies of kinetic parameter for thermal reaction [10]

k_{ti}	A_{ti} [kmol/ (m _f ³ h bar)]	E_{ati} [kJ/mol]
1	2.2215×10^{16}	272.23
2	2.4217×10^{20}	352.79
3	3.8224×10^{17}	313.06

$$k_i = A_i e^{-\frac{E_{ai}}{RT}}$$

$$K_i = A_i e^{-\frac{\Delta H_{ai}}{RT}}$$

Table B2 Preexponential factors and activation energies of kinetic parameter for catalytic reaction

Parameter	unit	This Research
A_1	kmol/(kgcat·hr)	2.33E+11
A_2	kmol/(kgcat·hr)	2.65E+16
A_3	kmol/(kgcat·hr)	9.01E+15
A_4	kmol/(kgcat·hr)	8.54E+17
A_{eb}	1/bar	2.55E-10
A_{st}	1/bar	2.26E-06
A_{h2}	1/bar	3.93E-09
E_1	kJ/mol	2.05E+02
E_2	kJ/mol	3.20E+02
E_3	kJ/mol	3.21E+02
E_4	kJ/mol	3.33E+02
H_{eb}	kJ/mol	-1.81E+02
H_{st}	kJ/mol	-1.22E+02
H_{h2}	kJ/mol	-1.52E+02

$$K_{eq} = \exp\left(-\frac{\Delta G^0}{RT}\right)$$

$$\Delta G^0 = \Delta H^0 - T\Delta S^0$$

$$\Delta H^0 = \Delta H_{298}^0 + \int_{298}^T \Delta C_p^0 dT$$

$$\Delta S^0 = \Delta S_{298}^0 + \int_{298}^T \Delta C_p^0 \frac{dT}{T}$$

$$\Delta C_p^0 = \Delta a + \Delta bT + \Delta cT^2 + \Delta dT^3$$

Table B3 Constants for the specific heat, the standard heats of formation, and the standard entropy change of reaction at reference temperature [10]

EB \leftrightarrow ST+ H ₂			
Component	EB	ST	H ₂
a [kJ/kmol·K]	-43.1	-28.35	27.14
b [kJ/kmol·K ²]	707.2 × 10 ⁻³	615.9 × 10 ⁻³	9.274 × 10 ⁻³
c [kJ/kmol·K ³]	-48.11 × 10 ⁻⁵	-40.23 × 10 ⁻⁵	-1.381 × 10 ⁻⁵
d [kJ/kmol·K ⁴]	130.1 × 10 ⁻⁹	99.35 × 10 ⁻⁹	7.645 × 10 ⁻⁹
ΔH _f ⁰ [kJ/kmol]	1.307 × 10 ⁵	1.475 × 10 ⁵	-
ΔS ⁰ [kJ/kmol·K]	115.7		

Heat of reaction

$$\Delta H_{r,i} = \Delta H_{298,i}^0 + \Delta a_i(T - 298.15) + \frac{\Delta b_i}{2}(T^2 - 298.15^2) + \frac{\Delta c_i}{3}(T^3 - 298.15^3) + \frac{\Delta d_i}{4}(T^4 - 298.15^4)$$

Table B4 Constants of the specific heats of the reactions [10]

Reaction, i	1	2	3	4
Δa_i [kJ/kmol·K]	41.99	12.986	10.86	-31.13
Δb_i [kJ/kmol·K ²]	-8.2026×10^{-2}	-7.67×10^{-2}	-15.1844×10^{-2}	-6.9818×10^{-2}
Δc_i [kJ/kmol·K ³]	6.499×10^{-5}	9.592×10^{-5}	23.04×10^{-5}	16.54×10^{-5}
Δd_i [kJ/kmol·K ⁴]	-2.311×10^{-8}	-4.125×10^{-8}	-9.9955×10^{-8}	-7.685×10^{-8}
$\Delta H_{298,i}^0$ [kJ/kmol]	117690	105510	-54680	-172370

Heat capacity

$$C_{p,j} = a_j + b_j T + c_j T^2 + d_j T^3$$

Table B5 Constants of the specific heats of components [10]

Component, j	Mw [g/mol]	a [kJ/kg·K]	b [kJ/kg·K ²]	c [kJ/kg·K ³]	d [kJ/kg·K ⁴]
EB	106.16	-0.43426	6.0671×10^{-3}	-3.8625×10^{-6}	9.1282×10^{-10}
ST	104.14	-0.26436	5.564×10^{-3}	-3.0018×10^{-6}	5.3317×10^{-10}
BZ	78.11	-0.40599	6.6616×10^{-3}	-4.5318×10^{-6}	12.255×10^{-10}
TO	92.11	-0.27127	5.9142×10^{-3}	-3.8631×10^{-6}	9.54×10^{-10}
H2	2	13.57	4.637×10^{-3}	-6.905×10^{-6}	38.23×10^{-10}
H2O	18	1.7911	0.1069×10^{-3}	0.58611×10^{-6}	-1.998×10^{-10}

Binary mass diffusion coefficient i in j [15]

$$D_{ij} = \frac{0.00143T^{1.75}}{PM_{ij}^{\frac{1}{2}} \left[(\sum v)_i^{\frac{1}{3}} + (\sum v)_j^{\frac{1}{3}} \right]}$$

$$M_{ij} = 2 \left[\frac{1}{M_{w_i}} + \frac{1}{M_{w_j}} \right]^{-1}$$

Where $\sum v$ is found for each component by summing atomic diffusion volumes in Table B6.

Table B6 Atomic Diffusion Volumes

Atomic and structural diffusion volume increments	
C	15.9
H	2.31
Diffusion volumes of simple molecules	
H ₂	6.12
H ₂ O	13.1

Thermal conductivity [15]

$$k_i = \frac{3.75\psi\mu}{M/R}$$

$$\psi = 1 + \alpha$$

$$\alpha = \left(\frac{C_v}{R} \right) - \frac{3}{2}$$

$$\beta = 0.7862 - 0.7109\omega + 1.3168\omega^2$$

$$Z = 2.0 + 10.5T_r^2$$

Table B7 Molecular weights and critical constant of component

Component	Molecular weight	T _c	P _c	ω
Ethylbenzene	106.167	617.2	36.06	0.303
Styrene	104.152	636	38.4	0.297
Benzene	78.114	562.2	48.98	0.210
Toluene	92.141	591.8	41.06	0.262
Hydrogen	2.061	33.19	13.13	0.216
Water	18.015	647.1	220.55	0.345



Appendix C Result of studied effect of catalyst that same equivalent
diameter

Result spherical shape

Table C1 Output result from different model

Output result	Model3	Model4	Model5	Model6
Reactor bed length [m]	1.187	1.193	1.201	1.201
Catalyst weight [kg]	7.39E+04	7.43 E+04	7.48 E+04	7.48 E+04
Pressure drop per length of reactor [bar/m]	0.360	0.373	0.361	0.370
Effectiveness factor	0.923	0.921	0.904	0.898

Table C2 Percent different of output result from model3

%Different	Model4	Model5	Model6
Reactor bed length [m]	0.50	1.17	1.17
Catalyst weight [kg]	0.50	1.17	1.17
Pressure drop per length of reactor [bar/m]	3.66	0.31	2.67
Effectiveness factor	-0.20	-2.12	-2.68

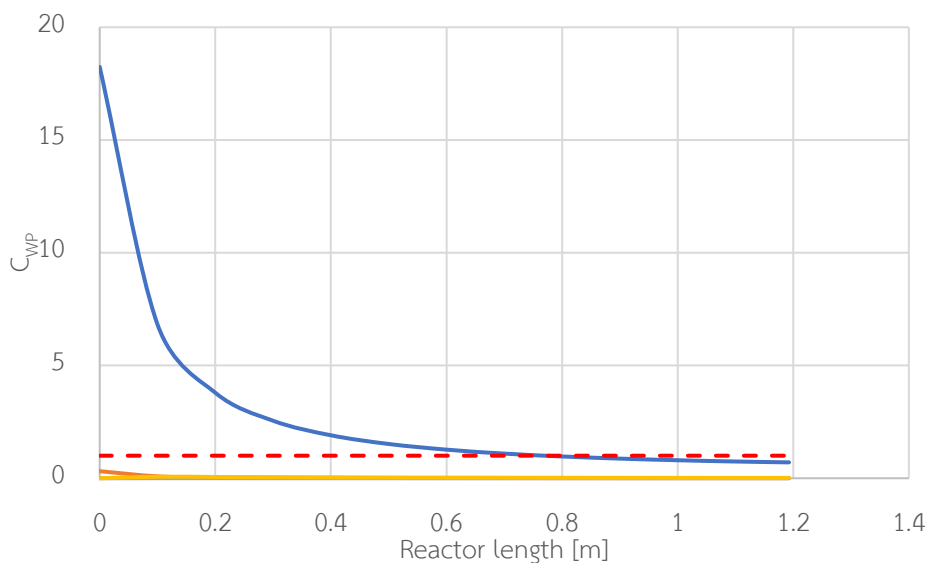


Figure C1 The value of Weisz-Prater parameter along the reactor length for reaction1 (blue), reaction2 (orange), reaction3 (grey), and reaction4 (yellow). Red line is criteria.

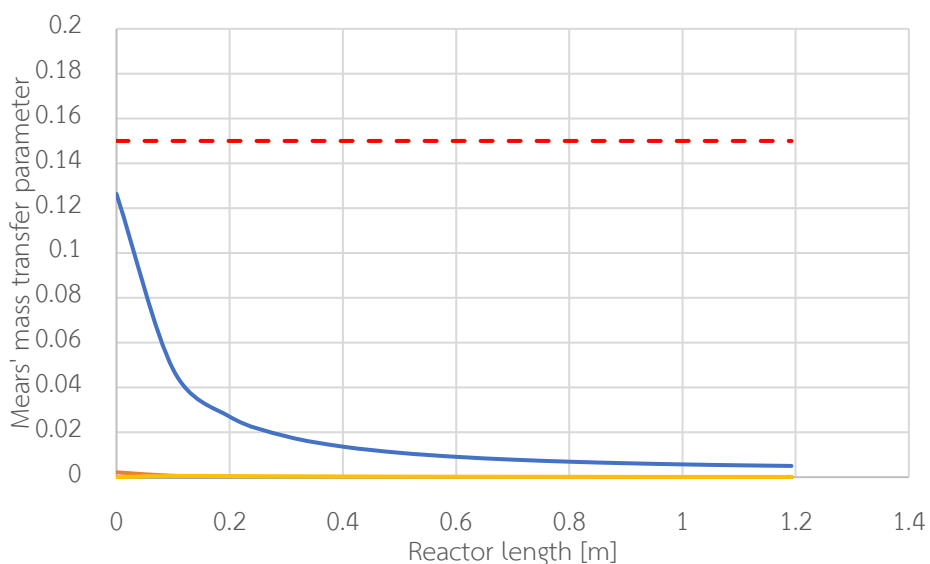


Figure C2 The absolute values of Mears' mass-transport parameter along the reactor for reaction1 (blue), reaction2 (orange), reaction3 (grey), and reaction4 (yellow). Red line is criteria.

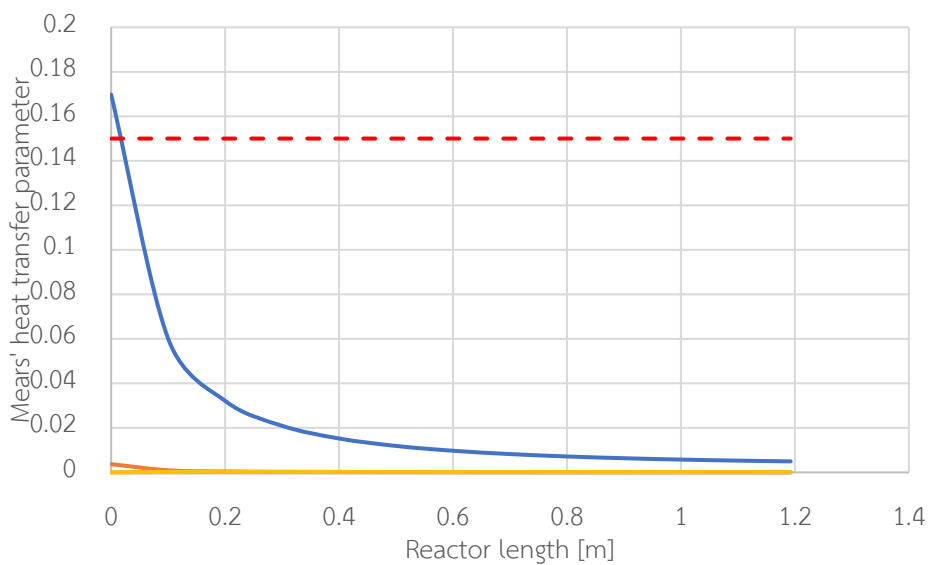


Figure C3 The absolute values of Mears' heat-transport parameter along the reactor for reaction1 (blue), reaction2 (orange), reaction3 (grey), and reaction4(yellow). Red line is criteria.

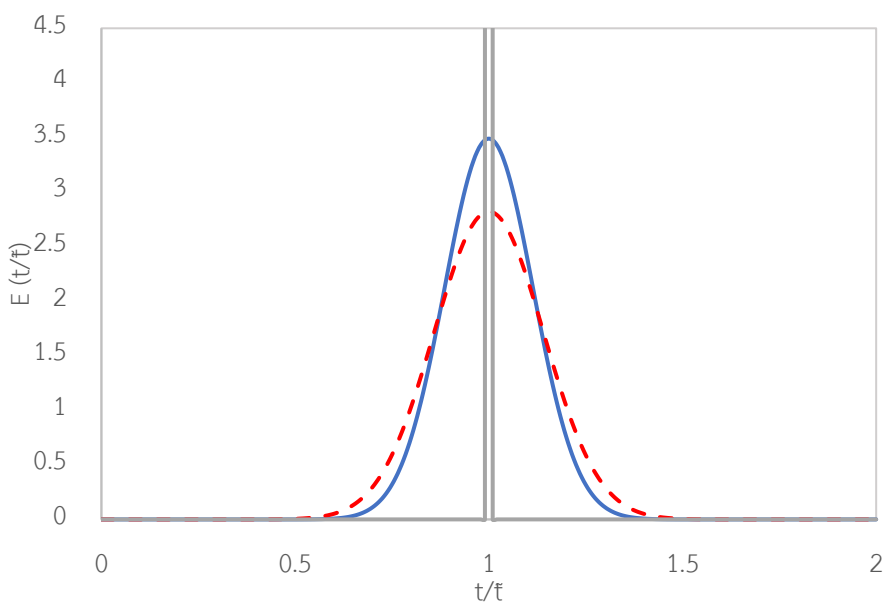


Figure C4 The residence time distribution curve of process (blue), plug flow (grey), and criteria (red), E is exit age distribution, t is actual residence time and \bar{t} is average residence time.

Result of Cylinder shape

Table C3 Output result from different model

Result output	Model3	Model4	Model5	Model6
Reactor bed length [m]	1.367	1.377	1.369	1.369
Catalyst weight [kg]	7.65E+04	7.70E+04	7.66E+04	7.66E+04
Pressure drop per length of reactor [bar/m]	0.175	0.180	0.175	0.178
Effectiveness factor	0.947	0.947	0.945	0.943

Table C4 Percent different of output result from model3

%Different	Model4	Model5	Model6
Reactor bed length [m]	0.67	0.12	0.12
Catalyst weight [kg]	0.67	0.12	0.12
Pressure drop per length of reactor [bar/m]	2.75	-0.02	1.69
Effectiveness factor	-0.09	-0.22	-0.45

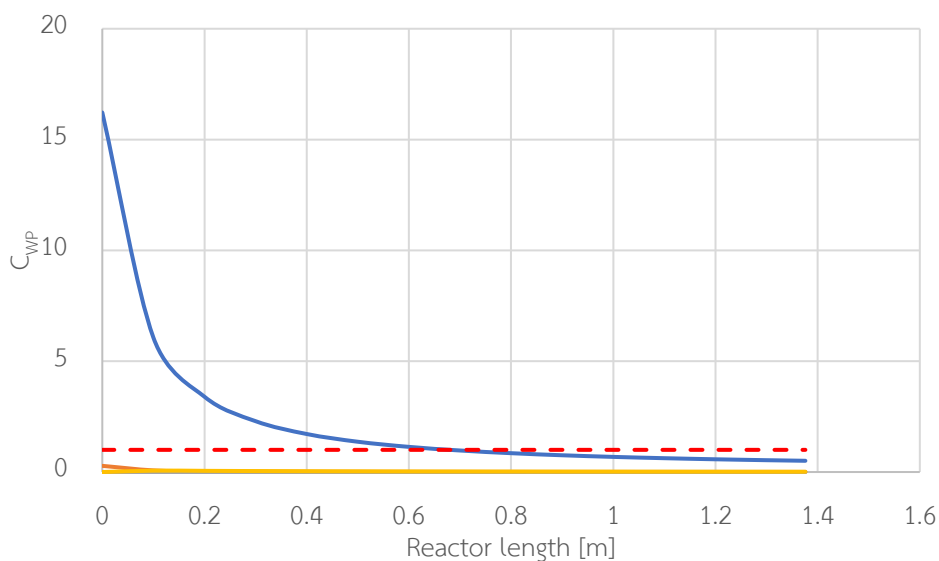


Figure C5 The value of Weisz-Prater parameter along the reactor length for reaction1 (blue), reaction2 (orange), reaction3 (grey), and reaction4 (yellow). Red line is criteria.

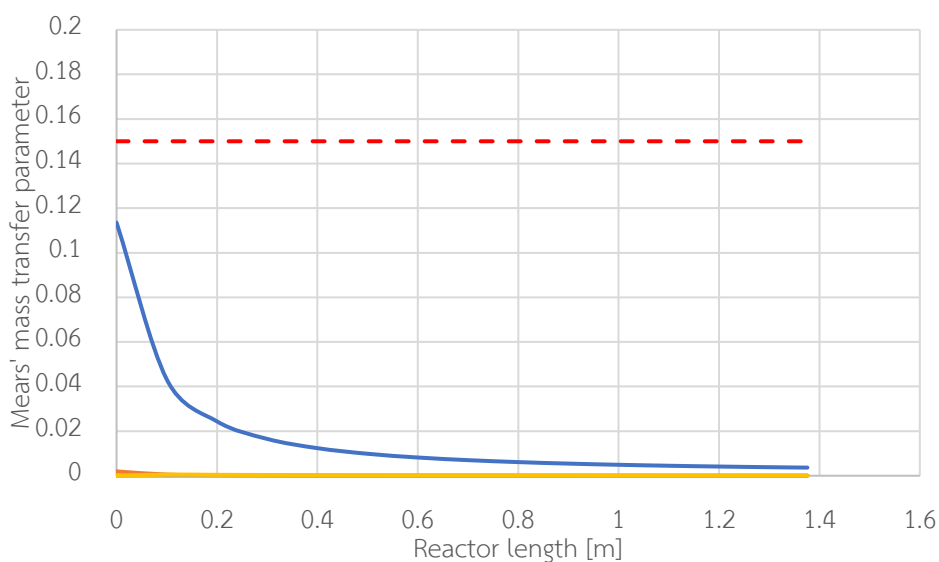


Figure C6 The absolute values of Mears' mass-transport parameter along the reactor for reaction1 (blue), reaction2 (orange), reaction3 (grey), and reaction4 (yellow). Red line is criteria.

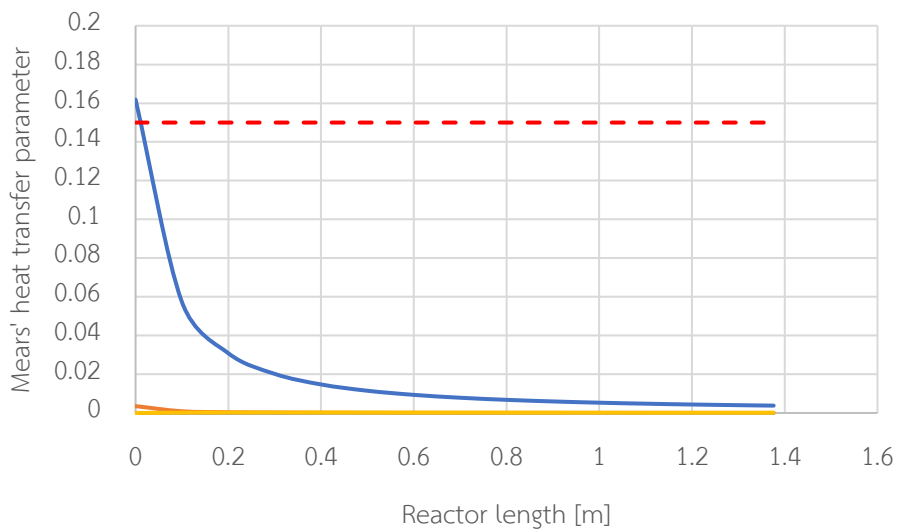


Figure C7 The absolute values of Mears' heat-transport parameter along the reactor for reaction1 (blue), reaction2 (orange), reaction3 (grey), and reaction4(yellow). Red line is criteria.

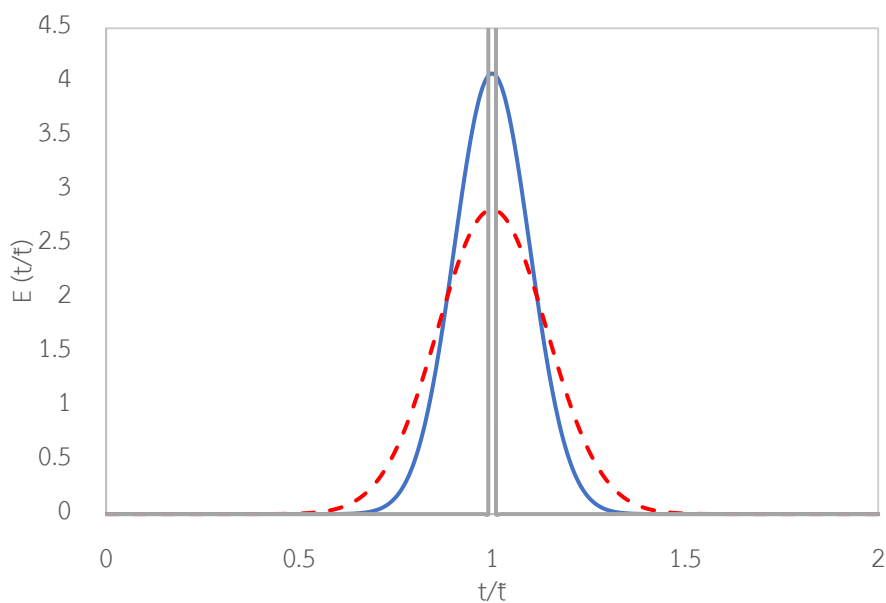


Figure C8 The residence time distribution curve of process (blue), plug flow (grey), and criteria (red), E is exit age distribution, t is actual residence time and \bar{t} is average residence time.

Result of trilobe shape

Table C5 Output result from different model

Result output	Model3	Model4	Model5	Model6
Reactor bed length [m]	1.446	1.455	1.468	1.468
Catalyst weight [kg]	7.29E+04	7.34+04	7.40+04	7.40+04
Pressure drop per length of reactor [bar/m]	0.102	0.103	0.102	0.110
Effectiveness factor	0.983	0.983	0.984	0.984

Table C6 Percent different of output result from model3

%Different	Model4	Model5	Model6
Reactor bed length [m]	0.56	1.49	1.49
Catalyst weight [kg]	0.56	1.49	1.49
Pressure drop per length of reactor [bar/m]	1.71	0.03	7.79
Effectiveness factor	-0.01	0.10	0.04

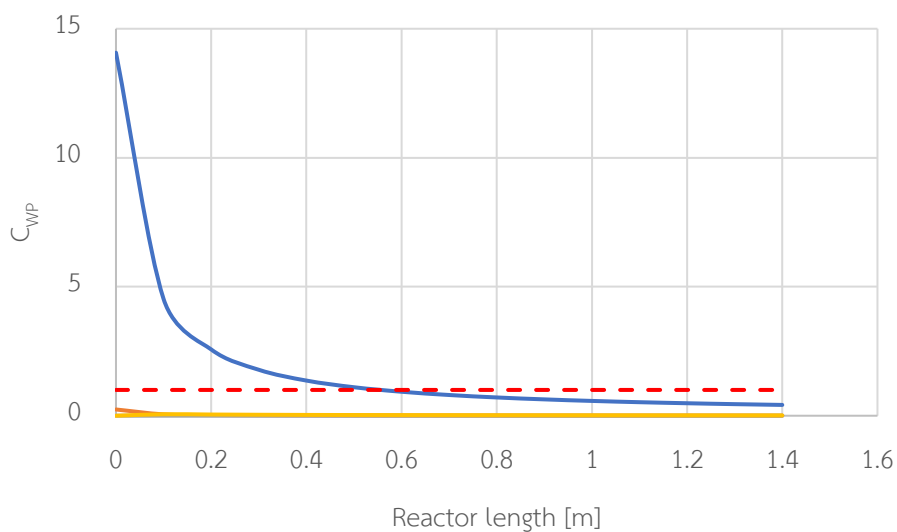


Figure C9 The value of Weisz-Prater parameter along the reactor length for reaction1 (blue), reaction2 (orange), reaction3 (grey), and reaction4 (yellow). Red line is criteria.

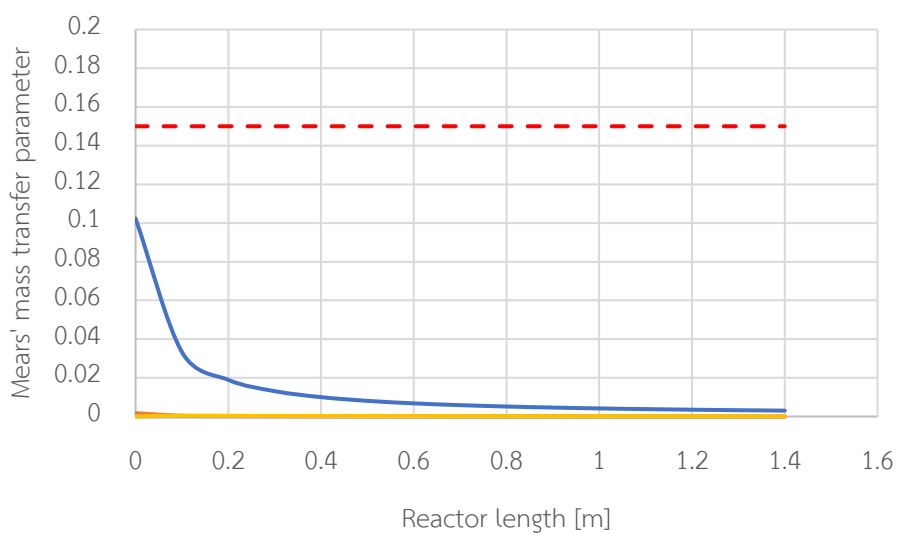


Figure C10 The absolute values of Mears' mass-transport parameter along the reactor for reaction1 (blue), reaction2 (orange), reaction3 (grey), and reaction4(yellow). Red line is criteria.

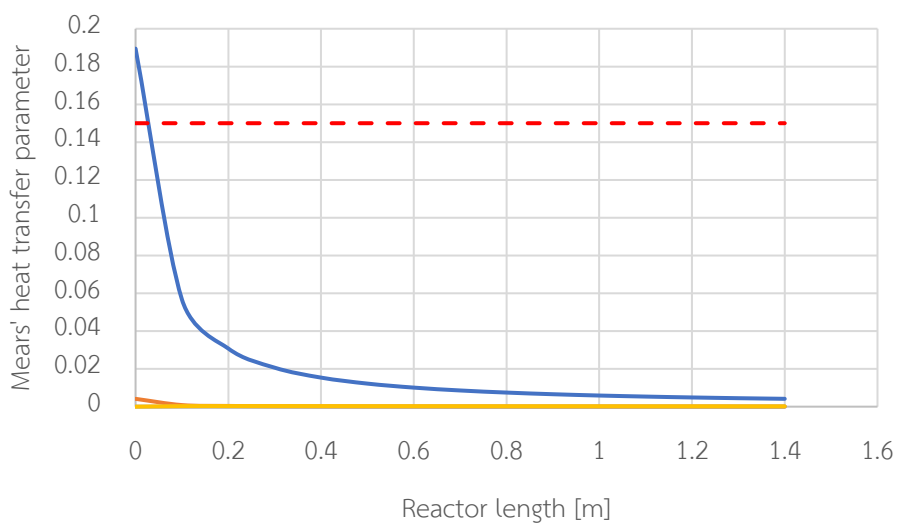


Figure C11 The absolute values of Mears' heat-transport parameter along the reactor for reaction1 (blue), reaction2 (orange), reaction3 (grey), and reaction4(yellow). Red line is criteria.

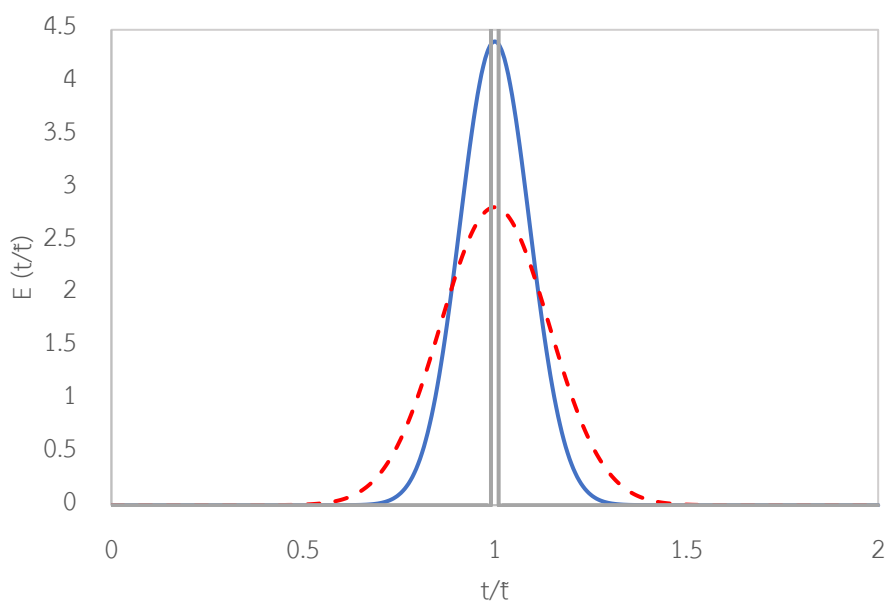


Figure C12 The residence time distribution curve of process (blue), plug flow (grey), and criteria (red), E is exit age distribution, t is actual residence time and τ is average residence time.

Appendix D Result of studied effect of commercial catalyst

Result of Sphere

Table D1 Output result from different model

Result output	Model2	Model3	Model4	Model5
Reactor bed length [m]	1.187	1.193	1.201	1.201
Catalyst weight [kg]	7.39E+04	7.43 E+04	7.48 E+04	7.48 E+04
Pressure drop per length of reactor [bar/m]	0.360	0.373	0.361	0.370
Effectiveness factor	0.923	0.921	0.904	0.898

Result of Cylinder

Table D2 Output result from different model

Result output	Model2	Model3	Model4	Model5
Reactor bed length [m]	1.246	1.251	1.261	1.258
Catalyst weight [kg]	7.37 E+04	7.40 E+04	7.46 E+04	7.44 E+04
Pressure drop per length of reactor [bar/m]	0.324	0.335	0.331479	0.324259
Effectiveness factor	0.930	0.929	0.910749	0.914973

Result of Trilobe

Table D3 Output result from different model

Result output	Model2	Model3	Model4	Model5
Reactor bed length [m]	1.290349	1.300001	1.301	1.301
Catalyst weight [kg]	7.28 E+04	7.33 E+04	7.34 E+04	7.34 E+04
Pressure drop per length of reactor [bar/m]	0.200667	0.20563	0.204078	0.200795
Effectiveness factor	0.965876	0.965457	0.962806	0.964115

Appendix E Fixed bed reactor model code

The following code is described in Chapter3 and was developed in EQUATRAN program.

1. Model1 : Pseudohomogeneous model

EQUATRAN code:

```
//Mass balance
us*Ceb'+us'*Ceb = -(rc1+rc2+rc3)*densityB-(rt1+rt2+rt3)*voidB ;Ceb#Ceb0
us*Cst'+us'*Cst = (rc1-rc4)*densityB+(rt1)*voidB ;Cst#Cst0
us*Cbz'+us'*Cbz = (rc2)*densityB+(rt2)*voidB ;Cbz#Cbz0
us*Cto'+us'*Cto = (rc3+rc4)*densityB+(rt3)*voidB ;Cto#Cto0
us*Ch2'+us'*Ch2 = (rc1-rc3-2*rc4)*densityB+(rt1-rt3)*voidB ;Ch2#Ch20
us'=R*(10^(-2))/Ac*((P*(Ft*T'+T*Ft')-T*Ft*P')/P^2) ;us#us0
Ft'/Ac = (rc1+rc2-rc4)*densityB+(rt1+rt2)*voidB ;Ft#Ft0

//Energy balance
(meb*Cpeb+mst*Cpst+mbz*Cpbz+mto*Cpto+mh2*Cph2+mh2o*Cph2o)/Ac*T'=(-rc1
*densityB+rt1*voidB)*HRX1-(rc2*densityB+rt2*voidB)*HRX2-(rc3*densityB
+rt3*voidB)*HRX3-rc4*densityB*HRX4) ;T#T0

//Momentum balance
P'*10^5 = -f*us*G/dp/3600^2 ;P#P0
f = (1-voidB)/voidB^3*(1.75+150*(1-voidB)/Re)

//Reaction
rc1 = kc1*KEB*(Peb-Pst*Ph2/Keq)/(1+KEB*Peb+KH2*Ph2+KST*Pst)^2
rc2 = kc2*KEB*Peb/(1+KEB*Peb+KH2*Ph2+KST*Pst)^2
rc3 = kc3*KEB*Peb*KH2*Ph2/(1+KEB*Peb+KH2*Ph2+KST*Pst)^2
rc4 = kc4*KST*Pst*KH2*Ph2/(1+KEB*Peb+KH2*Ph2+KST*Pst)^2
rt1 = kt1*(Peb-Pst*Ph2/Keq)
rt2 = kt2*Peb
rt3 = kt3*Peb
kc1 = A1*exp(-E1*10^3/R/T) ;A1=2.33293E+11 ;E1=204.6619326
kc2 = A2*exp(-E2*10^3/R/T) ;A2=2.65416E+16 ;E2=320.3544359
kc3 = A3*exp(-E3*10^3/R/T) ;A3=9.00967E+15 ;E3=320.9687204
kc4 = A4*exp(-E4*10^3/R/T) ;A4=8.53675E+17 ;E4=333.4837164
KEB = Aeb*exp(-Heb*10^3/R/T) ;Aeb=2.55449E-10 ;Heb=-180.5057701
KST = Ast*exp(-Hst*10^3/R/T) ;Ast=2.26449E-06 ;Hst=-122.2609362
KH2 = Ah2*exp(-Hh2*10^3/R/T) ;Ah2=3.92807E-09 ;Hh2=-152.1129516
kt1 = At1*exp(-Et1*10^3/R/T) ;At1=2.2215*10^16 ;Et1=272.23
kt2 = At2*exp(-Et2*10^3/R/T) ;At2=2.4217*10^20 ;Et2=352.79
kt3 = At3*exp(-Et3*10^3/R/T) ;At3=3.8224*10^17 ;Et3=313.06
Keq = exp(-deltaG/R/T)
deltaG = deltaH - T*deltaS
deltaH = deltaH0+deltaa*(T-298.15)+deltab/2*(T^2-298.15^2)+deltac/3*(T^3-
298.15^3)+deltad/4*(T^4-298.15^4)
deltaS = deltaS0+deltaa*loge(T/298.15)+deltab*(T-298.15)+deltac/2*(T^2-
298.15^2)+deltad/3*(T^3-298.15^3)
deltaH0= (1.475-0.2981)*10^5
deltaS0= 115.7
deltaa = -28.25+27.14+43.1 ;deltab=(615.9+9.274-707.2)*10^(-3)
;deltac=(-40.23-1.381+48.11)*10^(-5);deltad=(99.35+7.645-130.1)*10^(-9)
R = 8.314
```

```

HRX1 = HRX10+deltaa1*(T-298.15)+deltab1/2*(T^2-298.15^2)+deltac1/3*(T^3-
298.15^3)+deltad1/4*(T^4-298.15^4)
HRX2 = HRX20+deltaa2*(T-298.15)+deltab2/2*(T^2-298.15^2)+deltac2/3*(T^3-
298.15^3)+deltad2/4*(T^4-298.15^4)
HRX3 = HRX30+deltaa3*(T-298.15)+deltab3/2*(T^2-298.15^2)+deltac3/3*(T^3-
298.15^3)+deltad3/4*(T^4-298.15^4)
HRX4 = HRX40+deltaa4*(T-298.15)+deltab4/2*(T^2-298.15^2)+deltac4/3*(T^3-
298.15^3)+deltad4/4*(T^4-298.15^4)
HRX10=117690 ;deltaa1=41.99 ;deltab1=-8.2026*10^(-2)
;deltac1=6.499*10^(-5) ;deltad1=-2.311*10^(-8)
HRX20=105510 ;deltaa2=12.986 ;deltab2=-7.67*10^(-2)
;deltac2=9.592*10^(-5) ;deltad2=-4.125*10^(-8)
HRX30=-54680 ;deltaa3=10.86 ;deltab3=-15.1844*10^(-2)
;deltac3=23.04*10^(-5) ;deltad3=-9.9955*10^(-8)
HRX40=-172370 ;deltaa4=-31.13 ;deltab4=-6.9818*10^(-2)
;deltac4=16.54*10^(-5) ;deltad4=-7.685*10^(-8)

//Bed properties
voidB = 1-densityB/densityS
densityB = 1422
densityS = 2500
dp = 0.0055
Ac = _pi*rb^2
rb = 3.5
Lb = 1.33

//Properties of component
MWeb = 106.167
MWst = 104.151
MWbz = 78.113
MWto = 92.14
MWh2 = 2.016
MWh2o= 18.015
MWc1 = 16.043
MWc2 = 28.054

Cpeb = aeb+beb*T+ceb*T^2+deb*T^3 ;aeb=-0.43426
;beb=6.0671*10^(-3) ;ceb=-3.8625*10^(-6) ;deb=9.1282*10^(-10)
Cpst = ast+bst*T+cst*T^2+dst*T^3 ;ast=-0.26436
;bst=5.564*10^(-3) ;cst=-3.0018*10^(-6) ;dst=5.3317*10^(-10)
Cpbz = abz+bbz*T+cbz*T^2+dbz*T^3 ;abz=-0.40599
;bbz=6.6616*10^(-3) ;cbz=-4.5318*10^(-6) ;dbz=12.255*10^(-10)
Cpto = ato+bto*T+cto*T^2+dto*T^3 ;ato=-0.27127
;bto=5.9142*10^(-3) ;cto=-3.8631*10^(-6) ;dto=9.54*10^(-10)
Cph2 = ah2+bh2*T+ch2*T^2+dh2*T^3 ;ah2=13.57
;bh2=4.637*10^(-3) ;ch2=-6.905*10^(-6) ;dh2=38.23*10^(-10)
Cph2o= ah2o+bh2o*T+ch2o*T^2+dh2o*T^3;ah2o=1.79111
;bh2o=0.1069*10^(-3);ch2o=0.58611*10^(-6) ;dh2o=-1.998*10^(-10)

//Properties of fluid
v0 = Ft0*R*T0/P0*10^(-2)
us0= v0/Ac
Re = feedden0*dp*us0/(vis*3600)
us = v/Ac
G = feedden0*v0/Ac
feedden0 = (Feb0*MWeb+Fst0*MWst+Fbz0*MWbz+Fto0*MWto+Fh20*MWh2+Fh2o0*MWh2o
+Fc10*MWc1+Fc20*MWc2)/v0
vis=y1*vis1/(y1*phi11+y2*phi12+y3*phi13+y4*phi14+y5*phi15+y6*phi16)+y2*vis2/
(y1*phi21+y2*phi22+y3*phi23+y4*phi24+y5*phi25+y6*phi26)+y3*vis3/(y1*phi31+y2
*phi32+y3*phi33+y4*phi34+y5*phi35+y6*phi36)+y4*vis4/(y1*phi41+y2*phi42+y3*ph

```

```

i43+y4*phi44+y5*phi45+y6*phi46)+y5*vis5/(y1*phi51+y2*phi52+y3*phi53+y4*phi54
+y5*phi55+y6*phi56)+y6*vis6/(y1*phi61+y2*phi62+y3*phi63+y4*phi64+y5*phi65+y6
*phi66)
vis1=10^(-7)*(4.61*Tr1^0.618-2.04*exp(-0.449*Tr1)+1.94*exp(-4.058*Tr1)+0.1)
/(Tc1^(1/6)*MW1^(-1/2)*Pc1^(-2/3)) ;Tr1=T/Tc1 ;Tc1=617.2
;MW1=106.16 ;Pc1=36 //EB
vis2=10^(-7)*(4.61*Tr2^0.618-2.04*exp(-0.449*Tr2)+1.94*exp(-4.058*Tr2)+0.1)
/(Tc2^(1/6)*MW2^(-1/2)*Pc2^(-2/3)) ;Tr2=T/Tc2 ;Tc2=647.0
;MW2=104.14 ;Pc2=39.9 //ST
vis3=10^(-7)*(4.61*Tr3^0.618-2.04*exp(-0.449*Tr3)+1.94*exp(-4.058*Tr3)+0.1)
/(Tc3^(1/6)*MW3^(-1/2)*Pc3^(-2/3)) ;Tr3=T/Tc3 ;Tc3=562.2 ;MW3=78.11
;Pc3=48.9 //BZ
vis4=10^(-7)*(4.61*Tr4^0.618-2.04*exp(-0.449*Tr4)+1.94*exp(-4.058*Tr4)+0.1)
/(Tc4^(1/6)*MW4^(-1/2)*Pc4^(-2/3)) ;Tr4=T/Tc4 ;Tc4=591.8 ;MW4=92.11
;Pc4=41 //TO
vis5=10^(-7)*26.69*sqrt(MW5*T)/sigma5^2/omega5 ;MW5=2 ;sigma5=2.827
;omega5=1.16145/(T5)^0.14874+0.52487*exp(-0.77320*T5)+2.16178*exp(-
2.43787*T5) ;T5=T/59.7 //H2
vis6=10^(-7)*26.69*sqrt(MW6*T)/sigma6^2/omega62 ;MW6=18 ;sigma6=2.641
;omega6=1.16145/(T6)^0.14874+0.52487*exp(-0.77320*T6)+2.16178*exp(-
2.43787*T6) ;T6=T/809.1 ;omega62=omega6+0.2/T6 //H2O
phi11=(1+(vis1/vis1)^(1/2)*(MW1/MW1)^(1/4))^2/(8*(1+MW1/MW1))^(1/2)
phi12=(1+(vis1/vis2)^(1/2)*(MW2/MW1)^(1/4))^2/(8*(1+MW1/MW2))^(1/2)
phi13=(1+(vis1/vis3)^(1/2)*(MW3/MW1)^(1/4))^2/(8*(1+MW1/MW3))^(1/2)
phi14=(1+(vis1/vis4)^(1/2)*(MW4/MW1)^(1/4))^2/(8*(1+MW1/MW4))^(1/2)
phi15=(1+(vis1/vis5)^(1/2)*(MW5/MW1)^(1/4))^2/(8*(1+MW1/MW5))^(1/2)
phi16=(1+(vis1/vis6)^(1/2)*(MW6/MW1)^(1/4))^2/(8*(1+MW1/MW6))^(1/2)
phi21=(1+(vis2/vis1)^(1/2)*(MW1/MW2)^(1/4))^2/(8*(1+MW2/MW1))^(1/2)
phi22=(1+(vis2/vis2)^(1/2)*(MW2/MW2)^(1/4))^2/(8*(1+MW2/MW2))^(1/2)
phi23=(1+(vis2/vis3)^(1/2)*(MW3/MW2)^(1/4))^2/(8*(1+MW2/MW3))^(1/2)
phi24=(1+(vis2/vis4)^(1/2)*(MW4/MW2)^(1/4))^2/(8*(1+MW2/MW4))^(1/2)
phi25=(1+(vis2/vis5)^(1/2)*(MW5/MW2)^(1/4))^2/(8*(1+MW2/MW5))^(1/2)
phi26=(1+(vis2/vis6)^(1/2)*(MW6/MW2)^(1/4))^2/(8*(1+MW2/MW6))^(1/2)
phi31=(1+(vis3/vis1)^(1/2)*(MW1/MW3)^(1/4))^2/(8*(1+MW3/MW1))^(1/2)
phi32=(1+(vis3/vis2)^(1/2)*(MW2/MW3)^(1/4))^2/(8*(1+MW3/MW2))^(1/2)
phi33=(1+(vis3/vis3)^(1/2)*(MW3/MW3)^(1/4))^2/(8*(1+MW3/MW3))^(1/2)
phi34=(1+(vis3/vis4)^(1/2)*(MW4/MW3)^(1/4))^2/(8*(1+MW3/MW4))^(1/2)
phi35=(1+(vis3/vis5)^(1/2)*(MW5/MW3)^(1/4))^2/(8*(1+MW3/MW5))^(1/2)
phi36=(1+(vis3/vis6)^(1/2)*(MW6/MW3)^(1/4))^2/(8*(1+MW3/MW6))^(1/2)
phi41=(1+(vis4/vis1)^(1/2)*(MW1/MW4)^(1/4))^2/(8*(1+MW4/MW1))^(1/2)
phi42=(1+(vis4/vis2)^(1/2)*(MW2/MW4)^(1/4))^2/(8*(1+MW4/MW2))^(1/2)
phi43=(1+(vis4/vis3)^(1/2)*(MW3/MW4)^(1/4))^2/(8*(1+MW4/MW3))^(1/2)
phi44=(1+(vis4/vis4)^(1/2)*(MW4/MW4)^(1/4))^2/(8*(1+MW4/MW4))^(1/2)
phi45=(1+(vis4/vis5)^(1/2)*(MW5/MW4)^(1/4))^2/(8*(1+MW4/MW5))^(1/2)
phi46=(1+(vis4/vis6)^(1/2)*(MW6/MW4)^(1/4))^2/(8*(1+MW4/MW6))^(1/2)
phi51=(1+(vis5/vis1)^(1/2)*(MW1/MW5)^(1/4))^2/(8*(1+MW5/MW1))^(1/2)
phi52=(1+(vis5/vis2)^(1/2)*(MW2/MW5)^(1/4))^2/(8*(1+MW5/MW2))^(1/2)
phi53=(1+(vis5/vis3)^(1/2)*(MW3/MW5)^(1/4))^2/(8*(1+MW5/MW3))^(1/2)
phi54=(1+(vis5/vis4)^(1/2)*(MW4/MW5)^(1/4))^2/(8*(1+MW5/MW4))^(1/2)
phi55=(1+(vis5/vis5)^(1/2)*(MW5/MW5)^(1/4))^2/(8*(1+MW5/MW5))^(1/2)
phi56=(1+(vis5/vis6)^(1/2)*(MW6/MW5)^(1/4))^2/(8*(1+MW5/MW6))^(1/2)
phi61=(1+(vis6/vis1)^(1/2)*(MW1/MW6)^(1/4))^2/(8*(1+MW6/MW1))^(1/2)
phi62=(1+(vis6/vis2)^(1/2)*(MW2/MW6)^(1/4))^2/(8*(1+MW6/MW2))^(1/2)
phi63=(1+(vis6/vis3)^(1/2)*(MW3/MW6)^(1/4))^2/(8*(1+MW6/MW3))^(1/2)
phi64=(1+(vis6/vis4)^(1/2)*(MW4/MW6)^(1/4))^2/(8*(1+MW6/MW4))^(1/2)
phi65=(1+(vis6/vis5)^(1/2)*(MW5/MW6)^(1/4))^2/(8*(1+MW6/MW5))^(1/2)
phi66=(1+(vis6/vis6)^(1/2)*(MW6/MW6)^(1/4))^2/(8*(1+MW6/MW6))^(1/2)

```

```
//Feed
Feb0 = 707
Fst0 = 7.104
Fbz0 = 0.293
Fto0 = 4.968
Fh20 = 0
Fh2o0= 7777
Fc10 = 0
Fc20 = 0
Ft0 = Feb0+Fst0+Fbz0+Fto0+Fh20+Fh2o0+Fc10+Fc20
P0 = 1.25
T0 = 886
```

```
//Profile
Feb = Feb0*(1-XEB)
Fst = Fst0+Feb0*XST
Fbz = Fbz0+Feb0*XBZ
Fto = Fto0+Feb0*XTO
Fh2 = Fh20+Feb0*XH2
Fc1 = Fc10+Feb0*XTO
Fc2 = Fc20+Feb0*XBZ
```

```
Peb = Feb/Ft*P
Pst = Fst/Ft*P
Ph2 = Fh2/Ft*P
Pbz = Fbz/Ft*P
Pto = Fto/Ft*P
```

```
Ceb = Feb/v
Cst = Fst/v
Ch2 = Fh2/v
Cbz = Fbz/v
Cto = Fto/v
```

```
Ceb0 = Feb0/v0
Cst0 = Fst0/v0
Ch20 = Fh20/v0
Cbz0 = Fbz0/v0
Cto0 = Fto0/v0
```

```
mEb = MWeb*Feb
mSt = MWst*Fst
mBz = MWbz*Fbz
mTo = MWto*Fto
mH2 = MWh2*Fh2
mH2o= MWh2o*Fh2o0
mC1 = MWc1*Fc1
mC2 = MWc2*Fc2
mT = mEb+mSt+mBz+mH2+mTo+mC1+mC2+mH2o
```

```
y1=Feb/Ft
y2=Fst/Ft
y3=Fbz/Ft
y4=Fto/Ft
y5=Fh2/Ft
y6=Fh2o0/Ft
```



```
//Result
SST = XST/XEB*100
SBZ = XBZ/XEB*100
STO = XTO/XEB*100

integral z[0,Lb]
output XEB,SST,SBZ,STO,P,T
```

Result:

```
<< results >>
XEB      = 0.365168
SST      = 98.33506
SBZ      = 1.058546
STO      = 0.606362
P        = 1.046159
T        = 822.5684
```



2. Model2 : Heterogeneous model account for internal mass transfer

EQUATRAN code:

```

function diffus(Cseb0,Csst0,Csbz0,Csto0,Csh20,T0,P;Cseb,Csst,Csbz,Csto,Csh2
,rc1s,rc2s,rc3s,rc4s,rt1s,rt2s,rt3s,rc1sT,rc2sT,rc3sT,rc4sT)
Deebs*Cseb'+Cseb'*2/r*Deebs+Cseb'*Deebs'= (densityS*(rc1s+rc2s+rc3s)
+voidcat*(rt1s+rt2s+rt3s)) ;Cseb#Cseb0 ;Cseb'#0
Dests*Csst'+Csst'*2/r*Dests+Csst'*Dests'= -(densityS*(rc1s-rc4s)+voidcat
*(rt1s)) ;Csst#Csst0 ;Csst'#0
Debzs*Csbz'+Csbz'*2/r*Debzs+Csbz'*Debzs'= -(densityS*(rc2s)+voidcat*(rt2s))
;Csbz#Csbz0 ;Csbz'#0
Detos*Csto'+Csto'*2/r*Detos+Csto'*Detos'= -(densityS*(rc3s+rc4s)+voidcat
*(rt3s)) ;Csto#Csto0 ;Csto'#0
Deh2s*Csh2'+Csh2'*2/r*Deh2s+Csh2'*Deh2s'= -(densityS*(rc1s-rc3s-2*rc4s)
+voidcat*(rt1s-rt3s)) ;Csh2#Csh20 ;Csh2'#0

T'=0
T#T0

rc1sT' = (rc1s*densityS+rt1s*voidcat)*4*_pi*r^2 ;rc1sT#0
rc2sT' = (rc2s*densityS+rt2s*voidcat)*4*_pi*r^2 ;rc2sT#0
rc3sT' = (rc3s*densityS+rt3s*voidcat)*4*_pi*r^2 ;rc3sT#0
rc4sT' = rc4s*densityS*4*_pi*r^2 ;rc4sT#0

Cseb = Pseb/R/T*10^2
Csst = Psst/R/T*10^2
Csh2 = Psh2/R/T*10^2
Csbz = Psbz/R/T*10^2
Csto = Psto/R/T*10^2

Cseb0 = Pseb0/R/T0*10^2
Csst0 = Psst0/R/T0*10^2
Csh20 = Psh20/R/T0*10^2
Csbz0 = Psbz0/R/T0*10^2
Csto0 = Psto0/R/T0*10^2

rc1s = kc1*KEB*(Pseb-Psst*Psh2/Keq)/(1+KEB*Pseb+KH2*Psh2+KST*Psst)^2
rc2s = kc2*KEB*Pseb/(1+KEB*Pseb+KH2*Psh2+KST*Psst)^2
rc3s = kc3*KEB*Pseb*KH2*Psh2/(1+KEB*Pseb+KH2*Psh2+KST*Psst)^2
rc4s = kc4*KST*Psst*KH2*Psh2/(1+KEB*Pseb+KH2*Psh2+KST*Psst)^2
rt1s = kt1*(Pseb-Psst*Psh2/Keq)
rt2s = kt2*Pseb
rt3s = kt3*Pseb
kc1 = A1*exp(-E1*10^3/R/T) ;A1=2.33293E+11 ;E1=204.6619326
kc2 = A2*exp(-E2*10^3/R/T) ;A2=2.65416E+16 ;E2=320.3544359
kc3 = A3*exp(-E3*10^3/R/T) ;A3=9.00967E+15 ;E3=320.9687204
kc4 = A4*exp(-E4*10^3/R/T) ;A4=8.53675E+17 ;E4=333.4837164
KEB = Aeb*exp(-Heb*10^3/R/T) ;Aeb=2.55449E-10 ;Heb=-180.5057701
KST = Ast*exp(-Hst*10^3/R/T) ;Ast=2.26449E-06 ;Hst=-122.2609362
KH2 = Ah2*exp(-Hh2*10^3/R/T) ;Ah2=3.92807E-09 ;Hh2=-152.1129516
kt1 = At1*exp(-Et1*10^3/R/T) ;At1=2.2215*10^16 ;Et1=272.23
kt2 = At2*exp(-Et2*10^3/R/T) ;At2=2.4217*10^20 ;Et2=352.79
kt3 = At3*exp(-Et3*10^3/R/T) ;At3=3.8224*10^17 ;Et3=313.06
Keq = exp(-deltaG/R/T)
deltaG = deltaH - T*deltaS
deltaH = deltaH0+deltaa*(T-298.15)+deltab/2*(T^2-298.15^2)+deltac/3*(T^3-
298.15^3)+deltad/4*(T^4-298.15^4)
deltaS = deltaS0+deltaa*log_e(T/298.15)+deltab*(T-298.15)+deltac/2*(T^2-

```

```

298.15^2)+deltad/3*(T^3-298.15^3)
deltaH0= (1.475-0.2981)*10^5
deltaS0= 115.7
deltaa = -28.25+27.14+43.1 ;deltab=(615.9+9.274-707.2)*10^(-3)
;deltac=(-40.23-1.381+48.11)*10^(-5) ;deltad=(99.35+7.645-130.1)*10^(-9)
R = 8.314

```

```

Deebs' = voidcat/tor/10000*3600*(1-y1)/(y2/D12+y3/D13+y4/D14+y5/D15+y6/D16)
*1.75*T^(0.75)*T' ;Deebs#Deebs0
Dests' = voidcat/tor/10000*3600*(1-y2)/(y1/D21+y3/D23+y4/D24+y5/D25+y6/D26)
*1.75*T^(0.75)*T' ;Dests#Dests0
Debzs' = voidcat/tor/10000*3600*(1-y3)/(y1/D31+y2/D32+y4/D34+y5/D35+y6/D36)
*1.75*T^(0.75)*T' ;Debzs#Debzs0
Detos' = voidcat/tor/10000*3600*(1-y4)/(y1/D41+y2/D42+y3/D43+y5/D45+y6/D46)
*1.75*T^(0.75)*T' ;Detos#Detos0
Deh2s' = voidcat/tor/10000*3600*(1-y5)/(y1/D51+y2/D52+y3/D53+y4/D54+y6/D56)
*1.75*T^(0.75)*T' ;Deh2s#Deh2s0
Deebs0 = voidcat/tor/10000*3600*(1-y10)/(y20/D12+y30/D13+y40/D14+y50/D15
+y60/D16)*T0^1.75
Dests0 = voidcat/tor/10000*3600*(1-y20)/(y10/D21+y30/D23+y40/D24+y50/D25
+y60/D26)*T0^1.75
Debzs0 = voidcat/tor/10000*3600*(1-y30)/(y10/D31+y20/D32+y40/D34+y50/D35
+y60/D36)*T0^1.75
Detos0 = voidcat/tor/10000*3600*(1-y40)/(y10/D41+y20/D42+y30/D43+y50/D45
+y60/D46)*T0^1.75
Deh2s0 = voidcat/tor/10000*3600*(1-y50)/(y10/D51+y20/D52+y30/D53+y40/D54
+y60/D56)*T0^1.75
y10=Pseb0/P ;y20=Psst0/P ;y30=Psbz0/P ;y40=Psto0/P ;y50=Psh20/P
;y60=1-y10-y20-y30-y40-y50
y1=Pseb/P ;y2=Psst/P ;y3=Psbz/P ;y4=Psto/P ;y5=Psh2/P
;y6=1-y1-y2-y3-y4-y5
v1=132 ;v2=127.38 ;v3=90.96 ;v4=111.48 ;v5=6.12 ;v6=13.1
M1=106.16 ;M2=104.14 ;M3=78.11 ;M4=92.11 ;M5=2 ;M6=18
D12= 0.00143/P/M12^(1/2)/(v1^(1/3)+v2^(1/3))^2 ;M12 = 2*(1/M1+1/M2)^(-1)
D13= 0.00143/P/M13^(1/2)/(v1^(1/3)+v3^(1/3))^2 ;M13 = 2*(1/M1+1/M3)^(-1)
D14= 0.00143/P/M14^(1/2)/(v1^(1/3)+v4^(1/3))^2 ;M14 = 2*(1/M1+1/M4)^(-1)
D15= 0.00143/P/M15^(1/2)/(v1^(1/3)+v5^(1/3))^2 ;M15 = 2*(1/M1+1/M5)^(-1)
D16= 0.00143/P/M16^(1/2)/(v1^(1/3)+v6^(1/3))^2 ;M16 = 2*(1/M1+1/M6)^(-1)
D21= 0.00143/P/M21^(1/2)/(v2^(1/3)+v1^(1/3))^2 ;M21 = 2*(1/M2+1/M1)^(-1)
D23= 0.00143/P/M23^(1/2)/(v2^(1/3)+v3^(1/3))^2 ;M23 = 2*(1/M2+1/M3)^(-1)
D24= 0.00143/P/M24^(1/2)/(v2^(1/3)+v4^(1/3))^2 ;M24 = 2*(1/M2+1/M4)^(-1)
D25= 0.00143/P/M25^(1/2)/(v2^(1/3)+v5^(1/3))^2 ;M25 = 2*(1/M2+1/M5)^(-1)
D26= 0.00143/P/M26^(1/2)/(v2^(1/3)+v6^(1/3))^2 ;M26 = 2*(1/M2+1/M6)^(-1)
D31= 0.00143/P/M31^(1/2)/(v3^(1/3)+v1^(1/3))^2 ;M31 = 2*(1/M3+1/M1)^(-1)
D32= 0.00143/P/M32^(1/2)/(v3^(1/3)+v2^(1/3))^2 ;M32 = 2*(1/M3+1/M2)^(-1)
D34= 0.00143/P/M34^(1/2)/(v3^(1/3)+v4^(1/3))^2 ;M34 = 2*(1/M3+1/M4)^(-1)
D35= 0.00143/P/M35^(1/2)/(v3^(1/3)+v5^(1/3))^2 ;M35 = 2*(1/M3+1/M5)^(-1)
D36= 0.00143/P/M36^(1/2)/(v3^(1/3)+v6^(1/3))^2 ;M36 = 2*(1/M3+1/M6)^(-1)
D41= 0.00143/P/M41^(1/2)/(v4^(1/3)+v1^(1/3))^2 ;M41 = 2*(1/M4+1/M1)^(-1)
D42= 0.00143/P/M42^(1/2)/(v4^(1/3)+v2^(1/3))^2 ;M42 = 2*(1/M4+1/M2)^(-1)
D43= 0.00143/P/M43^(1/2)/(v4^(1/3)+v3^(1/3))^2 ;M43 = 2*(1/M4+1/M3)^(-1)
D45= 0.00143/P/M45^(1/2)/(v4^(1/3)+v5^(1/3))^2 ;M45 = 2*(1/M4+1/M5)^(-1)
D46= 0.00143/P/M46^(1/2)/(v4^(1/3)+v6^(1/3))^2 ;M46 = 2*(1/M4+1/M6)^(-1)
D51= 0.00143/P/M51^(1/2)/(v5^(1/3)+v1^(1/3))^2 ;M51 = 2*(1/M5+1/M1)^(-1)
D52= 0.00143/P/M52^(1/2)/(v5^(1/3)+v2^(1/3))^2 ;M52 = 2*(1/M5+1/M2)^(-1)
D53= 0.00143/P/M53^(1/2)/(v5^(1/3)+v3^(1/3))^2 ;M53 = 2*(1/M5+1/M3)^(-1)
D54= 0.00143/P/M54^(1/2)/(v5^(1/3)+v4^(1/3))^2 ;M54 = 2*(1/M5+1/M4)^(-1)
D56= 0.00143/P/M56^(1/2)/(v5^(1/3)+v6^(1/3))^2 ;M56 = 2*(1/M5+1/M6)^(-1)

```

```

densityS = 2500
voidcat = 0.4
tor = 3

integral r[0.0000001,0.00275]
END

//Solid phase
diffus (Cseb0, Csst0, Csbz0, Csto0, Csh20, T, P, Ceb, Cst, Cbz, Cto, Ch2, rcl1s, rc2s, rc3s,
rc4s, rtl1s, rt2s, rt3s, rcl1T, rc2sT, rc3sT, rc4sT)
eta1 = rcl1sT/((rcl1s*densityS+rtl1s*voidcat)*4/3*_pi*rp^3)
eta2 = rc2sT/((rc2s*densityS+rt2s*voidcat)*4/3*_pi*rp^3)
eta3 = rc3sT/((rc3s*densityS+rt3s*voidcat)*4/3*_pi*rp^3)
eta4 = rc4sT/(rc4s*densityS*4/3*_pi*rp^3)

//Gas phase
//Mass balance
us*Ceb'+us'*Ceb = -(eta1*rcl1+eta2*rc2+eta3*rc3)*densityB-(rt1+rt2+rt3)*voidB
;Ceb#Ceb0
us*Cst'+us'*Cst = (eta1*rcl1-eta4*rc4)*densityB+(rt1)*voidB
;Cst#Cst0
us*Cbz'+us'*Cbz = (eta2*rc2)*densityB+(rt2)*voidB
;Cbz#Cbz0
us*Cto'+us'*Cto = (eta3*rc3+eta4*rc4)*densityB+(rt3)*voidB
;Cto#Cto0
us*Ch2'+us'*Ch2 = (eta1*rcl1-eta3*rc3-2*eta4*rc4)*densityB+(rt1-rt3)*voidB
;Ch2#Ch20
us'=R*(10^(-2))/Ac*((P*(Ft*T'+T*Ft')-T*Ft*P')/P^2)
;us#us0
Ft'/Ac = (eta1*rcl1+eta2*rc2-eta4*rc4)*densityB+(rt1+rt2)*voidB
;Ft#Ft0

//Energy balance
(meb*Cpeb+mst*Cpst+mbz*Cpbz+mto*Cpto+mh2*Cph2+mh2o*Cph2o)/Ac*T'=(-
(eta1*rcl1*densityB+rt1*voidB)*HRX1-(eta2*rc2*densityB+rt2*voidB)*HRX2-
(eta3*rc3*densityB+rt3*voidB)*HRX3-eta4*rc4*densityB*HRX4)
;T#T0

//Momentum balance
P'*10^5 = -f*us*G/dp/3600^2
;P#P0
f = (1-voidB)/voidB^3*(1.75+150*(1-voidB)/Re)

//Reaction
rc1 = kc1*KEB*(Peb-Pst*Ph2/Keq)/(1+KEB*Peb+KH2*Ph2+KST*Pst)^2
rc2 = kc2*KEB*Peb/(1+KEB*Peb+KH2*Ph2+KST*Pst)^2
rc3 = kc3*KEB*Peb*KH2*Ph2/(1+KEB*Peb+KH2*Ph2+KST*Pst)^2
rc4 = kc4*KST*Pst*KH2*Ph2/(1+KEB*Peb+KH2*Ph2+KST*Pst)^2
rt1 = kt1*(Peb-Pst*Ph2/Keq)
rt2 = kt2*Peb
rt3 = kt3*Peb
kc1 = A1*exp(-E1*10^3/R/T)
;A1=2.33293E+11
;E1=204.6619326
kc2 = A2*exp(-E2*10^3/R/T)
;A2=2.65416E+16
;E2=320.3544359
kc3 = A3*exp(-E3*10^3/R/T)
;A3=9.00967E+15
;E3=320.9687204
kc4 = A4*exp(-E4*10^3/R/T)
;A4=8.53675E+17
;E4=333.4837164
KEB = Aeb*exp(-Heb*10^3/R/T)
;Aeb=2.55449E-10
;Heb=-180.5057701
KST = Ast*exp(-Hst*10^3/R/T)
;Ast=2.26449E-06
;Hst=-122.2609362
KH2 = Ah2*exp(-Hh2*10^3/R/T)
;Ah2=3.92807E-09
;Hh2=-152.1129516
kt1 = At1*exp(-Et1*10^3/R/T)
;At1=2.2215*10^16
;Et1=272.23
kt2 = At2*exp(-Et2*10^3/R/T)
;At2=2.4217*10^20
;Et2=352.79
kt3 = At3*exp(-Et3*10^3/R/T)
;At3=3.8224*10^17
;Et3=313.06
Keq = exp(-deltaG/R/T)
deltaG = deltaH - T*deltaS
deltaH = deltaH0+deltaa*(T-298.15)+deltab/2*(T^2-298.15^2)+deltac/3*(T^3-
298.15^3)+deltad/4*(T^4-298.15^4)
deltaS = deltaS0+deltaa*loge(T/298.15)+deltab*(T-298.15)+deltac/2*(T^2-
298.15^2)+deltad/3*(T^3-298.15^3)

```

```

deltaH0= (1.475-0.2981)*10^5
deltaS0= 115.7
deltaa = -28.25+27.14+43.1 ;deltab=(615.9+9.274-707.2)*10^(-3)
;deltac=(-40.23-1.381+48.11)*10^(-5) ;deltad=(99.35+7.645-130.1)*10^(-9)
R = 8.314

HRX1 = HRX10+deltaa1*(T-298.15)+deltab1/2*(T^2-298.15^2)+deltac1/3*(T^3-
298.15^3)+deltad1/4*(T^4-298.15^4)
HRX2 = HRX20+deltaa2*(T-298.15)+deltab2/2*(T^2-298.15^2)+deltac2/3*(T^3-
298.15^3)+deltad2/4*(T^4-298.15^4)
HRX3 = HRX30+deltaa3*(T-298.15)+deltab3/2*(T^2-298.15^2)+deltac3/3*(T^3-
298.15^3)+deltad3/4*(T^4-298.15^4)
HRX4 = HRX40+deltaa4*(T-298.15)+deltab4/2*(T^2-298.15^2)+deltac4/3*(T^3-
298.15^3)+deltad4/4*(T^4-298.15^4)
HRX10=117690 ;deltaa1=41.99 ;deltab1=-8.2026*10^(-2)
;deltac1=6.499*10^(-5) ;deltad1=-2.311*10^(-8)
HRX20=105510 ;deltaa2=12.986 ;deltab2=-7.67*10^(-2)
;deltac2=9.592*10^(-5) ;deltad2=-4.125*10^(-8)
HRX30=-54680 ;deltaa3=10.86 ;deltab3=-15.1844*10^(-2)
;deltac3=23.04*10^(-5) ;deltad3=-9.9955*10^(-8)
HRX40=-172370 ;deltaa4=-31.13 ;deltab4=-6.9818*10^(-2)
;deltac4=16.54*10^(-5) ;deltad4=-7.685*10^(-8)

//Bed properties
voidB = 1-densityB/densityS
densityB = 1422
densityS = 2500
voidcat = 0.4
dp = 0.0055
rp = dp/2
Ac = _pi*rb^2
rb = 3.5
Lb = 1.33

//Properties of component
MWeb = 106.167
MWst = 104.151
MWbz = 78.113
MWto = 92.14
MWh2 = 2.016
MWh2o= 18.015
MWc1 = 16.043
MWc2 = 28.054

Cpeb = aeb+beb*T+ceb*T^2+deb*T^3 ;aeb=-0.43426
;beb=6.0671*10^(-3) ;ceb=-3.8625*10^(-6) ;deb=9.1282*10^(-10)
Cpst = ast+bst*T+cst*T^2+dst*T^3 ;ast=-0.26436
;bst=5.564*10^(-3) ;cst=-3.0018*10^(-6) ;dst=5.3317*10^(-10)
Cpbz = abz+bbz*T+cbz*T^2+dbz*T^3 ;abz=-0.40599
;bbz=6.6616*10^(-3) ;cbz=-4.5318*10^(-6) ;dbz=12.255*10^(-10)
Cpto = ato+bto*T+cto*T^2+dto*T^3 ;ato=-0.27127
;bto=5.9142*10^(-3) ;cto=-3.8631*10^(-6) ;dto=9.54*10^(-10)
Cph2 = ah2+bh2*T+ch2*T^2+dh2*T^3 ;ah2=13.57
;bh2=4.637*10^(-3) ;ch2=-6.905*10^(-6) ;dh2=38.23*10^(-10)
Cph2o= ah2o+bh2o*T+ch2o*T^2+dh2o*T^3 ;ah2o=1.79111
;bh2o=0.1069*10^(-3) ;ch2o=0.58611*10^(-6) ;dh2o=-1.998*10^(-10)

//Properties of fluid
v0 = Ft0*R*T0/P0*10^(-2)
us0= v0/Ac

```

```

Re = feedden0*dp*us0/(vis*3600)
us = v/Ac
G = feedden0*v0/Ac
feedden0 =
(Feb0*MWeb+Fst0*MWst+Fbz0*MWbz+Fto0*MWto+Fh20*MWh2+Fh2o0*MWh2o+Fc10*MWc1+Fc2
0*MWc2)/v0
vis=y1*vis1/(y1*phi11+y2*phi12+y3*phi13+y4*phi14+y5*phi15+y6*phi16)+y2*vis2/
(y1*phi21+y2*phi22+y3*phi23+y4*phi24+y5*phi25+y6*phi26)+y3*vis3/(y1*phi31+y2
*phi32+y3*phi33+y4*phi34+y5*phi35+y6*phi36)+y4*vis4/(y1*phi41+y2*phi42+y3*ph
i43+y4*phi44+y5*phi45+y6*phi46)+y5*vis5/(y1*phi51+y2*phi52+y3*phi53+y4*phi54
+y5*phi55+y6*phi56)+y6*vis6/(y1*phi61+y2*phi62+y3*phi63+y4*phi64+y5*phi65+y6
*phi66)
vis1=10^(-7)*(4.61*Tr1^0.618-2.04*exp(-0.449*Tr1)+1.94*exp(-
4.058*Tr1)+0.1)/(Tc1^(1/6)*MW1^(-1/2)*Pc1^(-2/3)) ;Tr1=T/Tc1 ;Tc1=617.2
;MW1=106.16 ;Pc1=36 //EB
vis2=10^(-7)*(4.61*Tr2^0.618-2.04*exp(-0.449*Tr2)+1.94*exp(-
4.058*Tr2)+0.1)/(Tc2^(1/6)*MW2^(-1/2)*Pc2^(-2/3)) ;Tr2=T/Tc2 ;Tc2=647.0
;MW2=104.14 ;Pc2=39.9 //ST
vis3=10^(-7)*(4.61*Tr3^0.618-2.04*exp(-0.449*Tr3)+1.94*exp(-
4.058*Tr3)+0.1)/(Tc3^(1/6)*MW3^(-1/2)*Pc3^(-2/3)) ;Tr3=T/Tc3 ;Tc3=562.2
;MW3=78.11 ;Pc3=48.9 //BZ
vis4=10^(-7)*(4.61*Tr4^0.618-2.04*exp(-0.449*Tr4)+1.94*exp(-
4.058*Tr4)+0.1)/(Tc4^(1/6)*MW4^(-1/2)*Pc4^(-2/3)) ;Tr4=T/Tc4 ;Tc4=591.8
;MW4=92.11 ;Pc4=41 //TO
vis5=10^(-7)*26.69*sqrt(MW5*T)/sigma5^2/omega5 ;MW5=2 ;sigma5=2.827
;omega5=1.16145/(T5)^0.14874+0.52487*exp(-0.77320*T5)+2.16178*exp(-
2.43787*T5) ;T5=T/59.7 //H2
vis6=10^(-7)*26.69*sqrt(MW6*T)/sigma6^2/omega62 ;MW6=18
;sigma6=2.641 ;omega6=1.16145/(T6)^0.14874+0.52487*exp(-0.77320*T6)
+2.16178*exp(-2.43787*T6) ;T6=T/809.1 ;omega62=omega6+0.2/T6 //H20
phi11=(1+(vis1/vis1)^(1/2)*(MW1/MW1)^(1/4))^2/(8*(1+MW1/MW1))^(1/2)
phi12=(1+(vis1/vis2)^(1/2)*(MW2/MW1)^(1/4))^2/(8*(1+MW1/MW2))^(1/2)
phi13=(1+(vis1/vis3)^(1/2)*(MW3/MW1)^(1/4))^2/(8*(1+MW1/MW3))^(1/2)
phi14=(1+(vis1/vis4)^(1/2)*(MW4/MW1)^(1/4))^2/(8*(1+MW1/MW4))^(1/2)
phi15=(1+(vis1/vis5)^(1/2)*(MW5/MW1)^(1/4))^2/(8*(1+MW1/MW5))^(1/2)
phi16=(1+(vis1/vis6)^(1/2)*(MW6/MW1)^(1/4))^2/(8*(1+MW1/MW6))^(1/2)
phi21=(1+(vis2/vis1)^(1/2)*(MW1/MW2)^(1/4))^2/(8*(1+MW2/MW1))^(1/2)
phi22=(1+(vis2/vis2)^(1/2)*(MW2/MW2)^(1/4))^2/(8*(1+MW2/MW2))^(1/2)
phi23=(1+(vis2/vis3)^(1/2)*(MW3/MW2)^(1/4))^2/(8*(1+MW2/MW3))^(1/2)
phi24=(1+(vis2/vis4)^(1/2)*(MW4/MW2)^(1/4))^2/(8*(1+MW2/MW4))^(1/2)
phi25=(1+(vis2/vis5)^(1/2)*(MW5/MW2)^(1/4))^2/(8*(1+MW2/MW5))^(1/2)
phi26=(1+(vis2/vis6)^(1/2)*(MW6/MW2)^(1/4))^2/(8*(1+MW2/MW6))^(1/2)
phi31=(1+(vis3/vis1)^(1/2)*(MW1/MW3)^(1/4))^2/(8*(1+MW3/MW1))^(1/2)
phi32=(1+(vis3/vis2)^(1/2)*(MW2/MW3)^(1/4))^2/(8*(1+MW3/MW2))^(1/2)
phi33=(1+(vis3/vis3)^(1/2)*(MW3/MW3)^(1/4))^2/(8*(1+MW3/MW3))^(1/2)
phi34=(1+(vis3/vis4)^(1/2)*(MW4/MW3)^(1/4))^2/(8*(1+MW3/MW4))^(1/2)
phi35=(1+(vis3/vis5)^(1/2)*(MW5/MW3)^(1/4))^2/(8*(1+MW3/MW5))^(1/2)
phi36=(1+(vis3/vis6)^(1/2)*(MW6/MW3)^(1/4))^2/(8*(1+MW3/MW6))^(1/2)
phi41=(1+(vis4/vis1)^(1/2)*(MW1/MW4)^(1/4))^2/(8*(1+MW4/MW1))^(1/2)
phi42=(1+(vis4/vis2)^(1/2)*(MW2/MW4)^(1/4))^2/(8*(1+MW4/MW2))^(1/2)
phi43=(1+(vis4/vis3)^(1/2)*(MW3/MW4)^(1/4))^2/(8*(1+MW4/MW3))^(1/2)
phi44=(1+(vis4/vis4)^(1/2)*(MW4/MW4)^(1/4))^2/(8*(1+MW4/MW4))^(1/2)
phi45=(1+(vis4/vis5)^(1/2)*(MW5/MW4)^(1/4))^2/(8*(1+MW4/MW5))^(1/2)
phi46=(1+(vis4/vis6)^(1/2)*(MW6/MW4)^(1/4))^2/(8*(1+MW4/MW6))^(1/2)
phi51=(1+(vis5/vis1)^(1/2)*(MW1/MW5)^(1/4))^2/(8*(1+MW5/MW1))^(1/2)
phi52=(1+(vis5/vis2)^(1/2)*(MW2/MW5)^(1/4))^2/(8*(1+MW5/MW2))^(1/2)
phi53=(1+(vis5/vis3)^(1/2)*(MW3/MW5)^(1/4))^2/(8*(1+MW5/MW3))^(1/2)
phi54=(1+(vis5/vis4)^(1/2)*(MW4/MW5)^(1/4))^2/(8*(1+MW5/MW4))^(1/2)
phi55=(1+(vis5/vis5)^(1/2)*(MW5/MW5)^(1/4))^2/(8*(1+MW5/MW5))^(1/2)
phi56=(1+(vis5/vis6)^(1/2)*(MW6/MW5)^(1/4))^2/(8*(1+MW5/MW6))^(1/2)

```

```

phi61=(1+(vis6/vis1)^(1/2)*(MW1/MW6)^(1/4))^2/(8*(1+MW6/MW1))^(1/2)
phi62=(1+(vis6/vis2)^(1/2)*(MW2/MW6)^(1/4))^2/(8*(1+MW6/MW2))^(1/2)
phi63=(1+(vis6/vis3)^(1/2)*(MW3/MW6)^(1/4))^2/(8*(1+MW6/MW3))^(1/2)
phi64=(1+(vis6/vis4)^(1/2)*(MW4/MW6)^(1/4))^2/(8*(1+MW6/MW4))^(1/2)
phi65=(1+(vis6/vis5)^(1/2)*(MW5/MW6)^(1/4))^2/(8*(1+MW6/MW5))^(1/2)
phi66=(1+(vis6/vis6)^(1/2)*(MW6/MW6)^(1/4))^2/(8*(1+MW6/MW6))^(1/2)

```

```
//Feed
```

```

Feb0 = 707
Fst0 = 7.104
Fbz0 = 0.293
Fto0 = 4.968
Fh20 = 0
Fh2o0= 7777
Fc10 = 0
Fc20 = 0
Ft0 = Feb0+Fst0+Fbz0+Fto0+Fh20+Fh2o0+Fc10+Fc20
P0 = 1.25
T0 = 886

```

```
//Profile
```

```

Feb = Feb0*(1-XEB)
Fst = Fst0+Feb0*XST
Fbz = Fbz0+Feb0*XBZ
Fto = Fto0+Feb0*XTO
Fh2 = Fh20+Feb0*XH2
Fc1 = Fc10+Feb0*XTO
Fc2 = Fc20+Feb0*XBZ

```

```

Peb = Feb/Ft*P
Pst = Fst/Ft*P
Ph2 = Fh2/Ft*P
Pbz = Fbz/Ft*P
Pto = Fto/Ft*P

```

```

Ceb = Feb/v
Cst = Fst/v
Ch2 = Fh2/v
Cbz = Fbz/v
Cto = Fto/v

```

```

Ceb0 = Feb0/v0
Cst0 = Fst0/v0
Ch20 = Fh20/v0
Cbz0 = Fbz0/v0
Cto0 = Fto0/v0

```

```

meb = MWeb*Feb
mst = MWst*Fst
mbz = MWbz*Fbz
mto = MWto*Fto
mh2 = MWh2*Fh2
mh2o= MWh2o*Fh2o0
mc1 = Mwc1*Fc1
mc2 = Mwc2*Fc2
mt = meb+mst+mbz+mh2+mto+mc1+mc2+mh2o

```

```

y1=Feb/Ft
y2=Fst/Ft
y3=Fbz/Ft

```



```
y4=Fto/Ft
y5=Fh2/Ft
y6=Fh2o0/Ft

//Result
SST = XST/XEB*100
SBZ = XBZ/XEB*100
STO = XTO/XEB*100

integral z[0,Lb]
output XEB,SST,SBZ,STO,P,T
```

Result:

```
<<  results  >>
XEB      = 0.3449088
SST      = 97.89863
SBZ      = 1.129022
STO      = 0.9723437
P        = 1.044871
T        = 826.438
```



3. Model3 : Heterogeneous model account for internal mass and heat transfer

EQUATRAN code:

```

function diffus(Cseb0,Csst0,Csbz0,Csto0,Csh20,T0,P;Cseb,Csst,Csbz,Csto,Csh2,
T,rc1s,rc2s,rc3s,rc4s,rt1s,rt2s,rt3s,rc1sT,rc2sT,rc3sT,rc4sT)
Deebs*Cseb'+Cseb'*2/r*Deebs+Cseb'*Deebs'= (densityS*(rc1s+rc2s+rc3s)
+voidcat*(rt1s+rt2s+rt3s)) ;Cseb#Cseb0 ;Cseb'#0
Dests*Csst'+Csst'*2/r*Dests+Csst'*Dests'= -(densityS*(rc1s-
rc4s)+voidcat*(rt1s)) ;Csst#Csst0 ;Csst'#0
Debzs*Csbz'+Csbz'*2/r*Debzs+Csbz'*Debzs'= -(densityS*(rc2s)+voidcat*(rt2s))
;Csbz#Csbz0 ;Csbz'#0
Detos*Csto'+Csto'*2/r*Detos+Csto'*Detos'= -(densityS*(rc3s+rc4s)+voidcat
*(rt3s)) ;Csto#Csto0 ;Csto'#0
Deh2s*Csh2'+Csh2'*2/r*Deh2s+Csh2'*Deh2s'= -(densityS*(rc1s-rc3s-2*rc4s)
+voidcat*(rt1s-rt3s)) ;Csh2#Csh20 ;Csh2'#0

T'+T'*2/r = -(-(rc1s*densityS+rt1s*voidcat)*HRX1-
(rc2s*densityS+rt2s*voidcat)*HRX2-(rc3s*densityS+rt3s*voidcat)*HRX3-rc4s
*densityS*HRX4)/ke
T#T0 ;T'#0

rc1sT' = (rc1s*densityS+rt1s*voidcat)*4*_pi*r^2 ;rc1sT#0
rc2sT' = (rc2s*densityS+rt2s*voidcat)*4*_pi*r^2 ;rc2sT#0
rc3sT' = (rc3s*densityS+rt3s*voidcat)*4*_pi*r^2 ;rc3sT#0
rc4sT' = rc4s*densityS*4*_pi*r^2 ;rc4sT#0

Cseb = Pseb/R/T*10^2
Csst = Psst/R/T*10^2
Csh2 = Psh2/R/T*10^2
Csbz = Psbz/R/T*10^2
Csto = Psto/R/T*10^2

Cseb0 = Pseb0/R/T0*10^2
Csst0 = Psst0/R/T0*10^2
Csh20 = Psh20/R/T0*10^2
Csbz0 = Psbz0/R/T0*10^2
Csto0 = Psto0/R/T0*10^2

rc1s = kc1*KEB*(Pseb-Psst*Psh2/Keq) / (1+KEB*Pseb+KH2*Psh2+KST*Psst)^2
rc2s = kc2*KEB*Pseb/ (1+KEB*Pseb+KH2*Psh2+KST*Psst)^2
rc3s = kc3*KEB*Pseb*KH2*Psh2/ (1+KEB*Pseb+KH2*Psh2+KST*Psst)^2
rc4s = kc4*KST*Psst*KH2*Psh2/ (1+KEB*Pseb+KH2*Psh2+KST*Psst)^2
rt1s = kt1*(Pseb-Psst*Psh2/Keq)
rt2s = kt2*Pseb
rt3s = kt3*Pseb
kc1 = A1*exp(-E1*10^3/R/T) ;A1=2.33293E+11 ;E1=204.6619326
kc2 = A2*exp(-E2*10^3/R/T) ;A2=2.65416E+16 ;E2=320.3544359
kc3 = A3*exp(-E3*10^3/R/T) ;A3=9.00967E+15 ;E3=320.9687204
kc4 = A4*exp(-E4*10^3/R/T) ;A4=8.53675E+17 ;E4=333.4837164
KEB = Aeb*exp(-Heb*10^3/R/T) ;Aeb=2.55449E-10 ;Heb=-180.5057701
KST = Ast*exp(-Hst*10^3/R/T) ;Ast=2.26449E-06 ;Hst=-122.2609362
KH2 = Ah2*exp(-Hh2*10^3/R/T) ;Ah2=3.92807E-09 ;Hh2=-152.1129516
kt1 = At1*exp(-Et1*10^3/R/T) ;At1=2.2215*10^16 ;Et1=272.23
kt2 = At2*exp(-Et2*10^3/R/T) ;At2=2.4217*10^20 ;Et2=352.79
kt3 = At3*exp(-Et3*10^3/R/T) ;At3=3.8224*10^17 ;Et3=313.06
Keq = exp(-deltaG/R/T)
deltaG = deltaH - T*deltaS
deltaH = deltaH0+deltaa*(T-298.15)+deltab/2*(T^2-298.15^2)+deltac/3*(T^3-

```



```

298.15^3)+deltad/4*(T^4-298.15^4)
deltaS = deltaS0+deltaa*log(T/298.15)+deltab*(T-298.15)+deltac/2*(T^2-
298.15^2)+deltad/3*(T^3-298.15^3)
deltaH0= (1.475-0.2981)*10^5
deltaS0= 115.7
deltaa = -28.25+27.14+43.1 ;deltab=(615.9+9.274-707.2)*10^(-3)
;deltac=(-40.23-1.381+48.11)*10^(-5) ;deltad=(99.35+7.645-130.1)*10^(-9)
R = 8.314

```

```

HRX1 = HRX10+deltaa1*(T-298.15)+deltab1/2*(T^2-298.15^2)+deltac1/3*(T^3-
298.15^3)+deltad1/4*(T^4-298.15^4)
HRX2 = HRX20+deltaa2*(T-298.15)+deltab2/2*(T^2-298.15^2)+deltac2/3*(T^3-
298.15^3)+deltad2/4*(T^4-298.15^4)
HRX3 = HRX30+deltaa3*(T-298.15)+deltab3/2*(T^2-298.15^2)+deltac3/3*(T^3-
298.15^3)+deltad3/4*(T^4-298.15^4)
HRX4 = HRX40+deltaa4*(T-298.15)+deltab4/2*(T^2-298.15^2)+deltac4/3*(T^3-
298.15^3)+deltad4/4*(T^4-298.15^4)
HRX10=117690 ;deltaa1=41.99 ;deltab1=-8.2026*10^(-2)
;deltac1=6.499*10^(-5) ;deltad1=-2.311*10^(-8)
HRX20=105510 ;deltaa2=12.986 ;deltab2=-7.67*10^(-2)
;deltac2=9.592*10^(-5) ;deltad2=-4.125*10^(-8)
HRX30=-54680 ;deltaa3=10.86 ;deltab3=-15.1844*10^(-2)
;deltac3=23.04*10^(-5) ;deltad3=-9.9955*10^(-8)
HRX40=-172370 ;deltaa4=-31.13 ;deltab4=-6.9818*10^(-2)
;deltac4=16.54*10^(-5) ;deltad4=-7.685*10^(-8)
Cpeb = aeb+beb*T+ceb*T^2+deb*T^3 ;aeb=-0.43426
;beb=6.0671*10^(-3) ;ceb=-3.8625*10^(-6) ;deb=9.1282*10^(-10)
Cpst = ast+bst*T+cst*T^2+dst*T^3 ;ast=-0.26436
;bst=5.564*10^(-3) ;cst=-3.0018*10^(-6) ;dst=5.3317*10^(-10)
Cpbz = abz+bbz*T+cbz*T^2+dbz*T^3 ;abz=-0.40599
;bbz=6.6616*10^(-3) ;cbz=-4.5318*10^(-6) ;dbz=12.255*10^(-10)
Cpto = ato+bto*T+cto*T^2+dto*T^3 ;ato=-0.27127
;bto=5.9142*10^(-3) ;cto=-3.8631*10^(-6) ;dto=9.54*10^(-10)
Cph2 = ah2+bh2*T+ch2*T^2+dh2*T^3 ;ah2=13.57
;bh2=4.637*10^(-3) ;ch2=-6.905*10^(-6) ;dh2=38.23*10^(-10)
Cph2o= ah2o+bh2o*T+ch2o*T^2+dh2o*T^3 ;ah2o=1.79111
;bh2o=0.1069*10^(-3) ;ch2o=0.58611*10^(-6) ;dh2o=-1.998*10^(-10)

```

```

Deebs' = voidcat/tor/10000*3600*(1-y1)/(y2/D12+y3/D13+y4/D14+y5/D15+y6/D16)
*1.75*T^(0.75)*T' ;Deebs#Deebs0
Dests' = voidcat/tor/10000*3600*(1-y2)/(y1/D21+y3/D23+y4/D24+y5/D25+y6/D26)
*1.75*T^(0.75)*T' ;Dests#Dests0
Debzs' = voidcat/tor/10000*3600*(1-y3)/(y1/D31+y2/D32+y4/D34+y5/D35+y6/D36)
*1.75*T^(0.75)*T' ;Debzs#Debzs0
Detos' = voidcat/tor/10000*3600*(1-y4)/(y1/D41+y2/D42+y3/D43+y5/D45+y6/D46)
*1.75*T^(0.75)*T' ;Detos#Detos0
Deh2s' = voidcat/tor/10000*3600*(1-y5)/(y1/D51+y2/D52+y3/D53+y4/D54+y6/D56)
*1.75*T^(0.75)*T' ;Deh2s#Deh2s0
Deebs0 = voidcat/tor/10000*3600*(1-y10)/(y20/D12+y30/D13+y40/D14+y50/D15
+y60/D16)*T0^1.75
Dests0 = voidcat/tor/10000*3600*(1-y20)/(y10/D21+y30/D23+y40/D24+y50/D25
+y60/D26)*T0^1.75
Debzs0 = voidcat/tor/10000*3600*(1-y30)/(y10/D31+y20/D32+y40/D34+y50/D35
+y60/D36)*T0^1.75
Detos0 = voidcat/tor/10000*3600*(1-y40)/(y10/D41+y20/D42+y30/D43+y50/D45
+y60/D46)*T0^1.75
Deh2s0 = voidcat/tor/10000*3600*(1-y50)/(y10/D51+y20/D52+y30/D53+y40/D54
+y60/D56)*T0^1.75
y10=Pseb0/P ;y20=Psst0/P ;y30=Psbz0/P ;y40=Psto0/P ;y50=Psh20/P
;y60=1-y10-y20-y30-y40-y50

```

```

y1=Pseb/P ;y2=Psst/P ;y3=Psbz/P ;y4=Psto/P ;y5=Psh2/P
;y6=1-y1-y2-y3-y4-y5
v1=132 ;v2=127.38 ;v3=90.96 ;v4=111.48 ;v5=6.12 ;v6=13.1
M1=106.16 ;M2=104.14 ;M3=78.11 ;M4=92.11 ;M5=2 ;M6=18
D12= 0.00143/P/M12^(1/2)/(v1^(1/3)+v2^(1/3))^2 ;M12 = 2*(1/M1+1/M2)^(-1)
D13= 0.00143/P/M13^(1/2)/(v1^(1/3)+v3^(1/3))^2 ;M13 = 2*(1/M1+1/M3)^(-1)
D14= 0.00143/P/M14^(1/2)/(v1^(1/3)+v4^(1/3))^2 ;M14 = 2*(1/M1+1/M4)^(-1)
D15= 0.00143/P/M15^(1/2)/(v1^(1/3)+v5^(1/3))^2 ;M15 = 2*(1/M1+1/M5)^(-1)
D16= 0.00143/P/M16^(1/2)/(v1^(1/3)+v6^(1/3))^2 ;M16 = 2*(1/M1+1/M6)^(-1)
D21= 0.00143/P/M21^(1/2)/(v2^(1/3)+v1^(1/3))^2 ;M21 = 2*(1/M2+1/M1)^(-1)
D23= 0.00143/P/M23^(1/2)/(v2^(1/3)+v3^(1/3))^2 ;M23 = 2*(1/M2+1/M3)^(-1)
D24= 0.00143/P/M24^(1/2)/(v2^(1/3)+v4^(1/3))^2 ;M24 = 2*(1/M2+1/M4)^(-1)
D25= 0.00143/P/M25^(1/2)/(v2^(1/3)+v5^(1/3))^2 ;M25 = 2*(1/M2+1/M5)^(-1)
D26= 0.00143/P/M26^(1/2)/(v2^(1/3)+v6^(1/3))^2 ;M26 = 2*(1/M2+1/M6)^(-1)
D31= 0.00143/P/M31^(1/2)/(v3^(1/3)+v1^(1/3))^2 ;M31 = 2*(1/M3+1/M1)^(-1)
D32= 0.00143/P/M32^(1/2)/(v3^(1/3)+v2^(1/3))^2 ;M32 = 2*(1/M3+1/M2)^(-1)
D34= 0.00143/P/M34^(1/2)/(v3^(1/3)+v4^(1/3))^2 ;M34 = 2*(1/M3+1/M4)^(-1)
D35= 0.00143/P/M35^(1/2)/(v3^(1/3)+v5^(1/3))^2 ;M35 = 2*(1/M3+1/M5)^(-1)
D36= 0.00143/P/M36^(1/2)/(v3^(1/3)+v6^(1/3))^2 ;M36 = 2*(1/M3+1/M6)^(-1)
D41= 0.00143/P/M41^(1/2)/(v4^(1/3)+v1^(1/3))^2 ;M41 = 2*(1/M4+1/M1)^(-1)
D42= 0.00143/P/M42^(1/2)/(v4^(1/3)+v2^(1/3))^2 ;M42 = 2*(1/M4+1/M2)^(-1)
D43= 0.00143/P/M43^(1/2)/(v4^(1/3)+v3^(1/3))^2 ;M43 = 2*(1/M4+1/M3)^(-1)
D45= 0.00143/P/M45^(1/2)/(v4^(1/3)+v5^(1/3))^2 ;M45 = 2*(1/M4+1/M5)^(-1)
D46= 0.00143/P/M46^(1/2)/(v4^(1/3)+v6^(1/3))^2 ;M46 = 2*(1/M4+1/M6)^(-1)
D51= 0.00143/P/M51^(1/2)/(v5^(1/3)+v1^(1/3))^2 ;M51 = 2*(1/M5+1/M1)^(-1)
D52= 0.00143/P/M52^(1/2)/(v5^(1/3)+v2^(1/3))^2 ;M52 = 2*(1/M5+1/M2)^(-1)
D53= 0.00143/P/M53^(1/2)/(v5^(1/3)+v3^(1/3))^2 ;M53 = 2*(1/M5+1/M3)^(-1)
D54= 0.00143/P/M54^(1/2)/(v5^(1/3)+v4^(1/3))^2 ;M54 = 2*(1/M5+1/M4)^(-1)
D56= 0.00143/P/M56^(1/2)/(v5^(1/3)+v6^(1/3))^2 ;M56 = 2*(1/M5+1/M6)^(-1)

ke= Ks^(1-voidcat)*K^voidcat*10^(-3)*3600
K =yeb*k1/(yst*A12+ybz*A13+yto*A14+yh2*A15+yh2o*A16)+yst*k2/(yeb*A21+ybz*A23
+yto*A24+yh2*A25+yh2o*A26)+ybz*k3/(yeb*A31+yst*A32+yto*A34+yh2*A35+yh2o*A36)
+yto*k4/(yeb*A41+yst*A42+ybz*A43+yh2*A45+yh2o*A46)+yh2*k5/(yeb*A51+yst*A52+y
bz*A53+yto*A54+yh2o*A56)+yh2o*k6/(yeb*A61+yst*A62+ybz*A63+yto*A64+yh2*A65)
Ks = 44
Tc1= 617.2;Tc2 = 636 ;Tc3 = 562.2 ;Tc4 = 591.8 ;Tc5 = 33.19 ;Tc6 = 647.1
Pc1= 36.06;Pc2 = 38.4;Pc3 = 48.98;Pc4 = 41.06 ;Pc5 = 13.13 ;Pc6 = 220.55
Vc1= 374 ;Vc2 = 352 ;Vc3 = 259 ;Vc4 = 316 ;Vc5 = 64.1 ;Vc6 = 55.9
w1 = 0.303;w2 = 0.297;w3 = 0.21 ;w4 = 0.262 ;w5 = -0.216 ;w6 = 0.345
MW1 = 106.167;MW2 = 104.152;MW3 = 78.114
;MW4 = 92.141;MW5 = 2.061 ;MW6 = 18.015
L1= 377 ;L2 = 505.0424839 ;L3 = 412.3
;L4 = 377 ;L5 = 59.7 ;L6 = 809.1
yeb = y1;yst = y2 ;ybz = y3 ;yto = y4 ;yh2 = y5 ;yh2o = y6
T1 = 210*(Tc1*MW1^3/Pc1^4)^(1/6)
T2 = 210*(Tc2*MW2^3/Pc2^4)^(1/6)
T3 = 210*(Tc3*MW3^3/Pc3^4)^(1/6)
T4 = 210*(Tc4*MW4^3/Pc4^4)^(1/6)
T5 = 210*(Tc5*MW5^3/Pc5^4)^(1/6)
T6 = 210*(Tc6*MW6^3/Pc6^4)^(1/6)
Tr1 = T/Tc1
Tr2 = T/Tc2
Tr3 = T/Tc3
Tr4 = T/Tc4
Tr5 = T/Tc5
Tr6 = T/Tc6
A12 = voidcat*(1+(T2*(exp(0.0464*Tr1)-exp(-0.2412*Tr1)))/
T1/(exp(0.0464*Tr2)-exp(-0.2412*Tr2)))*(MW1/MW2)^0.25)^2/(8*(1+MW1/MW2))^0.5
A13 = voidcat*(1+(T3*(exp(0.0464*Tr1)-exp(-0.2412*Tr1)))/

```

$T1 / (\exp(0.0464 \cdot Tr3) - \exp(-0.2412 \cdot Tr3)) \cdot (MW1/MW3)^{0.25} / (8 \cdot (1 + MW1/MW3))^{0.5}$
A14 = voidcat*(1+(T4*(exp(0.0464*Tr1)-exp(-0.2412*Tr1)) /
 $T1 / (\exp(0.0464 \cdot Tr4) - \exp(-0.2412 \cdot Tr4)) \cdot (MW1/MW4)^{0.25} / (8 \cdot (1 + MW1/MW4))^{0.5}$
A15 = voidcat*(1+(T5*(exp(0.0464*Tr1)-exp(-0.2412*Tr1)) /
 $T1 / (\exp(0.0464 \cdot Tr5) - \exp(-0.2412 \cdot Tr5)) \cdot (MW1/MW5)^{0.25} / (8 \cdot (1 + MW1/MW5))^{0.5}$
A16 = voidcat*(1+(T6*(exp(0.0464*Tr1)-exp(-0.2412*Tr1)) /
 $T1 / (\exp(0.0464 \cdot Tr6) - \exp(-0.2412 \cdot Tr6)) \cdot (MW1/MW6)^{0.25} / (8 \cdot (1 + MW1/MW6))^{0.5}$
A21 = voidcat*(1+(T1*(exp(0.0464*Tr2)-exp(-0.2412*Tr2)) /
 $T2 / (\exp(0.0464 \cdot Tr1) - \exp(-0.2412 \cdot Tr1)) \cdot (MW2/MW1)^{0.25} / (8 \cdot (1 + MW2/MW1))^{0.5}$
A23 = voidcat*(1+(T3*(exp(0.0464*Tr2)-exp(-0.2412*Tr2)) /
 $T2 / (\exp(0.0464 \cdot Tr3) - \exp(-0.2412 \cdot Tr3)) \cdot (MW2/MW3)^{0.25} / (8 \cdot (1 + MW2/MW3))^{0.5}$
A24 = voidcat*(1+(T4*(exp(0.0464*Tr2)-exp(-0.2412*Tr2)) /
 $T2 / (\exp(0.0464 \cdot Tr4) - \exp(-0.2412 \cdot Tr4)) \cdot (MW2/MW4)^{0.25} / (8 \cdot (1 + MW2/MW4))^{0.5}$
A25 = voidcat*(1+(T5*(exp(0.0464*Tr2)-exp(-0.2412*Tr2)) /
 $T2 / (\exp(0.0464 \cdot Tr5) - \exp(-0.2412 \cdot Tr5)) \cdot (MW2/MW5)^{0.25} / (8 \cdot (1 + MW2/MW5))^{0.5}$
A26 = voidcat*(1+(T6*(exp(0.0464*Tr2)-exp(-0.2412*Tr2)) /
 $T2 / (\exp(0.0464 \cdot Tr6) - \exp(-0.2412 \cdot Tr6)) \cdot (MW2/MW6)^{0.25} / (8 \cdot (1 + MW2/MW6))^{0.5}$
A31 = voidcat*(1+(T1*(exp(0.0464*Tr3)-exp(-0.2412*Tr3)) /
 $T3 / (\exp(0.0464 \cdot Tr1) - \exp(-0.2412 \cdot Tr1)) \cdot (MW3/MW1)^{0.25} / (8 \cdot (1 + MW3/MW1))^{0.5}$
A32 = voidcat*(1+(T2*(exp(0.0464*Tr3)-exp(-0.2412*Tr3)) /
 $T3 / (\exp(0.0464 \cdot Tr2) - \exp(-0.2412 \cdot Tr2)) \cdot (MW3/MW2)^{0.25} / (8 \cdot (1 + MW3/MW2))^{0.5}$
A34 = voidcat*(1+(T4*(exp(0.0464*Tr3)-exp(-0.2412*Tr3)) /
 $T3 / (\exp(0.0464 \cdot Tr4) - \exp(-0.2412 \cdot Tr4)) \cdot (MW3/MW4)^{0.25} / (8 \cdot (1 + MW3/MW4))^{0.5}$
A35 = voidcat*(1+(T5*(exp(0.0464*Tr3)-exp(-0.2412*Tr3)) /
 $T3 / (\exp(0.0464 \cdot Tr5) - \exp(-0.2412 \cdot Tr5)) \cdot (MW3/MW5)^{0.25} / (8 \cdot (1 + MW3/MW5))^{0.5}$
A36 = voidcat*(1+(T6*(exp(0.0464*Tr3)-exp(-0.2412*Tr3)) /
 $T3 / (\exp(0.0464 \cdot Tr6) - \exp(-0.2412 \cdot Tr6)) \cdot (MW3/MW6)^{0.25} / (8 \cdot (1 + MW3/MW6))^{0.5}$
A41 = voidcat*(1+(T1*(exp(0.0464*Tr4)-exp(-0.2412*Tr4)) /
 $T4 / (\exp(0.0464 \cdot Tr1) - \exp(-0.2412 \cdot Tr1)) \cdot (MW4/MW1)^{0.25} / (8 \cdot (1 + MW4/MW1))^{0.5}$
A42 = voidcat*(1+(T2*(exp(0.0464*Tr4)-exp(-0.2412*Tr4)) /
 $T4 / (\exp(0.0464 \cdot Tr2) - \exp(-0.2412 \cdot Tr2)) \cdot (MW4/MW2)^{0.25} / (8 \cdot (1 + MW4/MW2))^{0.5}$
A43 = voidcat*(1+(T3*(exp(0.0464*Tr4)-exp(-0.2412*Tr4)) /
 $T4 / (\exp(0.0464 \cdot Tr3) - \exp(-0.2412 \cdot Tr3)) \cdot (MW4/MW3)^{0.25} / (8 \cdot (1 + MW4/MW3))^{0.5}$
A45 = voidcat*(1+(T5*(exp(0.0464*Tr4)-exp(-0.2412*Tr4)) /
 $T4 / (\exp(0.0464 \cdot Tr5) - \exp(-0.2412 \cdot Tr5)) \cdot (MW4/MW5)^{0.25} / (8 \cdot (1 + MW4/MW5))^{0.5}$
A46 = voidcat*(1+(T6*(exp(0.0464*Tr4)-exp(-0.2412*Tr4)) /
 $T4 / (\exp(0.0464 \cdot Tr6) - \exp(-0.2412 \cdot Tr6)) \cdot (MW4/MW6)^{0.25} / (8 \cdot (1 + MW4/MW6))^{0.5}$
A51 = voidcat*(1+(T1*(exp(0.0464*Tr5)-exp(-0.2412*Tr5)) /
 $T5 / (\exp(0.0464 \cdot Tr1) - \exp(-0.2412 \cdot Tr1)) \cdot (MW5/MW1)^{0.25} / (8 \cdot (1 + MW5/MW1))^{0.5}$
A52 = voidcat*(1+(T2*(exp(0.0464*Tr5)-exp(-0.2412*Tr5)) /
 $T5 / (\exp(0.0464 \cdot Tr2) - \exp(-0.2412 \cdot Tr2)) \cdot (MW5/MW2)^{0.25} / (8 \cdot (1 + MW5/MW2))^{0.5}$
A53 = voidcat*(1+(T3*(exp(0.0464*Tr5)-exp(-0.2412*Tr5)) /
 $T5 / (\exp(0.0464 \cdot Tr3) - \exp(-0.2412 \cdot Tr3)) \cdot (MW5/MW3)^{0.25} / (8 \cdot (1 + MW5/MW3))^{0.5}$
A54 = voidcat*(1+(T4*(exp(0.0464*Tr5)-exp(-0.2412*Tr5)) /
 $T5 / (\exp(0.0464 \cdot Tr4) - \exp(-0.2412 \cdot Tr4)) \cdot (MW5/MW4)^{0.25} / (8 \cdot (1 + MW5/MW4))^{0.5}$
A56 = voidcat*(1+(T6*(exp(0.0464*Tr5)-exp(-0.2412*Tr5)) /
 $T5 / (\exp(0.0464 \cdot Tr6) - \exp(-0.2412 \cdot Tr6)) \cdot (MW5/MW6)^{0.25} / (8 \cdot (1 + MW5/MW6))^{0.5}$
A61 = voidcat*(1+(T1*(exp(0.0464*Tr6)-exp(-0.2412*Tr6)) /
 $T6 / (\exp(0.0464 \cdot Tr1) - \exp(-0.2412 \cdot Tr1)) \cdot (MW6/MW1)^{0.25} / (8 \cdot (1 + MW6/MW1))^{0.5}$
A62 = voidcat*(1+(T2*(exp(0.0464*Tr6)-exp(-0.2412*Tr6)) /
 $T6 / (\exp(0.0464 \cdot Tr2) - \exp(-0.2412 \cdot Tr2)) \cdot (MW6/MW2)^{0.25} / (8 \cdot (1 + MW6/MW2))^{0.5}$
A63 = voidcat*(1+(T3*(exp(0.0464*Tr6)-exp(-0.2412*Tr6)) /
 $T6 / (\exp(0.0464 \cdot Tr3) - \exp(-0.2412 \cdot Tr3)) \cdot (MW6/MW3)^{0.25} / (8 \cdot (1 + MW6/MW3))^{0.5}$
A64 = voidcat*(1+(T4*(exp(0.0464*Tr6)-exp(-0.2412*Tr6)) /
 $T6 / (\exp(0.0464 \cdot Tr4) - \exp(-0.2412 \cdot Tr4)) \cdot (MW6/MW4)^{0.25} / (8 \cdot (1 + MW6/MW4))^{0.5}$
A65 = voidcat*(1+(T5*(exp(0.0464*Tr6)-exp(-0.2412*Tr6)) /
 $T6 / (\exp(0.0464 \cdot Tr5) - \exp(-0.2412 \cdot Tr5)) \cdot (MW6/MW5)^{0.25} / (8 \cdot (1 + MW6/MW5))^{0.5}$
 $\text{omegav1} = 1.16145 / (T/L1)^{0.14874} + 0.52487 \cdot \text{EXP}(-0.7732 \cdot (T/L1)) + 2.16178 \cdot \text{EXP}(-2.43787 \cdot (T/L1))$
 $\text{omegav2} = 1.16145 / (T/L2)^{0.14874} + 0.52487 \cdot \text{EXP}(-0.7732 \cdot (T/L2)) + 2.16178 \cdot \text{EXP}(-$

```

2.43787*(T/L2)
omegav3=1.16145/(T/L3)^0.14874+0.52487*EXP(-0.7732*(T/L3))+2.16178*EXP(-
2.43787*(T/L3))
omegav4=1.16145/(T/L4)^0.14874+0.52487*EXP(-0.7732*(T/L4))+2.16178*EXP(-
2.43787*(T/L4))
omegav5=1.16145/(T/L5)^0.14874+0.52487*EXP(-0.7732*(T/L5))+2.16178*EXP(-
2.43787*(T/L5))
omegav6=1.16145/(T/L6)^0.14874+0.52487*EXP(-0.7732*(T/L6))+2.16178*EXP(-
2.43787*(T/L6))
vis1=10^(-7)*(4.61*Tr1^0.618-2.04*exp(-0.449*Tr1)+1.94*exp(-4.058*Tr1)+0.1)
/(Tc1^(1/6)*MW1^(-1/2)*Pc1^(-2/3))
vis2=10^(-7)*(4.61*Tr2^0.618-2.04*exp(-0.449*Tr2)+1.94*exp(-4.058*Tr2)+0.1)
/(Tc2^(1/6)*MW2^(-1/2)*Pc2^(-2/3))
vis3=10^(-7)*(4.61*Tr3^0.618-2.04*exp(-0.449*Tr3)+1.94*exp(-4.058*Tr3)+0.1)
/(Tc3^(1/6)*MW3^(-1/2)*Pc3^(-2/3))
vis4=10^(-7)*(4.61*Tr4^0.618-2.04*exp(-0.449*Tr4)+1.94*exp(-4.058*Tr4)+0.1)
/(Tc4^(1/6)*MW4^(-1/2)*Pc4^(-2/3))
vis5=10^(-7)*26.69*sqrt(MW5*T)/sigma5^2/omega5 ; sigma5=2.827
;omega5=1.16145/(T55)^0.14874+0.52487*exp(-0.77320*T55)+2.16178*exp(-
2.43787*T55) ;T55=T/59.7 //H2
vis6=10^(-7)*26.69*sqrt(MW6*T)/sigma6^2/omega62 ; sigma6=2.641
;omega6=1.16145/(T66)^0.14874+0.52487*exp(-0.77320*T66)+2.16178*exp(-
2.43787*T66) ;T66=T/809.1 ;omega62=omega6+0.2/T6 //H20
a1=(Cpeb*MW1-8.314)/8.314-3/2
a2=(Cpst*MW2-8.314)/8.314-3/2
a3=(Cpbz*MW3-8.314)/8.314-3/2
a4=(Cpto*MW4-8.314)/8.314-3/2
a5=(Cph2*MW5-8.314)/8.314-3/2
a6=(Cph2o*MW6-8.314)/8.314-3/2
B1=0.7862-0.7109*w1+1.3168*w1^2
B2=0.7862-0.7109*w2+1.3168*w2^2
B3=0.7862-0.7109*w3+1.3168*w3^2
B4=0.7862-0.7109*w4+1.3168*w4^2
B5=0.7862-0.7109*w5+1.3168*w5^2
B6=0.7862-0.7109*w6+1.3168*w6^2
z1=2+10.5*(T/Tc1)^2
z2=2+10.5*(T/Tc2)^2
z3=2+10.5*(T/Tc3)^2
z4=2+10.5*(T/Tc4)^2
z5=2+10.5*(T/Tc5)^2
z6=2+10.5*(T/Tc6)^2
pi1=1+a1*((0.215+0.28288*a1-1.061*B1+0.26664*z1)/(0.6366+B1*z1+1.061*a1*B1))
pi2=1+a2*((0.215+0.28288*a2-1.061*B2+0.26664*z2)/(0.6366+B2*z2+1.061*a2*B2))
pi3=1+a3*((0.215+0.28288*a3-1.061*B3+0.26664*z3)/(0.6366+B3*z3+1.061*a3*B3))
pi4=1+a4*((0.215+0.28288*a4-1.061*B4+0.26664*z4)/(0.6366+B4*z4+1.061*a4*B4))
pi5=1+a5*((0.215+0.28288*a5-1.061*B5+0.26664*z5)/(0.6366+B5*z5+1.061*a5*B5))
pi6=1+a6*((0.215+0.28288*a6-1.061*B6+0.26664*z6)/(0.6366+B6*z6+1.061*a6*B6))
k1=3.75*pi1*8.314/(MW1*10^(-3))*vis1
k2=3.75*pi2*8.314/(MW2*10^(-3))*vis2
k3=3.75*pi3*8.314/(MW3*10^(-3))*vis3
k4=3.75*pi4*8.314/(MW4*10^(-3))*vis4
k5=3.75*pi5*8.314/(MW5*10^(-3))*vis5
k6=3.75*pi6*8.314/(MW6*10^(-3))*vis6

densityS = 2500
voidcat = 0.4
tor = 3

```

```

integral r[0.0000001,0.00275]
trend Deeb, Dest, Debz, Detos, Deh2s
END

//Solid phase
diffus(Cseb0,Csst0,Csbz0,Csto0,Csh20,Ts0,P,Ceb,Cst,Cbz,Cto,Ch2,T,rcl,rc2s,r
c3s,rc4s,rt1s,rt2s,rt3s,rclT,rc2sT,rc3sT,rc4sT)
eta1 = rclT/((rcl*densityS+rt1*voidcat)*4/3*_pi*rp^3)
eta2 = rc2sT/((rc2s*densityS+rt2s*voidcat)*4/3*_pi*rp^3)
eta3 = rc3sT/((rc3s*densityS+rt3s*voidcat)*4/3*_pi*rp^3)
eta4 = rc4sT/(rc4s*densityS*4/3*_pi*rp^3)

//Gas phase
//Mass balance
us*Ceb'+us'*Ceb = -(eta1*rcl+eta2*rc2+eta3*rc3)*densityB-(rt1+rt2+rt3)*voidB
;Ceb#Ceb0
us*Cst'+us'*Cst = (eta1*rcl-eta4*rc4)*densityB+(rt1)*voidB ;Cst#Cst0
us*Cbz'+us'*Cbz = (eta2*rc2)*densityB+(rt2)*voidB ;Cbz#Cbz0
us*Cto'+us'*Cto = (eta3*rc3+eta4*rc4)*densityB+(rt3)*voidB ;Cto#Cto0
us*Ch2'+us'*Ch2 = (eta1*rcl-eta3*rc3-2*eta4*rc4)*densityB+(rt1-rt3)*voidB
;Ch2#Ch20
us'=R*(10^(-2))/Ac*((P*(Ft*T'+T*Ft')-T*Ft*P')/P^2) ;us#us0
Ft'/Ac = (eta1*rcl+eta2*rc2-eta4*rc4)*densityB+(rt1+rt2)*voidB ;Ft#Ft0

//Energy balance
(meb*Cpeb+mst*Cpst+mbz*Cpbz+mto*Cpto+mh2*Cph2+mh2o*Cph2o)/Ac*T'=(-
(eta1*rcl*densityB+rt1*voidB)*HRX1-(eta2*rc2*densityB+rt2*voidB)*HRX2-
(eta3*rc3*densityB+rt3*voidB)*HRX3-eta4*rc4*densityB*HRX4) ;T#T0

//Momentum balance
P'*10^5 = -f*us*G/dp/3600^2 ;P#P0
f = (1-voidB)/voidB^3*(1.75+150*(1-voidB)/Re)

//Reaction
rc1 = kc1*KEB*(Peb-Pst*Ph2/Keq)/(1+KEB*Peb+KH2*Ph2+KST*Pst)^2
rc2 = kc2*KEB*Peb/(1+KEB*Peb+KH2*Ph2+KST*Pst)^2
rc3 = kc3*KEB*Peb*KH2*Ph2/(1+KEB*Peb+KH2*Ph2+KST*Pst)^2
rc4 = kc4*KST*Pst*KH2*Ph2/(1+KEB*Peb+KH2*Ph2+KST*Pst)^2
rt1 = kt1*(Peb-Pst*Ph2/Keq)
rt2 = kt2*Peb
rt3 = kt3*Peb
kc1 = A1*exp(-E1*10^3/R/T) ;A1=2.33293E+11 ;E1=204.6619326
kc2 = A2*exp(-E2*10^3/R/T) ;A2=2.65416E+16 ;E2=320.3544359
kc3 = A3*exp(-E3*10^3/R/T) ;A3=9.00967E+15 ;E3=320.9687204
kc4 = A4*exp(-E4*10^3/R/T) ;A4=8.53675E+17 ;E4=333.4837164
KEB = Aeb*exp(-Heb*10^3/R/T) ;Aeb=2.55449E-10 ;Heb=-180.5057701
KST = Ast*exp(-Hst*10^3/R/T) ;Ast=2.26449E-06 ;Hst=-122.2609362
KH2 = Ah2*exp(-Hh2*10^3/R/T) ;Ah2=3.92807E-09 ;Hh2=-152.1129516
kt1 = At1*exp(-Et1*10^3/R/T) ;At1=2.2215*10^16 ;Et1=272.23
kt2 = At2*exp(-Et2*10^3/R/T) ;At2=2.4217*10^20 ;Et2=352.79
kt3 = At3*exp(-Et3*10^3/R/T) ;At3=3.8224*10^17 ;Et3=313.06
Keq = exp(-deltaG/R/T)
deltaG = deltaH - T*deltaS
deltaH = deltaH0+deltaa*(T-298.15)+deltab/2*(T^2-298.15^2)+deltac/3*(T^3-
298.15^3)+deltad/4*(T^4-298.15^4)
deltaS = deltaS0+deltaa*log(T/298.15)+deltab*(T-298.15)+deltac/2*(T^2-
298.15^2)+deltad/3*(T^3-298.15^3)
deltaH0= (1.475-0.2981)*10^5
deltaS0= 115.7
deltaa = -28.25+27.14+43.1 ;deltab=(615.9+9.274-707.2)*10^(-3)

```

```
;deltac=(-40.23-1.381+48.11)*10^(-5) ;deltad=(99.35+7.645-130.1)*10^(-9)
R = 8.314
```

```
HRX1 = HRX10+deltaa1*(T-298.15)+deltab1/2*(T^2-298.15^2)+deltac1/3*(T^3-
298.15^3)+deltad1/4*(T^4-298.15^4)
HRX2 = HRX20+deltaa2*(T-298.15)+deltab2/2*(T^2-298.15^2)+deltac2/3*(T^3-
298.15^3)+deltad2/4*(T^4-298.15^4)
HRX3 = HRX30+deltaa3*(T-298.15)+deltab3/2*(T^2-298.15^2)+deltac3/3*(T^3-
298.15^3)+deltad3/4*(T^4-298.15^4)
HRX4 = HRX40+deltaa4*(T-298.15)+deltab4/2*(T^2-298.15^2)+deltac4/3*(T^3-
298.15^3)+deltad4/4*(T^4-298.15^4)
HRX10=117690 ;deltaa1=41.99 ;deltab1=-8.2026*10^(-2)
;deltac1=6.499*10^(-5) ;deltad1=-2.311*10^(-8)
HRX20=105510 ;deltaa2=12.986 ;deltab2=-7.67*10^(-2)
;deltac2=9.592*10^(-5) ;deltad2=-4.125*10^(-8)
HRX30=-54680 ;deltaa3=10.86 ;deltab3=-15.1844*10^(-2)
;deltac3=23.04*10^(-5) ;deltad3=-9.9955*10^(-8)
HRX40=-172370 ;deltaa4=-31.13 ;deltab4=-6.9818*10^(-2)
;deltac4=16.54*10^(-5) ;deltad4=-7.685*10^(-8)
```

```
//Bed properties
voidB = 1-densityB/densityS
densityB = 1422
densityS = 2500
voidcat = 0.4
dp = 0.0055
rp = dp/2
Ac = _pi*rb^2
rb = 3.5
Lb = 1.33
```

```
//Properties of component
MWeb = 106.167
MWst = 104.151
MWbz = 78.113
MWto = 92.14
MWh2 = 2.016
MWh2o= 18.015
MWc1 = 16.043
MWc2 = 28.054
```

```
Cpeb = aeb+beb*T+ceb*T^2+deb*T^3 ;aeb=-0.43426
;beb=6.0671*10^(-3) ;ceb=-3.8625*10^(-6) ;deb=9.1282*10^(-10)
Cpst = ast+bst*T+cst*T^2+dst*T^3 ;ast=-0.26436
;bst=5.564*10^(-3) ;cst=-3.0018*10^(-6) ;dst=5.3317*10^(-10)
Cpbz = abz+bbz*T+cbz*T^2+dbz*T^3 ;abz=-0.40599
;bbz=6.6616*10^(-3) ;cbz=-4.5318*10^(-6) ;dbz=12.255*10^(-10)
Cpto = ato+bto*T+cto*T^2+dto*T^3 ;ato=-0.27127
;bto=5.9142*10^(-3) ;cto=-3.8631*10^(-6) ;dto=9.54*10^(-10)
Cph2 = ah2+bh2*T+ch2*T^2+dh2*T^3 ;ah2=13.57
;bh2=4.637*10^(-3) ;ch2=-6.905*10^(-6) ;dh2=38.23*10^(-10)
Cph2o= ah2o+bh2o*T+ch2o*T^2+dh2o*T^3 ;ah2o=1.79111
;bh2o=0.1069*10^(-3) ;ch2o=0.58611*10^(-6) ;dh2o=-1.998*10^(-10)
```

```
//Properties of fluid
v0 = Ft0*R*T0/P0*10^(-2)
us0= v0/Ac
Re = feedden0*dp*us0/(vis*3600)
us = v/Ac
G = feedden0*v0/Ac
```



```

feedden0 = (Feb0*MWeb+Fst0*MWst+Fbz0*MWbz+Fto0*MWto+Fh20*MWh2+Fh2o0*MWh2o
+Fc10*MWc1+Fc20*MWc2)/v0
vis=y1*vis1/(y1*phi11+y2*phi12+y3*phi13+y4*phi14+y5*phi15+y6*phi16)+y2*vis2/
(y1*phi21+y2*phi22+y3*phi23+y4*phi24+y5*phi25+y6*phi26)+y3*vis3/(y1*phi31+y2
*phi32+y3*phi33+y4*phi34+y5*phi35+y6*phi36)+y4*vis4/(y1*phi41+y2*phi42+y3*ph
i43+y4*phi44+y5*phi45+y6*phi46)+y5*vis5/(y1*phi51+y2*phi52+y3*phi53+y4*phi54
+y5*phi55+y6*phi56)+y6*vis6/(y1*phi61+y2*phi62+y3*phi63+y4*phi64+y5*phi65+y6
*phi66)
vis1=10^(-7)*(4.61*Tr1^0.618-2.04*exp(-0.449*Tr1)+1.94*exp(-4.058*Tr1)+0.1)/
(Tc1^(1/6)*MW1^(-1/2)*Pc1^(-2/3))
;Tr1=T/Tc1 ;Tc1=617.2 ;MW1=106.16 ;Pc1=36 //EB
vis2=10^(-7)*(4.61*Tr2^0.618-2.04*exp(-0.449*Tr2)+1.94*exp(-4.058*Tr2)+0.1)/
(Tc2^(1/6)*MW2^(-1/2)*Pc2^(-2/3))
;Tr2=T/Tc2 ;Tc2=647.0 ;MW2=104.14 ;Pc2=39.9 //ST
vis3=10^(-7)*(4.61*Tr3^0.618-2.04*exp(-0.449*Tr3)+1.94*exp(-4.058*Tr3)+0.1)/
(Tc3^(1/6)*MW3^(-1/2)*Pc3^(-2/3))
;Tr3=T/Tc3 ;Tc3=562.2 ;MW3=78.11 ;Pc3=48.9 //BZ
vis4=10^(-7)*(4.61*Tr4^0.618-2.04*exp(-0.449*Tr4)+1.94*exp(-4.058*Tr4)+0.1)/
(Tc4^(1/6)*MW4^(-1/2)*Pc4^(-2/3))
;Tr4=T/Tc4 ;Tc4=591.8 ;MW4=92.11 ;Pc4=41 //TO
vis5=10^(-7)*26.69*sqrt(MW5*T)/sigma5^2/omega5 ;MW5=2 ;sigma5=2.827
;omega5=1.16145/(T5)^0.14874+0.52487*exp(-0.77320*T5)+2.16178*exp(-
2.43787*T5) ;T5=T/59.7 //H2
vis6=10^(-7)*26.69*sqrt(MW6*T)/sigma6^2/omega62 ;MW6=18 ;sigma6=2.641
;omega6=1.16145/(T6)^0.14874+0.52487*exp(-0.77320*T6)+2.16178*exp(-
2.43787*T6) ;T6=T/809.1 ;omega62=omega6+0.2/T6 //H2O
phi11=(1+(vis1/vis1)^(1/2)*(MW1/MW1)^(1/4))^2/(8*(1+MW1/MW1))^(1/2)
phi12=(1+(vis1/vis2)^(1/2)*(MW2/MW1)^(1/4))^2/(8*(1+MW1/MW2))^(1/2)
phi13=(1+(vis1/vis3)^(1/2)*(MW3/MW1)^(1/4))^2/(8*(1+MW1/MW3))^(1/2)
phi14=(1+(vis1/vis4)^(1/2)*(MW4/MW1)^(1/4))^2/(8*(1+MW1/MW4))^(1/2)
phi15=(1+(vis1/vis5)^(1/2)*(MW5/MW1)^(1/4))^2/(8*(1+MW1/MW5))^(1/2)
phi16=(1+(vis1/vis6)^(1/2)*(MW6/MW1)^(1/4))^2/(8*(1+MW1/MW6))^(1/2)
phi21=(1+(vis2/vis1)^(1/2)*(MW1/MW2)^(1/4))^2/(8*(1+MW2/MW1))^(1/2)
phi22=(1+(vis2/vis2)^(1/2)*(MW2/MW2)^(1/4))^2/(8*(1+MW2/MW2))^(1/2)
phi23=(1+(vis2/vis3)^(1/2)*(MW3/MW2)^(1/4))^2/(8*(1+MW2/MW3))^(1/2)
phi24=(1+(vis2/vis4)^(1/2)*(MW4/MW2)^(1/4))^2/(8*(1+MW2/MW4))^(1/2)
phi25=(1+(vis2/vis5)^(1/2)*(MW5/MW2)^(1/4))^2/(8*(1+MW2/MW5))^(1/2)
phi26=(1+(vis2/vis6)^(1/2)*(MW6/MW2)^(1/4))^2/(8*(1+MW2/MW6))^(1/2)
phi31=(1+(vis3/vis1)^(1/2)*(MW1/MW3)^(1/4))^2/(8*(1+MW3/MW1))^(1/2)
phi32=(1+(vis3/vis2)^(1/2)*(MW2/MW3)^(1/4))^2/(8*(1+MW3/MW2))^(1/2)
phi33=(1+(vis3/vis3)^(1/2)*(MW3/MW3)^(1/4))^2/(8*(1+MW3/MW3))^(1/2)
phi34=(1+(vis3/vis4)^(1/2)*(MW4/MW3)^(1/4))^2/(8*(1+MW3/MW4))^(1/2)
phi35=(1+(vis3/vis5)^(1/2)*(MW5/MW3)^(1/4))^2/(8*(1+MW3/MW5))^(1/2)
phi36=(1+(vis3/vis6)^(1/2)*(MW6/MW3)^(1/4))^2/(8*(1+MW3/MW6))^(1/2)
phi41=(1+(vis4/vis1)^(1/2)*(MW1/MW4)^(1/4))^2/(8*(1+MW4/MW1))^(1/2)
phi42=(1+(vis4/vis2)^(1/2)*(MW2/MW4)^(1/4))^2/(8*(1+MW4/MW2))^(1/2)
phi43=(1+(vis4/vis3)^(1/2)*(MW3/MW4)^(1/4))^2/(8*(1+MW4/MW3))^(1/2)
phi44=(1+(vis4/vis4)^(1/2)*(MW4/MW4)^(1/4))^2/(8*(1+MW4/MW4))^(1/2)
phi45=(1+(vis4/vis5)^(1/2)*(MW5/MW4)^(1/4))^2/(8*(1+MW4/MW5))^(1/2)
phi46=(1+(vis4/vis6)^(1/2)*(MW6/MW4)^(1/4))^2/(8*(1+MW4/MW6))^(1/2)
phi51=(1+(vis5/vis1)^(1/2)*(MW1/MW5)^(1/4))^2/(8*(1+MW5/MW1))^(1/2)
phi52=(1+(vis5/vis2)^(1/2)*(MW2/MW5)^(1/4))^2/(8*(1+MW5/MW2))^(1/2)
phi53=(1+(vis5/vis3)^(1/2)*(MW3/MW5)^(1/4))^2/(8*(1+MW5/MW3))^(1/2)
phi54=(1+(vis5/vis4)^(1/2)*(MW4/MW5)^(1/4))^2/(8*(1+MW5/MW4))^(1/2)
phi55=(1+(vis5/vis5)^(1/2)*(MW5/MW5)^(1/4))^2/(8*(1+MW5/MW5))^(1/2)
phi56=(1+(vis5/vis6)^(1/2)*(MW6/MW5)^(1/4))^2/(8*(1+MW5/MW6))^(1/2)
phi61=(1+(vis6/vis1)^(1/2)*(MW1/MW6)^(1/4))^2/(8*(1+MW6/MW1))^(1/2)
phi62=(1+(vis6/vis2)^(1/2)*(MW2/MW6)^(1/4))^2/(8*(1+MW6/MW2))^(1/2)
phi63=(1+(vis6/vis3)^(1/2)*(MW3/MW6)^(1/4))^2/(8*(1+MW6/MW3))^(1/2)
phi64=(1+(vis6/vis4)^(1/2)*(MW4/MW6)^(1/4))^2/(8*(1+MW6/MW4))^(1/2)

```

```
phi65=(1+(vis6/vis5)^(1/2)*(MW5/MW6)^(1/4))^2/(8*(1+MW6/MW5))^(1/2)
phi66=(1+(vis6/vis6)^(1/2)*(MW6/MW6)^(1/4))^2/(8*(1+MW6/MW6))^(1/2)
```

```
//Feed
Feb0 = 707
Fst0 = 7.104
Fbz0 = 0.293
Fto0 = 4.968
Fh20 = 0
Fh2o0= 7777
Fc10 = 0
Fc20 = 0
Ft0 = Feb0+Fst0+Fbz0+Fto0+Fh20+Fh2o0+Fc10+Fc20
P0 = 1.25
T0 = 886
```

```
//Profile
Feb = Feb0*(1-XEB)
Fst = Fst0+Feb0*XST
Fbz = Fbz0+Feb0*XBZ
Fto = Fto0+Feb0*XTO
Fh2 = Fh20+Feb0*XH2
Fc1 = Fc10+Feb0*XTO
Fc2 = Fc20+Feb0*XBZ
```

```
Peb = Feb/Ft*P
Pst = Fst/Ft*P
Ph2 = Fh2/Ft*P
Pbz = Fbz/Ft*P
Pto = Fto/Ft*P
```

```
Ceb = Feb/v
Cst = Fst/v
Ch2 = Fh2/v
Cbz = Fbz/v
Cto = Fto/v
```

```
Ceb0 = Feb0/v0
Cst0 = Fst0/v0
Ch20 = Fh20/v0
Cbz0 = Fbz0/v0
Cto0 = Fto0/v0
```

```
meb = MWeb*Feb
mst = MWst*Fst
mbz = MWbz*Fbz
mto = MWto*Fto
mh2 = MWh2*Fh2
mh2o= MWh2o*Fh2o0
mc1 = MWc1*Fc1
mc2 = MWc2*Fc2
mt = meb+mst+mbz+mh2+mto+mc1+mc2+mh2o
```

```
y1=Feb/Ft
y2=Fst/Ft
y3=Fbz/Ft
y4=Fto/Ft
y5=Fh2/Ft
y6=Fh2o0/Ft
```




```
//Result  
SST = XST/XEB*100  
SBZ = XBZ/XEB*100  
STO = XTO/XEB*100  
  
integral z[0,Lb]  
output XEB,SST,SBZ,STO,P,T
```

Result:

XEB	=	0.3448613
SST	=	97.90016
SBZ	=	1.128509
STO	=	0.9713318
P	=	1.044869
T	=	826.4452



4. Model4 : Heterogeneous model account for internal and external transfer

EQUATRAN code:

```

function diffus(Cseb0,Csst0,Csbz0,Csto0,Csh20,T0,P;Cseb,Csst,Csbz,Csto,Csh2,
T,Cseb',Csst',Csbz',Csto',Csh2',T',Deebs,Depts,Debzs,Detos,Deh2s,ke)
Deebs*Cseb'+Cseb'*2/r*Deebs+Cseb'*Deebs'= (densityS*(rc1s+rc2s+rc3s)
+voidcat*(rt1s+rt2s+rt3s)) ;Cseb#Cseb0 ;Cseb'#0
Depts*Csst'+Csst'*2/r*Depts+Csst'*Depts'= -(densityS*(rc1s-rc4s)+voidcat
*(rt1s)) ;Csst#Csst0 ;Csst'#0
Debzs*Csbz'+Csbz'*2/r*Debzs+Csbz'*Debzs'= -(densityS*(rc2s)+voidcat*(rt2s))
;Csbz#Csbz0 ;Csbz'#0
Detos*Csto'+Csto'*2/r*Detos+Csto'*Detos'= -(densityS*(rc3s+rc4s)+voidcat
*(rt3s)) ;Csto#Csto0 ;Csto'#0
Deh2s*Csh2'+Csh2'*2/r*Deh2s+Csh2'*Deh2s'= -(densityS*(rc1s-rc3s-2*rc4s)
+voidcat*(rt1s-rt3s)) ;Csh2#Csh20 ;Csh2'#0

T'+T'*2/r = -(-(rc1s*densityS+rt1s*voidcat)*HRX1-(rc2s*densityS+rt2s
*voidcat)*HRX2-(rc3s*densityS+rt3s*voidcat)*HRX3-rc4s*densityS*HRX4)/ke
T#T0 ;T'#0

Cseb = Pseb/R/T*10^2
Csst = Psst/R/T*10^2
Csh2 = Psh2/R/T*10^2
Csbz = Psbz/R/T*10^2
Csto = Psto/R/T*10^2

Cseb0 = Pseb0/R/T0*10^2
Csst0 = Psst0/R/T0*10^2
Csh20 = Psh20/R/T0*10^2
Csbz0 = Psbz0/R/T0*10^2
Csto0 = Psto0/R/T0*10^2

rc1s = kc1*KEB*(Pseb-Psst*Psh2/Keq)/(1+KEB*Pseb+KH2*Psh2+KST*Psst)^2
rc2s = kc2*KEB*Pseb/(1+KEB*Pseb+KH2*Psh2+KST*Psst)^2
rc3s = kc3*KEB*Pseb*KH2*Psh2/(1+KEB*Pseb+KH2*Psh2+KST*Psst)^2
rc4s = kc4*KST*Psst*KH2*Psh2/(1+KEB*Pseb+KH2*Psh2+KST*Psst)^2
rt1s = kt1*(Pseb-Psst*Psh2/Keq)
rt2s = kt2*Pseb
rt3s = kt3*Pseb
kc1 = A1*exp(-E1*10^3/R/T) ;A1=2.33293E+11 ;E1=204.6619326
kc2 = A2*exp(-E2*10^3/R/T) ;A2=2.65416E+16 ;E2=320.3544359
kc3 = A3*exp(-E3*10^3/R/T) ;A3=9.00967E+15 ;E3=320.9687204
kc4 = A4*exp(-E4*10^3/R/T) ;A4=8.53675E+17 ;E4=333.4837164
KEB = Aeb*exp(-Heb*10^3/R/T) ;Aeb=2.55449E-10 ;Heb=-180.5057701
KST = Ast*exp(-Hst*10^3/R/T) ;Ast=2.26449E-06 ;Hst=-122.2609362
KH2 = Ah2*exp(-Hh2*10^3/R/T) ;Ah2=3.92807E-09 ;Hh2=-152.1129516
kt1 = At1*exp(-Et1*10^3/R/T) ;At1=2.2215*10^16 ;Et1=272.23
kt2 = At2*exp(-Et2*10^3/R/T) ;At2=2.4217*10^20 ;Et2=352.79
kt3 = At3*exp(-Et3*10^3/R/T) ;At3=3.8224*10^17 ;Et3=313.06
Keq = exp(-deltaG/R/T)
deltaG = deltaH - T*deltaS
deltaH = deltaH0+deltaa*(T-298.15)+deltab/2*(T^2-298.15^2)+deltac/3*(T^3-
298.15^3)+deltad/4*(T^4-298.15^4)
deltaS = deltaS0+deltaa*loge(T/298.15)+deltab*(T-298.15)+deltac/2*(T^2-
298.15^2)+deltad/3*(T^3-298.15^3)
deltaH0= (1.475-0.2981)*10^5
deltaS0= 115.7
deltaa = -28.25+27.14+43.1 ;deltab=(615.9+9.274-707.2)*10^(-3)

```

```
;deltac=(-40.23-1.381+48.11)*10^(-5) ;deltad=(99.35+7.645-130.1)*10^(-9)
R = 8.314
```

```
HRX1 = HRX10+deltaa1*(T-298.15)+deltab1/2*(T^2-298.15^2)+deltac1/3*(T^3-
298.15^3)+deltad1/4*(T^4-298.15^4)
HRX2 = HRX20+deltaa2*(T-298.15)+deltab2/2*(T^2-298.15^2)+deltac2/3*(T^3-
298.15^3)+deltad2/4*(T^4-298.15^4)
HRX3 = HRX30+deltaa3*(T-298.15)+deltab3/2*(T^2-298.15^2)+deltac3/3*(T^3-
298.15^3)+deltad3/4*(T^4-298.15^4)
HRX4 = HRX40+deltaa4*(T-298.15)+deltab4/2*(T^2-298.15^2)+deltac4/3*(T^3-
298.15^3)+deltad4/4*(T^4-298.15^4)
```

```
HRX10=117690 ;deltaa1=41.99 ;deltab1=-8.2026*10^(-2)
;deltac1=6.499*10^(-5) ;deltad1=-2.311*10^(-8)
HRX20=105510 ;deltaa2=12.986 ;deltab2=-7.67*10^(-2)
;deltac2=9.592*10^(-5) ;deltad2=-4.125*10^(-8)
HRX30=-54680 ;deltaa3=10.86 ;deltab3=-15.1844*10^(-2)
;deltac3=23.04*10^(-5) ;deltad3=-9.9955*10^(-8)
HRX40=-172370 ;deltaa4=-31.13 ;deltab4=-6.9818*10^(-2)
;deltac4=16.54*10^(-5) ;deltad4=-7.685*10^(-8)
```

```
Cpeb = aeb+beb*T+ceb*T^2+deb*T^3 ;aeb=-0.43426
;beb=6.0671*10^(-3) ;ceb=-3.8625*10^(-6) ;deb=9.1282*10^(-10)
Cpst = ast+bst*T+cst*T^2+dst*T^3 ;ast=-0.26436
;bst=5.564*10^(-3) ;cst=-3.0018*10^(-6) ;dst=5.3317*10^(-10)
Cpbz = abz+bbz*T+cbz*T^2+dbz*T^3 ;abz=-0.40599
;bbz=6.6616*10^(-3) ;cbz=-4.5318*10^(-6) ;dbz=12.255*10^(-10)
Cpto = ato+bto*T+cto*T^2+dto*T^3 ;ato=-0.27127
;bto=5.9142*10^(-3) ;cto=-3.8631*10^(-6) ;dto=9.54*10^(-10)
Cph2 = ah2+bh2*T+ch2*T^2+dh2*T^3 ;ah2=13.57
;bh2=4.637*10^(-3) ;ch2=-6.905*10^(-6) ;dh2=38.23*10^(-10)
Cph2o= ah2o+bh2o*T+ch2o*T^2+dh2o*T^3 ;ah2o=1.79111
;bh2o=0.1069*10^(-3) ;ch2o=0.58611*10^(-6) ;dh2o=-1.998*10^(-10)
```

```
Deebs' = voidcat/tor/10000*3600*(1-y1)/(y2/D12+y3/D13+y4/D14+y5/D15+y6/D16)
*1.75*T^(0.75)*T' ;Deebs#Deebs0
```

```
Dests' = voidcat/tor/10000*3600*(1-y2)/(y1/D21+y3/D23+y4/D24+y5/D25+y6/D26)
*1.75*T^(0.75)*T' ;Dests#Dests0
```

```
Debzs' = voidcat/tor/10000*3600*(1-y3)/(y1/D31+y2/D32+y4/D34+y5/D35+y6/D36)
*1.75*T^(0.75)*T' ;Debzs#Debzs0
```

```
Detos' = voidcat/tor/10000*3600*(1-y4)/(y1/D41+y2/D42+y3/D43+y5/D45+y6/D46)
*1.75*T^(0.75)*T' ;Detos#Detos0
```

```
Deh2s' = voidcat/tor/10000*3600*(1-y5)/(y1/D51+y2/D52+y3/D53+y4/D54+y6/D56)
*1.75*T^(0.75)*T' ;Deh2s#Deh2s0
```

```
Deebs0 = voidcat/tor/10000*3600*(1-y10)/(y20/D12+y30/D13+y40/D14+y50/D15
+y60/D16)*T0^1.75
```

```
Dests0 = voidcat/tor/10000*3600*(1-y20)/(y10/D21+y30/D23+y40/D24+y50/D25
+y60/D26)*T0^1.75
```

```
Debzs0 = voidcat/tor/10000*3600*(1-y30)/(y10/D31+y20/D32+y40/D34+y50/D35
+y60/D36)*T0^1.75
```

```
Detos0 = voidcat/tor/10000*3600*(1-y40)/(y10/D41+y20/D42+y30/D43+y50/D45
+y60/D46)*T0^1.75
```

```
Deh2s0 = voidcat/tor/10000*3600*(1-y50)/(y10/D51+y20/D52+y30/D53+y40/D54
+y60/D56)*T0^1.75
```

```
y10=Pseb0/P ;y20=Psst0/P ;y30=Psbz0/P ;y40=Psto0/P ;y50=Psh20/P
;y60=1-y10-y20-y30-y40-y50
```

```
y1=Pseb/P ;y2=Psst/P ;y3=Psbz/P ;y4=Psto/P ;y5=Psh2/P
;y6=1-y1-y2-y3-y4-y5
```

```
v1=132 ;v2=127.38 ;v3=90.96 ;v4=111.48 ;v5=6.12 ;v6=13.1
M1=106.16 ;M2=104.14 ;M3=78.11 ;M4=92.11 ;M5=2 ;M6=18
```

```
D12= 0.00143/P/M12^(1/2)/(v1^(1/3)+v2^(1/3))^2 ;M12 = 2*(1/M1+1/M2)^(-1)
D13= 0.00143/P/M13^(1/2)/(v1^(1/3)+v3^(1/3))^2 ;M13 = 2*(1/M1+1/M3)^(-1)
```

$D14 = 0.00143/P/M14^{(1/2)} / (\sqrt{v1}^{(1/3)} + v4^{(1/3)})^2 ; M14 = 2 * (1/M1+1/M4)^{(-1)}$
 $D15 = 0.00143/P/M15^{(1/2)} / (\sqrt{v1}^{(1/3)} + v5^{(1/3)})^2 ; M15 = 2 * (1/M1+1/M5)^{(-1)}$
 $D16 = 0.00143/P/M16^{(1/2)} / (\sqrt{v1}^{(1/3)} + v6^{(1/3)})^2 ; M16 = 2 * (1/M1+1/M6)^{(-1)}$
 $D21 = 0.00143/P/M21^{(1/2)} / (\sqrt{v2}^{(1/3)} + v1^{(1/3)})^2 ; M21 = 2 * (1/M2+1/M1)^{(-1)}$
 $D23 = 0.00143/P/M23^{(1/2)} / (\sqrt{v2}^{(1/3)} + v3^{(1/3)})^2 ; M23 = 2 * (1/M2+1/M3)^{(-1)}$
 $D24 = 0.00143/P/M24^{(1/2)} / (\sqrt{v2}^{(1/3)} + v4^{(1/3)})^2 ; M24 = 2 * (1/M2+1/M4)^{(-1)}$
 $D25 = 0.00143/P/M25^{(1/2)} / (\sqrt{v2}^{(1/3)} + v5^{(1/3)})^2 ; M25 = 2 * (1/M2+1/M5)^{(-1)}$
 $D26 = 0.00143/P/M26^{(1/2)} / (\sqrt{v2}^{(1/3)} + v6^{(1/3)})^2 ; M26 = 2 * (1/M2+1/M6)^{(-1)}$
 $D31 = 0.00143/P/M31^{(1/2)} / (\sqrt{v3}^{(1/3)} + v1^{(1/3)})^2 ; M31 = 2 * (1/M3+1/M1)^{(-1)}$
 $D32 = 0.00143/P/M32^{(1/2)} / (\sqrt{v3}^{(1/3)} + v2^{(1/3)})^2 ; M32 = 2 * (1/M3+1/M2)^{(-1)}$
 $D34 = 0.00143/P/M34^{(1/2)} / (\sqrt{v3}^{(1/3)} + v4^{(1/3)})^2 ; M34 = 2 * (1/M3+1/M4)^{(-1)}$
 $D35 = 0.00143/P/M35^{(1/2)} / (\sqrt{v3}^{(1/3)} + v5^{(1/3)})^2 ; M35 = 2 * (1/M3+1/M5)^{(-1)}$
 $D36 = 0.00143/P/M36^{(1/2)} / (\sqrt{v3}^{(1/3)} + v6^{(1/3)})^2 ; M36 = 2 * (1/M3+1/M6)^{(-1)}$
 $D41 = 0.00143/P/M41^{(1/2)} / (\sqrt{v4}^{(1/3)} + v1^{(1/3)})^2 ; M41 = 2 * (1/M4+1/M1)^{(-1)}$
 $D42 = 0.00143/P/M42^{(1/2)} / (\sqrt{v4}^{(1/3)} + v2^{(1/3)})^2 ; M42 = 2 * (1/M4+1/M2)^{(-1)}$
 $D43 = 0.00143/P/M43^{(1/2)} / (\sqrt{v4}^{(1/3)} + v3^{(1/3)})^2 ; M43 = 2 * (1/M4+1/M3)^{(-1)}$
 $D45 = 0.00143/P/M45^{(1/2)} / (\sqrt{v4}^{(1/3)} + v5^{(1/3)})^2 ; M45 = 2 * (1/M4+1/M5)^{(-1)}$
 $D46 = 0.00143/P/M46^{(1/2)} / (\sqrt{v4}^{(1/3)} + v6^{(1/3)})^2 ; M46 = 2 * (1/M4+1/M6)^{(-1)}$
 $D51 = 0.00143/P/M51^{(1/2)} / (\sqrt{v5}^{(1/3)} + v1^{(1/3)})^2 ; M51 = 2 * (1/M5+1/M1)^{(-1)}$
 $D52 = 0.00143/P/M52^{(1/2)} / (\sqrt{v5}^{(1/3)} + v2^{(1/3)})^2 ; M52 = 2 * (1/M5+1/M2)^{(-1)}$
 $D53 = 0.00143/P/M53^{(1/2)} / (\sqrt{v5}^{(1/3)} + v3^{(1/3)})^2 ; M53 = 2 * (1/M5+1/M3)^{(-1)}$
 $D54 = 0.00143/P/M54^{(1/2)} / (\sqrt{v5}^{(1/3)} + v4^{(1/3)})^2 ; M54 = 2 * (1/M5+1/M4)^{(-1)}$
 $D56 = 0.00143/P/M56^{(1/2)} / (\sqrt{v5}^{(1/3)} + v6^{(1/3)})^2 ; M56 = 2 * (1/M5+1/M6)^{(-1)}$

ke = Ks^(1-voidcat)*K^voidcat*10^(-3)*3600

$K = yeb*k1 / (y1*A12+y2*A13+y3*A14+y4*A15+y5*A16)$
 $+ y1*k2 / (y1*A21+y2*A23+y3*A24+y4*A25+y5*A26) + y2*k3 / (y2*A31+y3*A32+y4*A34+y5*A35+y6*A36)$
 $+ y3*k4 / (y3*A41+y4*A42+y5*A43+y6*A45+y7*A46) + y4*k5 / (y4*A51+y5*A52+y6*A53+y7*A54+y8*A56)$
 $+ y5*k6 / (y5*A61+y6*A62+y7*A63+y8*A64+y9*A65)$

Ks = 44

Tc1 = 617.2 ; Tc2 = 636 ; Tc3 = 562.2

; Tc4 = 591.8 ; Tc5 = 33.19 ; Tc6 = 647.1

Pc1 = 36.06 ; Pc2 = 38.4 ; Pc3 = 48.98

; Pc4 = 41.06 ; Pc5 = 13.13 ; Pc6 = 220.55

Vc1 = 374 ; Vc2 = 352 ; Vc3 = 259

; Vc4 = 316 ; Vc5 = 64.1 ; Vc6 = 55.9

w1 = 0.303 ; w2 = 0.297 ; w3 = 0.21

; w4 = 0.262 ; w5 = -0.216 ; w6 = 0.345

MW1 = 106.167 ; MW2 = 104.152 ; MW3 = 78.114 ; MW4 = 92.141

; MW5 = 2.061 ; MW6 = 18.015

L1 = 377 ; L2 = 505.0424839 ; L3 = 412.3 ; L4 = 377

; L5 = 59.7 ; L6 = 809.1

yeb = y1 ; yst = y2 ; ybz = y3 ; yto = y4 ; yh2 = y5 ; yh2o = y6

T1 = 210*(Tc1*MW1^3/Pc1^4)^(1/6)

T2 = 210*(Tc2*MW2^3/Pc2^4)^(1/6)

T3 = 210*(Tc3*MW3^3/Pc3^4)^(1/6)

T4 = 210*(Tc4*MW4^3/Pc4^4)^(1/6)

T5 = 210*(Tc5*MW5^3/Pc5^4)^(1/6)

T6 = 210*(Tc6*MW6^3/Pc6^4)^(1/6)

Tr1 = T/Tc1

Tr2 = T/Tc2

Tr3 = T/Tc3

Tr4 = T/Tc4

Tr5 = T/Tc5

Tr6 = T/Tc6

$A12 = voidcat * (1 + (T2 * (\exp(0.0464*Tr1) - \exp(-0.2412*Tr1))) / T1$
 $/ (\exp(0.0464*Tr2) - \exp(-0.2412*Tr2))) * (MW1/MW2)^{0.25} / (8 * (1 + MW1/MW2))^{0.5}$

$A13 = voidcat * (1 + (T3 * (\exp(0.0464*Tr1) - \exp(-0.2412*Tr1))) / T1$
 $/ (\exp(0.0464*Tr3) - \exp(-0.2412*Tr3))) * (MW1/MW3)^{0.25} / (8 * (1 + MW1/MW3))^{0.5}$


```

omegav3=1.16145/(T/L3)^0.14874+0.52487*EXP(-0.7732*(T/L3))+2.16178*EXP(-
2.43787*(T/L3))
omegav4=1.16145/(T/L4)^0.14874+0.52487*EXP(-0.7732*(T/L4))+2.16178*EXP(-
2.43787*(T/L4))
omegav5=1.16145/(T/L5)^0.14874+0.52487*EXP(-0.7732*(T/L5))+2.16178*EXP(-
2.43787*(T/L5))
omegav6=1.16145/(T/L6)^0.14874+0.52487*EXP(-0.7732*(T/L6))+2.16178*EXP(-
2.43787*(T/L6))
vis1=10^(-7)*(4.61*Tr1^0.618-2.04*exp(-0.449*Tr1)+1.94*exp(-4.058*Tr1)+0.1)
/(Tc1^(1/6)*MW1^(-1/2)*Pc1^(-2/3))
vis2=10^(-7)*(4.61*Tr2^0.618-2.04*exp(-0.449*Tr2)+1.94*exp(-4.058*Tr2)+0.1)
/(Tc2^(1/6)*MW2^(-1/2)*Pc2^(-2/3))
vis3=10^(-7)*(4.61*Tr3^0.618-2.04*exp(-0.449*Tr3)+1.94*exp(-4.058*Tr3)+0.1)
/(Tc3^(1/6)*MW3^(-1/2)*Pc3^(-2/3))
vis4=10^(-7)*(4.61*Tr4^0.618-2.04*exp(-0.449*Tr4)+1.94*exp(-4.058*Tr4)+0.1)
/(Tc4^(1/6)*MW4^(-1/2)*Pc4^(-2/3))
vis5=10^(-7)*26.69*sqrt(MW5*T)/sigma5^2/omega5 ;sigma5=2.827
;omega5=1.16145/(T55)^0.14874+0.52487*exp(-0.77320*T55)+2.16178*exp(-
2.43787*T55) ;T55=T/59.7 //H2
vis6=10^(-7)*26.69*sqrt(MW6*T)/sigma6^2/omega62 ;sigma6=2.641
;omega6=1.16145/(T66)^0.14874+0.52487*exp(-0.77320*T66)+2.16178*exp(-
2.43787*T66) ;T66=T/809.1 ;omega62=omega6+0.2/T6 //H2O
a1=(Cpeb*MW1-8.314)/8.314-3/2
a2=(Cpst*MW2-8.314)/8.314-3/2
a3=(Cpbz*MW3-8.314)/8.314-3/2
a4=(Cpto*MW4-8.314)/8.314-3/2
a5=(Cph2*MW5-8.314)/8.314-3/2
a6=(Cph2o*MW6-8.314)/8.314-3/2
B1=0.7862-0.7109*w1+1.3168*w1^2
B2=0.7862-0.7109*w2+1.3168*w2^2
B3=0.7862-0.7109*w3+1.3168*w3^2
B4=0.7862-0.7109*w4+1.3168*w4^2
B5=0.7862-0.7109*w5+1.3168*w5^2
B6=0.7862-0.7109*w6+1.3168*w6^2
z1=2+10.5*(T/Tc1)^2
z2=2+10.5*(T/Tc2)^2
z3=2+10.5*(T/Tc3)^2
z4=2+10.5*(T/Tc4)^2
z5=2+10.5*(T/Tc5)^2
z6=2+10.5*(T/Tc6)^2
pi1=1+a1*((0.215+0.28288*a1-1.061*B1+0.26664*z1)/(0.6366+B1*z1+1.061*a1*B1))
pi2=1+a2*((0.215+0.28288*a2-1.061*B2+0.26664*z2)/(0.6366+B2*z2+1.061*a2*B2))
pi3=1+a3*((0.215+0.28288*a3-1.061*B3+0.26664*z3)/(0.6366+B3*z3+1.061*a3*B3))
pi4=1+a4*((0.215+0.28288*a4-1.061*B4+0.26664*z4)/(0.6366+B4*z4+1.061*a4*B4))
pi5=1+a5*((0.215+0.28288*a5-1.061*B5+0.26664*z5)/(0.6366+B5*z5+1.061*a5*B5))
pi6=1+a6*((0.215+0.28288*a6-1.061*B6+0.26664*z6)/(0.6366+B6*z6+1.061*a6*B6))
k1=3.75*pi1*8.314/(MW1*10^(-3))*vis1
k2=3.75*pi2*8.314/(MW2*10^(-3))*vis2
k3=3.75*pi3*8.314/(MW3*10^(-3))*vis3
k4=3.75*pi4*8.314/(MW4*10^(-3))*vis4
k5=3.75*pi5*8.314/(MW5*10^(-3))*vis5
k6=3.75*pi6*8.314/(MW6*10^(-3))*vis6

voidB = 1-densityB/densityS
densityB = 1422
densityS = 2500
voidcat = 0.4
tor = 3
integral r[0.0000001,0.00275]
END

```

```

//Solid phase
e1:diffus(Cseb0,Csst0,Csbz0,Csto0,Csh20,Ts0,P,CsebR,CsstR,CsbzR,CstoR,Csh2R,
Ts,kpeb*(Ceb-CsebR)/Deebs,kpst*(Cst-CsstR)/Dests,kpbz*(Czb-
CsbzR)/Debzs,kpto*(Cto-CstoR)/Detos,kph2*(Ch2-Csh2R)/Deh2s,h*(T-
Ts)/ke,Deebs,Dests,Debzs,Detos,Deh2s,ke)

//Gas phase
//Mass balance
us*Ceb'+us'*Ceb = -kpeb*as*(Ceb-CsebR)-voidB*(rt1+rt2+rt3) ;Ceb#Ceb0
us*Cst'+us'*Cst = -kpst*as*(Cst-CsstR)+voidB*(rt1) ;Cst#Cst0
us*Cbz'+us'*Cbz = -kpbz*as*(Cbz-CsbzR)+voidB*(rt2) ;Cbz#Cbz0
us*Cto'+us'*Cto = -kpto*as*(Cto-CstoR)+voidB*(rt3) ;Cto#Cto0
us*Ch2'+us'*Ch2 = -kph2*as*(Ch2-Csh2R)+voidB*(rt1-rt3) ;Ch2#Ch20
us'=R*(10^(-2))/Ac*( (P*(Ft*T'+T*Ft')-T*Ft*P')/P^2) ;us#us0
Ft'/Ac = (rc1+rc2-rc4)*densityB+(rt1+rt2)*voidB ;Ft#Ft0

//Energy balance
us*density*Cpm*T'=-as*h*(T-Ts) ;T#T0

//Momentum balance
P'*10^5 = -f*us*G/dp/3600^2 ;P#P0
f = (1-voidB)/voidB^3*(1.75+150*(1-voidB)/Re)

//Reaction
rc1 = kc1*KEB*(Peb-Pst*Ph2/Keq)/(1+KEB*Peb+KH2*Ph2+KST*Pst)^2
rc2 = kc2*KEB*Peb/(1+KEB*Peb+KH2*Ph2+KST*Pst)^2
rc3 = kc3*KEB*Peb*KH2*Ph2/(1+KEB*Peb+KH2*Ph2+KST*Pst)^2
rc4 = kc4*KST*Pst*KH2*Ph2/(1+KEB*Peb+KH2*Ph2+KST*Pst)^2
rt1 = kt1*(Peb-Pst*Ph2/Keq)
rt2 = kt2*Peb
rt3 = kt3*Peb
kc1 = A1*exp(-E1*10^3/R/T) ;A1=2.33293E+11 ;E1=204.6619326
kc2 = A2*exp(-E2*10^3/R/T) ;A2=2.65416E+16 ;E2=320.3544359
kc3 = A3*exp(-E3*10^3/R/T) ;A3=9.00967E+15 ;E3=320.9687204
kc4 = A4*exp(-E4*10^3/R/T) ;A4=8.53675E+17 ;E4=333.4837164
KEB = Aeb*exp(-Heb*10^3/R/T) ;Aeb=2.55449E-10 ;Heb=-180.5057701
KST = Ast*exp(-Hst*10^3/R/T) ;Ast=2.26449E-06 ;Hst=-122.2609362
KH2 = Ah2*exp(-Hh2*10^3/R/T) ;Ah2=3.92807E-09 ;Hh2=-152.1129516
kt1 = At1*exp(-Et1*10^3/R/T) ;At1=2.2215*10^16 ;Et1=272.23
kt2 = At2*exp(-Et2*10^3/R/T) ;At2=2.4217*10^20 ;Et2=352.79
kt3 = At3*exp(-Et3*10^3/R/T) ;At3=3.8224*10^17 ;Et3=313.06
Keq = exp(-deltaG/R/T)
deltaG = deltaH - T*deltaS
deltaH = deltaH0+deltaa*(T-298.15)+deltab/2*(T^2-298.15^2)+deltac/3*(T^3-
298.15^3)+deltad/4*(T^4-298.15^4)
deltaS = deltaS0+deltaa*loge(T/298.15)+deltab*(T-298.15)+deltac/2*(T^2-
298.15^2)+deltad/3*(T^3-298.15^3)
deltaH0= (1.475-0.2981)*10^5
deltaS0= 115.7
deltaa = -28.25+27.14+43.1 ;deltab=(615.9+9.274-707.2)*10^(-3)
;deltac=(-40.23-1.381+48.11)*10^(-5) ;deltad=(99.35+7.645-130.1)*10^(-9)
R = 8.314

HRX1 = HRX10+deltaa1*(T-298.15)+deltab1/2*(T^2-298.15^2)+deltac1/3*(T^3-
298.15^3)+deltad1/4*(T^4-298.15^4)
HRX2 = HRX20+deltaa2*(T-298.15)+deltab2/2*(T^2-298.15^2)+deltac2/3*(T^3-
298.15^3)+deltad2/4*(T^4-298.15^4)
HRX3 = HRX30+deltaa3*(T-298.15)+deltab3/2*(T^2-298.15^2)+deltac3/3*(T^3-
298.15^3)+deltad3/4*(T^4-298.15^4)

```

```

HRX4 = HRX40+deltaa4*(T-298.15)+deltab4/2*(T^2-298.15^2)+deltac4/3*(T^3-
298.15^3)+deltad4/4*(T^4-298.15^4)
HRX10=117690 ;deltaa1=41.99 ;deltab1=-8.2026*10^(-2)
;deltac1=6.499*10^(-5) ;deltad1=-2.311*10^(-8)
HRX20=105510 ;deltaa2=12.986 ;deltab2=-7.67*10^(-2)
;deltac2=9.592*10^(-5) ;deltad2=-4.125*10^(-8)
HRX30=-54680 ;deltaa3=10.86 ;deltab3=-15.1844*10^(-2)
;deltac3=23.04*10^(-5) ;deltad3=-9.9955*10^(-8)
HRX40=-172370 ;deltaa4=-31.13 ;deltab4=-6.9818*10^(-2)
;deltac4=16.54*10^(-5) ;deltad4=-7.685*10^(-8)

//Bed properties
voidB = 1-densityB/densityS
densityB = 1422
Ac = _pi*rb^2
rb = 3.5
Lb = 1.33
densityS = 2500
voidcat = 0.4
dp = 0.0055
rp = dp/2
as = 3/rp*(1-voidB)

//Properties of component
MWeb = 106.167
MWst = 104.151
MWbz = 78.113
MWto = 92.14
MWh2 = 2.016
MWh2o= 18.015
MWc1 = 16.043
MWc2 = 28.054

Cpeb = aeb+beb*T+ceb*T^2+deb*T^3 ;aeb=-0.43426
;beb=6.0671*10^(-3) ;ceb=-3.8625*10^(-6) ;deb=9.1282*10^(-10)
Cpst = ast+bst*T+cst*T^2+dst*T^3 ;ast=-0.26436
;bst=5.564*10^(-3) ;cst=-3.0018*10^(-6) ;dst=5.3317*10^(-10)
Cpbz = abz+bbz*T+cbz*T^2+dbz*T^3 ;abz=-0.40599
;bbz=6.6616*10^(-3) ;cbz=-4.5318*10^(-6) ;dbz=12.255*10^(-10)
Cpto = ato+bto*T+cto*T^2+dto*T^3 ;ato=-0.27127
;bto=5.9142*10^(-3) ;cto=-3.8631*10^(-6) ;dto=9.54*10^(-10)
Cph2 = ah2+bh2*T+ch2*T^2+dh2*T^3 ;ah2=13.57
;bh2=4.637*10^(-3) ;ch2=-6.905*10^(-6) ;dh2=38.23*10^(-10)
Cph2o= ah2o+bh2o*T+ch2o*T^2+dh2o*T^3 ;ah2o=1.79111
;bh2o=0.1069*10^(-3) ;ch2o=0.58611*10^(-6) ;dh2o=-1.998*10^(-10)

//Properties of fluid
v0 = Ft0*R*T0/P0*10^(-2)
us0= v0/Ac

us = v/Ac
density = (Feb*MWeb+Fst*MWst+Fbz*MWbz+Fto*MWto+Fh2*MWh2+Fh2o*MWh2o+Fc1*MWc1
+Fc2*MWc2)/v
Cpm = (meb*Cpeb+mst*Cpst+mbz*Cpbz+mto*Cpto+mh2*Cph2+mh2o*Cph2o)/mt
G = feedden0*v0/Ac
feedden0 = (Feb0*MWeb+Fst0*MWst+Fbz0*MWbz+Fto0*MWto+Fh20*MWh2+Fh2o0*MWh2o
+Fc10*MWc1+Fc20*MWc2)/v0
vis=y1*vis1/(y1*phi11+y2*phi12+y3*phi13+y4*phi14+y5*phi15+y6*phi16)+y2*vis2/
(y1*phi21+y2*phi22+y3*phi23+y4*phi24+y5*phi25+y6*phi26)+y3*vis3/(y1*phi31+y2
*phi32+y3*phi33+y4*phi34+y5*phi35+y6*phi36)+y4*vis4/(y1*phi41+y2*phi42+y3*ph

```



```

i43+y4*phi44+y5*phi45+y6*phi46)+y5*vis5/(y1*phi51+y2*phi52+y3*phi53+y4*phi54
+y5*phi55+y6*phi56)+y6*vis6/(y1*phi61+y2*phi62+y3*phi63+y4*phi64+y5*phi65+y6
*phi66)
vis1=10^(-7)*(4.61*Tr1^0.618-2.04*exp(-0.449*Tr1)+1.94*exp(-4.058*Tr1)+0.1)
/(Tc1^(1/6)*MW1^(-1/2)*Pc1^(-2/3)) //EB
vis2=10^(-7)*(4.61*Tr2^0.618-2.04*exp(-0.449*Tr2)+1.94*exp(-4.058*Tr2)+0.1)
/(Tc2^(1/6)*MW2^(-1/2)*Pc2^(-2/3)) //ST
vis3=10^(-7)*(4.61*Tr3^0.618-2.04*exp(-0.449*Tr3)+1.94*exp(-4.058*Tr3)+0.1)
/(Tc3^(1/6)*MW3^(-1/2)*Pc3^(-2/3)) //BZ
vis4=10^(-7)*(4.61*Tr4^0.618-2.04*exp(-0.449*Tr4)+1.94*exp(-4.058*Tr4)+0.1)
/(Tc4^(1/6)*MW4^(-1/2)*Pc4^(-2/3)) //TO
vis5=10^(-7)*26.69*sqrt(MW5*T)/sigma5^2/omega5 ;sigma5=2.827
;omega5=1.16145/(T55)^0.14874+0.52487*exp(-0.77320*T55)+2.16178*exp(-
2.43787*T5) ;T55=T/59.7 //H2
vis6=10^(-7)*26.69*sqrt(MW6*T)/sigma6^2/omega62 ;sigma6=2.641
;omega6=1.16145/(T66)^0.14874+0.52487*exp(-0.77320*T66)+2.16178*exp(-
2.43787*T6) ;T66=T/809.1 ;omega62=omega6+0.2/T66 //H20
phi11=(1+(vis1/vis1)^(1/2)*(MW1/MW1)^(1/4))^2/(8*(1+MW1/MW1))^(1/2)
phi12=(1+(vis1/vis2)^(1/2)*(MW2/MW1)^(1/4))^2/(8*(1+MW1/MW2))^(1/2)
phi13=(1+(vis1/vis3)^(1/2)*(MW3/MW1)^(1/4))^2/(8*(1+MW1/MW3))^(1/2)
phi14=(1+(vis1/vis4)^(1/2)*(MW4/MW1)^(1/4))^2/(8*(1+MW1/MW4))^(1/2)
phi15=(1+(vis1/vis5)^(1/2)*(MW5/MW1)^(1/4))^2/(8*(1+MW1/MW5))^(1/2)
phi16=(1+(vis1/vis6)^(1/2)*(MW6/MW1)^(1/4))^2/(8*(1+MW1/MW6))^(1/2)
phi21=(1+(vis2/vis1)^(1/2)*(MW1/MW2)^(1/4))^2/(8*(1+MW2/MW1))^(1/2)
phi22=(1+(vis2/vis2)^(1/2)*(MW2/MW2)^(1/4))^2/(8*(1+MW2/MW2))^(1/2)
phi23=(1+(vis2/vis3)^(1/2)*(MW3/MW2)^(1/4))^2/(8*(1+MW2/MW3))^(1/2)
phi24=(1+(vis2/vis4)^(1/2)*(MW4/MW2)^(1/4))^2/(8*(1+MW2/MW4))^(1/2)
phi25=(1+(vis2/vis5)^(1/2)*(MW5/MW2)^(1/4))^2/(8*(1+MW2/MW5))^(1/2)
phi26=(1+(vis2/vis6)^(1/2)*(MW6/MW2)^(1/4))^2/(8*(1+MW2/MW6))^(1/2)
phi31=(1+(vis3/vis1)^(1/2)*(MW1/MW3)^(1/4))^2/(8*(1+MW3/MW1))^(1/2)
phi32=(1+(vis3/vis2)^(1/2)*(MW2/MW3)^(1/4))^2/(8*(1+MW3/MW2))^(1/2)
phi33=(1+(vis3/vis3)^(1/2)*(MW3/MW3)^(1/4))^2/(8*(1+MW3/MW3))^(1/2)
phi34=(1+(vis3/vis4)^(1/2)*(MW4/MW3)^(1/4))^2/(8*(1+MW3/MW4))^(1/2)
phi35=(1+(vis3/vis5)^(1/2)*(MW5/MW3)^(1/4))^2/(8*(1+MW3/MW5))^(1/2)
phi36=(1+(vis3/vis6)^(1/2)*(MW6/MW3)^(1/4))^2/(8*(1+MW3/MW6))^(1/2)
phi41=(1+(vis4/vis1)^(1/2)*(MW1/MW4)^(1/4))^2/(8*(1+MW4/MW1))^(1/2)
phi42=(1+(vis4/vis2)^(1/2)*(MW2/MW4)^(1/4))^2/(8*(1+MW4/MW2))^(1/2)
phi43=(1+(vis4/vis3)^(1/2)*(MW3/MW4)^(1/4))^2/(8*(1+MW4/MW3))^(1/2)
phi44=(1+(vis4/vis4)^(1/2)*(MW4/MW4)^(1/4))^2/(8*(1+MW4/MW4))^(1/2)
phi45=(1+(vis4/vis5)^(1/2)*(MW5/MW4)^(1/4))^2/(8*(1+MW4/MW5))^(1/2)
phi46=(1+(vis4/vis6)^(1/2)*(MW6/MW4)^(1/4))^2/(8*(1+MW4/MW6))^(1/2)
phi51=(1+(vis5/vis1)^(1/2)*(MW1/MW5)^(1/4))^2/(8*(1+MW5/MW1))^(1/2)
phi52=(1+(vis5/vis2)^(1/2)*(MW2/MW5)^(1/4))^2/(8*(1+MW5/MW2))^(1/2)
phi53=(1+(vis5/vis3)^(1/2)*(MW3/MW5)^(1/4))^2/(8*(1+MW5/MW3))^(1/2)
phi54=(1+(vis5/vis4)^(1/2)*(MW4/MW5)^(1/4))^2/(8*(1+MW5/MW4))^(1/2)
phi55=(1+(vis5/vis5)^(1/2)*(MW5/MW5)^(1/4))^2/(8*(1+MW5/MW5))^(1/2)
phi56=(1+(vis5/vis6)^(1/2)*(MW6/MW5)^(1/4))^2/(8*(1+MW5/MW6))^(1/2)
phi61=(1+(vis6/vis1)^(1/2)*(MW1/MW6)^(1/4))^2/(8*(1+MW6/MW1))^(1/2)
phi62=(1+(vis6/vis2)^(1/2)*(MW2/MW6)^(1/4))^2/(8*(1+MW6/MW2))^(1/2)
phi63=(1+(vis6/vis3)^(1/2)*(MW3/MW6)^(1/4))^2/(8*(1+MW6/MW3))^(1/2)
phi64=(1+(vis6/vis4)^(1/2)*(MW4/MW6)^(1/4))^2/(8*(1+MW6/MW4))^(1/2)
phi65=(1+(vis6/vis5)^(1/2)*(MW5/MW6)^(1/4))^2/(8*(1+MW6/MW5))^(1/2)
phi66=(1+(vis6/vis6)^(1/2)*(MW6/MW6)^(1/4))^2/(8*(1+MW6/MW6))^(1/2)

Re = feedden0*dp*us0/(vis*3600)
Sc_eb = vis/density/(Deb/10000)
Sc_st = vis/density/(Dst/10000)
Sc_bz = vis/density/(Dbz/10000)
Sc_to = vis/density/(Dto/10000)
Sc_h2 = vis/density/(Dh2/10000)

```

$$Pr = K \cdot 10^{(-3)} / Cpm / vis$$

```
//Feed
Feb0 = 707
Fst0 = 7.104
Fbz0 = 0.293
Fto0 = 4.968
Fh20 = 0
Fh2o0= 7777
Fc10 = 0
Fc20 = 0
Ft0 = Feb0+Fst0+Fbz0+Fto0+Fh20+Fh2o0+Fc10+Fc20
P0 = 1.25
T0 = 886
```

```
//Profile
Feb = Feb0*(1-XEB)
Fst = Fst0+Feb0*XST
Fbz = Fbz0+Feb0*XBZ
Fto = Fto0+Feb0*XTO
Fh2 = Fh20+Feb0*XH2
Fc1 = Fc10+Feb0*XTO
Fc2 = Fc20+Feb0*XBZ
```

```
Peb = Feb/Ft*P
Pst = Fst/Ft*P
Ph2 = Fh2/Ft*P
Pbz = Fbz/Ft*P
Pto = Fto/Ft*P
```

```
Ceb = Feb/v
Cst = Fst/v
Ch2 = Fh2/v
Cbz = Fbz/v
Cto = Fto/v
```

```
Ceb0 = Feb0/v0
Cst0 = Fst0/v0
Ch20 = Fh20/v0
Cbz0 = Fbz0/v0
Cto0 = Fto0/v0
```

```
meb = MWeb*Feb
mst = MWst*Fst
mbz = MWbz*Fbz
mto = MWto*Fto
mh2 = MWh2*Fh2
mh2o = MWh2o*Fh2o0
mc1 = MWc1*Fc1
mc2 = MWc2*Fc2
mt = meb+mst+mbz+mh2+mto+mc1+mc2+mh2o
```

```
y1=Feb/Ft
y2=Fst/Ft
y3=Fbz/Ft
y4=Fto/Ft
y5=Fh2/Ft
y6=Fh2o0/Ft
```

```
yeb=Feb/Ft
```



```

yst=Fst/Ft
ybz=Fbz/Ft
yto=Fto/Ft
yh2=Fh2/Ft
yh2o=Fh2o0/Ft

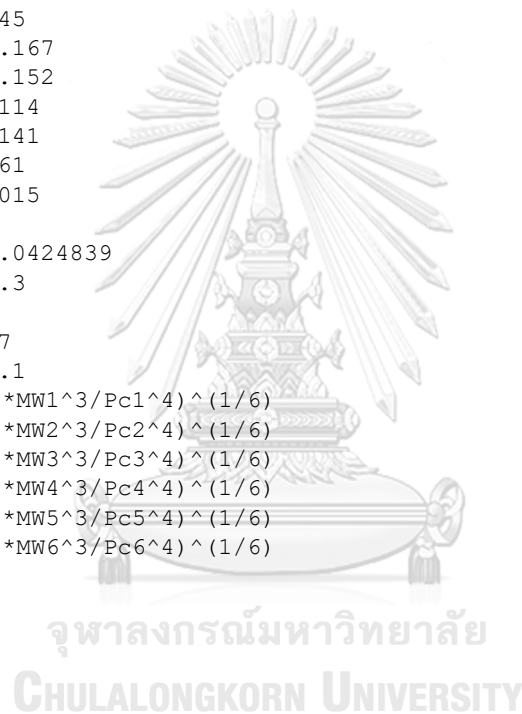
//Mass Transport parameter
v1=132      ;v2=127.38      ;v3=90.96      ;v4=111.48      ;v5=6.12      ;v6=13.1
M1=106.16 ;M2=104.14      ;M3=78.11      ;M4=92.11      ;M5=2          ;M6=18
1/Deb = 1/(1-y1)*(y2/D12+y3/D13+y4/D14+y5/D15+y6/D16)
D12=0.00143*T^1.75/P/M12^(1/2)/(v1^(1/3)+v2^(1/3))^2 ;M12=2*(1/M1+1/M2)^(-1)
D13=0.00143*T^1.75/P/M13^(1/2)/(v1^(1/3)+v3^(1/3))^2 ;M13=2*(1/M1+1/M3)^(-1)
D14=0.00143*T^1.75/P/M14^(1/2)/(v1^(1/3)+v4^(1/3))^2 ;M14=2*(1/M1+1/M4)^(-1)
D15=0.00143*T^1.75/P/M15^(1/2)/(v1^(1/3)+v5^(1/3))^2 ;M15=2*(1/M1+1/M5)^(-1)
D16=0.00143*T^1.75/P/M16^(1/2)/(v1^(1/3)+v6^(1/3))^2 ;M16=2*(1/M1+1/M6)^(-1)
1/Dst = 1/(1-y2)*(y1/D21+y3/D23+y4/D24+y5/D25+y6/D26)
D21=0.00143*T^1.75/P/M21^(1/2)/(v2^(1/3)+v1^(1/3))^2 ;M21=2*(1/M2+1/M1)^(-1)
D23=0.00143*T^1.75/P/M23^(1/2)/(v2^(1/3)+v3^(1/3))^2 ;M23=2*(1/M2+1/M3)^(-1)
D24=0.00143*T^1.75/P/M24^(1/2)/(v2^(1/3)+v4^(1/3))^2 ;M24=2*(1/M2+1/M4)^(-1)
D25=0.00143*T^1.75/P/M25^(1/2)/(v2^(1/3)+v5^(1/3))^2 ;M25=2*(1/M2+1/M5)^(-1)
D26=0.00143*T^1.75/P/M26^(1/2)/(v2^(1/3)+v6^(1/3))^2 ;M26=2*(1/M2+1/M6)^(-1)
1/Dbz = 1/(1-y3)*(y1/D31+y2/D32+y4/D34+y5/D35+y6/D36)
D31=0.00143*T^1.75/P/M31^(1/2)/(v3^(1/3)+v1^(1/3))^2 ;M31=2*(1/M3+1/M1)^(-1)
D32=0.00143*T^1.75/P/M32^(1/2)/(v3^(1/3)+v2^(1/3))^2 ;M32=2*(1/M3+1/M2)^(-1)
D34=0.00143*T^1.75/P/M34^(1/2)/(v3^(1/3)+v4^(1/3))^2 ;M34=2*(1/M3+1/M4)^(-1)
D35=0.00143*T^1.75/P/M35^(1/2)/(v3^(1/3)+v5^(1/3))^2 ;M35=2*(1/M3+1/M5)^(-1)
D36=0.00143*T^1.75/P/M36^(1/2)/(v3^(1/3)+v6^(1/3))^2 ;M36=2*(1/M3+1/M6)^(-1)
1/Dto = 1/(1-y4)*(y1/D41+y2/D42+y3/D43+y5/D45+y6/D46)
D41=0.00143*T^1.75/P/M41^(1/2)/(v4^(1/3)+v1^(1/3))^2 ;M41=2*(1/M4+1/M1)^(-1)
D42=0.00143*T^1.75/P/M42^(1/2)/(v4^(1/3)+v2^(1/3))^2 ;M42=2*(1/M4+1/M2)^(-1)
D43=0.00143*T^1.75/P/M43^(1/2)/(v4^(1/3)+v3^(1/3))^2 ;M43=2*(1/M4+1/M3)^(-1)
D45=0.00143*T^1.75/P/M45^(1/2)/(v4^(1/3)+v5^(1/3))^2 ;M45=2*(1/M4+1/M5)^(-1)
D46=0.00143*T^1.75/P/M46^(1/2)/(v4^(1/3)+v6^(1/3))^2 ;M46=2*(1/M4+1/M6)^(-1)
1/Dh2 = 1/(1-y5)*(y1/D51+y2/D52+y3/D53+y4/D54+y6/D56)
D51=0.00143*T^1.75/P/M51^(1/2)/(v5^(1/3)+v1^(1/3))^2 ;M51=2*(1/M5+1/M1)^(-1)
D52=0.00143*T^1.75/P/M52^(1/2)/(v5^(1/3)+v2^(1/3))^2 ;M52=2*(1/M5+1/M2)^(-1)
D53=0.00143*T^1.75/P/M53^(1/2)/(v5^(1/3)+v3^(1/3))^2 ;M53=2*(1/M5+1/M3)^(-1)
D54=0.00143*T^1.75/P/M54^(1/2)/(v5^(1/3)+v4^(1/3))^2 ;M54=2*(1/M5+1/M4)^(-1)
D56=0.00143*T^1.75/P/M56^(1/2)/(v5^(1/3)+v6^(1/3))^2 ;M56=2*(1/M5+1/M6)^(-1)

kpeb = 1.17*Re^(-0.42)*Sc_eb^(-0.67)*us
kpst = 1.17*Re^(-0.42)*Sc_st^(-0.67)*us
kpbz = 1.17*Re^(-0.42)*Sc_bz^(-0.67)*us
kpto = 1.17*Re^(-0.42)*Sc_to^(-0.67)*us
kph2 = 1.17*Re^(-0.42)*Sc_h2^(-0.67)*us

//Heat Transport parameter
Ks = 44
K = yeb*k1/(yst*A12+ybz*A13+yto*A14+yh2*A15+yh2o*A16)+yst*k2/(yeb*A21
+ybz*A23+yto*A24+yh2*A25+yh2o*A26)+ybz*k3/(yeb*A31+yst*A32+yto*A34+yh2*A35+y
h2o*A36)+yto*k4/(yeb*A41+yst*A42+ybz*A43+yh2*A45+yh2o*A46)+yh2*k5/(yeb*A51+y
st*A52+ybz*A53+yto*A54+yh2o*A56)+yh2o*k6/(yeb*A61+yst*A62+ybz*A63+yto*A64+yh
2*A65)
Tc1 = 617.2
Tc2 = 636
Tc3 = 562.2
Tc4 = 591.8
Tc5 = 33.19
Tc6 = 647.1
Pc1 = 36.06

```

Pc2 = 38.4
 Pc3 = 48.98
 Pc4 = 41.06
 Pc5 = 13.13
 Pc6 = 220.55
 Vc1 = 374
 Vc2 = 352
 Vc3 = 259
 Vc4 = 316
 Vc5 = 64.1
 Vc6 = 55.9
 w1 = 0.303
 w2 = 0.297
 w3 = 0.21
 w4 = 0.262
 w5 = -0.216
 w6 = 0.345
 MW1 = 106.167
 MW2 = 104.152
 MW3 = 78.114
 MW4 = 92.141
 MW5 = 2.061
 MW6 = 18.015
 L1 = 377
 L2 = 505.0424839
 L3 = 412.3
 L4 = 377
 L5 = 59.7
 L6 = 809.1
 $T1 = 210 * (Tc1 * MW1^3 / Pc1^4)^{1/6}$
 $T2 = 210 * (Tc2 * MW2^3 / Pc2^4)^{1/6}$
 $T3 = 210 * (Tc3 * MW3^3 / Pc3^4)^{1/6}$
 $T4 = 210 * (Tc4 * MW4^3 / Pc4^4)^{1/6}$
 $T5 = 210 * (Tc5 * MW5^3 / Pc5^4)^{1/6}$
 $T6 = 210 * (Tc6 * MW6^3 / Pc6^4)^{1/6}$
 Tr1 = T/Tc1
 Tr2 = T/Tc2
 Tr3 = T/Tc3
 Tr4 = T/Tc4
 Tr5 = T/Tc5
 Tr6 = T/Tc6
 $A12 = voidB * (1 + (T2 * (exp(0.0464 * Tr1) - exp(-0.2412 * Tr1)) / T1 / (exp(0.0464 * Tr2) - exp(-0.2412 * Tr2)))) * (MW1 / MW2)^{0.25} / (8 * (1 + MW1 / MW2))^{0.5}$
 $A13 = voidB * (1 + (T3 * (exp(0.0464 * Tr1) - exp(-0.2412 * Tr1)) / T1 / (exp(0.0464 * Tr3) - exp(-0.2412 * Tr3)))) * (MW1 / MW3)^{0.25} / (8 * (1 + MW1 / MW3))^{0.5}$
 $A14 = voidB * (1 + (T4 * (exp(0.0464 * Tr1) - exp(-0.2412 * Tr1)) / T1 / (exp(0.0464 * Tr4) - exp(-0.2412 * Tr4)))) * (MW1 / MW4)^{0.25} / (8 * (1 + MW1 / MW4))^{0.5}$
 $A15 = voidB * (1 + (T5 * (exp(0.0464 * Tr1) - exp(-0.2412 * Tr1)) / T1 / (exp(0.0464 * Tr5) - exp(-0.2412 * Tr5)))) * (MW1 / MW5)^{0.25} / (8 * (1 + MW1 / MW5))^{0.5}$
 $A16 = voidB * (1 + (T6 * (exp(0.0464 * Tr1) - exp(-0.2412 * Tr1)) / T1 / (exp(0.0464 * Tr6) - exp(-0.2412 * Tr6)))) * (MW1 / MW6)^{0.25} / (8 * (1 + MW1 / MW6))^{0.5}$
 $A21 = voidB * (1 + (T1 * (exp(0.0464 * Tr2) - exp(-0.2412 * Tr2)) / T2 / (exp(0.0464 * Tr1) - exp(-0.2412 * Tr1)))) * (MW2 / MW1)^{0.25} / (8 * (1 + MW2 / MW1))^{0.5}$
 $A23 = voidB * (1 + (T3 * (exp(0.0464 * Tr2) - exp(-0.2412 * Tr2)) / T2 / (exp(0.0464 * Tr3) - exp(-0.2412 * Tr3)))) * (MW2 / MW3)^{0.25} / (8 * (1 + MW2 / MW3))^{0.5}$
 $A24 = voidB * (1 + (T4 * (exp(0.0464 * Tr2) - exp(-0.2412 * Tr2)) / T2 / (exp(0.0464 * Tr4) - exp(-0.2412 * Tr4)))) * (MW2 / MW4)^{0.25} / (8 * (1 + MW2 / MW4))^{0.5}$
 $A25 = voidB * (1 + (T5 * (exp(0.0464 * Tr2) - exp(-0.2412 * Tr2)) / T2 / (exp(0.0464 * Tr5) - exp(-0.2412 * Tr5)))) * (MW2 / MW5)^{0.25} / (8 * (1 + MW2 / MW5))^{0.5}$
 $A26 = voidB * (1 + (T6 * (exp(0.0464 * Tr2) - exp(-0.2412 * Tr2)) / T2 / (exp(0.0464 * Tr6) - exp(-0.2412 * Tr6)))) * (MW2 / MW6)^{0.25} / (8 * (1 + MW2 / MW6))^{0.5}$



```

exp(-0.2412*Tr6)) * (MW2/MW6)^0.25^2 / (8 * (1+MW2/MW6))^0.5
A31 = voidB*(1+(T1*(exp(0.0464*Tr3)-exp(-0.2412*Tr3))/T3/(exp(0.0464*Tr1)-
exp(-0.2412*Tr1))) * (MW3/MW1)^0.25^2 / (8 * (1+MW3/MW1))^0.5
A32 = voidB*(1+(T2*(exp(0.0464*Tr3)-exp(-0.2412*Tr3))/T3/(exp(0.0464*Tr2)-
exp(-0.2412*Tr2))) * (MW3/MW2)^0.25^2 / (8 * (1+MW3/MW2))^0.5
A34 = voidB*(1+(T4*(exp(0.0464*Tr3)-exp(-0.2412*Tr3))/T3/(exp(0.0464*Tr4)-
exp(-0.2412*Tr4))) * (MW3/MW4)^0.25^2 / (8 * (1+MW3/MW4))^0.5
A35 = voidB*(1+(T5*(exp(0.0464*Tr3)-exp(-0.2412*Tr3))/T3/(exp(0.0464*Tr5)-
exp(-0.2412*Tr5))) * (MW3/MW5)^0.25^2 / (8 * (1+MW3/MW5))^0.5
A36 = voidB*(1+(T6*(exp(0.0464*Tr3)-exp(-0.2412*Tr3))/T3/(exp(0.0464*Tr6)-
exp(-0.2412*Tr6))) * (MW3/MW6)^0.25^2 / (8 * (1+MW3/MW6))^0.5
A41 = voidB*(1+(T1*(exp(0.0464*Tr4)-exp(-0.2412*Tr4))/T4/(exp(0.0464*Tr1)-
exp(-0.2412*Tr1))) * (MW4/MW1)^0.25^2 / (8 * (1+MW4/MW1))^0.5
A42 = voidB*(1+(T2*(exp(0.0464*Tr4)-exp(-0.2412*Tr4))/T4/(exp(0.0464*Tr2)-
exp(-0.2412*Tr2))) * (MW4/MW2)^0.25^2 / (8 * (1+MW4/MW2))^0.5
A43 = voidB*(1+(T3*(exp(0.0464*Tr4)-exp(-0.2412*Tr4))/T4/(exp(0.0464*Tr3)-
exp(-0.2412*Tr3))) * (MW4/MW3)^0.25^2 / (8 * (1+MW4/MW3))^0.5
A45 = voidB*(1+(T5*(exp(0.0464*Tr4)-exp(-0.2412*Tr4))/T4/(exp(0.0464*Tr5)-
exp(-0.2412*Tr5))) * (MW4/MW5)^0.25^2 / (8 * (1+MW4/MW5))^0.5
A46 = voidB*(1+(T6*(exp(0.0464*Tr4)-exp(-0.2412*Tr4))/T4/(exp(0.0464*Tr6)-
exp(-0.2412*Tr6))) * (MW4/MW6)^0.25^2 / (8 * (1+MW4/MW6))^0.5
A51 = voidB*(1+(T1*(exp(0.0464*Tr5)-exp(-0.2412*Tr5))/T5/(exp(0.0464*Tr1)-
exp(-0.2412*Tr1))) * (MW5/MW1)^0.25^2 / (8 * (1+MW5/MW1))^0.5
A52 = voidB*(1+(T2*(exp(0.0464*Tr5)-exp(-0.2412*Tr5))/T5/(exp(0.0464*Tr2)-
exp(-0.2412*Tr2))) * (MW5/MW2)^0.25^2 / (8 * (1+MW5/MW2))^0.5
A53 = voidB*(1+(T3*(exp(0.0464*Tr5)-exp(-0.2412*Tr5))/T5/(exp(0.0464*Tr3)-
exp(-0.2412*Tr3))) * (MW5/MW3)^0.25^2 / (8 * (1+MW5/MW3))^0.5
A54 = voidB*(1+(T4*(exp(0.0464*Tr5)-exp(-0.2412*Tr5))/T5/(exp(0.0464*Tr4)-
exp(-0.2412*Tr4))) * (MW5/MW4)^0.25^2 / (8 * (1+MW5/MW4))^0.5
A56 = voidB*(1+(T6*(exp(0.0464*Tr5)-exp(-0.2412*Tr5))/T5/(exp(0.0464*Tr6)-
exp(-0.2412*Tr6))) * (MW5/MW6)^0.25^2 / (8 * (1+MW5/MW6))^0.5
A61 = voidB*(1+(T1*(exp(0.0464*Tr6)-exp(-0.2412*Tr6))/T6/(exp(0.0464*Tr1)-
exp(-0.2412*Tr1))) * (MW6/MW1)^0.25^2 / (8 * (1+MW6/MW1))^0.5
A62 = voidB*(1+(T2*(exp(0.0464*Tr6)-exp(-0.2412*Tr6))/T6/(exp(0.0464*Tr2)-
exp(-0.2412*Tr2))) * (MW6/MW2)^0.25^2 / (8 * (1+MW6/MW2))^0.5
A63 = voidB*(1+(T3*(exp(0.0464*Tr6)-exp(-0.2412*Tr6))/T6/(exp(0.0464*Tr3)-
exp(-0.2412*Tr3))) * (MW6/MW3)^0.25^2 / (8 * (1+MW6/MW3))^0.5
A64 = voidB*(1+(T4*(exp(0.0464*Tr6)-exp(-0.2412*Tr6))/T6/(exp(0.0464*Tr4)-
exp(-0.2412*Tr4))) * (MW6/MW4)^0.25^2 / (8 * (1+MW6/MW4))^0.5
A65 = voidB*(1+(T5*(exp(0.0464*Tr6)-exp(-0.2412*Tr6))/T6/(exp(0.0464*Tr5)-
exp(-0.2412*Tr5))) * (MW6/MW5)^0.25^2 / (8 * (1+MW6/MW5))^0.5
omegav1=1.16145/(T/L1)^0.14874+0.52487*EXP(-0.7732*(T/L1))+2.16178*EXP(-
2.43787*(T/L1))
omegav2=1.16145/(T/L2)^0.14874+0.52487*EXP(-0.7732*(T/L2))+2.16178*EXP(-
2.43787*(T/L2))
omegav3=1.16145/(T/L3)^0.14874+0.52487*EXP(-0.7732*(T/L3))+2.16178*EXP(-
2.43787*(T/L3))
omegav4=1.16145/(T/L4)^0.14874+0.52487*EXP(-0.7732*(T/L4))+2.16178*EXP(-
2.43787*(T/L4))
omegav5=1.16145/(T/L5)^0.14874+0.52487*EXP(-0.7732*(T/L5))+2.16178*EXP(-
2.43787*(T/L5))
omegav6=1.16145/(T/L6)^0.14874+0.52487*EXP(-0.7732*(T/L6))+2.16178*EXP(-
2.43787*(T/L6))
a1=(Cpeb*MW1-8.314)/8.314-3/2
a2=(Cpst*MW2-8.314)/8.314-3/2
a3=(Cpbz*MW3-8.314)/8.314-3/2
a4=(Cpto*MW4-8.314)/8.314-3/2
a5=(Cph2*MW5-8.314)/8.314-3/2
a6=(Cph2o*MW6-8.314)/8.314-3/2
B1=0.7862-0.7109*w1+1.3168*w1^2

```

```

B2=0.7862-0.7109*w2+1.3168*w2^2
B3=0.7862-0.7109*w3+1.3168*w3^2
B4=0.7862-0.7109*w4+1.3168*w4^2
B5=0.7862-0.7109*w5+1.3168*w5^2
B6=0.7862-0.7109*w6+1.3168*w6^2
z1=2+10.5*(T/Tc1)^2
z2=2+10.5*(T/Tc2)^2
z3=2+10.5*(T/Tc3)^2
z4=2+10.5*(T/Tc4)^2
z5=2+10.5*(T/Tc5)^2
z6=2+10.5*(T/Tc6)^2
pi1=1+a1*((0.215+0.28288*a1-1.061*B1+0.26664*z1)/(0.6366+B1*z1+1.061*a1*B1))
pi2=1+a2*((0.215+0.28288*a2-1.061*B2+0.26664*z2)/(0.6366+B2*z2+1.061*a2*B2))
pi3=1+a3*((0.215+0.28288*a3-1.061*B3+0.26664*z3)/(0.6366+B3*z3+1.061*a3*B3))
pi4=1+a4*((0.215+0.28288*a4-1.061*B4+0.26664*z4)/(0.6366+B4*z4+1.061*a4*B4))
pi5=1+a5*((0.215+0.28288*a5-1.061*B5+0.26664*z5)/(0.6366+B5*z5+1.061*a5*B5))
pi6=1+a6*((0.215+0.28288*a6-1.061*B6+0.26664*z6)/(0.6366+B6*z6+1.061*a6*B6))
k1=3.75*pi1*8.314/(MW1*10^(-3))*vis1
k2=3.75*pi2*8.314/(MW2*10^(-3))*vis2
k3=3.75*pi3*8.314/(MW3*10^(-3))*vis3
k4=3.75*pi4*8.314/(MW4*10^(-3))*vis4
k5=3.75*pi5*8.314/(MW5*10^(-3))*vis5
k6=3.75*pi6*8.314/(MW6*10^(-3))*vis6

//Result
SST = XST/XEB*100
SBZ = XBZ/XEB*100
STO = XTO/XEB*100

integral z[0,Lb]
output XEB,SST,SBZ,STO,P,T

```

Result:

XEB	=	0.3446425
SST	=	97.88273
SBZ	=	1.130866
STO	=	0.9864085
P	=	1.037921
T	=	826.6271

5. Model5 : Heterogeneous model account for internal transfer and mass axial dispersion

EQUATRAN code:

```

function diffus(Cseb0,Csst0,Csbz0,Csto0,Csh20,T;Cseb,Csst,Csbz,Csto,Csh2
,rc1s,rc2s,rc3s,rc4s,rt1s,rt2s,rt3s,rc1sT,rc2sT,rc3sT,rc4sT)
Cseb'+Cseb'*2/r= 1/Deeb*(densityS*(rc1s+rc2s+rc3s) +voidcat*(rt1s+rt2s
+rt3s)) ;Cseb#Cseb0 ;Cseb'#0
Csst'+Csst'*2/r= -1/Dests*(densityS*(rc1s-rc4s)+voidcat*(rt1s))
;Csst#Csst0 ;Csst'#0
Csbz'+Csbz'*2/r= -1/Debzs*(densityS*(rc2s)+voidcat*(rt2s))
;Csbz#Csbz0 ;Csbz'#0
Csto'+Csto'*2/r= -1/Detos*(densityS*(rc3s+rc4s)+voidcat*(rt3s))
;Csto#Csto0 ;Csto'#0
Csh2'+Csh2'*2/r= -1/Deh2s*(densityS*(rc1s-rc3s-2*rc4s)+voidcat*(rt1s-rt3s))
;Csh2#Csh20 ;Csh2'#0

rc1sT' = (rc1s*densityS+rt1s*voidcat)*4*_pi*r^2 ;rc1sT#0
rc2sT' = (rc2s*densityS+rt2s*voidcat)*4*_pi*r^2 ;rc2sT#0
rc3sT' = (rc3s*densityS+rt3s*voidcat)*4*_pi*r^2 ;rc3sT#0
rc4sT' = rc4s*densityS*4*_pi*r^2 ;rc4sT#0

Cseb = Pseb/R/T*10^2
Csst = Psst/R/T*10^2
Csh2 = Psh2/R/T*10^2
Csbz = Psbz/R/T*10^2
Csto = Psto/R/T*10^2

rc1s = kc1*KEB*(Pseb-Psst*Psh2/Keq) / (1+KEB*Pseb+KH2*Psh2+KST*Psst) ^2
rc2s = kc2*KEB*Pseb/ (1+KEB*Pseb+KH2*Psh2+KST*Psst) ^2
rc3s = kc3*KEB*Pseb*KH2*Psh2/ (1+KEB*Pseb+KH2*Psh2+KST*Psst) ^2
rc4s = kc4*KST*Psst*KH2*Psh2/ (1+KEB*Pseb+KH2*Psh2+KST*Psst) ^2
rt1s = kt1*(Pseb-Psst*Psh2/Keq)
rt2s = kt2*Pseb
rt3s = kt3*Pseb
kc1 = A1*exp(-E1*10^3/R/T) ;A1=2.33293E+11 ;E1=204.6619326
kc2 = A2*exp(-E2*10^3/R/T) ;A2=2.65416E+16 ;E2=320.3544359
kc3 = A3*exp(-E3*10^3/R/T) ;A3=9.00967E+15 ;E3=320.9687204
kc4 = A4*exp(-E4*10^3/R/T) ;A4=8.53675E+17 ;E4=333.4837164
KEB = Aeb*exp(-Heb*10^3/R/T) ;Aeb=2.55449E-10 ;Heb=-180.5057701
KST = Ast*exp(-Hst*10^3/R/T) ;Ast=2.26449E-06 ;Hst=-122.2609362
KH2 = Ah2*exp(-Hh2*10^3/R/T) ;Ah2=3.92807E-09 ;Hh2=-152.1129516
kt1 = At1*exp(-Et1*10^3/R/T) ;At1=2.2215*10^16 ;Et1=272.23
kt2 = At2*exp(-Et2*10^3/R/T) ;At2=2.4217*10^20 ;Et2=352.79
kt3 = At3*exp(-Et3*10^3/R/T) ;At3=3.8224*10^17 ;Et3=313.06
Keq = exp(-deltaG/R/T)
deltaG = deltaH - T*deltaS
deltaH = deltaH0+deltaa*(T-298.15)+deltab/2*(T^2-298.15^2)+deltac/3*(T^3-
298.15^3)+deltad/4*(T^4-298.15^4)
deltaS = deltaS0+deltaa*log(T/298.15)+deltab*(T-298.15)+deltac/2*(T^2-
298.15^2)+deltad/3*(T^3-298.15^3)
deltaH0= (1.475-0.2981)*10^5
deltaS0= 115.7
deltaa = -28.25+27.14+43.1 ;deltab=(615.9+9.274-707.2)*10^(-3)
;deltac=(-40.23-1.381+48.11)*10^(-5) ;deltad=(99.35+7.645-130.1)*10^(-9)
R = 8.314

```

```

Deebs = 0.02248767
Dests = 0.02467243
Debzs = 0.02620409
Detos = 0.02359606
Deh2s = 0.2069529

densityS = 2500
voidcat = 0.4
tor = 3

integral r[0.0000001,0.00275]
END

//function
cal (Ceb0,Cst0,Cbz0,Cto0,Ch20;Ceb,Cst,Cbz,Cto,Ch2,Ceb',Cst',Cbz',Cto',Ch2')

//Solid phase
diffus (Cseb0,Csst0,Csbz0,Csto0,Csh20,T,Cseb,Csst,Csbz,Csto,Csh2,rc1s,rc2s,rc3s,rc4s,rt1s,rt2s,rt3s,rc1sT,rc2sT,rc3sT,rc4sT)
eta1 = rc1sT/((rc1s*densityS+rt1s*voidcat)*4/3*_pi*rp^3)
eta2 = rc2sT/((rc2s*densityS+rt2s*voidcat)*4/3*_pi*rp^3)
eta3 = rc3sT/((rc3s*densityS+rt3s*voidcat)*4/3*_pi*rp^3)
eta4 = rc4sT/(rc4s*densityS*4/3*_pi*rp^3)
e1:Cseb=Ceb
e2:Csst=Cst
e3:Csbz=Cbz
e4:Csto=Cto
e5:Csh2=Ch2
reset Cseb0#0.000337[0,1000] by e1 maxloop 1000,
Csst0#0.000953[0,1000] by e2 maxloop 1000,
Csbz0#0.000163[0,1000] by e3 maxloop 1000,
Csto0#0.0000238[0,1000] by e4 maxloop 1000,
Csh20#0.000115[0,1000] by e5 maxloop 1000

//Gas phase
//Mass balance
B*Da'*Ceb'+Ceb'-'-A*us*Ceb'-A*us'*Ceb-A*(eta1*rc1+eta2*rc2+eta3*rc3)*densityB
-A*(rt1+rt2+rt3)*voidB=0;Ceb#Ceb0;Ceb'#(us0/(voidB*Da0)*(Ceb0-Cebin))
B*Da'*Cst'+Cst'-'-A*us*Cst'-A*us'*Cst+A*(eta1*rc1-eta4*rc4)*densityB
+A*(rt1)*voidB=0;Cst#Cst0;Cst'#(us0/(voidB*Da0)*(Cst0-Cstin))
B*Da'*Cbz'+Cbz'-'-A*us*Cbz'-A*us'*Cbz+A*(eta2*rc2)*densityB+A*(rt2)*voidB=0
;Cbz#Cbz0;Cbz'#(us0/(voidB*Da0)*(Cbz0-Cbzin))
B*Da'*Cto'+Cto'-'-A*us*Cto'-A*us'*Cto+A*(eta3*rc3+eta4*rc4)*densityB
+A*(rt3)*voidB=0;Cto#Cto0;Cto'#(us0/(voidB*Da0)*(Cto0-Ctoin))
B*Da'*Ch2'+Ch2'-'-A*us*Ch2'-A*us'*Ch2+A*(eta1*rc1-eta3*rc3-2*eta4*rc4)
*densityB+A*(rt1-rt3)*voidB=0;Ch2#Ch20;Ch2'#(us0/(voidB*Da0)*(Ch20-Ch2in))
us'=R*(10^(-2))/Ac*((P*(Ft*T'+T*Ft')-T*Ft*P')/P^2);us#us0
Ft'/Ac=(eta1*rc1+eta2*rc2-eta4*rc4)*densityB+(rt1+rt2)*voidB;Ft#Ft0
Da'=0.5*(us'/voidB)*dp;Da#Da0
Da0=0.5*(us0/voidB)*dp
B=1/Da
A=1/(voidB*Da)

//Energy balance
(meb*Cpeb+mst*Cpst+mbz*Cpbz+mto*Cpto+mh2*Cph2+mh2o*Cph2o)/Ac*T'=(-
(eta1*rc1*densityB+rt1*voidB)*HRX1-(eta2*rc2*densityB+rt2*voidB)*HRX2-
(eta3*rc3*densityB+rt3*voidB)*HRX3-eta4*rc4*densityB*HRX4);T#T0

//Momentum balance
P'*10^5=-f*us*G/dp/3600^2;P#P0

```



```

f = (1-voidB)/voidB^3*(1.75+150*(1-voidB)/Re)

//Reaction
rc1 = kc1*KEB*(Peb-Pst*Ph2/Keq)/(1+KEB*Peb+KH2*Ph2+KST*Pst)^2
rc2 = kc2*KEB*Peb/(1+KEB*Peb+KH2*Ph2+KST*Pst)^2
rc3 = kc3*KEB*Peb*KH2*Ph2/(1+KEB*Peb+KH2*Ph2+KST*Pst)^2
rc4 = kc4*KST*Pst*KH2*Ph2/(1+KEB*Peb+KH2*Ph2+KST*Pst)^2
rt1 = kt1*(Peb-Pst*Ph2/Keq)
rt2 = kt2*Peb
rt3 = kt3*Peb
kc1 = A1*exp(-E1*10^3/R/T) ;A1=2.33293E+11 ;E1=204.6619326
kc2 = A2*exp(-E2*10^3/R/T) ;A2=2.65416E+16 ;E2=320.3544359
kc3 = A3*exp(-E3*10^3/R/T) ;A3=9.00967E+15 ;E3=320.9687204
kc4 = A4*exp(-E4*10^3/R/T) ;A4=8.53675E+17 ;E4=333.4837164
KEB = Aeb*exp(-Heb*10^3/R/T) ;Aeb=2.55449E-10 ;Heb=-180.5057701
KST = Ast*exp(-Hst*10^3/R/T) ;Ast=2.26449E-06 ;Hst=-122.2609362
KH2 = Ah2*exp(-Hh2*10^3/R/T) ;Ah2=3.92807E-09 ;Hh2=-152.1129516
kt1 = At1*exp(-Et1*10^3/R/T) ;At1=2.2215*10^16 ;Et1=272.23
kt2 = At2*exp(-Et2*10^3/R/T) ;At2=2.4217*10^20 ;Et2=352.79
kt3 = At3*exp(-Et3*10^3/R/T) ;At3=3.8224*10^17 ;Et3=313.06
Keq = exp(-deltaG/R/T)
deltaG = deltaH - T*deltaS
deltaH = deltaH0+deltaaa*(T-298.15)+deltab/2*(T^2-298.15^2)+deltac/3*(T^3-
298.15^3)+deltad/4*(T^4-298.15^4)
deltaS = deltaS0+deltaaa*loge(T/298.15)+deltab*(T-298.15)+deltac/2*(T^2-
298.15^2)+deltad/3*(T^3-298.15^3)
deltaH0= (1.475-0.2981)*10^5
deltaS0= 115.7
deltaaa = -28.25+27.14+43.1 ;deltab=(615.9+9.274-707.2)*10^(-3)
;deltac=(-40.23-1.381+48.11)*10^(-5) ;deltad=(99.35+7.645-130.1)*10^(-9)
R = 8.314

HRX1 = HRX10+deltaa1*(T-298.15)+deltab1/2*(T^2-298.15^2)+deltac1/3*(T^3-
298.15^3)+deltad1/4*(T^4-298.15^4)
HRX2 = HRX20+deltaa2*(T-298.15)+deltab2/2*(T^2-298.15^2)+deltac2/3*(T^3-
298.15^3)+deltad2/4*(T^4-298.15^4)
HRX3 = HRX30+deltaa3*(T-298.15)+deltab3/2*(T^2-298.15^2)+deltac3/3*(T^3-
298.15^3)+deltad3/4*(T^4-298.15^4)
HRX4 = HRX40+deltaa4*(T-298.15)+deltab4/2*(T^2-298.15^2)+deltac4/3*(T^3-
298.15^3)+deltad4/4*(T^4-298.15^4)
HRX10=117690 ;deltaa1=41.99 ;deltab1=-8.2026*10^(-2)
;deltac1=6.499*10^(-5) ;deltad1=-2.311*10^(-8)
HRX20=105510 ;deltaa2=12.986 ;deltab2=-7.67*10^(-2)
;deltac2=9.592*10^(-5) ;deltad2=-4.125*10^(-8)
HRX30=-54680 ;deltaa3=10.86 ;deltab3=-15.1844*10^(-2)
;deltac3=23.04*10^(-5) ;deltad3=-9.9955*10^(-8)
HRX40=-172370 ;deltaa4=-31.13 ;deltab4=-6.9818*10^(-2)
;deltac4=16.54*10^(-5) ;deltad4=-7.685*10^(-8)

//Bed properties
voidB = 1-densityB/densityS
densityB = 1422
densityS = 2500
voidcat = 0.4
dp = 0.0055
rp = dp/2
Ac = _pi*rb^2
rb = 3.5
Lb = 1.33

```

```

//Properties of component
MWeb = 106.167
MWst = 104.151
MWbz = 78.113
MWto = 92.14
MWh2 = 2.016
MWh2o= 18.015
MWc1 = 16.043
MWc2 = 28.054

Cpeb = aeb+beb*T+ceb*T^2+deb*T^3 ;aeb=-0.43426
;beb=6.0671*10^(-3) ;ceb=-3.8625*10^(-6) ;deb=9.1282*10^(-10)
Cpst = ast+bst*T+cst*T^2+dst*T^3 ;ast=-0.26436
;bst=5.564*10^(-3) ;cst=-3.0018*10^(-6) ;dst=5.3317*10^(-10)
Cpbz = abz+bbz*T+cbz*T^2+dbz*T^3 ;abz=-0.40599
;bbz=6.6616*10^(-3) ;cbz=-4.5318*10^(-6) ;dbz=12.255*10^(-10)
Cpto = ato+bto*T+cto*T^2+dto*T^3 ;ato=-0.27127
;bto=5.9142*10^(-3) ;cto=-3.8631*10^(-6) ;dto=9.54*10^(-10)
Cph2 = ah2+bh2*T+ch2*T^2+dh2*T^3 ;ah2=13.57
;bh2=4.637*10^(-3) ;ch2=-6.905*10^(-6) ;dh2=38.23*10^(-10)
Cph2o= ah2o+bh2o*T+ch2o*T^2+dh2o*T^3 ;ah2o=1.79111
;bh2o=0.1069*10^(-3) ;ch2o=0.58611*10^(-6) ;dh2o=-1.998*10^(-10)

//Properities of fluid
v0 = Ft0*R*T0/P0*10^(-2)
us0= v0/Ac

Re = feedden0*dp*us0/(vis*3600)
us = v/Ac
G = feedden0*v0/Ac
feedden0 = (Feb0*MWeb+Fst0*MWst+Fbz0*MWbz+Fto0*MWto+Fh20*MWh2+Fh2o0*MWh2o
+Fcl0*MWc1+Fc20*MWc2)/v0
vis=y1*vis1/(y1*phi11+y2*phi12+y3*phi13+y4*phi14+y5*phi15+y6*phi16)+y2*vis2/
(y1*phi21+y2*phi22+y3*phi23+y4*phi24+y5*phi25+y6*phi26)+y3*vis3/(y1*phi31+y2
*phi32+y3*phi33+y4*phi34+y5*phi35+y6*phi36)+y4*vis4/(y1*phi41+y2*phi42+y3*ph
i43+y4*phi44+y5*phi45+y6*phi46)+y5*vis5/(y1*phi51+y2*phi52+y3*phi53+y4*phi54
+y5*phi55+y6*phi56)+y6*vis6/(y1*phi61+y2*phi62+y3*phi63+y4*phi64+y5*phi65+y6
*phi66)
vis1=10^(-7)*(4.61*Tr1^0.618-2.04*exp(-0.449*Tr1)+1.94*exp(-4.058*Tr1)+0.1)/
(Tc1^(1/6)*MW1^(-1/2)*Pc1^(-2/3))
;Tr1=T/Tc1 ;Tc1=617.2 ;MW1=106.16 ;Pc1=36 //EB
vis2=10^(-7)*(4.61*Tr2^0.618-2.04*exp(-0.449*Tr2)+1.94*exp(-4.058*Tr2)+0.1)/
(Tc2^(1/6)*MW2^(-1/2)*Pc2^(-2/3))
;Tr2=T/Tc2 ;Tc2=647.0 ;MW2=104.14 ;Pc2=39.9 //ST
vis3=10^(-7)*(4.61*Tr3^0.618-2.04*exp(-0.449*Tr3)+1.94*exp(-4.058*Tr3)+0.1)/
(Tc3^(1/6)*MW3^(-1/2)*Pc3^(-2/3))
;Tr3=T/Tc3 ;Tc3=562.2 ;MW3=78.11 ;Pc3=48.9 //BZ
vis4=10^(-7)*(4.61*Tr4^0.618-2.04*exp(-0.449*Tr4)+1.94*exp(-4.058*Tr4)+0.1)/
(Tc4^(1/6)*MW4^(-1/2)*Pc4^(-2/3))
;Tr4=T/Tc4 ;Tc4=591.8 ;MW4=92.11 ;Pc4=41 //TO
vis5=10^(-7)*26.69*sqrt(MW5*T)/sigma5^2/omega5 ;MW5=2 ;sigma5=2.827
;omega5=1.16145/(T5)^0.14874+0.52487*exp(-0.77320*T5)+2.16178*exp(-
2.43787*T5) ;T5=T/59.7 //H2
vis6=10^(-7)*26.69*sqrt(MW6*T)/sigma6^2/omega62;MW6=18;sigma6=2.641
;omega6=1.16145/(T6)^0.14874+0.52487*exp(-0.77320*T6)+2.16178*exp(-
2.43787*T6) ;T6=T/809.1 ;omega62=omega6+0.2/T6 //H2O
phi11=(1+(vis1/vis1)^(1/2)*(MW1/MW1)^(1/4))^2/(8*(1+MW1/MW1))^(1/2)

```

```

phi12=(1+(vis1/vis2)^(1/2)*(MW2/MW1)^(1/4))^2/(8*(1+MW1/MW2))^(1/2)
phi13=(1+(vis1/vis3)^(1/2)*(MW3/MW1)^(1/4))^2/(8*(1+MW1/MW3))^(1/2)
phi14=(1+(vis1/vis4)^(1/2)*(MW4/MW1)^(1/4))^2/(8*(1+MW1/MW4))^(1/2)
phi15=(1+(vis1/vis5)^(1/2)*(MW5/MW1)^(1/4))^2/(8*(1+MW1/MW5))^(1/2)
phi16=(1+(vis1/vis6)^(1/2)*(MW6/MW1)^(1/4))^2/(8*(1+MW1/MW6))^(1/2)
phi21=(1+(vis2/vis1)^(1/2)*(MW1/MW2)^(1/4))^2/(8*(1+MW2/MW1))^(1/2)
phi22=(1+(vis2/vis2)^(1/2)*(MW2/MW2)^(1/4))^2/(8*(1+MW2/MW2))^(1/2)
phi23=(1+(vis2/vis3)^(1/2)*(MW3/MW2)^(1/4))^2/(8*(1+MW2/MW3))^(1/2)
phi24=(1+(vis2/vis4)^(1/2)*(MW4/MW2)^(1/4))^2/(8*(1+MW2/MW4))^(1/2)
phi25=(1+(vis2/vis5)^(1/2)*(MW5/MW2)^(1/4))^2/(8*(1+MW2/MW5))^(1/2)
phi26=(1+(vis2/vis6)^(1/2)*(MW6/MW2)^(1/4))^2/(8*(1+MW2/MW6))^(1/2)
phi31=(1+(vis3/vis1)^(1/2)*(MW1/MW3)^(1/4))^2/(8*(1+MW3/MW1))^(1/2)
phi32=(1+(vis3/vis2)^(1/2)*(MW2/MW3)^(1/4))^2/(8*(1+MW3/MW2))^(1/2)
phi33=(1+(vis3/vis3)^(1/2)*(MW3/MW3)^(1/4))^2/(8*(1+MW3/MW3))^(1/2)
phi34=(1+(vis3/vis4)^(1/2)*(MW4/MW3)^(1/4))^2/(8*(1+MW3/MW4))^(1/2)
phi35=(1+(vis3/vis5)^(1/2)*(MW5/MW3)^(1/4))^2/(8*(1+MW3/MW5))^(1/2)
phi36=(1+(vis3/vis6)^(1/2)*(MW6/MW3)^(1/4))^2/(8*(1+MW3/MW6))^(1/2)
phi41=(1+(vis4/vis1)^(1/2)*(MW1/MW4)^(1/4))^2/(8*(1+MW4/MW1))^(1/2)
phi42=(1+(vis4/vis2)^(1/2)*(MW2/MW4)^(1/4))^2/(8*(1+MW4/MW2))^(1/2)
phi43=(1+(vis4/vis3)^(1/2)*(MW3/MW4)^(1/4))^2/(8*(1+MW4/MW3))^(1/2)
phi44=(1+(vis4/vis4)^(1/2)*(MW4/MW4)^(1/4))^2/(8*(1+MW4/MW4))^(1/2)
phi45=(1+(vis4/vis5)^(1/2)*(MW5/MW4)^(1/4))^2/(8*(1+MW4/MW5))^(1/2)
phi46=(1+(vis4/vis6)^(1/2)*(MW6/MW4)^(1/4))^2/(8*(1+MW4/MW6))^(1/2)
phi51=(1+(vis5/vis1)^(1/2)*(MW1/MW5)^(1/4))^2/(8*(1+MW5/MW1))^(1/2)
phi52=(1+(vis5/vis2)^(1/2)*(MW2/MW5)^(1/4))^2/(8*(1+MW5/MW2))^(1/2)
phi53=(1+(vis5/vis3)^(1/2)*(MW3/MW5)^(1/4))^2/(8*(1+MW5/MW3))^(1/2)
phi54=(1+(vis5/vis4)^(1/2)*(MW4/MW5)^(1/4))^2/(8*(1+MW5/MW4))^(1/2)
phi55=(1+(vis5/vis5)^(1/2)*(MW5/MW5)^(1/4))^2/(8*(1+MW5/MW5))^(1/2)
phi56=(1+(vis5/vis6)^(1/2)*(MW6/MW5)^(1/4))^2/(8*(1+MW5/MW6))^(1/2)
phi61=(1+(vis6/vis1)^(1/2)*(MW1/MW6)^(1/4))^2/(8*(1+MW6/MW1))^(1/2)
phi62=(1+(vis6/vis2)^(1/2)*(MW2/MW6)^(1/4))^2/(8*(1+MW6/MW2))^(1/2)
phi63=(1+(vis6/vis3)^(1/2)*(MW3/MW6)^(1/4))^2/(8*(1+MW6/MW3))^(1/2)
phi64=(1+(vis6/vis4)^(1/2)*(MW4/MW6)^(1/4))^2/(8*(1+MW6/MW4))^(1/2)
phi65=(1+(vis6/vis5)^(1/2)*(MW5/MW6)^(1/4))^2/(8*(1+MW6/MW5))^(1/2)
phi66=(1+(vis6/vis6)^(1/2)*(MW6/MW6)^(1/4))^2/(8*(1+MW6/MW6))^(1/2)

```

```
//Feed
```

```

Feb0 = 707
Fst0 = 7.104
Fbz0 = 0.293
Fto0 = 4.968
Fh20 = 0
Fh2o0= 7777
Fc10 = 0
Fc20 = 0
Ft0 = Feb0+Fst0+Fbz0+Fto0+Fh20+Fh2o0+Fc10+Fc20
P0 = 1.25
T0 = 886

```

```
//Profile
```

```

Feb = Feb00*(1-XEB)
Fst = Fst00+Feb00*XST
Fbz = Fbz00+Feb00*XBZ
Fto = Fto00+Feb00*XTO
Fh2 = Fh200+Feb00*XH2
Fc1 = Fc10+Feb00*XTO
Fc2 = Fc20+Feb00*XBZ

```

```
Peb = Feb/Ft*P
```

```
Pst = Fst/Ft*P
```

Ph2 = Fh2/Ft*P
 Pbz = Fbz/Ft*P
 Pto = Fto/Ft*P

Ceb = Feb/v
 Cst = Fst/v
 Ch2 = Fh2/v
 Cbz = Fbz/v
 Cto = Fto/v

Cebin = Feb0/v0
 Cstin = Fst0/v0
 Ch2in = Fh20/v0
 Cbzin = Fbz0/v0
 Ctoin = Fto0/v0

Ceb0 = Feb00/v0
 Cst0 = Fst00/v0
 Ch20 = Fh200/v0
 Cbz0 = Fbz00/v0
 Cto0 = Fto00/v0

meb = MWeb*Feb
 mst = MWst*Fst
 mbz = MWbz*Fbz
 mto = MWto*Fto
 mh2 = MWh2*Fh2
 mh2o = MWh2o*Fh2o0
 mc1 = MWc1*Fc1
 mc2 = MWc2*Fc2
 mt = meb+mst+mbz+mh2+mto+mc1+mc2+mh2o

y1=Feb/Ft
 y2=Fst/Ft
 y3=Fbz/Ft
 y4=Fto/Ft
 y5=Fh2/Ft
 y6=Fh2o0/Ft

//Result
 SST = XST/XEB*100
 SBZ = XBZ/XEB*100
 STO = XTO/XEB*100

integral z[0,Lb] by trp step 0.133
 output Ceb',Cst',Cbz',Cto',Ch2',XEB,SST,SBZ,STO,P,TCeb0=0.0014073
 Cst0=0.000019
 Cbz0=0.0000006737844
 Cto0=0.000009939294
 Ch20=0.000004879009



Result:

```
<<  results  >>
Ceb'      = -8.348045e-005
Cst'      = -6.817745e-005
Cbx'      = -2.834605e-007
Cto'      = -2.082809e-007
Ch2'      = 3.116312e-006
XEB       = 0.3445653
SST       = 97.77636
SBZ       = 1.171451
STO       = 0.9487367
P         = 1.044915
T         = 826.0831
```



6. Model6 : Heterogeneous model account for internal transfer, external transfer and mass axial dispersion

EQUATRAN code:

```

function
diffus(Cseb0,Csst0,Csbz0,Csto0,Csh20,T0;Cseb,Csst,Csbz,Csto,Csh2,T,Cseb',Cst
t',Csbz',Csto',Csh2',T',Deebs,Deets,Debzs,Detos,Deh2s,ke)
Cseb'+Cseb'*2/r= 1/Deebs*(densityS*(rc1s+rc2s+rc3s) +voidcat*(rt1s+rt2s
+rt3s))
;Cseb#Cseb0 ;Cseb'#0
Csst'+Csst'*2/r= -1/Deets*(densityS*(rc1s-rc4s)+voidcat*(rt1s))
;Csst#Csst0 ;Csst'#0
Csbz'+Csbz'*2/r= -1/Debzs*(densityS*(rc2s)+voidcat*(rt2s))
;Csbz#Csbz0 ;Csbz'#0
Csto'+Csto'*2/r= -1/Detos*(densityS*(rc3s+rc4s)+voidcat*(rt3s))
;Csto#Csto0 ;Csto'#0
Csh2'+Csh2'*2/r= -1/Deh2s*(densityS*(rc1s-rc3s-2*rc4s)+voidcat*(rt1s-rt3s))
;Csh2#Csh20 ;Csh2'#0

T'+T'*2/r = -((rc1s*densityS+rt1s*voidcat)*HRX1-(rc2s*densityS+rt2s
*voidcat)*HRX2-(rc3s*densityS+rt3s*voidcat)*HRX3-rc4s*densityS*HRX4)/ke
;T#T0 ;T'#0

Cseb = Pseb/R/T*10^2
Csst = Psst/R/T*10^2
Csh2 = Psh2/R/T*10^2
Csbz = Psbz/R/T*10^2
Csto = Psto/R/T*10^2

Cseb0 = Pseb0/R/T0*10^2
Csst0 = Psst0/R/T0*10^2
Csh20 = Psh20/R/T0*10^2
Csbz0 = Psbz0/R/T0*10^2
Csto0 = Psto0/R/T0*10^2

rc1s = kc1*KEB*(Pseb-Psst*Psh2/Keq) / (1+KEB*Pseb+KH2*Psh2+KST*Psst)^2
rc2s = kc2*KEB*Pseb/ (1+KEB*Pseb+KH2*Psh2+KST*Psst)^2
rc3s = kc3*KEB*Pseb*KH2*Psh2/ (1+KEB*Pseb+KH2*Psh2+KST*Psst)^2
rc4s = kc4*KST*Psst*KH2*Psh2/ (1+KEB*Pseb+KH2*Psh2+KST*Psst)^2
rt1s = kt1*(Pseb-Psst*Psh2/Keq)
rt2s = kt2*Pseb
rt3s = kt3*Pseb
kc1 = A1*exp(-E1*10^3/R/T) ;A1=2.33293E+11 ;E1=204.6619326
kc2 = A2*exp(-E2*10^3/R/T) ;A2=2.65416E+16 ;E2=320.3544359
kc3 = A3*exp(-E3*10^3/R/T) ;A3=9.00967E+15 ;E3=320.9687204
kc4 = A4*exp(-E4*10^3/R/T) ;A4=8.53675E+17 ;E4=333.4837164
KEB = Aeb*exp(-Heb*10^3/R/T) ;Aeb=2.55449E-10 ;Heb=-180.5057701
KST = Ast*exp(-Hst*10^3/R/T) ;Ast=2.26449E-06 ;Hst=-122.2609362
KH2 = Ah2*exp(-Hh2*10^3/R/T) ;Ah2=3.92807E-09 ;Hh2=-152.1129516
kt1 = At1*exp(-Et1*10^3/R/T) ;At1=2.2215*10^16 ;Et1=272.23
kt2 = At2*exp(-Et2*10^3/R/T) ;At2=2.4217*10^20 ;Et2=352.79
kt3 = At3*exp(-Et3*10^3/R/T) ;At3=3.8224*10^17 ;Et3=313.06
Keq = exp(-deltaG/R/T)
deltaG = deltaH - T*deltaS
deltaH = deltaH0+deltaa*(T-298.15)+deltab/2*(T^2-298.15^2)+deltac/3*(T^3-
298.15^3)+deltad/4*(T^4-298.15^4)
deltaS = deltaS0+deltaa*log(T/298.15)+deltab*(T-298.15)+deltac/2*(T^2-
298.15^2)+deltad/3*(T^3-298.15^3)

```

```

deltaH0= (1.475-0.2981)*10^5
deltaS0= 115.7
deltaa = -28.25+27.14+43.1 ;deltab=(615.9+9.274-707.2)*10^(-3)
;deltac=(-40.23-1.381+48.11)*10^(-5) ;deltad=(99.35+7.645-130.1)*10^(-9)
R      = 8.314

```

```

HRX1 = HRX10+deltaa1*(T-298.15)+deltab1/2*(T^2-298.15^2)+deltac1/3*(T^3-
298.15^3)+deltad1/4*(T^4-298.15^4)
HRX2 = HRX20+deltaa2*(T-298.15)+deltab2/2*(T^2-298.15^2)+deltac2/3*(T^3-
298.15^3)+deltad2/4*(T^4-298.15^4)
HRX3 = HRX30+deltaa3*(T-298.15)+deltab3/2*(T^2-298.15^2)+deltac3/3*(T^3-
298.15^3)+deltad3/4*(T^4-298.15^4)
HRX4 = HRX40+deltaa4*(T-298.15)+deltab4/2*(T^2-298.15^2)+deltac4/3*(T^3-
298.15^3)+deltad4/4*(T^4-298.15^4)

```

```

HRX10=117690 ;deltaa1=41.99 ;deltab1=-8.2026*10^(-2)
;deltac1=6.499*10^(-5) ;deltad1=-2.311*10^(-8)
HRX20=105510 ;deltaa2=12.986 ;deltab2=-7.67*10^(-2)
;deltac2=9.592*10^(-5) ;deltad2=-4.125*10^(-8)
HRX30=-54680 ;deltaa3=10.86 ;deltab3=-15.1844*10^(-2)
;deltac3=23.04*10^(-5) ;deltad3=-9.9955*10^(-8)
HRX40=-172370 ;deltaa4=-31.13 ;deltab4=-6.9818*10^(-2)
;deltac4=16.54*10^(-5) ;deltad4=-7.685*10^(-8)
Cpeb = aeb+beb*T+ceb*T^2+deb*T^3 ;aeb=-0.43426
;beb=6.0671*10^(-3) ;ceb=-3.8625*10^(-6) ;deb=9.1282*10^(-10)
Cpst = ast+bst*T+cst*T^2+dst*T^3 ;ast=-0.26436
;bst=5.564*10^(-3) ;cst=-3.0018*10^(-6) ;dst=5.3317*10^(-10)
Cpbz = abz+bbz*T+cbz*T^2+dbz*T^3 ;abz=-0.40599
;bbz=6.6616*10^(-3) ;cbz=-4.5318*10^(-6) ;dbz=12.255*10^(-10)
Cpto = ato+bto*T+cto*T^2+dto*T^3 ;ato=-0.27127
;bto=5.9142*10^(-3) ;cto=-3.8631*10^(-6) ;dto=9.54*10^(-10)
Cph2 = ah2+bh2*T+ch2*T^2+dh2*T^3 ;ah2=13.57
;bh2=4.637*10^(-3) ;ch2=-6.905*10^(-6) ;dh2=38.23*10^(-10)
Cph2o= ah2o+bh2o*T+ch2o*T^2+dh2o*T^3 ;ah2o=1.79111
;bh2o=0.1069*10^(-3) ;ch2o=0.58611*10^(-6) ;dh2o=-1.998*10^(-10)

```

```

Deebs = 0.02248767
Dests = 0.02467243
Debzs = 0.02620409
Detos = 0.02359606
Deh2s = 0.2069529
ke = 19.35925

```

```

voidB = 1-densityB/densityS
densityB = 1422
densityS = 2500
voidcat = 0.4
tor = 3

```

```

integral r[0.0000001,0.00275]
END

```

```

//Solid phase
e:diffus(Cseb0,Csst0,Csbz0,Csto0,Csh20,Ts0,Cseb,Csst,Csbz,Csto,Csh2,Tss,kpeb
*(Ceb-Cseb)/Deebs,kpst*(Cst-Csst)/Dests,kpbz*(Czb-Csbz)/Debzs,kpto*(Cto-
Csto)/Detos,kph2*(Ch2-Csh2)/Deh2s,h*(T-Tss)/ke,Deebs,Dests,Debzs,Detos
,Deh2s,ke)
e1:Cseb=CseBR
e2:Csst=CsstR
e3:Csbz=CsbzR
e4:Csto=CstoR

```

```

e5:Csh2=Csh2R
e11:Tss=Ts
reset CsebR#0.0014064[0,1000]          by e1  maxloop 100000,
      CsstR#0.000320049[0,1000]        by e2  maxloop 100000,
      CsbzR#6.74E-07[0,1000]          by e3  maxloop 100000,
      CstoR#9.94E-06[0,1000]          by e4  maxloop 100000,
      Csh2R#4.88E-06[0,1000]          by e5  maxloop 100000,
      Ts#880[0,1000]                  by e11 maxloop 100000
reset  Cseb0#0.000351019[0,1000]      by e   maxloop 100000

//Gas phase
//Mass balance
voidB*Da'*Ceb'+voidB*Da*Ceb''-us*Ceb'-us'*Ceb-kpeb*as*(Ceb-CsebR)-
voidB*(rt1+rt2+rt3)=0          ;Ceb#Ceb0          ;Ceb'#(A0*(Ceb0-Cebin))
voidB*Da'*Cst'+voidB*Da*Cst''-us*Cst'-us'*Cst-kpst*as*(Cst-
CsstR)+voidB*(rt1)=0          ;Cst#Cst0          ;Cst'#(A0*(Cst0-Cstin))
voidB*Da'*Cbz'+voidB*Da*Cbz''-us*Cbz'-us'*Cbz-kpbz*as*(Cbz-
CsbzR)+voidB*(rt2)=0          ;Cbz#Cbz0          ;Cbz'#(A0*(Cbz0-Cbzin))
voidB*Da'*Cto'+voidB*Da*Cto''-us*Cto'-us'*Cto-kpto*as*(Cto-
CstoR)+voidB*(rt3)=0          ;Cto#Cto0          ;Cto'#(A0*(Cto0-Ctoin))
voidB*Da'*Ch2'+voidB*Da*Ch2''-us*Ch2'-us'*Ch2-kph2*as*(Ch2-
Csh2R)+voidB*(rt1-rt3)=0      ;Ch2#Ch20          ;Ch2'#(A0*(Ch20-Ch2in))
us'=R*(10^(-2))/Ac*((P*(Ft*T'+T*Ft')-T*Ft*P')/P^2)          ;us#us0
Ft'/Ac = (rc1+rc2-rc4)*densityB+(rt1+rt2)*voidB          ;Ft#Ft0
Da' = 0.5*(us'/voidB)*dp          ;Da#Da0
A0 = us0/(voidB*Da0)
Da0 = 0.5*(us0/voidB)*dp

//Energy balance
us*density*Cpm*T'=-as*h*(T-Ts)          ;T#T0

//Momentum balance
P'*10^5 = -f*us*G/dp/3600^2          ;P#P0
f = (1-voidB)/voidB^3*(1.75+150*(1-voidB)/Re)

//Reaction
rc1 = kc1*KEB*(Peb-Pst*Ph2/Keq)/(1+KEB*Peb+KH2*Ph2+KST*Pst)^2
rc2 = kc2*KEB*Peb/(1+KEB*Peb+KH2*Ph2+KST*Pst)^2
rc3 = kc3*KEB*Peb*KH2*Ph2/(1+KEB*Peb+KH2*Ph2+KST*Pst)^2
rc4 = kc4*KST*Pst*KH2*Ph2/(1+KEB*Peb+KH2*Ph2+KST*Pst)^2
rt1 = kt1*(Peb-Pst*Ph2/Keq)
rt2 = kt2*Peb
rt3 = kt3*Peb
kc1 = A1*exp(-E1*10^3/R/T)          ;A1=2.33293E+11          ;E1=204.6619326
kc2 = A2*exp(-E2*10^3/R/T)          ;A2=2.65416E+16          ;E2=320.3544359
kc3 = A3*exp(-E3*10^3/R/T)          ;A3=9.00967E+15          ;E3=320.9687204
kc4 = A4*exp(-E4*10^3/R/T)          ;A4=8.53675E+17          ;E4=333.4837164
KEB = Aeb*exp(-Heb*10^3/R/T)        ;Aeb=2.55449E-10          ;Heb=-180.5057701
KST = Ast*exp(-Hst*10^3/R/T)        ;Ast=2.26449E-06          ;Hst=-122.2609362
KH2 = Ah2*exp(-Hh2*10^3/R/T)        ;Ah2=3.92807E-09          ;Hh2=-152.1129516
kt1 = At1*exp(-Et1*10^3/R/T)        ;At1=2.2215*10^16          ;Et1=272.23
kt2 = At2*exp(-Et2*10^3/R/T)        ;At2=2.4217*10^20          ;Et2=352.79
kt3 = At3*exp(-Et3*10^3/R/T)        ;At3=3.8224*10^17          ;Et3=313.06
Keq = exp(-deltaG/R/T)
deltaG = deltaH - T*deltaS
deltaH = deltaH0+deltaa*(T-298.15)+deltab/2*(T^2-298.15^2)+deltac/3*(T^3-
298.15^3)+deltad/4*(T^4-298.15^4)
deltaS = deltaS0+deltaa*loge(T/298.15)+deltab*(T-298.15)+deltac/2*(T^2-
298.15^2)+deltad/3*(T^3-298.15^3)

```



```

deltaH0= (1.475-0.2981)*10^5
deltaS0= 115.7
deltaa = -28.25+27.14+43.1 ;deltab=(615.9+9.274-707.2)*10^(-3)
;deltac=(-40.23-1.381+48.11)*10^(-5) ;deltad=(99.35+7.645-130.1)*10^(-9)
R      = 8.314

HRX1 = HRX10+deltaa1*(T-298.15)+deltab1/2*(T^2-298.15^2)+deltac1/3*(T^3-
298.15^3)+deltad1/4*(T^4-298.15^4)
HRX2 = HRX20+deltaa2*(T-298.15)+deltab2/2*(T^2-298.15^2)+deltac2/3*(T^3-
298.15^3)+deltad2/4*(T^4-298.15^4)
HRX3 = HRX30+deltaa3*(T-298.15)+deltab3/2*(T^2-298.15^2)+deltac3/3*(T^3-
298.15^3)+deltad3/4*(T^4-298.15^4)
HRX4 = HRX40+deltaa4*(T-298.15)+deltab4/2*(T^2-298.15^2)+deltac4/3*(T^3-
298.15^3)+deltad4/4*(T^4-298.15^4)
HRX10=117690 ;deltaa1=41.99 ;deltab1=-8.2026*10^(-2)
;deltac1=6.499*10^(-5) ;deltad1=-2.311*10^(-8)
HRX20=105510 ;deltaa2=12.986 ;deltab2=-7.67*10^(-2)
;deltac2=9.592*10^(-5) ;deltad2=-4.125*10^(-8)
HRX30=-54680 ;deltaa3=10.86 ;deltab3=-15.1844*10^(-2)
;deltac3=23.04*10^(-5) ;deltad3=-9.9955*10^(-8)
HRX40=-172370 ;deltaa4=-31.13 ;deltab4=-6.9818*10^(-2)
;deltac4=16.54*10^(-5) ;deltad4=-7.685*10^(-8)

//Bed properties
voidB = 1-densityB/densityS
densityB = 1422
Ac = _pi*rb^2
rb = 3.5
Lb = 1.33
densityS = 2500
voidcat = 0.4
dp = 0.0055
rp = dp/2
as = 3/rp*(1-voidB)

//Properties of component
MWeb = 106.167
MWst = 104.151
MWbz = 78.113
MWto = 92.14
MWh2 = 2.016
MWh2o= 18.015
MWcl = 16.043
MWc2 = 28.054

Cpeb = aeb+beb*T+ceb*T^2+deb*T^3 ;aeb=-0.43426
;beb=6.0671*10^(-3) ;ceb=-3.8625*10^(-6) ;deb=9.1282*10^(-10)
Cpst = ast+bst*T+cst*T^2+dst*T^3 ;ast=-0.26436
;bst=5.564*10^(-3) ;cst=-3.0018*10^(-6) ;dst=5.3317*10^(-10)
Cpbz = abz+bbz*T+cbz*T^2+dbz*T^3 ;abz=-0.40599
;bbz=6.6616*10^(-3) ;cbz=-4.5318*10^(-6) ;dbz=12.255*10^(-10)
Cpto = ato+bto*T+cto*T^2+dto*T^3 ;ato=-0.27127
;bto=5.9142*10^(-3) ;cto=-3.8631*10^(-6) ;dto=9.54*10^(-10)
Cph2 = ah2+bh2*T+ch2*T^2+dh2*T^3 ;ah2=13.57
;bh2=4.637*10^(-3) ;ch2=-6.905*10^(-6) ;dh2=38.23*10^(-10)
Cph2o= ah2o+bh2o*T+ch2o*T^2+dh2o*T^3 ;ah2o=1.79111
;bh2o=0.1069*10^(-3) ;ch2o=0.58611*10^(-6) ;dh2o=-1.998*10^(-10)

//Properties of fluid
v0 = Ft0*R*T0/P0*10^(-2)

```

```

us0= v0/Ac
us = v/Ac
density = (Feb*MWeb+Fst*MWst+Fbz*MWbz+Fto*MWto+Fh2*MWh2+Fh2o0*MWh2o+Fc1*MWc1
+Fc2*MWc2)/v
Cpm = (meb*Cpeb+mst*Cpst+mbz*Cpbz+mto*Cpto+mh2*Cph2+mh2o*Cph2o)/mt
G = feedden0*v0/Ac
feedden0 = (Feb0*MWeb+Fst0*MWst+Fbz0*MWbz+Fto0*MWto+Fh20*MWh2+Fh2o0*MWh2o
+Fc10*MWc1+Fc20*MWc2)/v0
Re = feedden0*dp*us0/(vis*3600)
vis=y1*vis1/(y1*phi11+y2*phi12+y3*phi13+y4*phi14+y5*phi15+y6*phi16)+y2*vis2/
(y1*phi21+y2*phi22+y3*phi23+y4*phi24+y5*phi25+y6*phi26)+y3*vis3/(y1*phi31+y2
*phi32+y3*phi33+y4*phi34+y5*phi35+y6*phi36)+y4*vis4/(y1*phi41+y2*phi42+y3*ph
i43+y4*phi44+y5*phi45+y6*phi46)+y5*vis5/(y1*phi51+y2*phi52+y3*phi53+y4*phi54
+y5*phi55+y6*phi56)+y6*vis6/(y1*phi61+y2*phi62+y3*phi63+y4*phi64+y5*phi65+y6
*phi66)
vis1=10^(-7)*(4.61*Tr1^0.618-2.04*exp(-0.449*Tr1)+1.94*exp(-4.058*Tr1)+0.1)/
(Tc1^(1/6)*MW1^(-1/2)*Pc1^(-2/3))
;Tr1=T/Tc1 ;Tc1=617.2 ;MW1=106.16 ;Pc1=36 //EB
vis2=10^(-7)*(4.61*Tr2^0.618-2.04*exp(-0.449*Tr2)+1.94*exp(-4.058*Tr2)+0.1)/
(Tc2^(1/6)*MW2^(-1/2)*Pc2^(-2/3))
;Tr2=T/Tc2 ;Tc2=647.0; MW2=104.14 ;Pc2=39.9 //ST
vis3=10^(-7)*(4.61*Tr3^0.618-2.04*exp(-0.449*Tr3)+1.94*exp(-4.058*Tr3)+0.1)/
(Tc3^(1/6)*MW3^(-1/2)*Pc3^(-2/3))
;Tr3=T/Tc3 ;Tc3=562.2 ;MW3=78.11 ;Pc3=48.9 //BZ
vis4=10^(-7)*(4.61*Tr4^0.618-2.04*exp(-0.449*Tr4)+1.94*exp(-4.058*Tr4)+0.1)/
(Tc4^(1/6)*MW4^(-1/2)*Pc4^(-2/3))
;Tr4=T/Tc4 ;Tc4=591.8 ;MW4=92.11 ;Pc4=41 //TO
vis5=10^(-7)*26.69*sqrt(MW5*T)/sigma5^2/omega5 ;MW5=2 ;sigma5=2.827
;omega5=1.16145/(T5)^0.14874+0.52487*exp(-0.77320*T5)+2.16178*exp(-
2.43787*T5) ;T5=T/59.7 //H2
vis6=10^(-7)*26.69*sqrt(MW6*T)/sigma6^2/omega62;MW6=18 ;sigma6=2.641
;omega6=1.16145/(T6)^0.14874+0.52487*exp(-0.77320*T6)+2.16178*exp(-
2.43787*T6) ;T6=T/809.1 ;omega62=omega6+0.2/T6 //H2O
phi11=(1+(vis1/vis1)^(1/2)*(MW1/MW1)^(1/4))^2/(8*(1+MW1/MW1))^(1/2)
phi12=(1+(vis1/vis2)^(1/2)*(MW2/MW1)^(1/4))^2/(8*(1+MW1/MW2))^(1/2)
phi13=(1+(vis1/vis3)^(1/2)*(MW3/MW1)^(1/4))^2/(8*(1+MW1/MW3))^(1/2)
phi14=(1+(vis1/vis4)^(1/2)*(MW4/MW1)^(1/4))^2/(8*(1+MW1/MW4))^(1/2)
phi15=(1+(vis1/vis5)^(1/2)*(MW5/MW1)^(1/4))^2/(8*(1+MW1/MW5))^(1/2)
phi16=(1+(vis1/vis6)^(1/2)*(MW6/MW1)^(1/4))^2/(8*(1+MW1/MW6))^(1/2)
phi21=(1+(vis2/vis1)^(1/2)*(MW1/MW2)^(1/4))^2/(8*(1+MW2/MW1))^(1/2)
phi22=(1+(vis2/vis2)^(1/2)*(MW2/MW2)^(1/4))^2/(8*(1+MW2/MW2))^(1/2)
phi23=(1+(vis2/vis3)^(1/2)*(MW3/MW2)^(1/4))^2/(8*(1+MW2/MW3))^(1/2)
phi24=(1+(vis2/vis4)^(1/2)*(MW4/MW2)^(1/4))^2/(8*(1+MW2/MW4))^(1/2)
phi25=(1+(vis2/vis5)^(1/2)*(MW5/MW2)^(1/4))^2/(8*(1+MW2/MW5))^(1/2)
phi26=(1+(vis2/vis6)^(1/2)*(MW6/MW2)^(1/4))^2/(8*(1+MW2/MW6))^(1/2)
phi31=(1+(vis3/vis1)^(1/2)*(MW1/MW3)^(1/4))^2/(8*(1+MW3/MW1))^(1/2)
phi32=(1+(vis3/vis2)^(1/2)*(MW2/MW3)^(1/4))^2/(8*(1+MW3/MW2))^(1/2)
phi33=(1+(vis3/vis3)^(1/2)*(MW3/MW3)^(1/4))^2/(8*(1+MW3/MW3))^(1/2)
phi34=(1+(vis3/vis4)^(1/2)*(MW4/MW3)^(1/4))^2/(8*(1+MW3/MW4))^(1/2)
phi35=(1+(vis3/vis5)^(1/2)*(MW5/MW3)^(1/4))^2/(8*(1+MW3/MW5))^(1/2)
phi36=(1+(vis3/vis6)^(1/2)*(MW6/MW3)^(1/4))^2/(8*(1+MW3/MW6))^(1/2)
phi41=(1+(vis4/vis1)^(1/2)*(MW1/MW4)^(1/4))^2/(8*(1+MW4/MW1))^(1/2)
phi42=(1+(vis4/vis2)^(1/2)*(MW2/MW4)^(1/4))^2/(8*(1+MW4/MW2))^(1/2)
phi43=(1+(vis4/vis3)^(1/2)*(MW3/MW4)^(1/4))^2/(8*(1+MW4/MW3))^(1/2)
phi44=(1+(vis4/vis4)^(1/2)*(MW4/MW4)^(1/4))^2/(8*(1+MW4/MW4))^(1/2)
phi45=(1+(vis4/vis5)^(1/2)*(MW5/MW4)^(1/4))^2/(8*(1+MW4/MW5))^(1/2)
phi46=(1+(vis4/vis6)^(1/2)*(MW6/MW4)^(1/4))^2/(8*(1+MW4/MW6))^(1/2)
phi51=(1+(vis5/vis1)^(1/2)*(MW1/MW5)^(1/4))^2/(8*(1+MW5/MW1))^(1/2)
phi52=(1+(vis5/vis2)^(1/2)*(MW2/MW5)^(1/4))^2/(8*(1+MW5/MW2))^(1/2)
phi53=(1+(vis5/vis3)^(1/2)*(MW3/MW5)^(1/4))^2/(8*(1+MW5/MW3))^(1/2)

```

```

phi54=(1+(vis5/vis4)^(1/2)*(MW4/MW5)^(1/4))^2/(8*(1+MW5/MW4))^(1/2)
phi55=(1+(vis5/vis5)^(1/2)*(MW5/MW5)^(1/4))^2/(8*(1+MW5/MW5))^(1/2)
phi56=(1+(vis5/vis6)^(1/2)*(MW6/MW5)^(1/4))^2/(8*(1+MW5/MW6))^(1/2)
phi61=(1+(vis6/vis1)^(1/2)*(MW1/MW6)^(1/4))^2/(8*(1+MW6/MW1))^(1/2)
phi62=(1+(vis6/vis2)^(1/2)*(MW2/MW6)^(1/4))^2/(8*(1+MW6/MW2))^(1/2)
phi63=(1+(vis6/vis3)^(1/2)*(MW3/MW6)^(1/4))^2/(8*(1+MW6/MW3))^(1/2)
phi64=(1+(vis6/vis4)^(1/2)*(MW4/MW6)^(1/4))^2/(8*(1+MW6/MW4))^(1/2)
phi65=(1+(vis6/vis5)^(1/2)*(MW5/MW6)^(1/4))^2/(8*(1+MW6/MW5))^(1/2)
phi66=(1+(vis6/vis6)^(1/2)*(MW6/MW6)^(1/4))^2/(8*(1+MW6/MW6))^(1/2)

```

```
//Feed
```

```

Feb0 = 707
Fst0 = 7.104
Fbz0 = 0.293
Fto0 = 4.968
Fh20 = 0
Fh2o0= 7777
Fc10 = 0
Fc20 = 0
Ft0 = Feb0+Fst0+Fbz0+Fto0+Fh20+Fh2o0+Fc10+Fc20
P0 = 1.25
T0 = 886

```

```
//Profile
```

```

Ceb0 = Feb00/v0
Cst0 = Fst00/v0
Ch20 = Fh200/v0
Cbz0 = Fbz00/v0
Cto0 = Fto00/v0
Feb = Feb00*(1-XEB)
Fst = Fst00+Feb00*XST
Fbz = Fbz00+Feb00*XBZ
Fto = Fto00+Feb00*XTO
Fh2 = Fh200+Feb00*XH2
Fc1 = Fc10+Feb00*XTO
Fc2 = Fc20+Feb00*XBZ

```

```

Peb = Feb/Ft*P
Pst = Fst/Ft*P
Ph2 = Fh2/Ft*P
Pbz = Fbz/Ft*P
Pto = Fto/Ft*P

```

```

Ceb = Feb/v
Cst = Fst/v
Ch2 = Fh2/v
Cbz = Fbz/v
Cto = Fto/v

```

```

Cebin = Feb0/v0
Cstin = Fst0/v0
Ch2in = Fh20/v0
Cbzin = Fbz0/v0
Ctoin = Fto0/v0

```

```

meb = MWeb*Feb
mst = MWst*Fst
mbz = MWbz*Fbz
mto = MWto*Fto

```



```

mh2    = MWh2*Fh2
mh2o   = MWh2o*Fh2o0
mc1    = MWc1*Fc1
mc2    = MWc2*Fc2
mt     = meb+mst+mbz+mh2+mto+mc1+mc2+mh2o

y1=Feb/Ft
y2=Fst/Ft
y3=Fbz/Ft
y4=Fto/Ft
y5=Fh2/Ft
y6=Fh2o0/Ft

yeb=Feb/Ft
yst=Fst/Ft
ybz=Fbz/Ft
yto=Fto/Ft
yh2=Fh2/Ft
yh2o=Fh2o0/Ft

//Mass Transport parameter
kpeb   =    1197.351
kpst   =    1070.464
kpbz   =    1204.048
kpto   =    1122.234
kph2   =    4835.582

//Heat Transport parameter
h      =    2974.605

//Result
SST = XST/XEB*100
SBZ = XBZ/XEB*100
STO = XTO/XEB*100

integral z[0,Lb] by trp step 0.133
output XEB,SST,SBZ,STO,P,T,Ceb',Cst',Czb',Cto',Ch2'

Ceb0=0.00140705
Cst0=0.0000187
Czb0=0.0000006737844
Cto0=0.000009939294
Ch20=0.0000046

```

Result:

```

<<  results  >>
XEB      = 0.3445987
SST      = 97.98518
SBZ      = 1.171413
STO      = 0.9758352
P        = 1.039764
T        = 826.4305
Ceb'     = 9.607248e-005
Cst'     = -6.354263e-006
Czb'     = 6.51771e-006
Cto'     = 4.353134e-006
Ch2'     = 7.573117e-005

```

VITA

NAME Pawinee Maithong

DATE OF BIRTH 27 Oct 1994

PLACE OF BIRTH Chonburi, Thailand

INSTITUTIONS ATTENDED Chulalongkorn university

HOME ADDRESS 2/7 Soi 2 Adunthammapas Road
Paknam Meung Rayong Thailand 21000

